Journal of Physical and Chemical Reference Data

An Organized Collection of Theoretical Gas-Phase Geometric, Spectroscopic, and Thermochemical Data of Oxygenated Hydrocarbons, $C_xH_yO_z$ (x, y = 1, 2; z = 1–8), of Relevance to Atmospheric, Astrochemical, and Combustion Sciences

Cite as: J. Phys. Chem. Ref. Data **49**, 023102 (2020); https://doi.org/10.1063/1.5132628
Submitted: 18 October 2019 • Accepted: 03 March 2020 • Published Online: 28 May 2020

John M. Simmie and Judith Würmel

Journal of Physical and Chemical Reference Data ARTICLE scitation.org/journal/jpr

An Organized Collection of Theoretical Gas-Phase Geometric, Spectroscopic, and Thermochemical Data of Oxygenated Hydrocarbons, $C_xH_yO_z$ (x, y = 1, 2; z = 1–8), of Relevance to Atmospheric, Astrochemical, and Combustion Sciences

Cite as: J. Phys. Chem. Ref. Data 49, 023102 (2020); doi: 10.1063/1.5132628
Submitted: 18 October 2019 • Accepted: 3 March 2020 •
Published Online: 28 May 2020

John M. Simmie[1,a)] and Judith Würmel[2]

AFFILIATIONS

[1] School of Chemistry, National University of Ireland, Galway H91 TK33, Ireland
[2] Galway Mayo Institute of Technology, Galway H91 T8NW, Ireland

[a)] **Author to whom correspondence should be addressed:** john.simmie@nuigalway.ie

ABSTRACT

The objective of this work is to present a unified collection of structural and chemical information on a series of neutral chemical tri-elemental species up to a molecular formula $C_2H_2O_8$, which may be used for validation purposes, for deep structured learning or indeed more simply for basic data of a single species. Such a collection vastly is tightly focused in terms of its component parts, contains novel results, and covers a number of chemical classes including stable molecules, radicals, carbenes, dipolar species, and excited states. Wherever possible, comparisons are made to the experimental and quantum chemical literature of gas-phase molecules, but the paucity of such means that there is only a very limited scope for validation. The primary data consist of structural information in the form of Cartesian coordinates, rotational constants together with vibrational frequencies, and anharmonicity coefficients, all obtained through density functional, B3LYP, calculations with the cc-pVTZ+d basis set. Standard statistical thermodynamic relations are then used to compute entropy, specific heat at constant pressure, and an enthalpy function over temperatures from 298.15 K to 2000 K. Supplementary material contains all the information necessary to carry out these calculations over different conditions as required as well as the raw species data. High-level quantum mechanical computations employing composite model chemistries, including CBS-QB3, CBS-APNO, G3, G4, W1BD, WMS, W2X, and W3X-L, are used to derive formation enthalpies via atomization and/or isodesmic calculations as appropriate.

Key words: formation enthalpies; entropy; isobaric heat capacity; enthalpy function; quantum chemistry; frequencies; anharmonicities; quantum chemistry; DFT; W3X-L; WMS.

CONTENTS

List of Tables

1. Introduction

Helium excepted hydrogen, oxygen, and carbon are the most abundant elements in the universe [T90], and hence, the widespread occurrence and importance of compounds of these elements is unsurprising. There has been increasing interest in very recent times in the properties of highly oxygenated species as combustion temperatures are lowered in order to improve efficiency and minimize emissions with multiple radical + O_2 reactions increasingly dominating the mechanistic landscape. This "low temperature" regime has begun to overlap with atmospheric temperatures [VABB18, WPCM17], increasing the commonality of interest. Astronomical measurements and mechanistic studies of the complex chemistry that may take place in star-forming regions have expanded in recent years [GWH08, KT14], highlighting the need to identify and quantify these data.

However, many of these oxygenates are highly reactive, have a transient existence, and thus are not readily amenable to experiment [IRK19]. In addition, the number of possible conformers and close-lying electronic states of some, as well as their multi-reference nature, renders theoretical calculations quite challenging.

There have been a number of attempts to create systematic archives of thermodynamic data for species, which are important to atmospheric, combustion, and wider communities. None of these can be considered as definitive or complete, but new initiatives are beginning to appear, which show considerable promise. As Amabilino and others have pointed out [ABBV19, LHGG19, GLG19, NRAC19, MP19, MKK19], the rise in machine learning technologies has increased the value of the underlying data in terms of their quality, bias, and size. It is to be hoped that the data herein presented offer an opportunity for such an exercise.

2. Methodology

A search of the SciFinder® database created a list of known species that conformed to the molecular formula $C_{1-2}H_{1-2}O_{1-x}$; this list was amplified in a non-systematic manner by unknown species thrown up during erratic optimizations and by obvious additions such as extending O–O chains. In some cases, non-systematic nomenclature has been used because previous authors have employed different naming conventions such as *cis/trans* or *syn/anti*—where possible, we have followed the original naming convention.

A preliminary investigation of possible ground state structures was undertaken, as required, by a conformational search using a molecular mechanics forcefield amplified on occasion by a density functional method with the application Spartan [S18]. Unless otherwise specified, the lowest energy conformer is featured.

A combination of the B3LYP functional and the cc-pVTZ+d basis set is used to optimize the geometry and determine the vibrational modes as implemented in Gaussian [FTSS16] with the keywords Opt=VTight and Int=SuperFine where feasible. The output of such calculations is therefore proscribed by the application so that the Cartesian coordinates are shown in angstroms, the rotational constants are the equilibrium values, and the wavenumbers ("frequencies") are reported in the non-SI units of cm^{-1}. The same level of theory is used for relaxed potential energy scans of dihedrals implicated in hindered internal rotations that are carried out over 360° in 10° steps and fitted to a Fourier series, both for the potential energy, $V(\chi)$, and for the rotational constant, $B(\chi)$,

$$V(\chi) = V_0 + \sum_{n=1}^{N} C_n \cos\left(n\sigma_V\{\chi + \varphi_V\}\right) + \sum_{n=1}^{N} S_n \sin\left(n\sigma_V\{\chi + \varphi_V\}\right),$$

$$B(\chi) = B_0 + \sum_{n=1}^{N} B_n \cos\left(n\sigma_B\{\chi + \varphi_B\}\right),$$

where χ is the dihedral angle in radians, σ_V is the symmetry number for the potential energy, and φ_V is a phase angle for the potential. A similar description applies to the equation relating the rotational constant as a function of dihedral angle. The reliability and accuracy of this density functional, B3LYP, has recently been tested and compared against CCSD(T)-level rotational profiles and shown to perform adequately [TBRL18]—specifically for one of the species, namely, glyoxal, in our dataset.

The wavenumbers are scaled by 0.989 in harmonic oscillator/rigid rotor treatments [CR15] but are unscaled when anharmonic frequencies are available. This approach has been validated by Jacobson *et al.* in their comprehensive study of anharmonic vibrational frequency calculations [JJ13]. On occasion, anharmonic analysis via second-order perturbation theory with an anharmonic reference wave function (VPT2) gives unreasonable predictions and a purely harmonic treatment is resorted to. Although such cases can be dealt with by a de-perturbation analysis [PBB15], the caveats outlined by Irikura [I14] apply. In some cases, simply replacing B3LYP/cc-pVTZ+d by MP2/cc-pVTZ may yield reasonable anharmonic corrections [KHR17].

In general, the methodology is suited to represent the complex multi-species and multi-conformer potential energy surface in a tractable way [ZM19]—more elaborate treatments involving coupled rotors, for example, such as Q2DTor [FCTF18], which show considerable promise, are eschewed here.

2.1. Thermodynamic parameters: $S°$, $C_p°$, and $H°(T) - H°(0)$

The THERMO module of the MultiWell Program Suite [BNSA18] is employed to compute thermodynamic parameters from the species data and is presented *here* at 1 bar and temperatures from 298.15 K to 2000 K. The input includes the enthalpy of formation of the species in question at 0 K, $\Delta_f H°(0\ K)$, the molecular formula (from which a natural molecular weight M_0 is derived), the external symmetry number (σ), the number of optical isomers, the degeneracy (g), and the number of electronic energy levels. If it is desired to include the excited electronic states, then their energy relative to the ground state and their degeneracy can be additionally specified. Finally, each of vibrational mode and rotation is listed together with the appropriate theoretical treatment to be used. In many cases, the vibrational modes are presented as "harmonic frequencies," $\bar{\upsilon}$, with their associated anharmonicities, namely, the diagonal elements, x_{ii}, of the anharmonic matrix. Finally, the input is completed by including terms for the treatment of external molecular rotations; the equilibrium moments of inertia generated by Gaussian (I_A, I_B, and I_C or their related rotational constants A, B, and C) were used to determine whether a symmetric top is appropriate, that is, are two rotational constants equal. If not, then the resulting asymmetric top was approximated as a quasi-symmetric top, where $B \approx C$ and neither are equal to A; in that case, a two-dimensional separable rotor $B_2 = (B \times C)^{1/2}$ and a 1D separable rotor A treatment were used.

Although it is convenient to enter a non-zero value for $\Delta_f H(0\ K)$, it plays no real part in the subsequent computation, which, however, does perform the essential calculation of the difference $|\Delta_f H°(0\ K) - \Delta_f H°(298.15\ K)|$. All of the input data files required to create the outputs presented *here* are archived in the supplementary material as well as references to the physical constants employed by THERMO.

There are numerous advantages to the THERMO code: principally, in the exploration of different scenarios such as replacing specific vibrations by a hindered rotor and harmonic frequencies by anharmonic ones and seeing directly the impact that this has both sequentially and in total. The identification of specific vibrational modes as potential hindered rotors in non-obvious cases was devolved to Gaussian, and corrections reported by that application were used sporadically as cross-checks. The two applications do not, as far as one can tell, employ the same methodology, and hence, if the resultant thermochemistry is to be used for chemical kinetic [VGP15] or equilibrium purposes, then one or the other should be chosen to benefit from cancellation of errors. A useful guide as to whether a specific mode is more appropriately classified as either a "free" rotor or a "hindered" rotor or, indeed, a pure vibration is provided by the ratio (V/RT) of the barrier V to a relaxed potential energy dihedral scan to the thermal energy RT. If the reduced barrier height $V/RT \ll 1$, then a free rotor is most appropriate (indicated by "qro" in the input file), whereas if $V/RT \gg 1$, then a vibrational mode is indicated ("vib"); for $V/RT \sim 1$, then a hindered rotor approach ("hra" or "hrb"or "hrc" or "hrd") should be considered.

The absence of comprehensive validated benchmarks for entropy ($S°$), specific heat ($C_p°$), and enthalpy function ($H°_T - H°_0$) makes it difficult to establish reliable uncertainties for the calculations presented *here*, which are based on the assumption that rigid rotors, anharmonic frequencies, and, as appropriate, one-dimensional hindered rotors are a sufficient treatment. Where high-level data exist, for example, for methanal, the agreement is excellent to within 99.8% or 0.37 J K^{-1} mol^{-1} for $S(298.15\ K)$. However, this entropy is dominated by translational and external rotational contributions that are rarely in dispute with the vibrational contribution amounting to only <0.2% of the total. By way of contrast for $C_2H_2O_8$, the vibrational contribution to the entropy rises to 29%, and now the determination of the precise nature of each vibrational mode requires much more careful consideration with a concomitant rise in the uncertainty. Note that in common with all quantum chemistry codes, Gaussian works on the assumption that the most abundant isotopes comprise the species in question, and therefore, "$C_2H_2O_8$" has a molecular mass

of 153.975 derived from $^{12}C_2^1H_2^{16}O_8$, which it uses in determining equilibrium moments of inertia and thence rotational constants. In contrast, THERMO employs standard atomic weights to determine the molecular mass from the molecular formula that (in this worst case scenario) would be 154.030—the difference is slight and further mitigated by the fact that the translational entropy (S_t) depends upon the molecular mass (m) as $S_t \propto \ln(\sqrt{m})$.

It is possible to estimate the uncertainty in the computed thermochemical properties by making a number of assumptions about the uncertainties in rovibrational parameters such as vibrational frequencies, hindered rotor potentials, and rotational constants. Thus, for example, Goldsmith and co-workers [GMG12] assumed upper and lower bounds of 10% on the frequencies, ±20% on potentials, and ±5% on rotational constants. As the authors acknowledge that such an exercise does not consider other issues, we do not consider *here* such a mode–mode coupling and other anharmonic behavior as such.

2.2. Enthalpy of formation $\Delta_f H(0\ \mathrm{K})$

The following two approaches have been used:

1. The first uses the composite methods W2X and W3X-L to calculate the atomization energy and hence the formation enthalpy. These protocols are detailed in the original work of Chan and Radom [CR15] but essentially consists of energy determinations (at a B3LYP/cc-pVTZ+d geometry) by combining conventional and explicitly correlated coupled-cluster calculations extrapolated to the complete basis set limit with aug′-ccpVnZ up to aug′-cc-pVQZ basis sets. Core–valence correlation and scalar relativistic calculations at the CCSD(T)/cc-pCVTZ level using non-relativistic frozen-core and all-electron Douglas–Kroll–Hess methods and an amalgam of MP2 and CCSD(T) energies. These computations, obtained with MOLPRO [WKKM18], summarizes the W2X method; additional post-CCSD(T) effects up to CCSDT(Q), which comprises the W3X-L approach, are obtained using multi-reference methods embodied in the MRCC code [KRCN13]. These methods are computationally quite demanding, and only a limited number of species could be so treated.
   A more recent composite method, WMS, which is claimed to perform comparably to W3X-L but at a significantly reduced computational cost, is tested here [ZXLH18]. The geometry and frequencies employed *here* for these calculations are the same as those used for W3X-L calculations, namely, B3LYP/cc-pVTZ+d. This differs from the CCSD(T)/cc-pV(Q+d)Z, QCISD/MG3, and CCSD(T)-F12a/T-F12 methodologies variously used by the developers [KRCN13].
2. The second uses multiple composite methods [MFOP00, OPM96, CRRRP98, CRR07, BPMF09] (CBS-QB3, CBS-APNO, G3, G4, and W1BD) to compute the average reaction enthalpy, $\Delta_r H(0\ \mathrm{K})$, of a carefully chosen isodesmic reaction, **X** + **A** = **B** + **C**, which, in conjunction with well-known formation enthalpies of the accompanying species or chaperones **A**, **B**, and **C**, leads to an averaged formation enthalpy of the target species, **X**,

$$\Delta_f H(\mathbf{X}) = \Delta_f H(\mathbf{B}) + \Delta_f H(\mathbf{C}) - \Delta_f H(\mathbf{A}) - \Delta_r H(0\,\mathrm{K}).$$

The uncertainty in the target formation enthalpy, u_X, is simply $u_X = \left(u_A^2 + u_B^2 + u_C^2 + u_r^2\right)^{1/2}$, where u_r is the standard deviation in the reaction enthalpy and u_i are the chaperone uncertainties.

If more than one isodesmic reaction can be framed, then inverse-variance weighting is used to derive the average and the uncertainty. If it is not possible to frame good isodesmic reactions, then a multi-composite atomization procedure can be used.

The advantages and disadvantages of these methodologies are discussed in recent publications [SBCH08, SS16, SS15], but, in essence, these computations are relatively inexpensive and use differing geometry optimization routines and varying corrections. To some extent, this multiple composite approach produces results that are less dependent upon any one particular procedure. The determination of the reaction enthalpy of an isodesmic reaction allows some degree of error cancellation, and the use of many different procedures provides a statistical measure of the uncertainties *appropriate to each reaction enthalpy* rather than a transferable uncertainty garnered elsewhere and based on a specific method. Naturally, the success of this method is entirely predicated on the existence of suitable companion species.

For atomization calculations, the atomic values and the uncertainties, u, used are (kJ mol^{-1}) as follows:

	H ($^2S_{½}$)	C (^3P)	O ($^3P_2$)
0 K	216.034	711.401	246.844
298.15 K	217.998	716.892	249.229
u	±0.000	±0.048	±0.0021

Formation enthalpies computed from multi-composite atomization calculations are of a more limited value and are only relied upon if suitable isodesmic reactions cannot be found. The multi-composite approach used here has been validated for closed [SS15] and open [SS15] shell species previously, and measures of dispersion established, which indicate that standard deviations of ±4.8 kJ mol^{-1} and ±4.0 kJ mol^{-1}, respectively, apply. However, there is a caveat [SS15], namely, that the "predictive power of the statistics depends on both the extent to which the electronic structure of the target molecules is well represented by the reference set and the accuracy of the reference set." Since it is unclear to what extent there is overlap between previous and current datasets, the measures of dispersion quoted above may be unduly optimistic.

2.3. Comparisons with literature

In the following, each species is discussed in detail and any comparisons that can be made with the existing literature data are made. Apart from a very few cases, there is a dearth of such information available even for neutral closed-shell species. The most useful general repositories of data include the Active Thermochemical Tables (ATcT) [RB16], the NIST-JANAF Thermochemical Tables [C63], the Third Millennium Ideal Gas Thermochemical Database [GBR18], the NIST WebBook [NIST69], the Comprehensive Handbook of Chemical Bond Energies [L07], and miscellaneous recent publications [I14, L07, NRAC19].

The most useful as regards formation enthalpies is the ATcT that tabulates values and uncertainties at both 0 and 298.15 K and crucially adds an audit trail to the final result produced by analyzing and solving a large network. However, a cautionary note must be struck, namely, "*the reduction in uncertainty possible when taking into account many inter-related experimental and theoretical determinations will produce a final result with a drastically reduced uncertainty, which is probably beyond the reach of even the highest-level theoretical computations available today.*" This observation [SS16] applies to species containing more than a trivial number of "heavy" atoms.

2.4. Units

Units of J mol^{-1} K^{-1} are used throughout the document for both the entropy, $S^{o}(T)$, and the constant pressure heat capacity, $C_{p}^{o}(T)$, while enthalpies of formation, $\Delta_{f}H^{o}(0\ \mathrm{K})$ and $\Delta_{f}H^{o}(298.15\ \mathrm{K})$, and the enthalpy function, $H^{o}(T) - H^{o}(0)$, are all expressed in kJ mol^{-1}. As regards the geometric and frequency data for the various species, these are in Angstroms (1 Å = 1 × 10^{-10} m) for the Cartesian coordinates, the rotational constant B is in GHz and related to the moment of inertia I through B GHz = 505.38/I amu Å^{2}. Wavenumbers or "frequencies," $\overline{\upsilon}$, as well as anharmonicity coefficients, x_{ii}, are in cm^{-1}.

References for methodology

T90 V. Trimble, "The origin and abundances of the chemical elements revisited," Astro. Astrophys. Rev. **3**(1), 1–46 (1991).

VABB18 L. Vereecken, B. Aumont, I. Barnes, J. W. Bozzelli, M. J. Goldman, W. H. Green, S. Madronich, M. R. Mcgillen, A. Mellouki, J. J. Orlando, B. Picquet-Varrault, A. R. Rickard, W. R. Stockwell, T. J. Wallington, and W. P. L. Carter, "Perspective on mechanism development and structure-activity relationships for gas-phase atmospheric chemistry," Int. J. Chem. Kinet. **50**(6), 435–469 (2018).

WPCM17 Z. Wang, D. M. Popolan-Vaida, B. Chen, K. Moshammer, S. Y. Mohamed, H. Wang, S. Sioud, M. A. Raji, K. Kohse-Höinghaus, N. Hansen, P. Dagaut, S. R. Leone, and S. M. Sarathy, "Unraveling the structure and chemical mechanisms of highly oxygenated intermediates in oxidation of organic compounds," Proc. Natl. Acad. Sci. U. S. A. **114**(50), 13102–13107 (2017).

GWH08 R. T. Garrod, S. L. W. Weaver, and E. Herbst, "Complex chemistry in star-forming regions: An expanded gas-grain warm-up chemical model," Astrophys. J. **682**(1), 283–302 (2008).

KT14 A. Karton and D. Talbi, "Pinning the most stable $H_xC_yO_z$ isomers in space by means of high-level theoretical procedures," Chem. Phys. **436-437**, 22–28 (2014).

IRK19 S. Iyer, M. P. Rissanen, and T. Kurtén, "Reaction between peroxy and alkoxy radicals can form stable Adducts," J. Phys. Chem. Lett. **10**(9), 2051–2057 (2019).

ABBV19 S. Amabilino, L. A. Bratholm, S. J. Bennie, A. C. Vaucher, M. Reiher, and D. R. Glowacki, "Training neural nets to learn reactive potential energy surfaces using interactive quantum chemistry in virtual reality," J. Phys. Chem. A **123**(20), 4486–4499 (2019).

LHGG19 Y.-P. Li, K. Han, C. A. Grambow, and W. H. Green, "Self-evolving machine: A continuously improving model for molecular thermochemistry," J. Phys. Chem. A **123**, 2142–2152 (2019).

GLG19 C. A. Grambow, Y.-P. Li, and W. H. Green, "Accurate thermochemistry with small datasets: A bond additivity correction and transfer learning approach," J. Phys. Chem. A **123**(27), 5826–5835 (2019).

NRAC19 B. Narayanan, P. C. Redfern, R. S. Assary, and L. A. Curtiss, "Accurate quantum chemical energies for 133 000 organic molecules," Chem. Sci. **10**, 7449–7455 (2019).

MP19 P. Morgante and R. Peverati, "Statistically representative databases for density functional theory *via* data science," Phys. Chem. Chem. Phys. **21**, 19092–19103 (2019).

MKK19 A. Menon, N. B. Krdzavac, and M. Kraft, "From database to knowledge graph—Using data in chemistry," Curr. Opin. Chem. Eng. **26**, 33 (2019).

S18 Spartan'18, version 1.4.0, Wavefunction, Inc., Irvine, CA, USA.

FTSS16 M. J. Frisch, G. W. Trucks, H. B. Schlegel, G. E. Scuseria, M. A. Robb, J. R. Cheeseman, G. Scalmani, V. Barone, G. A. Petersson, H. Nakatsuji, X. Li, M. Caricato, A. V. Marenich, J. Bloino, B. G. Janesko, R. Gomperts,B. Mennucci, H. P. Hratchian, J. V. Ortiz, A. F. Izmaylov, J. L. Sonnenberg, D. Williams-Young, F. Ding, F. Lipparini, F. Egidi, J. Goings, B. Peng, A. Petrone, T. Henderson, D. Ranasinghe, V. G. Zakrzewski, J. Gao, N. Rega, G. Zheng, W. Liang, M. Hada, M. Ehara, K. Toyota, R. Fukuda, J. Hasegawa, M. Ishida, T. Nakajima, Y. Honda, O. Kitao, H. Nakai, T. Vreven, K. Throssell, J. A. Montgomery, Jr., J. E. Peralta, F. Ogliaro, M. J. Bearpark, ; J. J. Heyd, E. N. Brothers, K. N. Kudin, V. N. Staroverov, T. A. Keith, R. Kobayashi, J. Normand, K. Raghavachari, A. P. Rendell, J. C. Burant, S. S. Iyengar, J. Tomasi, M. Cossi, J. M. Millam, M. Klene, C. Adamo, R. Cammi, J. W. Ochterski, R. L. Martin, K. Morokuma, O. Farkas, J. B. Foresman, and D. J. Fox, Gaussian 16, Revision A.03, Gaussian, Inc., Wallingford, CT, 2016.

TBRL18 D. N. Tahchieva, D. Bakowies, R. Ramakrishnan, and O. A. von Lilienfeld, "Torsional potentials of glyoxal, oxalyl halides, and their thiocarbonyl derivatives: Challenges for popular density functional approximations," J. Chem. Theory Comput. **14**(9), 4806–4817 (2018).

CR15 B. Chan and L. Radom, "W2X and W3X-L: Cost-effective approximations to W2 and W4 with kJ mol^{-1} accuracy," J. Chem. Theory Comput. **11**(5), 2109–2119 (2015).

JJ13 R. L. Jacobsen, R. D. Johnson, K. K. Irikura, and R. N. Kacker, "Anharmonic vibrational frequency calculations are not worthwhile for small basis sets," J. Chem. Theor. Comput. **9**, 951–954 (2013).

PBB15 M. Piccardo, J. Bloino, and V. Barone, "Generalized vibrational perturbation theory for rotovibrational energies of linear, symmetric and asymmetric tops: Theory, approximations, and automated approaches to deal with medium-to-large molecular systems," Int. J. Quantum Chem. **115**(15), 948–982 (2015).

I14 K. K. Irikura, "Anharmonic partition functions for polyatomic thermochemistry," J. Chem. Thermodyn. **73**, 183–189 (2014).

KHR17 S. J. Klippenstein, L. B. Harding, and B. Ruscic, "*Ab initio* computations and active thermochemical tables hand in hand: Heats of formation of core combustion species," J. Phys. Chem. A **121**(35), 6580–6602 (2017).

ZM19 J. Zádor and J. A. Miller, "Comment on influence of multiple conformations and paths on rate constants and product branching ratios. Thermal decomposition of 1-propanol radicals," J. Phys. Chem. A **123**(5), 1129–1130 (2019).

FCCTF18 D. Ferro-Costas, M. N. D. S. Cordeiro, D. G. Truhlar, and A. Fernández-Ramos, "Q2DTor: A program to treat torsional anharmonicity through coupled pair torsions in flexible molecules," Comput. Phys. Commun. **232**, 190–205 (2018).

RNSA18 J. R. Barker, T. L. Nguyen, J. F. Stanton, C. Aieta, M. Ceotto, F. Gabas, T. J. D. Kumar, C. G. L. Li, L. L. Lohr, A. Maranzana, N. F. Ortiz, J. M. Preses, J. M. Simmie, J. A. Sonk, and P. J. Stimac, MultiWell-2017 Software Suite, J. R. Barker, University of Michigan, Ann Arbor, MI, USA, http://clasp-research.engin.umich.edu/multiwell/, 2018.

VGP15 L. Vereecken, D. R. Glowacki, and M. J. Pilling, "Theoretical chemical kinetics in tropospheric chemistry: Methodologies and applications," Chem. Rev. **115**(10), 4063–4114 (2015).

GMG12 C. F. Goldsmith, G. R. Magoon, and W. H. Green, "Database of small molecule thermochemistry for combustion," J. Phys. Chem. A **116**(36), 9033–9057 (2012).

WKKM18 written by H.-J. Werner, P. J. Knowles, G. Knizia, F. R.Manby, M. Schütz, P. Celani, W. Györffy, D. Kats, T. Korona, R. Lindh, A. Mitrushenkov, G. Rauhut, K. R. Shamasundar, T. B. Adler, R. D. Amos, S. J. Bennie, A. Bernhardsson, A. Berning, D. L. Cooper, M. J. O. Deegan, A. J. Dobbyn, F. Eckert, E. Goll, C. Hampel, A. Hesselmann, G. Hetzer, T. Hrenar, G. Jansen, C. Köppl, S. J. R. Lee, Y. Liu, A. W. Lloyd, Q. Ma, R. A. Mata, A. J. May, S. J. McNicholas, W. Meyer, T. F. Miller III, M. E. Mura, A. Nicklaß, D. P. O'Neill, P. Palmieri, D. Peng, K. Pflüger, R. Pitzer, M. Reiher, T. Shiozaki, H. Stoll, A. J. Stone, R. Tarroni, T. Thorsteinsson, M. Wang, and M. Welborn, MOLPRO, version 2018.1, a package of *ab initio* programs, http://www.molpro.net.

KRCN13 MRCC, a quantum chemical program suite written by M. Kállay, Z. Rolik, J. Csontos, P. Nagy, G. Samu, D. Mester, J. Csóka, I. Ladjánszki, L. Szegedy, B. Ladóczki, K. Petrov, M. Farkas, and B. Hégely, see also Z. Rolik, L. Szegedy, I. Ladjánszki, B. Ladóczki, and M. Kállay, J. Chem. Phys. **139**, 094105 (2013), see htpp://www.mrcc.hu

ZXLH18 Y. Zhao, L. Xia, X. Liao, Q. He, M. X. Zhao, and D. G. Truhlar, "Extrapolation of high-order correlation energies: The WMS model," Phys. Chem. Chem. Phys. **20**(43), 27375–27384 (2018).

MFOP00 J. A. Montgomery, M. J. Frisch, J. W. Ochterski, and G. A. Petersson, "A complete basis set model chemistry. VII. Use of the minimum population localization method," J. Chem. Phys. **112**(15), 6532–6542 (2000).

OPM96 J. W. Ochterski, G. A. Petersson, and J. A. Montgomery, "A complete basis set model chemistry. V. Extensions to six or more heavy atoms," J. Chem. Phys. **104**(7), 2598–2619 (1996).

CRRRP98 L. A. Curtiss, K. Raghavachari, P. C. Redfern, V. Rassolov, and J. A. Pople, "Gaussian-3 (G3) theory for molecules containing first and second-row atoms," J. Chem. Phys. **109**(18), 7764–7776 (1998).

CRR07 L. A. Curtiss, P. C. Redfern, and K. Raghavachari, "Gaussian-4 theory using reduced order perturbation theory," J. Chem. Phys. **127**(12), 124105 (2007).

BPMF09 E. C. Barnes, G. A. Petersson, J. A. Montgomery, M. J. Frisch, and J. M. L. Martin, "Unrestricted coupled cluster and Brueckner doubles variations of W1 theory," J. Chem. Theory Comput. **5**(10), 2687–2693 (2009).

SBCH08 J. M. Simmie, G. Black, H. J. Curran, and J. P. Hinde, "Enthalpies of formation and bond dissociation energies of lower alkyl hydroperoxides and related hydroperoxy and alkoxy radicals," J. Phys. Chem. A **112**(22), 5010–5016 (2008).

SS16 J. M. Simmie and J. N. Sheahan, "Validation of a database of formation enthalpies and of mid-level model chemistries," J. Phys. Chem. A **120**(37), 7370–7384 (2016).

SS15 K. P. Somers and J. M. Simmie, "Benchmarking compound methods (CBS-QB3, CBS-APNO, G3, G4, W1BD) against the active thermochemical tables: Formation enthalpies of radicals," J. Phys. Chem. A **119**(33), 8922–8933 (2015).

SS15 J. M. Simmie and K. P. Somers, "Benchmarking compound methods (CBS-QB3, CBS-APNO, G3, G4, W1BD) against the active thermochemical tables: A litmus test for cost-effective molecular formation enthalpies," J. Phys. Chem. A **119**(28), 7235–7246 (2015).

RB16 B. Ruscic and D. H. Bross, Active Thermochemical Tables (ATcT) values based on ver. 1.122 of the Thermochemical Network, 2016, available at https://ATcT.anl.gov.

C63 *NIST-JANAF Thermochemical Tables*, 4th ed., Journal of Physical and Chemical Reference Data, Monograph Vol. 9, edited by M. W. Chase, Jr. (U.S. Department of Commerce, Gaithersburg, MD, 1963).

GBR18 E. Goos, A. Burcat, and B. Ruscic, "Extended third Millennium ideal gas and condensed phase thermochemical database for combustion with updates from active thermochemical tables," Mirrored at http://garfield.chem.elte.hu/Burcat/burcat.html; 12 January 2018.

NIST69 NIST Chemistry WebBook, Standard Reference Database No. 69, https://doi.org/10.18434/T4D303.

L07 Y.-R. Luo, *Comprehensive Handbook of Chemical Bond Energies* (CRC Press, Boca Raton, USA, 2007).

NRAC19 B. Narayanan, P. C. Redfern, R. S. Assary, and L. A. Curtiss, "Accurate quantum chemical energies for 133 000 organic molecules," Chem. Sci. **10**, 7449 (2019).

PHG84 J.-Y. Park, M. C. Heaven, and D. Gutman, "Kinetics and mechanism of the reaction of vinyl radicals with molecular-oxygen," Chem. Phys. Lett. **104**, 469–474 (1984).

3. Thermochemical Data

3.1. $C_1H_1O_1$

3.1.1. Formyl; oxomethyl

$^2A'$ g = 2 C_S σ = 1 M_0 = 29.0180

The formyl radical, H–Ċ=O, is a key intermediate species in the combustion of hydrocarbon fuels, confirmed experimentally by the use of various techniques including laser photolysis/photoionization mass spectrometry [PHG84, SPHG84] and time-resolved Fourier transform infrared emission spectroscopy [WWHK01]. Formyl has long been known to exist in the interstellar medium and is probably formed by hydrogenation of abundant CO on dust grains [BF16].

3.1.1.1 Species data.

8	0.061 930	−0.589 615	0.000 000
6	0.061 930	0.583 359	0.000 000
1	−0.867 014	1.216 771	0.000 000
B (GHz)	716.057	45.042 4	42.376 8

No.	$\bar{\nu}$ (cm^{-1})	x_{ii}
1	2637.24	−113.89
2	1936.04	−11.57
3	1108.05	−9.29

3.1.1.2. Formation enthalpy, $\Delta_f H$(0 K). The most accurate experimental determination is that of Terentis and Kable [TK96] who measured the dissociation energy of the reaction $H_2CO \rightarrow HC^{\bullet}O + H^{\bullet}$ in a supersonic free jet as 30 328.5 ± 0.5 cm^{-1}; using the latest values of constants and formation enthalpies for the H-atom and formaldehyde, this equates to a formyl 0 K formation enthalpy of $\Delta_f H^o$(0 K) = 41.4 ± 0.5 kJ mol^{-1} (41.8 kJ mol^{-1} at 298.15 K). An earlier [CFM87] dissociation energy of 30 250 ± 60 cm^{-1} was obtained by Chuang *et al.* by measuring the appearance of $H^{\bullet}$ by vacuum ultraviolet laser-induced fluorescence in the photo-fragmentation of formaldehyde; this translates to $\Delta_f H^o$(0 K) = 40.5 ± 0.8 kJ mol^{-1} (40.9 kJ mol^{-1} at 298.15 K).

Becerra *et al.* measured the kinetics of the reaction $HC^{\bullet}O$ + HI/HBr → $CH_2O + I^{\bullet}/Br^{\bullet}$ over a range of temperatures from 293 K to 540 K and used third law methods to deduce $\Delta_f H^o$(298.15 K) = 44.29 ± 0.43 kJ mol^{-1}; of necessity, there is quite a complex chain of reasoning between the experimental data and the final outcome—this may account for the difference [BCW97].

Among the theoretical determinations, the most careful and reliable is that due to Feller *et al.* who estimated [FPD08] a total atomization energy of 1132.44 ± 1.3 kJ mol^{-1}, which translates to $\Delta_f H^o$(0 K) = 41.8 ± 1.3 kJ mol^{-1}. An identical atomization energy was later found by Karton *et al.* using their W4.2 protocol [KSM17]. Marenich and Boggs [MB03] reported values of $\Delta_f H^o$(0 K) = 41.9 kJ mol^{-1} (42.3 kJ mol^{-1} at 298.15 K) from CCSD(T)/CBS calculations. The recent high-level Argonne National Laboratory schemes [KHB17] ANL0 and ANL1 predict $\Delta_f H^o$(0 K) = 40.8 kJ mol^{-1}.

Hence, a case can be made for recommending $\Delta_f H^o$(0 K) = 41.4 kJ mol^{-1} (41.8 kJ mol^{-1} at 298.15 K) based entirely on the experiments and theoretical calculations considered above, to which a modest uncertainty of ±0.8 kJ mol^{-1} can be ascribed.

Note that the latest v1.122d ATcT recommendation of $\Delta_f H^o$(0 K) = 41.805 ± 0.098 kJ mol^{-1} depends upon a large number of inter-

related values (148 contributions account for 90% of the provenance) but does not include recent high-level results. As discussed above, it is doubtful that any single theoretical method with near universal applicability can approach that level of uncertainty.

Here, a W3X-L calculation yields $\Delta_f H^o(0\ K) = 40.4\ kJ\ mol^{-1}$ ($40.8\ kJ\ mol^{-1}$ at 298.15 K)—the good agreement obtained helps us to validate the methodology employed in W3X-L. Note also that the W2X method, which does not include post-CCSD(T) terms up to CCSDT(Q), returns 41.1 kJ mol^{-1} (41.4 kJ mol^{-1} at 298.15 K).

3.1.1.3. Results. Our calculated values of entropy and heat capacity are in excellent agreement with the literature values: Goos *et al.* [GBR18] reported $S^o = 224.28\ J\ mol^{-1}\ K^{-1}$ and $C_p^o = 34.68\ J\ mol^{-1}\ K^{-1}$, while Goldsmith *et al.* [GMG12] reported $S^o = 223.84\ J\ mol^{-1}\ K^{-1}$ and $C_p^o(300\ K) = 34.72\ J\ mol^{-1}\ K^{-1}$. Literature [MB03] values obtained by direct summation of the rovibrational energy levels yielded S^o = 224.3 J mol^{-1} K^{-1}, C_p^o = 34.6 J mol^{-1} K^{-1}, and $H^o(T) - H^o(0)$ = 10.001 kJ mol^{-1}, which are in excellent agreement with our computed results not just near 300 K but also at 2000 K, for example, $S^o = 310.6\ J\ mol^{-1}\ K^{-1}$ (309.6 J mol^{-1} K^{-1}), $C_p^o = 58.1\ J\ mol^{-1}\ K^{-1}$ (56.43 J mol^{-1} K^{-1}), and $H^o(T) - H^o(0) = 93.667\ kJ\ mol^{-1}$ (92.36 kJ mol^{-1}). Earlier results by Gurvich and co-workers [GVA89] are in substantial agreement at 298.15 K, viz., $S^o = 224.339\ J\ mol^{-1}\ K^{-1}$, C_p^o = 34.586 J mol^{-1} K^{-1}, and $H^o(T) - H^o(0) = 9.989\ kJ\ mol^{-1}$.

T (K)	$S^o(T)$	$C_p^o(T)$	$H^o(T) - H^o(0)$
298.15	224.33	34.55	9.98
300.	224.54	34.58	10.04
400.	234.73	36.42	13.59
500.	243.09	38.60	17.34
600.	250.33	40.85	21.31
700.	256.79	43.01	25.50
800.	262.66	44.99	29.91
900.	268.06	46.74	34.49
1000.	273.07	48.28	39.25
1100.	277.74	49.62	44.14
1200.	282.11	50.79	49.16
1300.	286.21	51.81	54.29
1400.	290.08	52.70	59.52
1500.	293.75	53.49	64.83
1600.	297.22	54.19	70.21
1800.	303.68	55.41	81.18
2000.	309.57	56.43	92.36

References for formyl; oxomethyl.

PHG84 J.-Y. Park, M. C. Heaven, and D. Gutman, "Kinetics and mechanism of the reaction of vinyl radicals with molecular-oxygen," Chem. Phys. Lett. **104**, 469–474 (1984).

SPHG84 I. R. Slagle, J. Y. Park, M. C. Heaven, and D. Gutman, "Kinetics of polyatomic free-radicals produced by laser photolysis. III. Reaction of vinyl radicals with molecular-oxygen," J. Am. Chem. Soc. **106**, 4356–4361 (1984).

WWHK01 H. Wang, B. Wang, Y. He, and F. Kong, "The gaseous reaction of vinyl radical with oxygen," J. Chem. Phys. **115**, 1742–1746 (2001).

BF16 A. Bacmann and A. Faure, "The origin of gas-phase HCO and CH_3O radicals in prestellar cores," Astro. Astrophys. **587**, A130 (2016).

TK96 A. C. Terentis and S. H. Kable, "Near threshold dynamics and dissociation energy of the reaction $H_2CO \rightarrow HC_2O + H$," Chem. Phys. Lett. **258**, 626–632 (1996).

CFM87 M. C. Chuang, M. F. Foltz, and C. B. Moore, "T_1 barrier height, S_1-T_1 intersystem crossing rate, and S_0 radical dissociation threshold for H_2CO, D_2CO and HDCO," J. Chem. Phys. **87**, 3855–3864 (1987).

BCW97 R. Becerra, I. W. Carpenter, and R. Walsh, "Time-resolved studies of the kinetics of the reactions of CHO with HI and HBr: Thermochemistry of the CHO radical and the C-H bond strengths in CH_2O and CHO," J. Phys. Chem. A **101**(23), 4185–4190 (1997).

FPD08 D. Feller, K. A. Peterson, and D. A. Dixon, "A survey of factors contributing to accurate theoretical predictions of atomization energies and molecular structures," J. Chem. Phys. **129**, 204105 (2008).

KSM17 A. Karton, N. Sylvetsky, and J. M. L. Martin, "W4-17: A diverse and high-confidence dataset of atomization energies for benchmarking high-level electronic structure methods," J. Comput. Chem. **38**, 2063–2075 (2017).

MB03 A. V. Marenich and J. E. Boggs, "Coupled cluster CCSD(T) calculation of equilibrium geometries, anharmonic force fields and thermodynamic properties of the formyl (HCO) and isoformyl (COH) radical species," J. Phys. Chem. A **107**, 2343–2350 (2003).

KHR17 S. J. Klippenstein, L. B. Harding, and B. Ruscic, "*Ab initio* computations and active thermochemical tables hand in hand: Heats of formation of core combustion species," J. Phys. Chem. A **121**, 6580–6602 (2017).

GBR18 E. Goos, A. Burcat and B. Ruscic Extended third Millennium ideal gas and condensed phase thermochemical database for combustion with updates from active thermochemical tables. Mirrored at http://garfield.chem.elte.hu/Burcat/burcat.html; 12 January 2018.

GMG12 C. F. Goldsmith, G. R. Magoon, and W. H. Green, "Database of small molecule thermochemistry for combustion," J. Phys. Chem. A **116**, 9033–9057 (2012).

GVA89 L. V. Gurvich, I. V. Veyts, and C. B. Alcock, *Thermodynamic Properties of Individual Substances: Elements and Compounds* (Hemisphere, New York, 1989), Vol. 2.

3.1.2. Isoformyl; hydroxymethylidyne

$^2A'$ g = 2 C_S σ = 1 M_0 = 29.0180

Isoformyl, H–O=C$^\bullet$, is the less stable isomer of formyl predicted in an early study to lie ~170 kJ mol^{-1} above formyl [D80]. While the thioformyl radical HSC has been found in interstellar space, its oxygen analog HOC$^\bullet$ has so far not [AMCT18], even though HC$^\bullet$O is abundant.

3.1.2.1. Species data.

8	0.059 775	−0.480 442	0.000 000
6	0.059775	0.789 502	0.000 000
1	−0.836 851	−0.893 480	0.000 000
B (GHz)	701.942 7	42.075 7	39.696 2

No.	$\bar{\upsilon}$ (cm^{-1})	x_{ii}
1	3263.24	−242.22
2	1388.55	−13.57
3	1133.10	−11.53

3.1.2.2. Formation enthalpy, $\Delta_f H(0\ K)$. A W3X-L value of $\Delta_f H^o(0\ K) = 216.4\ kJ\ mol^{-1}$ (216.8 kJ mol^{-1} at 298.15 K) has been noted by Simmie and Sheahan [SS16]. Marenich and Boggs [MB03] obtained 217.8 kJ mol^{-1} (218.1 kJ mol^{-1}) from atomization calculations at CCSD(T)/CBS. ANL0 and ANL1 results [KHR17] show ATcT differences of 0.4 kJ mol^{-1} and 0.6 kJ mol^{-1}, which can be interpreted to indicate $\Delta_f H^o(0\ K) = 217.8\ kJ\ mol^{-1}$.

ATcT v1.122d values [RB16] of 217.29 ± 0.69 kJ mol^{-1} (217.67 kJ mol^{-1} at 298.15 K) rely heavily on the computed enthalpy of the isomerization reaction of HC$^{\bullet}$O ↔ C$^{\bullet}$OH by Marenich and Boggs; It is probable that when post-2015 data are incorporated, there will be some revision.

3.1.2.3. Results. Our computed values, shown in brackets, are in excellent agreement with those calculated by the direct summation of rovibrational energy levels by Marenich and Boggs [MB03] at 298.15 K of $S^o = 225.0\ J\ mol^{-1}\ K^{-1}$ (225.03 J mol^{-1} K^{-1}), $C_p^o = 35.0\ J\ mol^{-1}\ K^{-1}$ (34.90 J mol^{-1} K^{-1}), and $H^o(T) - H^o(0) = 10.008\ kJ\ mol^{-1}$ (10.00 kJ mol^{-1}) and at 2000 K of $S^o = 311.8\ J\ mol^{-1}\ K^{-1}$ (312.11 J mol^{-1} K^{-1}), $C_p^o = 57.9\ J\ mol^{-1}\ K^{-1}$ (57.57 J mol^{-1} K^{-1}), and $H^o(T) - H^o(0) = 93.707\ kJ\ mol^{-1}$ (93.98 kJ mol^{-1}), respectively.

T (K)	$S^o(T)$	$C_p^o(T)$	$H^o(T) - H^o(0)$
298.15	225.03	34.90	10.00
300.	225.24	34.94	10.06
400.	235.61	37.36	13.67
500.	244.23	39.91	17.53
600.	251.71	42.24	21.64
700.	258.38	44.30	25.97
800.	264.42	46.11	30.49
900.	269.94	47.70	35.19
1000.	275.04	49.10	40.03
1100.	279.78	50.36	45.00
1200.	284.21	51.48	50.09
1300.	288.37	52.49	55.29
1400.	292.30	53.42	60.59
1500.	296.01	54.26	65.97
1600.	299.54	55.04	71.44
1800.	306.10	56.41	82.58
2000.	312.11	57.57	93.98

References for isoformyl; hydroxymethylidyne.

D80 T. H. Dunning, "Theoretical characterization of the potential energy surface of the ground state of the HCO system," J. Chem. Phys. **73**, 2304–2309 (1980).

AMCT18 M. Agundez, N. Marcelino, J. Cernicharo, and M. Tafalla, "Detection of interstellar HCS and its metastable isomer HSC: New pieces in the puzzle of sulfur chemistry," Astron. Astrophys. **611**, L1 (2018).

SS16 J. M. Simmie and J. N. Sheahan, "Validation of a database of formation enthalpies and of mid-level model chemistries," J. Phys. Chem. A **120**, 7370–7384 (2016).

MB03 A. V. Marenich and J. E. Boggs, "Coupled cluster CCSD(T) calculation of equilibrium geometries, anharmonic force fields and thermodynamic properties of the formyl (HCO) and isoformyl (COH) radical species," J. Phys. Chem. A **107**, 2343–2350 (2003).

KHR17 S. J. Klippenstein, L. B. Harding, and B. Ruscic, "*Ab initio* computations and active thermochemical tables hand in hand: Heats of formation of core combustion species," J. Phys. Chem. A **121**, 6580–6602 (2017).

RB16 B. Ruscic and D. H. Bross, Active Thermochemical Tables (ATcT) values based on ver. 1.122 of the Thermochemical Network, 2016, available at https://ATcT.anl.gov.

3.2. $C_1H_1O_2$

3.2.1. Dioxiranyl

$^2A_1$ g = 2 C_S σ = 1 M_0 = 45.0177

This species has cropped up in a theoretical study of the CH ($^2\Pi$) + O_2 ($^3\Sigma_g^-$) reaction [HCW02].

3.2.1.1. Species data.

6	−0.035 985	0.744 750	0.000 000
1	0.791 667	1.461 201	0.000 000
8	−0.035 985	−0.370 606	0.767 379
8	−0.035 985	−0.370 606	−0.767 379
B (GHz)	36.542 6	26.064 3	15.736 1

No.	$\bar{\nu}$ (cm^{-1})	x_{ii}	
1	3012.72	−75.01	a'
2	1410.77	−4.99	a'
3	1071.12	−14.25	a'
4	792.51	−3.67	a'
5	1086.24	−6.31	a''
6	860.23	2.54	a''

3.2.1.2. Formation enthalpy, $\Delta_f H^o(0\ K)$. The isodesmic reaction

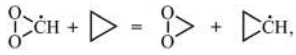

which employs the reference [RB16] chaperones, cyclopropane (70.77 ± 0.47 kJ mol^{-1}), dioxirane (9.45 ± 0.55 kJ mol^{-1}), and cyclopropyl (302.7 ± 1.6 kJ mol^{-1}), has a reaction enthalpy of 25.52 ± 1.96 kJ mol^{-1} from which $\Delta_f H^o(0\ K) = 215.9 \pm 2.6\ kJ\ mol^{-1}$ can be gleaned.

This is in excellent agreement with our W3X-L atomization values at 0 K of $\Delta_f H^o(0\ K) = 215.9\ kJ\ mol^{-1}$ (212.4 kJ mol^{-1} at 298.15 K). These are in very good agreement with the ATcT values of $\Delta_f H^o(0\ K) = 216.2 \pm 2.4\ kJ\ mol^{-1}$ that are based on lower levels of theory primarily.

3.2.1.3. Results. A standard rigid-rotor anharmonic oscillator treatment is employed here, neglecting ring-puckering.

T (K)	$S^o(T)$	$C_p^o(T)$	$H^o(T) - H^o(0)$
298.15	250.57	41.49	10.47
300.	250.83	41.63	10.54
400.	263.79	48.69	15.06
500.	275.32	54.69	20.24
600.	285.73	59.44	25.96
700.	295.19	63.19	32.10
800.	303.83	66.20	38.57
900.	311.77	68.66	45.32
1000.	319.11	70.70	52.29
1100.	325.93	72.41	59.44
1200.	332.30	73.86	66.76
1300.	338.26	75.11	74.21
1400.	343.87	76.18	81.77
1500.	349.16	77.12	89.44
1600.	354.16	77.95	97.19
1800.	363.42	79.34	112.92
2000.	371.84	80.48	128.91

References for dioxiranyl.

HCW02 M.-B. Huang, B.-Z. Chen, and Z.-X. Wang, "Theoretical study of CH + O_2 reactions," J. Phys. Chem. A **106**(22), 5490–5497 (2002).

RB16 B. Ruscic and D. H. Bross, Active Thermochemical Tables (ATcT) values based on ver. 1.122 of the Thermochemical Network, 2016, available at https://ATcT.anl.gov.

3.2.2. *Dioxymethylene* anti/syn

$^2A'$ g = 2 C_S σ = 1 M_0 = 45.0177

	anti				*syn*		
8	−1.128 527	−0.427 730	0.000 000	8	−1.109 858	−0.528 134	0.000 000
8	0.000 000	0.296 691	0.000 000	8	0.000 000	0.386 898	0.000 000
6	1.198 796	0.021 909	0.000 000	6	1.188 887	0.296 369	0.000 000
1	1.834 380	0.916 853	0.000 000	1	1.745 547	−0.648 326	0.000 000
B (GHz)	186.492	11.645 5	10.961 0	B (GHz)	127.711	11.476 7	10.530 4

No.	$\bar{\upsilon}$ (cm^{-1})	x_{ii}		No.	$\bar{\upsilon}$ (cm^{-1})	x_{ii}	
1	3006.47	−71.18	a'	1	3004.13	−79.54	a'
2	1497.96	−18.40	a'	2	1744.80	−15.81	a'
3	1050.42	−7.86	a'	3	870.33	−0.41	a'
4	781.69	−11.20	a'	4	429.24	−188.41	a'
5	522.59	−99.44	a'	5	422.31	−76.63	a'
6	556.30	2.23	a''	6	528.08	5.79	a''

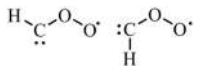

This species is an intermediate discovered during a theoretical study of the reaction between carbonyl oxide and hydroxyl radical [MA06] leading ultimately to the formation of formaldehyde and hydroperoxyl radical, $H_2COO + OH \rightarrow H_2C = O + HO_2$. Formation of the *syn* conformer is endothermic by +6.0 kJ mol^{-1}, whereas the channel to the *anti* is exothermic by −27.3 kJ mol^{-1}. In a theoretical DFT study of the CH + O_2 reaction, Huang and co-workers [HCW02] identified three σ states of the *anti* formyloxy radical, namely, $^2A_1$, $^2B_2$, and $^2A'$, with the latter being a first order saddle point although these classifications are quite dependent on the basis set used. We find in common with Mansergas and Anglada [MA06] that the $^2A'$ state with an OOC angle of ~134° is the ground state.

3.2.2.1. Species data.

3.2.2.2. Formation enthalpy, $\Delta_f H(0\ K)$. The presence of considerable multi-reference character (a T_1 diagnostic of 0.068) makes it difficult to establish reliable formation enthalpies or indeed relative energies. Thus, at CCSD(T)/aug-cc-pVTZ//QCISD/6-311+G(d,p), the *syn* is more stable, whereas at CASPT2(17,14)/6-311+G(2df,2p)//CASSCF(11,10)/6-311+G(2df,2p), this conclusion is completely reversed with the *anti* some 7.1 kJ mol^{-1} more stable than the *syn* [MA06].

G3B3, G4, W1BD, and W1RO methods indicate that the *anti* conformer is more stable by 8.6 kJ mol^{-1}, 7.9 kJ mol^{-1}, 7.8 kJ mol^{-1}, and 10.2 kJ mol^{-1}, respectively, a conclusion reinforced by W2X and W3X-L calculations. The highest level W3X-L has the *anti* at $\Delta_f H^o(0\ K) = 349.2$ kJ mol^{-1} (347.0 kJ mol^{-1} at 298.15 K) and the *syn* at $\Delta_f H^o(0\ K) = 358.1$ kJ mol^{-1} (355.8 kJ mol^{-1} at 298.15 K). WMS similarly puts the $|syn - anti|$ difference at +13.5 kJ mol^{-1}.

There is considerable disagreement with ATcT values, which have values for the *trans* or *anti* of $\Delta_f H^o(0\ K) = 364.0 \pm 2.7$ kJ mol^{-1} and for the *cis* or *syn* of 341.1 ± 3.4 kJ mol^{-1} and with previous work [SS15]. An audit trail of the reference ATcT data show that the bulk of the provenance in the values is derived from single reference composite methods, and additionally, the *trans* conformer illustrated is not the ground state.

3.2.2.3. Results. The relaxed potential energy scans are unfeasible; a hindered rotor analysis from Gaussian suggests that any correction is slight, $S_{hin}-S_{har} = 1.7$ J K^{-1} mol^{-1} for the *syn*, and less than half of that for the *anti*-conformer. Literature [MA06] values of 251.8–254.3 J K^{-1} mol^{-1} for the *anti* and those of 256.4–258.1 J K^{-1} mol^{-1} for the *syn* are close to those reported *here*.

References for dioxymethylene *anti/syn*.

MA06 A. Mansergas and J. M. Anglada, "Reaction mechanism between carbonyl oxide and hydroxyl radical: A theoretical study," J. Phys. Chem. A **110**(11), 4001–4011 (2006).

HCW02 M.-B. Huang, B.-Z. Chen, and Z.-X. Wang, "Theoretical study of CH + O_2 reactions," J. Phys. Chem. A **106**(22), 5490–5497 (2002).

SS15 K. P. Somers and J. M. Simmie, "Benchmarking compound methods (CBS-QB3, CBS-apno, G3, G4, W1BD) against the active thermochemical tables: Formation enthalpies of radicals," J. Phys. Chem. A **119**(33), 8922–8933 (2015).

3.2.3. Formyloxy; formyloxidanyl

$^2A_1$ g = 2 σ = 2 C_{2v} $M_0 = 45.0177$

$^2B_2$ g = 2 σ = 2 C_{2v} $M_0 = 45.0177$

This radical was first observed experimentally by Kim *et al.* in negative ion photoelectron spectroscopic experiments [KBAM95]. Döntgen and Leonhard [DL16] found that formyloxy is an intermediate in the reactions of chemically activated formic acid formed via the radical recombination reaction HC$^{\bullet}$O + $^{\bullet}$OH. While there has been much debate about the electronic ground state of formyloxy, it now appears from both experimental and theoretical work that the $^2A_1$ state is the global minimum structure with the $^2B_2$ state, also C_{2v}, some 3.8 ± 0.1 kJ mol^{-1} higher [OKKL14, GKSZ10]. Structurally, the principal difference between them is the O–C–O angle, which is 144.7° for the ground state and 112.9° for $^2B_2$; Oyeyemi *et al.*

	anti			*syn*		
T (K)	$S^o(T)$	$C_p^o(T)$	$H^o(T) - H^o(0)$	$S^o(T)$	$C_p^o(T)$	$H^o(T) - H^o(0)$
298.15	255.92	47.75	11.81	257.91	44.60	11.71
300.	256.21	47.83	11.90	258.19	44.63	11.79
400.	270.49	51.56	16.87	271.29	46.53	16.35
500.	282.36	54.78	22.19	281.88	48.42	21.10
600.	292.59	57.52	27.81	290.87	50.25	26.03
700.	301.64	59.86	33.68	298.75	51.97	31.14
800.	309.77	61.87	39.77	305.79	53.54	36.42
900.	317.16	63.60	46.05	312.18	54.95	41.84
1000.	323.94	65.11	52.48	318.03	56.21	47.40
1100.	330.21	66.43	59.06	323.44	57.32	53.08
1200.	336.04	67.60	65.76	328.47	58.29	58.86
1300.	341.49	68.62	72.57	333.17	59.14	64.73
1400.	346.61	69.54	79.48	337.58	59.88	70.68
1500.	351.44	70.37	86.48	341.74	60.54	76.70
1600.	356.00	71.12	93.55	345.66	61.11	82.78
1800.	364.46	72.44	107.91	352.92	62.07	95.11
2000.	372.15	73.58	122.51	359.50	62.84	107.60

concluded [OKKL14] that both states will be important at combustion temperatures.

3.2.3.1. Species data.

	$^2A_1$				$^2B_2$		
1	0.000 000	0.000 000	1.368 605	1	0.000 000	0.000 000	1.529 058
6	0.000 000	0.000 000	0.207 283	6	0.000 000	0.000 000	0.433 056
8	0.000 000	1.164 008	−0.163 269	8	0.000 000	1.042 166	−0.257 962
8	0.000 000	−1.164 008	−0.163 269	8	0.000 000	−1.042 166	−0.257 962
B (GHz)	157.184	11.659 9	10.854 7	B (GHz)	75.604 1	14.545 6	12.198 7

	$^2A_1$				$^2B_2$		
No.	$\bar{\upsilon}$ (cm^{-1})	x_{ii}		No.	$\bar{\upsilon}$ (cm^{-1})	x_{ii}	
1	2309.43	−164.23	a_1	1	3047.24	−61.78	a_1
2	1212.30	−5.21	a_1	2	1496.42	−4.82	a_1
3	677.37	2.48	a_1	3	652.45	0.66	a_1
4	852.64	−2.02	b_1	4	1026.91	−2.78	b_1
5	1663.28	−24.84	b_2	5	1288.96	−5.28	b_2
6	120.87	679.74	b_2	6	1061.91	17.39	b_2

3.2.3.2. Formation enthalpy, $\Delta_f H$(0 K). Feller *et al.* derived corresponding values of $\Delta_f H^o$(0 K) = −123.0 kJ mol^{-1} (−126.4 ± 1.7 kJ mol^{-1} at 298.15 K) from extensive CCSD(T)/CBS calculations [FDF03] on an electronically challenging system and $\Delta_f H^o$(0 K) = −123.9 kJ mol^{-1} in the work of Dixon *et al.* [DFF03]. Fabian and Janoschek [FJ05] studied the role of formyloxy in the reaction CO + $^{\bullet}$OH → CO_2 + H$^{\bullet}$ and noted $\Delta_f H^o$(298.15 K) = −127.1 kJ mol^{-1} from W1U computations. In G3(MP2) isodesmic calculations, Yu, Rauk, and Armstrong [YRA94] found $\Delta_f H^o$(298.15 K) = −126.6 ± 3.2 kJ mol^{-1} (our W2X suggests −128.4 kJ mol^{-1}); there is therefore very good agreement among these methods centering around −127 ± 1 kJ mol^{-1} at 298.15 K.

Our W3X-L calculations for the $^2A_1$ ground state indicate $\Delta_f H^o$(0 K) = −130.0 kJ mol^{-1} (−131.6 kJ mol^{-1} at 298.15 K), respectively, which are significantly more negative.

None of the above agree with ATcT values of $\Delta_f H^o$(0 K) = −125.57 ± 0.56 kJ mol^{-1} (−127.23 kJ mol^{-1} at 298.15 K), which rely mainly on the work by Feller [FDF03, DFF03] or on lower level calculations. All three flavors of the ANL protocol [KHR17] indicate that the ATcT values are in need of substantial downward correction by between 4 kJ mol^{-1} and 5 kJ mol^{-1}, which at −129.5 kJ mol^{-1} to −130.5 kJ mol^{-1} would bring them into agreement with our results.

We conclude that the newer results (W3X-L and ANLs) will change the tabulated value substantially.

The formation enthalpy for the $^2B_2$ state lies, according to W3X-L, at $\Delta_f H^o$(0 K) = −123.8 kJ mol^{-1} (−127.3 kJ mol^{-1} at 298.15 K), some 6.2 kJ mol^{-1} higher at 0 K and 4.4 kJ mol^{-1} higher at 298.15 K than the $^2A_1$ state. There is substantial disagreement with the Dixon *et al.* values of −116.3 kJ mol^{-1} (−120.5 kJ mol^{-1} at 298.15 K) although the difference $|^2A_1 - {}^2B_2|$ does agree within 1.3 kJ mol^{-1}.

3.2.3.3. Results. The lowest b_2 mode in the ground state ($^2A_1$) is highly anharmonic, and we have therefore included a simple rigid rotor (RR) and harmonic oscillator (HO) or RRHO treatment; however, for the excited state, this is not required. In an *ab initio* study of the radicals and ions of formic and acetic acids, Yu *et al.* reported [YRA94] C_p^o = 43.4 J K^{-1} mol^{-1} and S^o = 244.7 J K^{-1} mol^{-1} at 298.15 K from scaled HF/6-31G(d) frequencies, whereas the corresponding values from the work of Goldsmith *et al.* [GMG12] are 51.0 ± 1.7 J K^{-1} mol^{-1} and 252.3 ± 2.1 J K^{-1} mol^{-1}. We obtain very satisfactory agreement with those of Fabian and Janoschek [FJ05] who reported C_p^o = 48.44 J K^{-1} mol^{-1} and S^o = 256.49 J K^{-1} mol^{-1} for the ground $^2A_1$ state and C_p^o = 40.90 J K^{-1} mol^{-1} and S^o = 245.23 J K^{-1} mol^{-1} for the $^2B_2$ state.

$^2A_1$				$^2B_2$			
T (K)	$S°(T)$	$C_p°(T)$	$H°(T) - H°(0)$	T (K)	$S°(T)$	$C_p°(T)$	$H°(T) - H°(0)$
298.15	256.71	48.55	12.30	298.15	245.31	40.76	10.46
300.	257.01	48.65	12.39	300.	245.57	40.88	10.54
400.	271.73	53.81	17.52	400.	258.19	47.16	14.94
500.	284.24	58.36	23.13	500.	269.34	52.84	19.95
600.	295.23	62.23	29.16	600.	279.40	57.51	25.47
700.	305.07	65.45	35.55	700.	288.56	61.29	31.42
800.	313.99	68.11	42.23	800.	296.95	64.36	37.71
900.	322.14	70.29	49.16	900.	304.68	66.87	44.27
1000.	329.64	72.08	56.28	1000.	311.84	68.95	51.07
1100.	336.58	73.55	63.56	1100.	318.50	70.69	58.05
1200.	343.04	74.77	70.98	1200.	324.71	72.15	65.19
1300.	349.07	75.79	78.51	1300.	330.54	73.39	72.47
1400.	354.71	76.65	86.13	1400.	336.02	74.45	79.86
1500.	360.03	77.37	93.83	1500.	341.18	75.36	87.36
1600.	365.04	77.98	101.60	1600.	346.07	76.15	94.93
1800.	374.28	78.95	117.29	1800.	355.12	77.43	110.29
2000.	382.64	79.68	133.16	2000.	363.33	78.42	125.88

References for formyloxy; formyloxidanyl.

KBAM95 E. H. Kim, S. E. Bradforth, D. W. Arnold, and R. B. Metz, "Study of HCO_2 and DCO_2 by negative ion photoelectron spectroscopy," J. Chem. Phys. **103**, 7801–7814 (1995).

DL16 M. Döntgen and K. Leonhard, "Reactions of chemically activated formic acid formed via HĊO + H," J. Phys. Chem. A **120**(11), 1819–1824 (2016).

OKKL14 V. B. Oyeyemi, D. B. Krisiloff, J. A. Keith, F. Libisch, M. Pavone, and E. A. Carter, "Size-extensivity-corrected multireference configuration interaction schemes to accurately predict bond dissociation energies of oxygenated hydrocarbons," J. Chem. Phys. **140**(4), 044317 (2014).

GKSZ10 E. Garand, K. Klein, J. F. Stanton, J. Zhou, T. I. Yacovitch, and D. M. Neumark, "Vibronic structure of the formyloxyl radical (HCO_2) via slow photoelectron velocity-map imaging spectroscopy and model Hamiltonian calculations," J. Phys. Chem. A **114**(3), 1374–1383 (2010).

FDF03 D. Feller, D. A. Dixon, and J. S. Francisco, "Coupled cluster theory determination of the heats of formation of combustion-related Compounds: CO, HCO, CO_2, HCO_2, HOCO, HC(O)OH, and HC(O)OOH," J. Phys. Chem. A **107**(10), 1604–1617 (2003).

DFF03 D. A. Dixon, D. Feller, and J. S. Francisco, "Molecular structure, vibrational frequencies, and energetics of the HCO, HOCO, and HCO_2 anions," J. Phys. Chem. A **107**, 186–190 (2003).

FJ05 W. M. F. Fabian and R. Janoschek, "Thermochemical properties of the hydroxy-formyl radical, HOCO, and the formyloxy radical, HC(O)O, and their role in the reaction OH + CO → H + CO_2. Computational G3MP2B3 and CCSD(T)-CBS studies," J. Mol. Struct.: THEOCHEM **713**, 227–234 (2005).

YRA94 D. Yu, A. Rauk, and D. A. Armstrong, "Radicals and ions of formic and acetic acids: An *ab initio* study of the structures and gas and solution thermochemistry," J. Chem. Soc. Perkin Trans. **2**, 2207–2215 (1994).

KHR17 S. J. Klippenstein, L. B. Harding, and B. Ruscic, "*Ab initio* computations and active thermochemical tables hand in hand: Heats of formation of core combustion species," J. Phys. Chem. A **121**, 6580–6602 (2017).

GMG12 C. F. Goldsmith, G. R. Magoon, and W. H. Green, "Database of small molecule thermochemistry for combustion," J. Phys. Chem. A **116**(36), 9033–9057 (2012).

3.2.4. *Hydroxyformyl anti/syn*

$^2A'$ g = 2 C_S σ = 1 M_0 = 45.0177

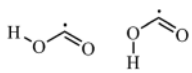

Hydroxyformyl or HOCO is an important atmospheric radical and intermediate combustion species [W84, NK16]. It is believed to form via the reaction of OH and CO, decompose to H and CO_2, and stabilized through collision with an inert species. A full understanding of the chemistry of the HOCO radical could lead to a better understanding of atmospheric and terrestrial chemistry. The *trans* or *anti* conformer is more stable by 5.7 kJ mol^{-1}, which agrees well with the predictions by Fortenberry *et al.* [FHFC11]. A review article [FMY10] summarizes many of the properties of HOCO up to 2010.

3.2.4.1. Species data.

	anti				*syn*		
1	−1.752 291	0.467 866	0.000 025	1	−0.766 128	−1.288 105	0.000 000
8	−1.067 423	−0.212 428	0.000 004	8	−1.059 113	−0.355 753	0.000 000
8	1.186 672	−0.137 386	−0.000 012	8	1.154 879	0.186 370	0.000 000
6	0.133 050	0.388 441	0.000 007	6	0.000 000	0.440 528	0.000 000
B (GHz)	166.609	11.485	10.744	*B* (GHz)	142.696	11.792	10.892

	anti				*syn*		
No.	$\bar{\upsilon}$ (cm^{-1})	x_{ii}		No.	$\bar{\upsilon}$ (cm^{-1})	x_{ii}	
1	3793.95	−83.76	a'	1	3571.85	−106.47	a′
2	1902.57	−13.00	a'	2	1867.00	−13.28	a′
3	1242.68	−12.12	a'	3	1298.90	−7.78	a′
4	1084.31	−9.29	a'	4	1073.70	−7.26	a′
5	622.11	−0.05	a'	5	599.69	0.48	a′
6	545.59	0.13	a''	6	594.42	−21.73	a″

3.2.4.2. Formation enthalpy, Δ_fH (0 K). Feller *et al.* computed [FDF03] a value of $\Delta_f H^o$(0 K) = −183.7 ± 2.1 kJ mol^{-1} for the *anti*-conformer from coupled-cluster theory, which is to be compared to a revised [RL00] quasi-experimental value of ≥ −195 ± 3 kJ mol^{-1}. Nagy and co-workers [NCKT10] used the HEAT345-Q model chemistry to determine −181.32 kJ mol^{-1} and −174.63 kJ mol^{-1} for the *anti* and *syn*, respectively; two years later, Nguyen *et al.* used the HEAT model [NXWBS12] similarly deriving −180.40 kJ mol^{-1} and −174.05 kJ mol^{-1}.

W3X-L atomization calculations [SS16] gave $\Delta_f H^o$(0 K) = −183.2 kJ mol^{-1} (−185.8 kJ mol^{-1} at 298.15 K) for the *anti* and $\Delta_f H^o$(0 K) = −176.7 kJ mol^{-1} (−179.8 kJ mol^{-1} at 298.15 K) for the *syn*.

ATcT v1.122d has, based primarily on the coupled-cluster work [FDF03, NCKT10, NXWBS12] and on lower levels of theory, $\Delta_f H^o$(0 K) = −181.19 ± 0.50 kJ mol^{-1} (−184.16 kJ mol^{-1} at 298.15 K) for the *anti* and $\Delta_f H^o$(0 K) = −174.34 ± 0.53 kJ mol^{-1} (−177.37 kJ mol^{-1} at 298.15 K) for the *syn*. A companion work [KHR17] using various high-level ANL protocols indicates that the tabulated values of −181.19 kJ mol^{-1} for the *anti* are still somewhat too high by some 0.6 kJ mol^{-1}.

3.2.4.3. Results. Fortenberry *et al.* [FHFC11] carried out a comprehensive study of the *anti*-HOCO radical; their vibrational frequencies and other data closely match our lower level ones, as they do for the syn [FHFC11]. In computing entropy, the torsional mode no. 6 is replaced by a hindered rotor treatment; Nagy *et al.* reported an entropy of 251.4 J K^{-1} mol^{-1} from a rigid rotor harmonic oscillator treatment for the *anti* conformer [NCKT10].

The species labeled "carboxyl" by Gurvich *et al.* [GVA89], which SciFinder classifies as an alternative name for "COOH," has quite different values, viz., S^o = 251.732 J K^{-1} mol^{-1}, C_p^o = 43.609 J K^{-1} mol^{-1}, and H^o(T) − H^o(0) = 10.813 kJ mol^{-1}.

	anti			*syn*		
T (K)	$S^o(T)$	$C_p^o(T)$	$H^o(T) - H^o(0)$	$S^o(T)$	$C_p^o(T)$	$H^o(T) - H^o(0)$
298.15	253.43	48.08	11.35	254.02	48.15	11.37
300.	253.72	48.21	11.44	254.31	48.27	11.46
400.	268.44	54.08	16.56	269.03	54.04	16.59
500.	281.01	58.58	22.21	281.59	58.51	22.22
600.	292.02	62.17	28.25	292.58	62.12	28.26
700.	301.83	65.08	34.62	302.39	65.09	34.62
800.	310.68	67.47	41.25	311.25	67.55	41.26
900.	318.74	69.43	48.09	319.32	69.57	48.12
1000.	326.14	71.05	55.12	326.74	71.24	55.16
1100.	332.98	72.39	62.29	333.60	72.61	62.35
1200.	339.33	73.50	69.59	339.97	73.74	69.67
1300.	345.25	74.43	76.98	345.91	74.68	77.09
1400.	350.79	75.21	84.47	351.47	75.46	84.60
1500.	356.01	75.87	92.02	356.70	76.11	92.18
1600.	360.92	76.43	99.64	361.63	76.66	99.82
1800.	369.98	77.35	115.02	370.71	77.54	115.24
2000.	378.17	78.07	130.56	378.92	78.20	130.82

References for hydroxyformyl *anti/syn*.

W84 J. Warnatz, *Combustion Chemistry*, edited by W. C. Gardiner (Springer, New York, 1984), Chap. 5.

NK16 E. J. K. Nilsson and A. A. Konnov, "Role of HOCO chemistry in syngas combustion," Energy Fuels **30**, 2443–2457 (2016).

FHFC11 R. C. Fortenberry, X. Huang, J. S. Francisco, T. D. Crawford, and T. J. Lee, "The *trans*-HOCO radical: Quartic force fields, vibrational frequencies, and spectroscopic constants," J. Chem. Phys. **135**, 134301 (2011).

FMY10 J. S. Francisco, J. T. Muckerman, and H.-G. Yu, "HOCO radical chemistry," Acc. Chem. Res. **43**(12), 1519–1526 (2010).

FDF03 D. Feller, D. A. Dixon, and J. S. Francisco, "Coupled cluster theory determination of the heats of formation of combustion-related Compounds: CO, HCO, CO_2, HCO_2, HOCO, HC(O)OH, and HC(O)OOH," J. Phys. Chem. A **107**(10), 1604–1617 (2003).

RL00 B. Ruscic and M. Litorja, "Photo-ionization of HOCO revisited: A new upper limit to the adiabatic ionization energy and lower limit to the enthalpy of formation," Chem. Phys. Lett. **316**, 45–50 (2000).

NCKT10 B. Nagy, J. Csontos, M. Kállay, and G. Tasi, "High-accuracy theoretical study on the thermochemistry of several formaldehyde derivatives," J. Phys. Chem. A **114**(50), 13213–13221 (2010).

NXWBS12 T. L. Nguyen, B. C. Xue, R. E. Weston, Jr., J. R. Barker, and J. F. Stanton, "Reaction of HO with CO: Tunneling is indeed important," J. Phys. Chem. Lett. **3**, 1549 (2012).

SS16 J. M. Simmie and J. N. Sheahan, "Validation of a database of formation enthalpies and of mid-level model chemistries," J. Phys. Chem. A **120**(37), 7370–7384 (2016).

FHFC11 R. C. Fortenberry, X. Huang, J. S. Francisco, T. D. Crawford, and T. J. Lee, "Vibrational frequencies, and spectroscopic constants from quartic force fields for *cis*-HOCO: The radical and the anion," J. Chem. Phys. **135**, 214303 (2011).

KHR17 S. J. Klippenstein, L. B. Harding, and B. Ruscic, "*Ab initio* computations and active thermochemical tables hand in hand: Heats of formation of core combustion species," J. Phys. Chem. A **121**, 6580–6602 (2017).

GVA89 L. V. Gurvich, I. V. Veyts, and C. B. Alcock, *Thermodynamic Properties of Individual Substances: Elements and Compounds* (Hemisphere, New York, 1989), Vol. 2.

3.3. $C_1H_1O_3$

3.3.1. 3-Dioxyranyloxyl

$^2A''$ g = 2 C_S σ = 1 M_0 = 61.0171

The O-centered radical has a simpler structure and higher-symmetry than the corresponding carbon-centered radical (see 3-hydroxydioxyranyl below) as well as a T_1 of 0.027.

3.3.1.1. Species data.

8	0.773 284	1.212 314	0.000 000
6	−0.228 974	0.349 016	0.000 000
8	−0.228 974	−0.797 186	0.763 265
8	−0.228 974	−0.797 186	−0.763 265
1	−1.148 839	0.962 377	0.000 000
B (GHz)	21.666 8	8.508 4	6.890 4

No.	$\bar{\upsilon}$ (cm^{-1})	x_{ii}	
1	2919.17	−81.14	a'
2	1378.91	−10.39	a'
3	1262.53	−3.72	a'
4	1025.48	−3.13	a'
5	774.69	−3.00	a'
6	475.66	1.10	a'
7	1066.61	−7.58	a''
8	853.32	−1.49	a''
9	367.64	−36.65	a''

3.3.1.2. Formation enthalpy, $\Delta_f H$(0 K). A W3X-L atomization calculation returns $\Delta_f H^o$(0 K) = 80.1 kJ mol^{-1} at 0 K (74.4 kJ mol^{-1} at 298.15 K).

3.3.1.3. Results. Harmonic and anharmonic treatments are in good agreement near 300 K but show appreciable differences at higher temperatures.

T (K)	$S^o(T)$	$C_p^o(T)$	$H^o(T) - H^o(0)$
298.15	275.35	56.10	12.56
300.	275.70	56.26	12.67
400.	292.99	64.02	18.70
500.	307.96	70.19	25.42
600.	321.21	75.08	32.69
700.	333.09	78.98	40.40
800.	343.85	82.12	48.46
900.	353.67	84.70	56.80
1000.	362.71	86.83	65.38
1100.	371.07	88.61	74.16
1200.	378.85	90.12	83.09
1300.	386.11	91.40	92.17
1400.	392.93	92.51	101.37
1500.	399.34	93.46	110.66
1600.	405.40	94.30	120.05
1800.	416.59	95.69	139.06
2000.	426.74	96.80	158.31

3.3.2. 3-Hydroxydioxyranyl

syn $^2A'$ g = 2 C_S σ = 1 M_0 = 61.0171;

gauche ^2A g = 2 C_1 σ = 1 M_0 = 61.0171

This carbon-centered radical exists in two conformers that can be described as *syn* or *anti* based on the dihedral HOCX, where X is the O–O bond midpoint. In reality, the *anti* is a saddle point and the

actual conformer is probably best described as *gauche* with a dihedral of ca. 151°. Neither radical is currently included in the SciFinder database.

3.3.2.1. Species data.

	syn				*gauche*		
1	1.034 288	−1.397 790	0.000 000	1	2.006 479	0.407 955	0.354 970
8	0.060 208	−1.404 138	0.000 000	8	1.362 618	−0.057 794	−0.190 696
6	−0.413 215	−0.162 210	0.000 000	6	0.150 543	0.014 496	0.389 731
8	0.060 208	0.850 259	0.773 956	8	−0.881 782	0.769 404	−0.094 801
8	0.060 208	0.850 259	−0.773 956	8	−0.844 553	−0.773 476	−0.051 173
B (GHz)	22.517	8.395 1	6.642 7	*B* (GHz)	23.027	8.348 0	6.556 7

	syn				*gauche*		
No.	$\bar{\upsilon}$ (cm^{-1})	x_{ii}		No.	$\bar{\upsilon}$ (cm^{-1})	x_{ii}	
1	3620.48	−100.46	a'	1	3814.56	−82.39	*a*
2	1436.40	−6.41	a'	2	1475.15	−6.04	*a*
3	1294.01	−8.14	a'	3	1215.52	−10.15	*a*
4	1044.91	−3.09	a'	4	1078.27	−4.15	*a*
5	768.37	−3.33	a'	5	868.66	0.81	*a*
6	543.37	0.59	a'	6	780.87	−3.38	*a*
7	865.11	0.62	a''	7	569.32	−0.03	*a*
8	490.60	−1.84	a''	8	460.66	−1.47	*a*
9	122.48	64.71	a''	9	219.95	−80.49	*a*

3.3.2.2. Formation enthalpy, $\Delta_f H$(0 K). Atomization calculations based on W3X-L protocols yield $\Delta_f H^\circ$(0 K) = 12.4 kJ mol^{-1} (7.4 kJ mol^{-1} at 298.15 K) for the more symmetrical *syn* conformer and $\Delta_f H^\circ$(0 K) = 10.9 kJ mol^{-1} (5.6 kJ mol^{-1} at 298.15 K) for the *gauche* form. Multi-composite treatment returns 11.0 ± 4.3 kJ mol^{-1} for the *syn*, but CBS-APNO and G3 calculations fail for the *gauche*.

3.3.2.3. Results. An anharmonic and hindered rotor treatment is used for both conformers with replacement of the highly anharmonic mode no. 9. A larger effect of the hindered rotor was observed for the *gauche* conformer. The *syn–gauche* barrier to a relaxed potential energy about C–O is 8.4 kJ mol^{-1}, while interconversion *g*,*g*′ faces a much lower barrier of <1 kJ mol^{-1}. Gaussian's own hindered rotor treatment concurs, identifying ν_9 as a hindered rotor with a ratio of barrier height to thermal energy or the reduced barrier height (*V*/*RT*), of 0.626 (*syn*) and 1.589 (*gauche*).

	syn			*gauche*		
T (K)	$S^\circ(T)$	$C_p^\circ(T)$	$H^\circ(T) - H^\circ(0)$	$S^\circ(T)$	$C_p^\circ(T)$	$H^\circ(T) - H^\circ(0)$
298.15	284.17	60.48	13.61	284.04	60.43	13.60
300.	284.54	60.65	13.72	284.41	60.60	13.72
400.	303.13	68.61	20.20	302.99	68.60	20.19
500.	319.13	74.75	27.38	318.99	74.75	27.37
600.	333.19	79.43	35.10	333.05	79.42	35.09
700.	345.72	83.05	43.23	345.57	83.00	43.22
800.	357.00	85.93	51.68	356.85	85.82	51.66
900.	367.26	88.27	60.39	367.09	88.11	60.36
1000.	376.67	90.23	69.32	376.48	90.02	69.27
1100.	385.35	91.89	78.43	385.14	91.65	78.36
1200.	393.40	93.32	87.69	393.17	93.06	87.59
1300.	400.92	94.56	97.08	400.67	94.28	96.96
1400.	407.97	95.64	106.59	407.70	95.36	106.44
1500.	414.60	96.60	116.21	414.31	96.32	116.03
1600.	420.86	97.45	125.91	420.55	97.18	125.70
1800.	432.43	98.90	145.55	432.09	98.64	145.29
2000.	442.91	100.07	165.45	442.54	99.84	165.14

3.3.3. Hydroxyoxomethoxy

$^2A'$ g = 2 C_S σ = 1 M_0 = 61.0171

Formation of the bicarbonate radical $HOCO_2^{\bullet}$ was proposed by Ghoshal and Hazra [GH16] to proceed from the OH radical initiated reaction of carbonic acid H_2CO_3 via the pre-reactive entrance channel complex $H_2CO_3\cdots OH$ and the exit channel $HCO_3\cdots H_2O$ product complex. Puzzarini *et al.* [PBPFL17] have characterized this radical in its ground and excited states at very high levels of theory, emphasizing its connection with the atmospherically and flame chemistry relevant hydroxyformyl HOCO radical.

3.3.3.1. Species data.

8	0.896 058	0.932 089	0.000 000
6	0.054 878	0.001 985	0.000 000
8	0.520 571	−1.151 373	0.000 000
8	−1.239 852	0.285 541	0.000 000
1	1.743 484	−0.541 965	0.000 000
B (GHz)	13.813 7	11.249 2	6.200 1

No.	$\bar{\upsilon}$ (cm^{-1})	x_{ii}	
1	3750.69	−84.31	*a′*
2	1577.90	−7.56	*a′*
3	1272.91	−5.58	*a′*
4	1149.89	−0.63	*a′*
5	1032.83	−3.25	*a′*
6	554.74	0.29	*a′*
7	512.81	−1.29	*a′*
8	760.33	−0.96	*a″*
9	473.63	−14.37	*a″*

3.3.3.2. Formation enthalpy, $\Delta_f H$(0 K). W2X and W3X-L atomization calculations return values of −359.6 kJ mol^{-1} and −362.8 kJ mol^{-1}, respectively, which translate to −365.9 kJ mol^{-1} and −369.0 kJ mol^{-1} at 298.15 K. A value of −364.1 kJ mol^{-1} at 298.15 K was extracted from the isodesmic reaction

$$HOCO_2^{\cdot} + CH_4 = HCO_2^{\cdot} + CH_3OH$$

from CBS-RAD calculations [AWR06]. The comparable number obtained *here* from multiple composites is −362.9 ± 6.4 kJ mol^{-1}—the large uncertainty arising from the outlying CBS-QB3 and CBS-APNO reaction enthalpies. A total atomization energy of 2030.1 kJ mol^{-1} was obtained from CCSD(T)/CBS calculations by Puzzarini *et al.* [PBPFL17]—this translates to $\Delta_f H^o$(0 K) = −362.1 kJ mol^{-1}, which is in very good agreement with our W3X-L value as is the −361.3 kJ mol^{-1} ANL0 value [KHR17].

Hence, $\Delta_f H^o$(0 K) = −362.4 ± 0.6 kJ mol^{-1} (−368.6 kJ mol^{-1} at 298.15 K) can be confidently recommended.

3.3.3.3. Results. Hindered rotor analysis identified frequency no. 9 as a hindered rotor with a reduced barrier height V/RT = 12.3. A relaxed potential energy barrier scan shows a barrier of 28.8 kJ mol^{-1}, incorporation of which results in a difference in entropy of 0.4 J K^{-1} mol^{-1} at 298.15 K, which increases to 1.3 J K^{-1} mol^{-1} at 2000 K according to the THERMO module of MultiWell. Armstrong *et al.* [AWR06] computed the thermochemistry of a number of carbonic acid species and reported 298.15 K values of 273.0 J K^{-1} mol^{-1} and 12.0 kJ mol^{-1} for the entropy and enthalpy function, respectively.

T (K)	$S^o(T)$	$C_p^o(T)$	$H^o(T) - H^o(0)$
298.15	273.47	55.57	12.13
300.	273.81	55.78	12.23
400.	291.29	65.89	18.33
500.	306.90	73.94	25.34
600.	320.95	80.06	33.05
700.	333.66	84.66	41.30
800.	345.20	88.13	49.95
900.	355.74	90.77	58.90
1000.	365.42	92.83	68.08
1100.	374.35	94.47	77.45
1200.	382.63	95.80	86.97
1300.	390.34	96.89	96.61
1400.	397.56	97.81	106.34
1500.	404.33	98.59	116.16
1600.	410.72	99.26	126.06
1800.	422.48	100.36	146.02
2000.	433.10	101.22	166.19

References for hydroxyoxomethoxy.

GH16 S. Ghoshal and M. K. Hazra, "Impact of OH radical-initiated H_2CO_3 degradation in the earth's atmosphere via proton-coupled electron transfer mechanism," J. Phys. Chem. A **120**, 562–575 (2016).

PBPFL17 C. Puzzarini, M. Biczysko, K. A. Peterson, J. S. Francisco, and R. Linguerri, "Accurate spectroscopic characterization of the HOC(O)O radical: A route toward its experimental identification," J. Chem. Phys. **147**(2), 024302 (2017).

AWR06 D. A. Armstrong, W. L. Waltz, and A. Rauk, "Carbonate radical anion—Thermochemistry," Can. J. Chem. **84**, 1614–1619 (2006).

KHR17 S. J. Klippenstein, L. B. Harding, and B. Ruscic, "*Ab initio* computations and active thermochemical tables hand in hand: Heats of formation of core combustion species," J. Phys. Chem. A **121**, 6580–6602 (2017).

3.3.4. Hydroperoxyoxomethyl

^2A g = 2 C_1 σ = 1 M_0 = 61.0171

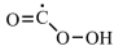

It has been reported [S10] as an intermediate in the photochemical oxidation of glyoxal, reacting to regenerate the hydroxyl radical: $O\dot{C}OOH \rightarrow CO_2 + OH^{\bullet}$.

3.3.4.1. Species data.

6	−0.650 792	−0.340 417	0.024 362
8	−1.783 919	−0.011 826	0.014 968
8	0.387 293	0.505 617	−0.043 917
8	1.628 047	−0.250 657	−0.079 180
1	2.053 378	0.097 430	0.718 860
B (GHz)	70.890 9	4.785 2	4.533 4

No.	$\bar{\upsilon}$ (cm^{-1})	x_{ii}
1	3742.68	−81.78
2	1865.96	−13.83
3	1414.42	−10.63
4	1025.10	−13.13
5	944.57	−6.70
6	598.30	−0.36
7	350.68	−0.33
8	257.60	0.18
9	156.66	−30.22

3.3.4.2. Formation enthalpy, $\Delta_f H$(0 K). A formation enthalpy of −76.2 kJ mol^{-1} at 298.15 K was noted by da Silva [S10] from G3SX calculations. A multi-composite treatment returns $\Delta_f H^o$(0 K) = −75.4 ± 3.9 kJ mol^{-1}, while W3X-L gives $\Delta_f H^o$(0 K) = −74.6 kJ mol^{-1} (−78.6 kJ mol^{-1} at 298.15 K), in good agreement with an ANL0 value [KHR17] of −73.3 kJ mol^{-1}. These results can be summarized as $\Delta_f H^o$(0 K) = −74.4 ± 1.2 kJ mol^{-1} (−78.4 kJ mol^{-1} at 298.15 K).

3.3.4.3. Results. Literature values [S10] of S^o = 286.6 J mol^{-1} K^{-1} and C_p^o = 63.17 J mol^{-1} K^{-1} are in very good agreement with our computed results that are based on a hindered rotor treatment for a relaxed potential energy scan of the HOOC dihedral (mode no. 9), as well as anharmonic frequencies.

T (K)	$S^o(T)$	$C_p^o(T)$	$H^o(T) - H^o(0)$
298.15	291.65	62.29	14.32
300.	292.04	62.43	14.44
400.	310.97	69.28	21.04
500.	327.03	74.66	28.24
600.	341.04	78.91	35.93
700.	353.47	82.32	44.00
800.	364.65	85.12	52.37
900.	374.81	87.47	61.00
1000.	384.13	89.46	69.85
1100.	392.74	91.19	78.89
1200.	400.74	92.69	88.08
1300.	408.22	94.01	97.42
1400.	415.23	95.18	106.87
1500.	421.83	96.22	116.44
1600.	428.07	97.15	126.11
1800.	439.61	98.75	145.71
2000.	450.08	100.09	165.59

References for hydroperoxyoxomethyl.

S10 G. da Silva, "Hydroxyl radical regeneration in the photochemical oxidation of glyoxal:kinetics and mechanism of the HC(O)CO + O2 reaction," Phys. Chem. Chem. Phys. **12**, 6698–6705 (2010).

KHR17 S. J. Klippenstein, L. B. Harding, and B. Ruscic, "*Ab initio* computations and active thermochemical tables hand in hand: Heats of formation of core combustion species," J. Phys. Chem. A **121**, 6580–6602 (2017).

3.3.5. Methylenetrioxygen radical

$^2A'$ g = 2 C_S σ = 1 M_0 = 61.0171

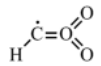

3.3.5.1. Species data.

6	−0.117 262	1.449 738	0.000 000
8	0.000 000	0.192 057	0.000 000
1	−1.205 750	1.620 532	0.000 000
8	−0.931 150	−0.911 943	0.000 000
8	1.169 816	−0.569 984	0.000 000
B (GHz)	13.568	10.746	5.996 6

No.	$\bar{\upsilon}$ (cm^{-1})	x_{ii}	
1	3001.99	−64.15	*a*′
2	1373.83	−7.96	*a*′
3	1156.77	−9.81	*a*′
4	784.49	−6.32	*a*′
5	643.46	−21.80	*a*′
6	440.41	−1.07	*a*′
7	338.34	−11.55	*a*′
8	821.38	−1.99	*a*″
9	359.71	−1.61	*a*″

3.3.5.2. Formation enthalpy, $\Delta_f H$(0 K). A multi-composite calculation, *sans* CBS-APNO, returns $\Delta_f H^o$(0 K) = 688.4 ± 8.0 kJ mol^{-1} (683.7 kJ mol^{-1} at 298.15 K). A C–H bond dissociation energy of 487 kJ mol^{-1} can be calculated, which is stronger than the corresponding bond in ethylene [L07] of 464 kJ mol^{-1}.

3.3.5.3. Results. A hindered rotor analysis identifies mode no. 8 at 821 cm^{-1}, but a reduced barrier height (*V*/*RT*) of 21.6 means that it has little impact over a conventional RR anharmonic treatment; in addition, a scan of the HCOO dihedral fails.

T (K)	$S^o(T)$	$C_p^o(T)$	$H^o(T) - H^o(0)$
298.15	282.14	65.14	13.64
300.	282.54	65.36	13.76
400.	302.83	75.68	20.84
500.	320.59	83.41	28.81
600.	336.32	88.99	37.45
700.	350.36	92.93	46.55
800.	362.96	95.71	55.99
900.	374.35	97.67	65.67
1000.	384.72	99.04	75.51
1100.	394.21	99.98	85.46
1200.	402.94	100.59	95.49
1300.	411.01	100.95	105.57
1400.	418.50	101.12	115.68
1500.	425.47	101.16	125.79
1600.	432.00	101.11	135.91
1800.	443.90	100.85	156.11
2000.	454.51	100.53	176.25

References for methylenetrioxygen radical.

L07 Y.-R. Luo, *Comprehensive Handbook of Chemical Bond Energies* (CRC Press, Boca Raton, USA, 2007).

3.3.6. Peroxyformyl; formylperoxy

$^2A''$ g = 2 C_S σ = 1 M_0 = 61.0171
trans/*E*

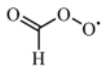

The peroxyformyl radical has been implicated in the photochemistry of polluted atmospheres and in other planetary atmospheres. In agreement with previous work [ETS15] that computed a difference of 10.1 kJ mol^{-1} in zero-point corrected electronic energies, we find that the *trans* or *E* OCOO conformer is more stable than the *cis or Z* by 12.7 kJ mol^{-1} at the W3X-L level.

3.3.6.1. Species data.

8	−0.185 307	−0.713 298	0.000 000
8	−0.933 283	1.415 356	0.000 000
6	0.000 000	0.696 374	0.000 000
1	1.072 576	0.926 302	0.000 000
8	0.984 519	−1.340 126	0.000 000
B (GHz)	60.5414	5.1384	4.7364

3.3.6.2. Formation enthalpy, $\Delta_f H(0\ K)$. A W3X-L atomization calculation returns $\Delta_f H^o(0\ K) = -102.5$ kJ mol^{-1} (−107.6 kJ mol^{-1} at 298.15 K) for the *trans* conformer whose T_1 diagnostic of 0.032 is indicative of some not inconsiderable multireference character. This is in accord with the experimentally determined value of −98 ± 12 kJ mol^{-1} via energy-resolved collision-induced dissociation with a tandem mass spectrometer and thermochemical cycles by Nickel *et al.* [NLE13] and the value of −95 ± 15 kJ mol^{-1} of an earlier study by Villano *et al.* [VEWE10]. There is also very satisfactory agreement with an ANL0 calculation [VEWE10] of $\Delta_f H^o(0\ K) = -101.3$ kJ mol^{-1}.

No.	$\bar{\upsilon}$ (cm^{-1})	x_{ii}	
1	3049.48	−60.73	a'
2	1887.92	−11.13	a'
3	1331.88	−7.05	a'
4	1152.33	−6.63	a'
5	972.39	−4.99	a'
6	593.05	−1.66	a'
7	407.78	−0.63	a'
8	1017.27	−2.70	a''
9	174.45	−2.32	a''

3.3.6.3. Results. Hindered rotor analysis indicates that only minor changes to the thermodynamic data at room temperature are required, since the reduced barrier height V/RT = 12.1, and this is corroborated by a MultiWell calculation in which a relaxed potential energy scan about the OC–OO dihedral reveals a barrier of 38.3 kJ mol^{-1}. Nevertheless, a full anharmonic hindered rotor treatment is used, which is in agreement with the literature [GMG12], viz., $S^o(298.15\ K) = 281.2 \pm 3.8$ J mol^{-1} K^{-1} and $C_p^o(300\ K) = 59.8 \pm 3.8$ J mol^{-1} K^{-1}.

T (K)	$S^o(T)$	$C_p^o(T)$	$H^o(T) - H^o(0)$
298.15	279.61	58.89	13.21
300.	279.98	59.08	13.32
400.	298.28	68.35	19.70
500.	314.37	75.81	26.93
600.	328.73	81.66	34.81
700.	341.67	86.22	43.21
800.	353.43	89.81	52.02
900.	364.18	92.64	61.15
1000.	374.06	94.88	70.53
1100.	383.19	96.66	80.11
1200.	391.66	98.09	89.85
1300.	399.56	99.26	99.72
1400.	406.96	100.21	109.69
1500.	413.90	101.00	119.75
1600.	420.44	101.66	129.88
1800.	432.47	102.70	150.32
2000.	443.34	103.50	170.94

References for peroxyformyl; formylperoxy.

ETS15 S. N. Elliott, J. M. Turney, and H. F. Schaefer, "The *cis*- and *trans*-formylperoxy radical: Fundamental vibrational frequencies and relative

energies of the (X) $^2A''$ and (A) $^2A'$ states," RSC Adv. **5**(130), 107254–107265 (2015).

ETS15 In [ETS15], above their Fig. 3 contradicts both the text and their Table 3 about which is the more stable conformer.

NLE13 A. A. Nickel, J. G. Lanorio, and K. M. Ervin, "Energy-Resolved collision-induced dissociation of peroxyformate anion: Enthalpies of formation of peroxyformic acid and peroxyformyl radical," J. Phys. Chem. A **117**(6), 1021–1029 (2013).

VEWE10 S. M. Villano, N. Eyet, S. W. Wren, G. B. Ellison, V. M. Bierbaum, and W. C. Lineberger, "Photoelectron spectroscopy and thermochemistry of the peroxyformate anion," J. Phys. Chem. A **114**(1), 191–200 (2010).

KHR17 S. J. Klippenstein, L. B. Harding, and B. Ruscic, "*Ab initio* computations and active thermochemical tables hand in hand: Heats of formation of core combustion species," J. Phys. Chem. A **121**(35), 6580–6602 (2017).

GMG12 C. F. Goldsmith, G. R. Magoon, and W. H. Green, "Database of small molecule thermochemistry for combustion," J. Phys. Chem. A **116**(36), 9033–9057 (2012).

3.3.7. Peroxyformyl; formylperoxy

$^2A''$ g = 2 C_S σ = 1 M_0 = 61.0171

cis/*Z*

In agreement with previous work [ETS15] that computed a difference of 10.1 kJ mol^{-1} in zero-point corrected electronic energies, we find that the *cis* or *Z* OCOO conformer is less stable than the *trans* or *E* by 12.7 kJ mol^{-1} at the W3X-L level.

3.3.7.1. Species data.

8	−0.867 458	−0.262 907	0.000 000
8	1.176 605	0.821 169	0.000 000
6	0.000 000	0.864 177	0.000 000
1	−0.655 200	1.742 719	0.000 000
8	−0.227 246	−1.424 234	0.000 000
B (GHz)	24.678 3	7.091 8	5.508 8

3.3.7.2. Formation enthalpy, $\Delta_f H(0\ K)$. A W3X-L atomization calculation returns $\Delta_f H^\circ(0\ K)$ = −89.8 kJ mol^{-1} (−94.8 kJ mol^{-1} at 298.15 K) for the *cis* conformer whose T_1 diagnostic of 0.031 indicates some multi-reference character.

No.	$\bar{\upsilon}$ (cm^{-1})	x_{ii}	
1	3056.77	−59.93	*a*′
2	1879.69	−11.30	*a*′
3	1366.50	−8.14	*a*′
4	1105.65	−7.23	*a*′
5	878.19	−8.38	*a*′
6	783.38	−4.06	*a*′
7	326.30	0.01	*a*′
8	981.44	−1.55	*a*″
9	242.61	−0.53	*a*″

3.3.7.3. Results. Hindered rotor analysis indicates that only minor changes to the thermodynamic data at room temperature are required since the reduced barrier height *V*/*RT* = 12.1, and this is corroborated by a MultiWell calculation in which a relaxed potential energy scan about the OC–OO dihedral reveals a barrier of 38.3 kJ mol^{-1} at B3LYP/cc-pVTZ+d. If CCSD(T)/ANO2 wavenumbers and CCSD(T)/ANO1 anharmonicities are used [ETS15] instead of our values, then the entropies differ by 1.5 J mol^{-1} K^{-1} at 298.15 K and by 11.1 J mol^{-1} K^{-1} at 2000 K. A full hindered rotor anharmonic treatment is shown here.

T (K)	$S^\circ(T)$	$C_p^\circ(T)$	$H^\circ(T) - H^\circ(0)$
298.15	282.12	58.86	13.30
300.	282.49	59.05	13.41
400.	300.79	68.41	19.79
500.	316.90	75.94	27.02
600.	331.29	81.82	34.92
700.	344.26	86.40	43.34
800.	356.04	90.00	52.17
900.	366.81	92.83	61.31
1000.	376.71	95.07	70.71
1100.	385.86	96.86	80.31
1200.	394.35	98.31	90.07
1300.	402.27	99.48	99.96
1400.	409.68	100.44	109.96
1500.	416.64	101.25	120.04
1600.	423.19	101.93	130.20
1800.	435.27	103.02	150.70
2000.	446.16	103.86	171.39

References for peroxyformyl; formylperoxy.

ETS15 S. N. Elliott, J. M. Turney, and H. F. Schaefer, "The *cis*- and *trans*-formylperoxy radical: Fundamental vibrational frequencies and relative energies of the ($\tilde{X}$) $^2A''$ and ($\tilde{A}$) $^2A'$ states," RSC Adv. **5**(130), 107254–107265 (2015).

3.3.8. Trioxetanyl

$^2A'$ g = 2 C_S σ = 1 M_0 = 61.0171

The radical of trioxetane *quod vide* (q.v.) is unknown in the chemical literature.

3.3.8.1. Species data.

6	0.046 007 000	0.967 357 000	0.000 000 000
8	0.017 962 000	0.035 481 000	1.020 059 000
8	0.017 962 000	−1.016 250 000	0.000 000 000
8	0.017 962 000	0.035 481 000	−1.020 059 000
1	−0.707 128 000	1.758 166 000	0.000 000 000
B (GHz)	16.099	14.956	7.875 5

No.	$\bar{\upsilon}$ (cm^{-1})	x_{ii}	
1	3036.73	−76.83	a'
2	1161.10	−3.33	a'
3	990.63	−17.11	a'
4	896.98	−2.63	a'
5	821.00	−42.54	a'
6	227.07	5.90	a'
7	1200.68	−9.96	a''
8	1097.11	−2.87	a''
9	842.94	−31.68	a''

3.3.8.2. Formation enthalpy, $\Delta_f H(0\ K)$. A multi-composite value of $\Delta_f H^o(0\ K) = 270.1 \pm 6.8$ kJ mol^{-1} is in agreement with a W3X-L of 270.6 kJ mol^{-1} (264.4 kJ mol^{-1} at 298.15 K) and a WMS of 267.7 kJ mol^{-1}. A C–H bond energy of (218.0 + 264.4–92.7) = 390 kJ mol^{-1} is obtained, which is similar [L07] to that in ethane-1,2-diol, $H_2C(OH)_2$.

3.3.8.3. Results. A standard rigid rotor anharmonic treatment is employed.

T (K)	$S^o(T)$	$C_p^o(T)$	$H^o(T) - H^o(0)$
298.15	271.79	53.50	12.09
300.	272.12	53.71	12.19
400.	289.12	64.72	18.13
500.	304.58	73.81	25.07
600.	318.70	80.97	32.82
700.	331.62	86.63	41.21
800.	343.50	91.13	50.11
900.	354.44	94.67	59.41
1000.	364.57	97.40	69.02
1100.	373.95	99.45	78.87
1200.	382.67	100.92	88.89
1300.	390.79	101.93	99.04
1400.	398.37	102.57	109.26
1500.	405.47	102.92	119.54
1600.	412.11	103.07	129.84
1800.	424.25	102.95	150.45
2000.	435.08	102.53	171.00

References for trioxetanyl.

L07 Y.-R. Luo, *Comprehensive Handbook of Chemical Bond Energies* (CRC Press, Boca Raton, USA, 2007).

3.4. $C_1H_1O_4$

3.4.1. Bis-dioxymethylene radical

$^2A_2$ g = 2 C_{2v} σ = 2 M_0 = 77.0165;

$^2A''$ g = 2 C_S σ = 1 M_0 = 77.0165

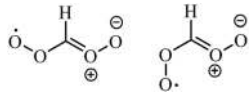

The *syn/syn*-conformer OOCH/HCOO appears to be the ground state at G4 with the *s/a* at + 4.0 kJ mol^{-1}, which agrees at WMS although now the difference only amounts to 1.2 kJ mol^{-1}, but this is contradicted at W1BD, which reverses the order and places the *sa* above at +1.3 kJ mol^{-1}. T_1 diagnostics of 0.055 and 0.032 indicates considerable multi-reference character, which accounts for the variability.

3.4.1.1. Species data.

	ss				*sa*		
6	0.000 000	0.231 297	0.000 000	6	0.000 000	0.642 646	0.000 000
1	−0.000 071	1.313 135	0.000 000	1	0.353 315	1.663 384	0.000 000
8	−1.091 659	−0.457 236	0.000 000	8	0.829 737	−0.348 394	0.000 000
8	1.091 062	−0.457 370	0.000 000	8	−1.276 360	0.450 807	0.000 000
8	−2.220 900	0.289 963	0.000 000	8	2.129 615	0.028 600	0.000 000
8	2.221 506	0.287 029	0.000 000	8	−1.727 156	−0.820 921	0.000 000
B (GHz)	43.157	2.579 4	2.433 9	*B* (GHz)	22.080	3.193 4	2.790 0

	ss				*sa*		
No.	$\bar{\upsilon}$ (cm^{-1})	x_{ii}		No.	$\bar{\upsilon}$ (cm^{-1})	x_{ii}	
1	3214.37	−55.67	a_1	1	3229.75	−54.42	a'
2	1299.40	−6.67	a_1	2	1380.13	−7.88	a'
3	1070.17	−3.78	a_1	3	1243.65	−8.91	a'
4	545.04	−0.15	a_1	4	1166.80	−7.43	a'
5	253.89	−9.72	a_1	5	1056.86	−8.13	a'
6	243.89	0.27	a_2	6	967.97	−6.73	a'
7	903.64	−6.90	b_1	7	722.59	−0.92	a'
8	207.12	0.07	b_1	8	430.72	−0.18	a'
9	1365.48	−9.07	b_2	9	246.25	0.14	a'
10	1152.67	−4.59	b_2	10	834.08	−6.10	a''
11	1003.79	−7.67	b_2	11	375.50	−2.16	a''
12	502.81	−0.81	b_2	12	177.18	0.32	a''

3.4.1.2. Formation enthalpy, $\Delta_f H(0\ K)$. A W3X-L calculation yields $\Delta_f H^o(0\ K)$ = 177.2 kJ mol^{-1} (170.3 kJ mol^{-1} at 298.15 K) for the *ss* conformer with the *sa* at $\Delta_f H^o(0\ K)$ = 178.7 kJ mol^{-1} (171.2 kJ mol^{-1} at 298.15 K).

3.4.1.3. Results. A relaxed potential energy scan encounters a barrier in excess of 56 kJ mol^{-1} as rotation about the C–O bond from the *ss* transforms into the *sa*, which lies at 4.6 kJ mol^{-1} above. Hence, a RR anharmonic treatment is applied.

	ss				*sa*		
T (K)	$S^o(T)$	$C_p^o(T)$	$H^o(T) - H^o(0)$	T (K)	$S^o(T)$	$C_p^o(T)$	$H^o(T) - H^o(0)$
298.15	297.40	75.21	15.71	298.15	301.48	72.15	15.17
300.	297.87	75.46	15.85	300.	301.93	72.40	15.31
400.	321.28	87.36	24.02	400.	324.46	84.45	23.17
500.	341.76	95.90	33.21	500.	344.37	93.94	32.11
600.	359.79	101.70	43.11	600.	362.17	101.15	41.88
700.	375.78	105.74	53.49	700.	378.19	106.64	52.28
800.	390.11	108.72	64.22	800.	392.72	110.92	63.16
900.	403.05	111.03	75.21	900.	405.99	114.34	74.43
1000.	414.85	112.90	86.41	1000.	418.18	117.12	86.01
1100.	425.69	114.47	97.78	1100.	429.46	119.44	97.84
1200.	435.70	115.79	109.29	1200.	439.94	121.39	109.88
1300.	445.02	116.94	120.93	1300.	449.72	123.06	122.10
1400.	453.72	117.94	132.67	1400.	458.90	124.51	134.48
1500.	461.89	118.82	144.51	1500.	467.53	125.77	147.00
1600.	469.58	119.60	156.43	1600.	475.68	126.89	159.63
1800.	483.75	120.93	180.49	1800.	490.74	128.80	185.20
2000.	496.55	122.01	204.78	2000.	504.40	130.39	211.12

3.4.2. Bis-hydroperoxymethylene radical

$^2A''$ g = 2 C_S σ = 1 M_0 = 77.0165

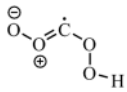

Tha *asa* conformer is the ground state, classified according to the dihedrals HOOC/(H)OOCO/OCOO.

3.4.2.1. Species data.

6	0.000 000	0.843 784	0.000 000
8	0.875 240	−0.194 292	0.000 000
8	2.147 710	0.225 512	0.000 000
8	−1.186 315	0.526 261	0.000 000
8	−1.525 983	−1.072 551	0.000 000
1	−2.485 211	−0.942 144	0.000 000
B (GHz)	17.333	3.230 3	2.722 8

No.	$\bar{\upsilon}$ (cm^{-1})	x_{ii}	
1	3771.75	−78.72	a'
2	1524.78	−23.23	a'
3	1184.74	−11.48	a'
4	1096.17	−4.76	a'
5	1003.27	−15.23	a'
6	682.49	−1.20	a'
7	491.69	−3.34	a'
8	398.51	−3.80	a'
9	204.60	−0.28	a'
10	466.19	−1.75	a''
11	200.06	−21.05	a''
12	147.55	−0.61	a''

3.4.2.2. Formation enthalpy, $\Delta_f H$(0 K). The high-level W3X-L for this species with T_1 = 0.037 returns $\Delta_f H^o$(0 K) = 159.2 kJ mol^{-1} (154.2 kJ mol^{-1} at 298.15 K). The multi-composite result shows a large uncertainty 150.8 ± 18.2 kJ mol^{-1} largely due to the G4 value, the omission of which value gives 158.8 ± 4.5 kJ mol^{-1} and WMS/W2X values of 162.5 kJ mol^{-1}/168 kJ mol^{-1} round out the picture.

3.4.2.3. Results. A relaxed potential energy scan about the HOOC dihedral, mode no. 11, is well-behaved but not that about (H)OOCO, which leads to dissociation to O_2 + CO + OH$^\bullet$. Hence, a simple hindered rotor anharmonic treatment is used.

T (K)	$S^o(T)$	$C_p^o(T)$	$H^o(T) - H^o(0)$
298.15	317.89	84.90	17.62
300.	318.42	85.13	17.78
400.	344.46	95.75	26.86
500.	366.65	103.01	36.82
600.	385.91	108.06	47.38
700.	402.86	111.78	58.38
800.	417.98	114.70	69.71
900.	431.64	117.13	81.30
1000.	444.09	119.23	93.12
1100.	455.54	121.13	105.14
1200.	466.16	122.87	117.34
1300.	476.06	124.49	129.71
1400.	485.34	126.01	142.23
1500.	494.08	127.44	154.90
1600.	502.35	128.78	167.72
1800.	517.66	131.19	193.72
2000.	531.59	133.20	220.16

3.4.3. Carbonoperoxyl

^2A g = 2 C_1 σ = 1 M_0 = 77.0165

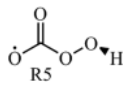

Saenz Méndez *et al.* identified two radicals [SEV09] derived from carbonoperoxoic acid by removal of the carboxylic hydrogen (**R5** and **R6**). Only the non-planar **R5** exists at our chosen DFT and basis set combination, B3LYP/cc-pVTZ+d.

3.4.3.1. Species data.

8	−1.641 354	−0.566 943	0.007 271
8	−0.529 957	1.242 612	0.006 074
6	−0.534 940	−0.005 688	−0.001 312
8	0.576 535	−0.766 846	−0.002 007
8	1.736 579	0.089 345	−0.110 061
1	2.075 220	0.048 781	0.797 650
B (GHz)	12.579	4.607 6	3.408 8

No.	$\bar{\upsilon}$ (cm^{-1})	x_{ii}
1	3732.42	−82.44
2	1521.25	−7.29
3	1407.32	−9.26
4	1201.35	6.53
5	1008.48	−5.64
6	923.36	−2.24
7	739.64	0.51
8	633.10	−0.59
9	521.26	−0.44
10	262.89	−0.63
11	211.72	−12.53
12	139.78	−2.20

3.4.3.2. Formation enthalpy, $\Delta_f H(0\ K)$. A direct comparison, via multi-composite calculations, with the cognate radical **R1** below suggests a difference of 88.48 ± 4.48 kJ mol^{-1} so that $\Delta_f H^o(0\ K) = -243.5 \pm 4.9$ kJ mol^{-1} (−249.9 kJ mol^{-1} at 298.15 K) is indicated for **R5**.

3.4.3.3. Results. Hindered rotor analysis reveals two significant modes, nos. 12 and 11, which have some impact, given the reduced barrier height (*V*/*RT*) values of 9.5 and 3.5, respectively. However, a relaxed potential energy scan about the O=C–OO(H) bond leads to dissociation, so only a single hindered rotor, mode no. 11, is included in the anharmonic treatment, inclusion of which negates the optical isomer correction.

T (K)	$S^o(T)$	$C_p^o(T)$	$H^o(T) - H^o(0)$
298.15	316.38	74.11	16.24
300.	316.84	74.32	16.38
400.	339.76	85.22	24.37
500.	359.75	93.84	33.34
600.	377.43	99.99	43.05
700.	393.18	104.20	53.27
800.	407.30	107.09	63.85
900.	420.04	109.15	74.66
1000.	431.62	110.70	85.66
1100.	442.23	111.93	96.79
1200.	452.01	112.95	108.03
1300.	461.09	113.82	119.37
1400.	469.55	114.58	130.79
1500.	477.48	115.26	142.28
1600.	484.94	115.87	153.84
1800.	498.65	116.93	177.12
2000.	511.02	117.82	200.59

References for Carbonoperoxyl.

SEV09 P. Saenz Méndez, L. A. Eriksson, and O. N. Ventura, "Theoretical study of the structure of neutral, radical and anionic monoperoxo carbonic acid," J. Mol. Struct.: THEOCHEM **913**(1), 131–138 (2009).

3.4.4. Carboxydioxy

$^2A'$ g = 2 C_S σ = 1 M_0 = 77.0165

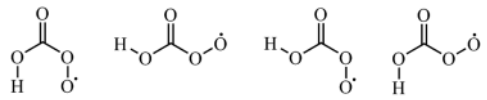

R1 R2 R3 R4

Saenz Méndez *et al.* have identified six radicals [SEV09] derived from carbonoperoxoic acid, four (**R1–R4**) resulting from removal of the peroxylic hydrogen, and two derived from removal of the carboxylic hydrogen (**R5–R6**). The first set can be further described as *aa*, *ss*, *sa*, and *as*; **R2** lies at +11.25 ± 0.83 kJ mol^{-1}, **R3** at +15.28 ± 0.70 kJ mol^{-1}, and **R4** at +17.01 ± 0.78 kJ mol^{-1} relative to the ground state **R1**.

3.4.4.1. Species data.

1	1.384 524	−0.620 324	0.000 000
8	1.282 265	0.357 964	0.000 000
8	−0.590 759	1.623 402	0.000 000
6	0.000 000	0.603 579	0.000 000
8	−0.801 157	−0.633 067	0.000 000
8	−0.063 415	−1.723 444	0.000 000
B (GHz)	11.459	4.911 6	3.438 0

No.	$\bar{\nu}$ (cm^{-1})	x_{ii}	
1	3477.60	−142.15	a'
2	1966.28	−11.88	a'
3	1392.27	−15.21	a'
4	1201.67	−3.68	a'
5	1122.36	−2.78	a'
6	766.54	−4.50	a'
7	633.40	−1.13	a'
8	513.13	−1.90	a'
9	383.74	−0.91	a'
10	749.65	−10.63	a''
11	719.53	−2.34	a''
12	189.47	−1.04	a''

3.4.4.2. Formation enthalpy, $\Delta_f H(0\ K)$. An isodesmic reaction **R1** + CH_4 = $CH_3OO\bullet$ + HCOOH featuring reference values for methane (−66.550 ± 0.057 kJ mol^{-1}), methyl peroxy (22.29 ± 0.49 kJ mol^{-1}), and *syn*-formic acid (−371.06 ± 0.22 kJ mol^{-1}) has a reaction enthalpy of +49.71 ± 1.76 kJ mol^{-1}; this leads to $\Delta_f H^o(0\ K) = -331.9 \pm 1.8$ kJ mol^{-1} (−341.5 kJ mol^{-1} at 298.15 K)—in good agreement with a W3X-L of $\Delta_f H^o(0\ K) = -334.8$ kJ mol^{-1} (−344.2 kJ mol^{-1} at 298.15 K).

3.4.4.3. Results. Hindered rotor analysis reveals two significant modes, nos. 1 and 6, which, however, have little impact, given the reduced barrier height *V*/*RT* values of 15.8 and 32.8, respectively.

T (K)	$S°(T)$	$C_p°(T)$	$H°(T) - H°(0)$
298.15	295.18	69.03	14.20
300.	295.61	69.29	14.32
400.	317.32	81.73	21.90
500.	336.64	91.31	30.57
600.	353.97	98.69	40.09
700.	369.63	104.50	50.26
800.	383.91	109.19	60.95
900.	397.00	113.05	72.07
1000.	409.08	116.31	83.54
1100.	420.30	119.11	95.31
1200.	430.77	121.56	107.35
1300.	440.59	123.72	119.61
1400.	449.83	125.64	132.08
1500.	458.56	127.36	144.73
1600.	466.83	128.90	157.54
1800.	482.16	131.52	183.59
2000.	496.14	133.62	210.11

References for Carboxydioxy.

SEV09 P. Saenz Méndez, L. A. Eriksson, and O. N. Ventura, "Theoretical study of the structure of neutral, radical and anionic monoperoxo carbonic acid," J. Mol. Struct.: THEOCHEM **913**(1), 131–138 (2009).

3.4.5. Dioxiraneperoxyl; dioxymethylenebisoxy

$^2A''$ g = 2 C_S σ = 1 M_0 = 77.0165

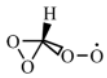

There are two conformers with the H–C–O–O• dihedral at either 0° or 180°, with the former as the ground state and the latter at +5.42 ± 0.62 kJ mol^{-1}.

3.4.5.1. Species data.

6	0.299 562	0.336 005	0.000 000
8	−0.326 513	1.277 938	0.758 662
8	−0.326 513	1.277 938	−0.758 662
1	1.380 705	0.236 191	0.000 000
8	−0.326 513	−0.936 616	0.000 000
8	0.582 278	−1.900 788	0.000 000
B (GHz)	18.895	3.636 2	3.390 3

No.	$\bar{\upsilon}$ (cm^{-1})	x_{ii}	
1	3156.07	−57.46	a'
2	1416.27	−4.98	a'
3	1299.97	−3.22	a'
4	1175.29	−6.71	a'
5	1007.43	−7.47	a'
6	825.15	−3.14	a'
7	513.01	−0.61	a'
8	400.00	−0.92	a'
9	1183.49	−6.35	a''
10	908.74	−2.28	a''
11	431.45	−0.22	a''
12	67.83	0.17	a''

3.4.5.2. Formation enthalpy, $\Delta_f H$(0 K).

An isodesmic reaction featuring reference values for methane (−66.550 ± 0.057 kJ mol^{-1}) and methyl peroxy (22.29 ± 0.49 kJ mol^{-1}) as well as dioxirane (9.45 ± 0.55 kJ mol^{-1})

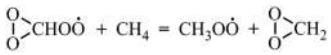

has a reaction enthalpy of 49.02 ± 1.76 kJ mol^{-1}, which yields $\Delta_f H°$(0 K) = 49.29 ± 1.91 kJ mol^{-1} (41.7 kJ mol^{-1} at 298.15 K). A very similar number is obtained of $\Delta_f H°$(0 K) = 49.96 ± 1.92 kJ mol^{-1} if ethane (−68.33 ± 0.3 kJ mol^{-1})/ethyl peroxy chaperones are used instead, but with the Klippenstein *et al.* value of −5.80 ± 1 kJ mol^{-1} for the ethyl peroxy radical [KHR17] and the reaction enthalpy of 22.02 ± 1.53 kJ mol^{-1}. The inverse-variance weighted average and uncertainty is $\Delta_f H°$(0 K) = 49.63 ± 1.35 kJ mol^{-1}.

A W3X-L value of $\Delta_f H°$(0 K) = 50.1 kJ mol^{-1} (42.3 kJ mol^{-1} at 298.15 K) rounds out the picture for this radical with a T_1 of 0.029.

3.4.5.3. Results.

Hindered rotor analysis identifies mode no. 12 as important, contributing +1.3 J K^{-1} mol^{-1} to the room temperature entropy. A relaxed potential energy scan shows a barrier of 19.3 kJ mol^{-1}.

T (K)	$S^o(T)$	$C_p^o(T)$	$H^o(T) - H^o(0)$
298.15	303.37	69.96	14.89
300.	303.80	70.22	15.02
400.	325.84	83.18	22.71
500.	345.53	93.17	31.55
600.	363.20	100.47	41.25
700.	379.11	105.80	51.58
800.	393.51	109.79	62.37
900.	406.63	112.88	73.51
1000.	418.65	115.34	84.92
1100.	429.74	117.34	96.56
1200.	440.02	119.00	108.37
1300.	449.61	120.40	120.35
1400.	458.57	121.60	132.45
1500.	467.00	122.64	144.66
1600.	474.94	123.54	156.97
1800.	489.58	125.05	181.83
2000.	502.83	126.27	206.96

References for dioxiraneperoxyl; dioxymethylenebisoxy.

KHR17 S. J. Klippenstein, L. B. Harding, and B. Ruscic, "*Ab initio* computations and active thermochemical tables hand in hand: Heats of formation of core combustion species," J. Phys. Chem. A **121**(35), 6580–6602 (2017).

3.4.6. Hydrogentrioxide oxomethyl

^{2}A g = 2 C_1 σ = 1 M_0 = 77.0165

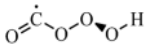

A radical of formyl hydrotrioxide, the conformer with an OOOH dihedral of 85.2°, is the ground state, which lies 2.3 ± 0.6 kJ mol^{-1} below the state with an OOOH dihedral of −90.8°.

3.4.6.1. Species data.

8	0.163 981	0.533 097	0.401 628
8	2.216 811	−0.279 825	0.034 637
6	1.092 877	−0.141 590	−0.294 693
8	−1.111 245	0.523 405	−0.347 867
8	−1.805 760	−0.627 498	0.028 298
1	−2.267 569	−0.343 894	0.834 592
B (GHz)	21.884 4	2.860 6	2.698 9

No.	$\bar{\upsilon}$ (cm^{-1})	x_{ii}	No.	$\bar{\upsilon}$ (cm^{-1})	x_{ii}
1	3687.94	−87.17	7	632.34	−4.54
2	1867.48	−14.18	8	486.19	10.60
3	1431.99	−12.13	9	425.88	−4.93
4	1005.60	−9.77	10	319.39	−0.25
5	967.00	−4.53	11	240.95	0.54
6	733.99	−3.81	12	92.48	−1.28

3.4.6.2. Formation enthalpy, $\Delta_f H$(0 K).

An isodesmic reaction that makes use of our value for hydroperoxyoxomethyl (−74.4 ± 1.2 kJ mol^{-1}) together with reference values for water (−238.931 ± 0.027 kJ mol^{-1}) and hydrogen peroxide (−129.472 ± 0.064 kJ mol^{-1})

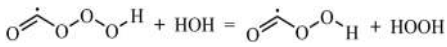

has an enthalpy change of 58.05 ± 1.13 kJ mol^{-1}; this gives rise to $\Delta_f H^o$(0 K) = −23.0 ± 1.7 kJ mol^{-1} (−29.0 kJ mol^{-1} at 298.15 K). This compares to a multi-composite result of −20.6 ± 3.5 kJ mol^{-1}.

3.4.6.3. Results.

The relaxed potential energy scans are compromised, so a default RR anharmonic treatment is used.

T (K)	$S^o(T)$	$C_p^o(T)$	$H^o(T) - H^o(0)$
298.15	319.83	81.14	16.84
300.	320.34	81.39	16.99
400.	345.37	92.51	25.71
500.	366.87	99.94	35.36
600.	385.56	104.94	45.62
700.	402.02	108.56	56.30
800.	416.71	111.41	67.31
900.	429.98	113.82	78.57
1000.	442.08	115.91	90.06
1100.	453.22	117.75	101.74
1200.	463.53	119.35	113.60
1300.	473.14	120.72	125.60
1400.	482.13	121.89	137.73
1500.	490.57	122.86	149.97
1600.	498.53	123.66	162.29
1800.	513.17	124.80	187.15
2000.	526.35	125.47	212.18

3.4.7. Oxomethyltrioxy

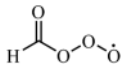

In a photochemical study [KBWJ04] of benzoyl, Kolano *et al.* discussed a simpler model system, namely, diformyl tetraoxide that can dissociate to *E* and *Z* formylperoxy radicals or disproportionate to formyloxy and formyltrioxy radicals,

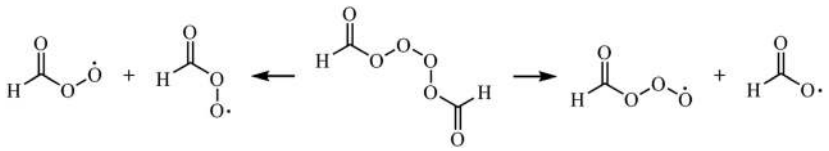

They reported that oxomethyltrioxy is not a minimum at B3LYP/6-31+G(d) and it is not at our chosen protocol either.

References for oxomethyltrioxy.

KBWJ04 C. Kolano, G. Bucher, H. H. Wenk, M. Jäger, O. Schade, and W. Sander, "Photochemistry of 9-fluorenone oxime phenylglyoxylate: A combined TRIR, TREPR and *ab initio* study," J. Phys. Org. Chem. **17**(3), 207–214 (2004).

3.5. $C_1H_1O_5$

3.5.1. Carbonodiperoxoic acid radical

$^2A''$ g = 2 C_S σ = 1 M_0 = 77.0165

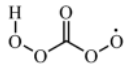

The *saa* conformer HOCO/OOCO/OCOO• is the lowest in energy and is considered *here*.

3.5.1.1. Species data.

6	0.000 000	0.111 107	0.000 000
8	−0.744 590	−0.993 344	0.000 000
8	−2.141 198	−0.654 030	0.000 000
8	1.324 033	−0.356 535	0.000 000
8	2.196 572	0.640 410	0.000 000
1	−2.109 794	0.326 271	0.000 000
8	−0.371 093	1.239 384	0.000 000
B (GHz)	11.303	2.460 3	2.020 5

No.	$\bar{\upsilon}$ (cm^{-1})	x_{ii}	
1	3544.72	−96.75	a'
2	1876.36	−10.82	a'
3	1498.14	−9.25	a'
4	1221.54	−5.69	a'
5	1139.75	−5.53	a'
6	986.81	−3.28	a'
7	947.25	−1.67	a'
8	722.87	−0.89	a'
9	487.05	−1.54	a'
10	381.54	−0.27	a'
11	260.31	0.02	a'
12	724.79	−0.23	a''
13	367.30	−33.09	a''
14	178.84	−0.46	a''
15	102.41	−0.43	a''

3.5.1.2. Formation enthalpy, $\Delta_f H$(0 K). A multi-composite calculation returns $\Delta_f H^\circ$(0 K) = −215.7 ± 5.7 kJ mol^{-1} (−222.1 kJ mol^{-1} at 298.15 K).

3.5.1.3. Results. Hindered rotor analysis identifies two cases, mode nos. 1 and 4, whose reduced barrier heights (V/RT)s of 7.9 and 9.2, respectively, indicate small impact at room temperature. The relaxed potential energy scans of the O=COO•, the (H)OOC=O, and HOOC dihedrals (mode nos. 15, 14, and 13) are well-behaved.

T (K)	$S^\circ(T)$	$C_p^\circ(T)$	$H^\circ(T) - H^\circ(0)$
298.15	341.79	100.90	20.58
300.	342.41	101.14	20.76
400.	373.16	112.73	31.48
500.	399.32	121.55	43.21
600.	422.07	127.92	55.70
700.	442.15	132.46	68.73
800.	460.07	135.74	82.15
900.	476.20	138.15	95.85
1000.	490.85	139.95	109.76
1100.	504.26	141.33	123.82
1200.	516.60	142.39	138.01
1300.	528.03	143.23	152.29
1400.	538.67	143.90	166.65
1500.	548.62	144.45	181.06
1600.	557.96	144.90	195.53
1800.	575.07	145.62	224.58
2000.	590.44	146.18	253.76

3.5.2. Formylhydrotetroxide radical

^2A g = 2 C_1 σ = 1 M_0 = 77.0165

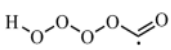

3.5.2.1. Species data.

6	1.588 113	0.085 074	0.269 021
8	2.640 836	−0.424 047	0.114 666
8	0.600 451	0.104 068	−0.636 976
8	−0.543 837	0.888 684	−0.088 459
8	−1.322 972	0.049 986	0.661 146
8	−2.200 911	−0.677 841	−0.209 057
1	−2.917 203	−0.037 245	−0.344 681
B(GHz)	13.073 2	1.793 6	1.746 1

No.	$\bar{\upsilon}$ (cm^{-1})	x_{ii}
1	3713.26	−83.45
2	1866.76	−14.40
3	1401.19	−11.10
4	1000.00	−9.11
5	942.98	−2.68
6	826.09	−3.91
7	684.45	−2.34
8	621.38	−3.48
9	559.71	−4.75
10	392.96	−29.96
11	333.82	−11.86
12	302.13	−0.79
13	237.60	0.58
14	154.59	−0.74
15	60.28	−0.53

3.5.2.2. Formation enthalpy, $\Delta_f H(0\ K)$. A multi-composite value of 26.5 ± 10.0 kJ mol^{-1} (19.4 kJ mol^{-1} at 298.15 K) shows a large scatter, whereas the isodesmic reaction

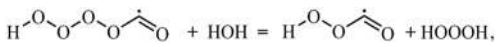

which utilizes our W3X-L value for hydroperoxyoxomethyl (−74.4 ± 1.2 kJ mol^{-1}) as well as reference values for water (−238.931 ± 0.027 kJ mol^{-1}) and dihydrogen trioxide (−81.43 ± 0.7 kJ mol^{-1}), gives $\Delta_f H°(0\ K)$ = 28.0 ± 2.2 kJ mol^{-1} (21.5 kJ mol^{-1} at 298.15 K) from the reaction enthalpy of 55.09 ± 1.68 kJ mol^{-1}. WMS returns 24.9 kJ mol^{-1} for this T_1 = 0.024 radical.

The aldehydic C–H bond dissociation energy of 415 kJ mol^{-1} is somewhat stronger than the same bond in formic acid [BEG94] BDE [H–C(O)OH] = 404 kJ mol^{-1}.

3.5.2.3. Results. Four hindered rotors are identifiable associated with mode nos. 15, 14, 13, and 11. The relaxed potential energy scans are problematic and are not considered with instead of a default rigid rotor anharmonic treatment.

T (K)	$S°(T)$	$C_p°(T)$	$H°(T) - H°(0)$
298.15	352.08	102.91	20.50
300.	352.71	103.23	20.69
400.	384.43	116.76	31.74
500.	411.40	124.51	43.84
600.	434.50	128.60	56.52
700.	454.50	130.67	69.49
800.	472.03	131.72	82.62
900.	487.58	132.32	95.82
1000.	501.54	132.76	109.07
1100.	514.22	133.18	122.37
1200.	525.82	133.62	135.71
1300.	536.54	134.10	149.09
1400.	546.49	134.59	162.52
1500.	555.79	135.09	176.01
1600.	564.53	135.57	189.54
1800.	580.55	136.46	216.74
2000.	594.97	137.20	244.11

References for formylhydrotetroxide radical.

BEG94 J. Berkowitz, G. B. Ellison, and D. Gutman, "Three methods to measure RH bond energies," J. Phys. Chem. **98**, 2744 (1994).

3.6. $C_1H_2O_1$

3.6.1. Hydroxymethylene singlet syn/anti; triplet

$^1A'$ g = 1 C_S σ = 1 M_0 = 30.0263;

^3A g = 3 C_1 σ = 1 M_0 = 30.0263

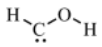

Hydroxymethylene has been isolated in helium nanodroplets following from the pyrolysis of glyoxylic acid. The singlets result from the photo-dissociation of hydroxymethyl, $\dot{C}H_2OH$, beyond its electronic ground state [LMSD14]. *Syn* and *anti* (shown) conformers of the singlet exist, whereas the triplet has a *gauche* configuration with a dihedral of 109°.

3.6.1.2. Species data.

	anti				*syn*				*triplet*		
8	0.121 774	−0.565 560	0.0	8	0.010 693	−0.568 965	0.0	8	−0.588 335	−0.127 321	−0.018 748
6	0.121 774	0.740 446	0.0	6	0.010 693	0.741 902	0.0	6	0.717 819	0.109 873	−0.127 816
1	−0.947 946	1.072 927	0.0	1	−1.078 187	0.978 450	0.0	1	1.466 047	−0.272 212	0.568 609
1	−0.756 887	−0.991 123	0.0	1	0.928 478	−0.878 146	0.0	1	−1.066 278	0.631 541	0.348 270
B (GHz)	290.31	36.551	32.464	*B* (GHz)	281.37	36.483	32.297	*B* (GHz)	359.86	32.150	31.732

anti				*syn*				*triplet*			
No.	$\bar{\upsilon}$ (cm^{-1})	x_{ii}		No.	$\bar{\upsilon}$ (cm^{-1})	x_{ii}		No.	$\bar{\upsilon}$ (cm^{-1})	x_{ii}	
1	3696.93	−98.32	a'	1	3522.9	−124.58	a'	1	3657.38	−117.52	a
2	2832.95	−66.66	a'	2	2751.04	−73.49	a'	2	3051.05	−75.22	a
3	1508.06	−0.66	a'	3	1475.28	0.22	a'	3	1301.78	−8.54	a
4	1326.04	−10.83	a'	4	1334.38	−9.61	a'	4	1155.73	−10.27	a
5	1216.88	−6.11	a'	5	1221.1	−5.51	a'	5	1077.66	−6.10	a
6	1092.65	−9.55	a''	6	1019.85	−7.97	a''	6	456.92	−32.08	a

3.6.1.2. Formation enthalpy, $\Delta_f H(0\ \mathrm{K})$. A composite, convergent, statistically calibrated coupled-cluster based treatment of the *anti* gave 112.3 ± 1.3 kJ mol^{-1} (108.4 kJ mol^{-1} at 298.15 K) in an application of the FPD method [FPD12]. Vogiatzis *et al.* reported [VHK14] an atomization energy from interference-corrected explicitly correlated second-order perturbation theory of 1276.9 kJ mol^{-1}, which equates to $\Delta_f H^\circ(0\ \mathrm{K})$ = 113.4 kJ mol^{-1} for the *anti* conformer.

Nguyen and Stanton [NS15] used their HEAT-345(Q) formulation to compute energy differences relative to O ($^1\Delta_g$) and methane to yield $\Delta_f H^\circ(0\ \mathrm{K})$ = 112.8 kJ mol^{-1} and $\Delta_f H(0\ \mathrm{K})$ = 131.3 kJ mol^{-1} for the *anti* and *syn* conformers, respectively.

W3X-L results are as follows: for the *anti* of 111.6 kJ mol^{-1} (107.8 kJ mol^{-1} at 298.15 K), for the *syn* comformer of 129.9 kJ mol^{-1} (126.1 kJ mol^{-1} at 298.15 K), and for the triplet of 217.1 kJ mol^{-1} (214.3 kJ mol^{-1} at 298.15 K).

These results can be summarized as the *anti* at $\Delta_f H^\circ(0\ \mathrm{K})$ = 112.2 ± 1.0 kJ mol^{-1}, the *syn* at $\Delta_f H^\circ(0\ \mathrm{K})$ = 130.2 ± 0.9 kJ mol^{-1}, and the triplet at $\Delta_f H^\circ(0\ \mathrm{K})$ = 217.1 ± 1.5 kJ mol^{-1}, all of which are in good agreement with ATcT that lists the *anti* at $\Delta_f H^\circ(0\ \mathrm{K})$ = 112.70 ± 0.28 kJ mol^{-1}, the *syn* at $\Delta_f H^\circ(0\ \mathrm{K})$ = 131.12 ± 0.29 kJ mol^{-1}, and the triplet at $\Delta_f H^\circ(0\ \mathrm{K})$ = 219.3 ± 1.1 kJ mol^{-1}.

3.6.1.3. Results. In all three cases, mode no. 6 is replaced by a hindered rotor and the remaining modes are treated as anharmonics; good agreement for the singlets with data in the 3rd Millennium Database [GBR18], viz., S° = 225.212 J K^{-1} mol^{-1}, C_p° = 36.066 J K^{-1} mol^{-1}, and $H(T)$-$H(0)$ = 10.059 kJ mol^{-1} for the *anti* and S° = 225.93 J K^{-1} mol^{-1}, C_p° = 36.260 J K^{-1} mol^{-1}, and $H(T) - H(0)$ = 10.075 kJ mol^{-1} for the *syn* is obtained. As regards the triplet state, there is good agreement [GMG12] with Goldsmith *et al.* S° (298.15 K) of 243.9 ± 1.7 J K^{-1} mol^{-1} and C_p° (300 K) of 42.7 ± 1.3 J K^{-1} mol^{-1}.

	anti			*syn*			*triplet*		
T (K)	$S^\circ(T)$	$C_p^\circ(T)$	$H^\circ(T) - H^\circ(0)$	$S^\circ(T)$	$C_p^\circ(T)$	$H^\circ(T) - H^\circ(0)$	$S^\circ(T)$	$C_p^\circ(T)$	$H^\circ(T) - H^\circ(0)$
298.15	225.10	36.58	10.08	225.27	36.62	10.08	244.12	42.70	10.99
300.	225.33	36.66	10.15	225.50	36.70	10.15	244.39	42.78	11.07
400.	236.58	42.01	14.07	236.76	42.10	14.08	257.32	47.26	15.58
500.	246.58	47.83	18.56	246.80	47.99	18.58	268.30	51.22	20.50
600.	255.78	53.09	23.61	256.03	53.34	23.66	277.94	54.50	25.80
700.	264.31	57.54	29.15	264.60	57.88	29.22	286.55	57.25	31.39
800.	272.24	61.23	35.10	272.59	61.65	35.20	294.35	59.61	37.23
900.	279.63	64.28	41.37	280.03	64.77	41.53	301.50	61.70	43.30
1000.	286.54	66.82	47.93	287.00	67.37	48.14	308.09	63.55	49.56
1100.	293.01	68.97	54.72	293.52	69.55	54.99	314.23	65.21	56.00
1200.	299.09	70.80	61.71	299.65	71.39	62.04	319.97	66.70	62.60
1300.	304.82	72.37	68.87	305.43	72.98	69.26	325.36	68.03	69.33
1400.	310.24	73.73	76.18	310.89	74.34	76.62	330.45	69.23	76.20
1500.	315.37	74.93	83.61	316.06	75.54	84.12	335.26	70.31	83.17
1600.	320.24	75.99	91.16	320.97	76.59	91.73	339.83	71.29	90.25
1800.	329.29	77.76	106.54	330.10	78.36	107.23	348.33	72.97	104.68
2000.	337.56	79.20	122.24	338.43	79.78	123.04	356.09	74.36	119.42

References for hydroxymethylene *syn/anti/triplet*.

LMSD14 C. M. Leavitt, C. P. Moradi, J. F. Stanton, and G. E. Douberly, "Helium nanodroplet isolation and rovibrational spectroscopy of hydroxymethylene," J. Chem. Phys. **140**, 171102 (2014).

FPD12 D. Feller, K. A. Peterson, and D. A. Dixon, "Further benchmarks of a composite, convergent, statistically calibrated coupled-cluster-based approach for thermochemical and spectroscopic studies," Mol. Phys. **110**, 2381–2399 (2012).

NS15 T. L. Nguyen and J. F. Stanton, "A steady-state approximation to the two-dimensional master equation for chemical kinetics calculations," J. Phys. Chem. A **119**(28), 7627–7636 (2015).

VHK14 K. D. Vogiatzis, R. Haunschild, and W. Klopper, "Accurate atomization energies from combining coupled-cluster computations with interference-corrected explicitly correlated second-order perturbation theory," Theor. Chem. Acc. **133**, 1446 (2014).

GBR18 E. Goos, A. Burcat, and B. Ruscic, "Extended third Millennium ideal gas and condensed phase thermochemical database for combustion with updates from active thermochemical tables," Mirrored at http://garfield.chem.elte.hu/Burcat/burcat.html; 12 January 2018.

GMG12 C. F. Goldsmith, G. R. Magoon, and W. H. Green, "Database of small molecule thermochemistry for combustion," J. Phys. Chem. A **116**(36), 9033–9057 (2012).

3.6.2. Methanal; formaldehyde

$^1A_1$ g = 1 C_{2v} σ = 2 M_0 = 30.0263

There are too many possible references for this very well-known molecule, suffice it to say that it is encountered in tropospheric emissions, planetary surfaces, and non-thermal plasmas as well as the usual combustion environments [ZLSP17, DPSH17, O16, S03].

3.6.2.1. Species data.

8	0.000 000	0.000 000	0.673 127
6	0.000 000	0.000 000	−0.526 010
1	0.000 000	0.937 251	−1.114 477
1	0.000 000	−0.937 251	−1.114 477
B (GHz)	285.452	39.151 8	34.429 5

No.	$\bar{\upsilon}$ (cm^{-1})	x_{ii}	
1	2877.04	−30.71	a_1
2	1824.03	−9.34	a_1
3	1536.41	0.90	a_1
4	1202.70	−2.94	b_1
5	2930.94	−36.32	b_2
6	1268.23	−2.04	b_2

3.6.2.2. Formation enthalpy, $\Delta_f H(0\ K)$. Flame calorimetric measurements by Fletcher and Pilcher [FP70] gave a heat of combustion at 298.15 K of −570.77 ± 0.42 kJ mol^{-1} that translates to $\Delta_f H^o$(298.15 K) = −108.6 ± 0.7 kJ mol^{-1}. Recent high-quality theoretical calculations included those of Martin *et al.* [KRMR06] of −109.18 kJ mol^{-1}, of da Silva *et al.* [SBSB06] of −109.0 ± 1.8 kJ mol^{-1}, and probably the most comprehensive and careful focal-point analysis [CMSC08] by Czakó *et al.* of −109.23 ± 0.33 kJ mol^{-1}. Published W3X-L values of −109.8 kJ mol^{-1} (−105.9 kJ mol^{-1} at 0 K) are in very good agreement [SS16].

The ATcT value of $\Delta_f H^o$(0 K) = −105.347 ± 0.098 kJ mol^{-1} (−109.186 kJ mol^{-1} at 298.15 K) is based on a very large number of determinations, the most important contribution, which amounts to 22% of the provenance, comes from the focal-point analysis study [CMSC08].

3.6.2.3. Results. Excellent agreement with the literature [C63, GVA89] is obtained, viz., entropies of 218.95 and 218.760 J K^{-1} mol^{-1}, specific heats of 35.402 and 35.387 J K^{-1} mol^{-1}, and enthalpy functions of 10.01 and 10.020 kJ mol^{-1}, all at 298.15 K

T (K)	$S^o(T)$	$C_p^o(T)$	$H^o(T) - H^o(0)$
298.15	218.58	35.20	10.00
300.	218.80	35.25	10.07
400.	229.40	38.87	13.76
500.	238.54	43.25	17.87
600.	246.82	47.65	22.41
700.	254.48	51.76	27.39
800.	261.64	55.45	32.75
900.	268.36	58.72	38.46
1000.	274.70	61.58	44.48
1100.	280.69	64.07	50.76
1200.	286.36	66.23	57.28
1300.	291.73	68.10	64.00
1400.	296.84	69.72	70.89
1500.	301.70	71.14	77.94
1600.	306.33	72.38	85.11
1800.	314.98	74.41	99.80
2000.	322.91	76.00	114.84

References for methanal; formaldehyde.

ZLSP17 P. Zoogman, X. Liu, R. M. Suleiman, W. F. Pennington, D. E. Flittner, J. A. Al-Saadi, B. B. Hilton, D. K. Nicks, M. J. Newchurch, J. L. Carr, S. J. Janz, M. R. Andraschko, A. Arola, B. D. Baker, B. P. Canova, C. Chan Miller, R. C. Cohen, J. E. Davis, M. E. Dussault, D. P. Edwards, J. Fishman, A. Ghulam, G. González Abad, M. Grutter, J. R. Herman, J. Houck, D. J. Jacob, J. Joiner, B. J. Kerridge, J. Kim, N. A. Krotkov, L. Lamsal, C. Li, A. Lindfors, R. V. Martin, C. T. McElroy, C. McLinden, V. Natraj, D. O. Neil, C. R. Nowlan, E. J. O'Sullivan, P. I. Palmer, R. B. Pierce, M. R. Pippin, A. Saiz-Lopez, R. J. D. Spurr, J. J. Szykman, O. Torres, J. P. Veefkind, B. Veihelmann, H. Wang, J. Wang, and K. Chance, "Tropospheric emissions: Monitoring of

pollution (TEMPO)," J. Quant. Spectrosc. Radiat. Transfer **186**, 17–39 (2017).

DPSH17 M. L. Delitsky, D. A. Paige, M. A. Siegler, E. R. Harju, D. Schriver, R. E. Johnson, and P. Travnicek, "Ices on Mercury: Chemistry of volatiles in permanently cold areas of Mercury's north polar region," Icarus **281**, 19–31 (2017).

O16 R. Ono, "Optical diagnostics of reactive species in atmospheric-pressure nonthermal plasma," J. Phys. D: Appl. Phys. **49**(8), 083001-1–083001-34 (2016).

S03 J. M. Simmie, "Detailed chemical kinetic models for the combustion of hydrocarbon fuels," Prog. Energy Combust. Sci. **29**(6), 599–634 (2003).

FP70 R. A. Fletcher and G. Pilcher, "Measurements of heats of combustion by flame calorimetry. Part 6. Formaldehyde, glyoxal," Trans. Faraday Soc. **66**, 794–799 (1970).

KRMR06 A. Karton, E. Rabinovich, J. M. L. Martin, and B. Ruscic, "W4 theory for computational thermochemistry: In pursuit of confident sub-kJ/mol predictions," J. Chem. Phys. **125**, 144108 (2006).

SBSB06 G. da Silva, J. W. Bozzelli, N. Sebbar, and H. Bockhorn, "Thermodynamic and *ab initio* analysis of the controversial enthalpy of formation of formaldehyde," Chem. Phys. Chem. **7**, 1119–1126 (2006).

CMSC08 G. Czakó, E. Mátyus, A. C. Simmonett, A. G. Császár, H. F. Schaefer, and W. D. Allen, "Anchoring the absolute proton affinity scale," J. Chem. Theor. Comput. **4**(8), 1220–1229 (2008).

SS16 J. M. Simmie and J. N. Sheahan, "Validation of a database of formation enthalpies and of mid-level model chemistries," J. Phys. Chem. A **120**, 7370–7384 (2016).

C63 *NIST-JANAF Thermochemical Tables*, 4th ed., Journal of Physical and Chemical Reference Data Monographs Vol. 9, editor by M. W.ChaseJr. (U.S. Dept. of Commerce, Gaithersburg, MD, 1963).

GVA89 L. V. Gurvich, I. V. Veyts, and C. B. Alcock, *Thermodynamic Properties of Individual Substances: Elements and Compounds* (Hemisphere, New York, 1989), Vol. 2.

3.7. $C_1H_2O_2$

3.7.1. Dihydroxycarbene; dihydroxymethylene

$^1A_1$ g = 1 C_{2v} σ = 2 M_0 = 46.0257

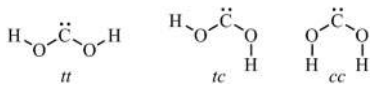

The singlet carbene produced via pyrolysis of oxalic acid, in its *trans/trans* and *trans/cis* forms, has recently had its IR laser Stark spectrum explored in helium nanodroplets [BMMSD15]. In a molecular dynamics simulation of the classic Urey–Miller experiment, the carbene was seen as an intermediate in the reaction between CO and H_2O leading to the amino acid, glycine [WTML14]. The singlet-triplet gap is known to be large, favoring the singlet [AE18, VPAD17]. Conformationally, the most stable is the *tt* followed by the *ct* and *cc*.

3.7.1.1. Species data.

6	0.000 000	0.000 000	0.558 763
8	0.000 000	1.051 376	−0.249 001
8	0.000 000	−1.051 376	−0.249 001
1	0.000 000	1.831 200	0.315 723
1	0.000 000	−1.831 200	0.315 723
B (GHz)	85.332	11.998 4	10.519 3

No.	$\bar{\upsilon}$ (cm^{-1})	x_{ii}	
1	3828.47	−41.68	a_1
2	1423.91	−5.11	a_1
3	1141.27	−3.12	a_1
4	644.08	−0.05	a_1
5	666.48	0.18	a_2
6	733.42	−3.42	b_1
7	3823.74	−41.38	b_2
8	1347.92	−7.45	b_2
9	1133.15	−4.02	b_2

3.7.1.2. Formation enthalpy, Δ_fH(0 K).

A W3X-L calculation returns Δ_fH^o(0 K) = −200.1 kJ mol^{-1} (−206.2 kJ mol^{-1} at 298.15 K) for the lowest conformer *tt*, which is in excellent agreement with a multi-composite value of Δ_fH^o(0 K) = −199.5 ± 2.1 kJ mol^{-1}. These are also in very good agreement with HEAT-345(Q) calculations [NLMMS15], a high-level extrapolated thermochemical procedure, which has Δ_fH^o(0 K) = −199.12 kJ mol^{-1} (−206.20 kJ mol^{-1} at 298.15 K). Values of −197.7 kJ mol^{-1} and −199.5 kJ mol^{-1} have also been derived by Schreiner and Reisenauer [SR08]. The *ct* and *cc* conformers lie 3.1 kJ mol^{-1} and 32.8 kJ mol^{-1} higher, in good agreement with the literature [NLMMS15] values of 2.85 kJ mol^{-1} and 31.94 kJ mol^{-1}.

3.7.1.3. Results.

A standard anharmonic oscillator hindered rotor treatment is employed replacing mode nos. 5 and 6 that are anti-symmetric and symmetric HO–CO rotors, respectively.

T (K)	$S^o(T)$	$C_p^o(T)$	$H^o(T) - H^o(0)$
298.15	253.83	48.87	12.15
300.	254.13	49.03	12.24
400.	269.42	57.60	17.58
500.	283.10	65.01	23.72
600.	295.49	70.94	30.53
700.	306.80	75.68	37.87
800.	317.17	79.58	45.63
900.	326.74	82.89	53.76
1000.	335.62	85.77	62.20
1100.	343.92	88.32	70.90
1200.	351.70	90.59	79.85
1300.	359.04	92.61	89.01
1400.	365.96	94.39	98.36
1500.	372.53	95.97	107.88
1600.	378.77	97.35	117.55
1800.	390.37	99.58	137.25
2000.	400.95	101.24	157.34

References for dihydroxycarbene; dihydroxymethylene.

BMMSD15 B. M. Broderick, L. McCaslin, C. P. Moradi, J. F. Stanton, and G. E. Douberly, "Reactive intermediates in ^{4}He nanodroplets: Infrared laser Stark spectroscopy of dihydroxycarbene," J. Chem. Phys. **142**(14), 144309 (2015).

WTML14 L.-P. Wang, A. Titov, R. McGibbon, F. Liu, V. S. Pande, and T. J. Martínez, "Discovering chemistry with an *ab initio* nanoreactor," Nat. Chem. **6**(12), 1044–1048 (2014).

AE18 I. Alkorta and J. Elguero, "A LFER analysis of the singlet-triplet gap in a series of sixty-six carbenes," Chem. Phys. Lett. **691**, 33–36 (2018).

VPAD17 M. Vasiliu, K. A. Peterson, A. J. Arduengo, and D. A. Dixon, "Characterization of carbenes via hydrogenation energies, stability, and reactivity: What's in a name?," Chem. - Eur. J. **23**(69), 17556–17565 (2017).

NLMMS15 T. L. Nguyen, H. Lee, D. A. Matthews, M. C. McCarthy, and J. F. Stanton, 8Stabilization of the simplest criegee intermediate from the reaction between ozone and ethylene: A high-level quantum chemical and kinetic analysis of ozonolysis," J. Phys. Chem. A **119**(22), 5524–5533 (2015).

SR08 P. R. Schreiner and H. P. Reisenauer, "Spectroscopic identification of dihydroxycarbene," Angew. Chem., Int. Ed. **47**, 7071–7074 (2008).

3.7.2. Dioxirane

$^1A_1$ g = 1 C_{2v} σ = 2 M_0 = 46.0257

Decomposition of carbonyl oxide via the "ester channel" involves unimolecular isomerization to dioxirane, which then decomposes into smaller species such as CO, CO_2, H, and H_2O [ACB99, NNNN07].

3.7.2.1. Species data.

6	0.000 000	0.000 000	0.730 478
1	0.925 557	0.000 000	1.303 190
1	−0.925 557	0.000 000	1.303 190
8	0.000 000	0.749 045	−0.436 828
8	0.000 000	−0.749 045	−0.436 828
B (GHz)	28.858 2	25.686 1	14.981 1

No.	$\bar{\upsilon}$ (cm^{-1})	x_{ii}	
1	3052.41	−29.10	a_1
2	1548.39	−0.098	a_1
3	1310.82	−3.69	a_1
4	822.93	−3.00	a_1
5	1026.37	−1.19	a_2
6	3145.58	−34.39	b_1
7	1179.98	−1.13	b_1
8	1259.38	−4.33	b_2
9	896.31	−1.71	b_2

3.7.2.2. Formation enthalpy, $\Delta_f H$(0 K).

Recent high-level computation by Klippenstein *et al.* [KHR17] of $\Delta_f H$(0 K) = 8.9 kJ mol^{-1} is in very good agreement with Simmie and Sheahan's [SS16] published W3X-L value of $\Delta_f H^o$(0 K) = 8.8 kJ mol^{-1} (1.1 kJ mol^{-1} at 298.15 K) and with the $\Delta_f H^o$(0 K) = 8.97 kJ mol^{-1} (1.32 kJ mol^{-1} at 298.15 K) from a HEAT calculation [NLMMS15]. These indicate that the ATcT database [RB16] value of 9.45 ± 0.55 kJ mol^{-1} based largely on earlier work by Karton *et al.* [KDM11] in 2011 and Nguyen *et al.* [NNNN07] in 2007 may need slight revision.

3.7.2.3. Results.

Harmonic and anharmonic treatments lead to almost identical results that are slightly lower than the literature values of Dorofeeva [D92]: S^o(298.15 K) = 241.368 J mol^{-1} K^{-1} and C_p^o = 43.877 J mol^{-1} K^{-1}.

T (K)	$S^o(T)$	$C_p^o(T)$	$H^o(T) - H^o(0)$
298.15	240.53	42.00	10.46
300.	240.79	42.16	10.54
400.	254.15	51.13	15.20
500.	266.47	59.43	20.74
600.	277.94	66.37	27.04
700.	288.62	72.08	33.97
800.	298.56	76.81	41.43
900.	307.84	80.76	49.31
1000.	316.53	84.11	57.56
1100.	324.68	86.96	66.11
1200.	332.36	89.40	74.94
1300.	339.60	91.50	83.98
1400.	346.45	93.32	93.23
1500.	352.94	94.90	102.64
1600.	359.11	96.28	112.20
1800.	370.59	98.56	131.69
2000.	381.07	100.34	151.59

References for dioxirane.

ACB99 J. M. Anglada, R. Crehuet, and J. M. Bofill, "The ozonolysis of ethylene: A theoretical study of the gas-phase reaction mechanism," Chem. Eur. J. **5**(6), 1809–1822 (1999).

NNNN07 M. T. Nguyen, T. L. Nguyen, V. T. Ngan, and H. M. T. Nguyen, "Heats of formation of the Criegee formaldehyde oxide and dioxirane," Chem. Phys. Lett. **448**, 183–188 (2007).

KHR17 S. J. Klippenstein, L. B. Harding, and B. Ruscic, "*Ab initio* computations and active thermochemical tables hand in hand: Heats of formation of core combustion species," J. Phys. Chem. A **121**, 6580–6602 (2017).

SS16 J. M. Simmie and J. N. Sheahan, "Validation of a database of formation enthalpies and of mid-level model chemistries," J. Phys. Chem. A **120**, 7370–7384 (2016).

NLMMS15 T. L. Nguyen, H. Lee, D. A. Matthews, M. C. McCarthy, and J. F. Stanton, "Stabilization of the simplest criegee intermediate from the reaction between ozone and ethylene: A high-level quantum chemical and kinetic analysis of ozonolysis," J. Phys. Chem. A **119**(22), 5524–5533 (2015).

RB16 B. Ruscic and D. H. Bross, Active Thermochemical Tables (ATcT) values based on ver. 1.122 of the Thermochemical Network, 2016, available at https://ATcT.anl.gov.

KDM11 A. Karton, S. Daon, and J. M. L. Martin, "W4-11: A high-confidence benchmark dataset for computational thermochemistry derived from first-principles W4 data," Chem. Phys. Lett. **510**, 165–178 (2011).

D92 O. V. Dorofeeva, "Ideal gas thermodynamic properties of oxygen heterocyclic compounds. Part 1. Three-membered, four-membered and five-membered rings," Thermochim. Acta **194**, 9–46 (1992).

3.7.3. Dioxymethane; methylenebis(oxy)

$^3A_2$ g = 3 C_{2v} σ = 2 M_0 = 46.0257;

$^3B_1$ g = 3 C_{2v} σ = 2 M_0 = 46.0257

Carbonyl oxides including dioxymethane or methylenebis(oxy) play important roles in synthetic and mechanistic chemistry [CCA01]. Two electronic states are discernible, which are principally distinguishable by their OCO bond angle with the $^3A_2$ at 107.4° and the $^3B_1$ at 134.4°.

3.7.3.1. Species data.

	$^3A_2$				$^3B_1$		
8	0.000 000	1.067 275	−0.320 875	8	0.000 000	1.203 927	−0.227 695
6	0.000 000	0.000 000	0.463 116	6	0.000 000	0.000 000	0.278 463
8	0.000 000	−1.067 275	−0.320 875	8	0.000 000	−1.203 927	−0.227 695
1	−0.873 261	0.000 000	1.177 647	1	−0.911 519	0.000 000	0.986 170
1	0.873 261	0.000 000	1.177 647	1	0.911 519	0.000 000	0.986 170
B (GHz)	50.129	13.307 9	11.234 8	*B* (GHz)	82.296	10.519 5	9.941 8

No.	$\bar{\upsilon}$ (cm^{-1})	x_{ii}		No.	$\bar{\upsilon}$ (cm^{-1})	x_{ii}	
1	2667.13	−43.86	a_1	1	2380.85	−70.20	a_1
2	1246.97	−2.47	a_1	2	1159.33	−5.63	a_1
3	1113.64	−1.51	a_1	3	974.14	−7.23	a_1
4	567.13	0.64	a_1	4	606.74	0.26	a_1
5	1033.13	−2.93	a_2	5	1401.12	−42.69	a_2
6	2603.60	−62.55	b_1	6	2333.84	−95.26	b_1
7	573.06	25.37	b_1	7	840.42	−0.21	b_1
8	1283.88	−1.16	b_2	8	1438.08	−26.29	b_2
9	1092.19	−10.42	b_2	9	778.22	20.00	b_2

3.7.3.2. Formation enthalpy, $\Delta_f H(0\ K)$. For the ground $^3A_2$ state, an ANL0 calculation [K18] suggests $\Delta_f H^o(0\ K) = 82.5$ kJ mol^{-1}, in good agreement with a W3X-L value of $\Delta_f H(0\ K) = 82.9$ kJ mol^{-1} (75.6 kJ mol^{-1} at 298.15 K), while the $^3B_1$ state is at $\Delta_f H^o(0\ K) = 122.3$ kJ mol^{-1} (115.1 kJ mol^{-1} at 298.15 K).

3.7.3.3. Results. Anharmonic frequencies and a rigid rotor approach are used.

8	0.000 000	0.457 112	0.000 000
6	1.069 517	−0.202 038	0.000 000
8	−1.177 059	−0.193 248	0.000 000
1	1.023 068	−1.283 908	0.000 000
1	1.976 305	0.385 222	0.000 000
B (GHz)	81.325	12.418 7	10.773 5

	$^3A_2$			$^3B_1$		
T (K)	$S^o(T)$	$C_p^o(T)$	$H^o(T) - H^o(0)$	$S^o(T)$	$C_p^o(T)$	$H^o(T) - H^o(0)$
298.15	254.02	47.12	11.05	252.72	46.42	10.91
300.	254.31	47.29	11.14	253.00	46.61	10.99
400.	269.21	56.59	16.34	267.77	56.39	16.15
500.	282.73	64.63	22.41	281.31	65.02	22.23
600.	295.12	71.22	29.22	293.82	72.22	29.10
700.	306.51	76.58	36.61	305.41	78.15	36.63
800.	317.04	80.99	44.50	316.17	83.01	44.70
900.	326.79	84.62	52.78	326.19	87.02	53.20
1000.	335.87	87.64	61.40	335.54	90.34	62.08
1100.	344.35	90.17	70.30	344.28	93.13	71.25
1200.	352.29	92.30	79.42	352.49	95.50	80.69
1300.	359.75	94.11	88.74	360.22	97.54	90.34
1400.	366.78	95.65	98.23	367.51	99.32	100.18
1500.	373.42	96.97	107.86	374.42	100.90	110.20
1600.	379.72	98.12	117.62	380.98	102.31	120.36
1800.	391.39	99.99	137.43	393.17	104.77	141.07
2000.	402.00	101.45	157.58	404.32	106.84	162.23

References for dioxymethane; methylenebis(oxy).

CCA01 D. Cremer, R. Crehuet, and J. Anglada, "The ozonolysis of acetylene-A quantum chemical investigation," J. Am. Chem. Soc. **123**, 6127–6141 (2001).

K18 S. J. Klippenstein (personal communication, 21 December 2018)

3.7.4. Dioxymethyl; methanal oxide; Criegee intermediate

$^1A'$ g = 1 C_S σ = 1 M_0 = 46.0257

As an intermediate in the ozonolysis of ethene, this formaldehyde oxide was postulated by Criegee [C75] and its identity and properties were subsequently confirmed [TMST08, SHWL13].

3.7.4.1. Species data.

3.7.4.2. Formation enthalpy, $\Delta_f H(0\ K)$. The W3X-L protocol gives $\Delta_f H^o(0\ K) = 110.8$ kJ mol^{-1} (103.7 kJ mol^{-1} at 298.15 K), which is in excellent agreement with ATcT of 111.90 ± 0.63 kJ mol^{-1} (104.90 kJ mol^{-1} at 298.15 K).

No.	$\bar{\upsilon}$ (cm^{-1})	x_{ii}	
1	3270.79	−32.42	a'
2	3118.97	−28.53	a'
3	1538.84	−5.71	a'
4	1399.92	−3.58	a'
5	1243.03	−0.45	a'
6	932.52	−7.13	a'
7	931.27	1.11	a'
8	675.00	−3.46	a''
9	531.22	−0.43	a''

3.7.4.3. Results. A relaxed potential energy scan about the C–O bond is problematic; hence, a rigid rotor anharmonic approximation is presented. There is no significant difference (~1 J

mol^{-1} K^{-1} in entropy at 2000 K) between our results and those obtained from the comprehensive analysis of Yu *et al.* utilizing the Lanczos algorithm and a multi-configurational time-dependent Hartree method [HNLDG15].

T (K)	$S^o(T)$	$C_p^o(T)$	$H^o(T) - H^o(0)$
298.15	249.25	47.35	11.10
300.	249.54	47.51	11.19
400.	264.44	56.29	16.39
500.	277.83	63.78	22.40
600.	290.02	69.89	29.10
700.	301.18	74.89	36.34
800.	311.46	79.05	44.05
900.	320.98	82.58	52.13
1000.	329.84	85.59	60.54
1100.	338.12	88.19	69.23
1200.	345.89	90.44	78.17
1300.	353.21	92.41	87.31
1400.	360.12	94.12	96.64
1500.	366.67	95.63	106.13
1600.	372.89	96.96	115.76
1800.	384.44	99.18	135.38
2000.	394.98	100.95	155.40

SHWL13 Y.-T. Su, Y.-H. Huang, H. A. Witek, and Y.-P. Lee, "Infrared absorption spectrum of the simplest criegee intermediate CH_2OO," Science **340**, 174–176 (2013).

HNLDG15 H.-G. Hu, S. Ndengue, J. Li, R. Dawes, and H. Guo, "Vibrational energy levels of the simplest Criegee intermediate (CH_2OO) from full-dimensional Lanczos, MCTDH, and MULTIMODE calculations," J. Chem. Phys. **143**, 084311 (2015).

3.7.5. *Formic acid; methanoic acid* syn/anti

$^1A'$ g = 1 C_S σ = 1 M_0 = 46.0257

This extremely well-known compound, the simplest carboxylic acid, is featured in over 90 000 publications. Formic acid is one of the so-called oxidized volatile organic compounds or OVOCs that are products of the photolysis and oxidation of compounds such as isoprene, which are emitted by forest plants [MJPL15]. It is an intermediate, for example, in the low temperature oxidation of dimethyl ether [NCTSP15] and has been detected in the interstellar medium [VCLB14].

Two conformers exist with the *syn* HOCO ground state lying some 16.9 kJ mol^{-1} below the *anti*.

3.7.5.1. *Species data.*

syn				*anti*			
1	−0.654 054	−1.341 791	0.000 000	1	−1.791 062	−0.274 027	0.000 000
8	−1.027 943	−0.446 436	0.000 000	8	−0.893 754	−0.628 976	0.000 000
8	1.158 010	0.117 914	0.000 000	8	1.176 407	0.202 214	0.000 000
6	0.000 000	0.420 533	0.000 000	6	0.000 000	0.384 279	0.000 000
1	−0.386 484	1.446 769	0.000 000	1	−0.470 163	1.382 451	0.000 000
B (GHz)	78.147	12.062 2	10.449 3	B(GHz)	87.545 5	11.694 3	10.316 2

References for dioxymethyl; methanal oxide; Criegee intermediate.

C75 R. Criegee, "Mechanism of ozonolysis," Angew. Chem., Int. Ed. **14**, 745–752 (1975).

TMST08 C. A. Taatjes, G. Meloni, T. M. Selby, A. J. Trevitt, D. L. Osborn, C. J. Percival, and D. E. Shallcross, "Direct observation of the gas-phase criegee intermediate (CH_2OO)," J. Am. Chem. Soc. **130**(36), 11883–11885 (2008).

syn				*anti*			
No.	$\bar{\upsilon}$ (cm^{-1})	x_{ii}		No.	$\bar{\upsilon}$ (cm^{-1})	x_{ii}	
1	3720.79	−84.98	a'	1	3787.84	−85.21	a'
2	3042.96	−60.98	a'	2	2952.62	−65.41	a'
3	1825.99	−9.36	a'	3	1870.85	−9.53	a'
4	1405.60	−7.78	a'	4	1420.60	1.03	a'
5	1306.00	−6.47	a'	5	1275.07	−11.29	a'
6	1124.79	−5.83	a'	6	1111.17	−4.75	a'
7	630.08	0.52	a'	7	662.00	0.13	a'
8	1055.77	−2.91	a''	8	1036.84	−2.73	a''
9	684.18	−11.28	a''	9	530.33	−15.08	a''

3.7.5.2. Formation enthalpy, $\Delta_f H$(0 K). There are a considerable number of experimental determinations [S59, L64, G74] using a variety of methods for the 298.15 K formation enthalpy ranging from −378.5 ± 0.6 kJ mol^{-1} in 1959 through −379.0 ± 0.6 kJ mol^{-1} in 1964 and −378.6 kJ mol^{-1} in 1974. Many of these results have been subsequently revised by others [B19] employing updated values for vaporization enthalpies.

ATcT v1.122d includes these and cognate results and presents a summary of −378.36 ± 0.22 kJ mol^{-1} with a corresponding $\Delta_f H^\circ$ (0 K) = −371.06 kJ mol^{-1} for the ground state *syn* conformer. The *anti* is placed at −361.96 ± 0.39 kJ mol^{-1} (−354.70 at 0 K).

Purely theoretical values for the *syn* include −378.7 ± 0.4 kJ mol^{-1} at 298.15 K from RQCISD(T)/cc-pV∞QZ//B3LYP/6-311++G(d,p) calculations.

WMS, W2X, and W3X-L return $\Delta_f H^\circ$(0 K) of −372.2, −372.7, and −373.3 kJ mol^{-1}, respectively, for the *syn* and $\Delta_f H^\circ$(0 K) = −355.4, −355.7, and −356.3 kJ mol^{-1} similarly for the *anti*. These can be summarized as follows: *syn* $\Delta_f H^\circ$(0 K) = −372.7 ± 0.6 kJ mol^{-1}, $\Delta_f H^\circ$(298.15 K) = −380.1 ± 0.6 kJ mol^{-1} and *anti* $\Delta_f H^\circ$(0 K) = −355.8 ± 0.5 kJ mol^{-1}, $\Delta_f H^\circ$(298.15 K) = −362.2 ± 0.5 kJ mol^{-1}, which are in reasonable agreement with all extant data.

3.7.5.3. Results. A relaxed potential energy scan of the HOCO dihedral and an HR treatment are used to replace mode no. 9 with all other modes considered as anharmonics.

At 298.15 K, an entropy of 248.70 ± 0.42 J K^{-1} mol^{-1} by Millikan [MP57] and a C_p° of 45.68 ± 0.07 J K^{-1} mol^{-1} by Chao [CHMW86] are usually considered to represent the best known values [B19]; these are in good agreement with those derived *here*. Those given by Fukushima *et al.* [FCZ71], which agree with those given by Chao, are, in fact, for natural formic acid, that is, an equilibrium mixture of *syn* and *anti* and not for pure *syn* as reported here; at or near room temperature, this distinction is slight.

The tabulation of Gurvich *et al.* [GVA89] contains results for *trans*-formic acid, which corresponds to our *anti*-formic acid, for *cis*-formic acid, and for formic acid. Their data for the ground state *cis* or *syn* compare very favorably with those shown here, for example, S° = 248.911 J K^{-1} mol^{-1} as indeed it does for the *anti* conformer, viz., S°(298.15 K) = 248.787 and C_p°(298.15 K) = 45.306 J K^{-1} mol^{-1}.

	syn			*anti*		
T (K)	$S^\circ(T)$	$C_p^\circ(T)$	$H^\circ(T) - H^\circ(0)$	$S^\circ(T)$	$C_p^\circ(T)$	$H^\circ(T) - H^\circ(0)$
298.15	248.56	45.28	10.85	247.92	44.83	10.77
300.	248.84	45.44	10.93	248.19	45.00	10.86
400.	263.19	54.80	15.94	262.44	54.49	15.83
500.	276.38	63.55	21.87	275.57	63.34	21.73
600.	288.64	70.98	28.61	287.80	70.87	28.45
700.	300.06	77.05	36.02	299.21	77.04	35.86
800.	310.68	81.97	43.98	309.84	82.07	43.82
900.	320.57	85.96	52.38	319.75	86.15	52.24
1000.	329.80	89.21	61.14	329.00	89.48	61.03
1100.	338.43	91.86	70.20	337.66	92.19	70.11
1200.	346.52	94.02	79.50	345.78	94.40	79.45
1300.	354.12	95.80	88.99	353.41	96.21	88.98
1400.	361.28	97.27	98.64	360.60	97.69	98.67
1500.	368.03	98.48	108.43	367.38	98.90	108.50
1600.	374.42	99.49	118.33	373.80	99.91	118.45
1800.	386.23	101.06	138.39	385.66	101.45	138.59
2000.	396.94	102.20	158.72	396.41	102.55	158.99

References for formic acid; methanoic acid *syn/anti*.

MJPL15 K. Moshammer, A. W. Jasper, D. M. Popolan-Vaida, A. Lucassen, P. Diévart, H. Selim, A. J. Eskola, C. A. Taatjes, S. R. Leone, S. M. Sarathy, Y. Ju, P. Dagaut, K. Kohse-Höinghaus, and N. Hansen, "Detection and identification of the keto-hydroperoxide ($HOOCH_2OCHO$) and other intermediates during low-temperature oxidation of dimethyl ether," J. Phys. Chem. A **119**(28), 7361–7374 (2015).

NCTSP15 T. B. Nguyen, J. D. Crounse, A. P. Teng, J. M. St. Clair, F. Paulot, G. M. Wolfe, and P. O. Wennberg, Rapid deposition of oxidized biogenic compounds to a temperate forest, Proc. Natl. Acad. Sci. U. S. A. **112**(5), E392–E401 (2015).

VCLB14 C. Vastel, C. Ceccarelli, B. Lefloch, and R. Bachiller, "The origin of complex organic molecules in prestellar cores," Astrophys. J. Lett. **795**, L2 (2014).

S59 G. C. Sinke, "The heat of formation of formic acid," J. Phys. Chem. **63**, 2063 (1959).

L64 N. D. Lebedeva, "Heats of combustion of monocarboxylic acids," Russ. J. Phys. Chem. **38**, 1435–1437 (1964).

G74 J. P. Guthrie, "Hydration of carboxamides. Evaluation of the free energy change for addition of water to acetamide and formamide derivatives," J. Am. Chem. Soc. **96**, 3608–3615 (1974).

B19 D. R. Burgess, Jr., ""Thermochemical data" and Glushko thermocenter, Russian Academy of Sciences, Moscow entropy and heat capacity of organic compounds," in *NIST Chemistry WebBook, NIST Standard Reference Database Number 69*, edited by P. J. Linstrom and W. G. Mallard (National Institute of Standards and Technology, Gaithersburg, MD, 2019) (retrieved October 4, 2019).

MP57 R. C. Millikan and K. S. Pitzer, "Infrared spectra and vibrational assignment of monomeric formic acid," J. Chem. Phys. **27**, 1305–1308 (1957).

CHMW86 J. Chao, K. R. Hall, K. N. Marsh, and R. C. Wilhoit, "Thermodynamic properties of key organic oxygen compounds in the carbon range C1 to C4. Part 2. Ideal gas properties," J. Phys. Chem. Ref. Data **15**, 1369–1436 (1986).

FCZ71 K. Fukushima, J. Chao, and B. J. Zwolinski, "Normal coordinate treatment and thermodynamic properties of the *cis-trans* isomers of formic acid and its deutero-analog," J. Chem. Thermodyn. **3**, 553–562 (1971).

GVA89 L. V. Gurvich, I. V. Veyts, and C. B. Alcock, *Thermodynamic Properties of Individual Substances: Elements and Compounds* (Hemisphere, New York, 1989), Vol 2.

3.7.6. Hydroperoxycarbene; hydroperoxymethylene

$^1A'$ g = 1 C_S σ = 1 M_0 = 46.0257

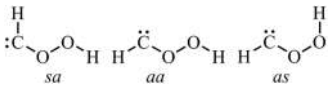

Global reaction route mapping by Ohno and Maeda [OM06] on the potential energy surfaces of formic acid revealed three conformers of hydroperoxycarbene with the *syn/anti* ground state followed by the *anti/anti* at +51.2 kJ mol^{-1} and finally the *anti/syn* at +64.0 kJ mol^{-1} based on HCOO and COOH dihedrals in sequence. Their work utilized B3LYP/6-311++G(d,p) geometries and energies, and our multi-composite results are not dissimilar, 0 kJ mol^{-1}: +64.4 kJ mol^{-1}: +74.2 kJ mol^{-1}.

In contrast, Richardson *et al.* reported [RRS99] relative energies in the order *sa* at 0, *as* at +43.1 kJ mol^{-1}, and *ss* at +48.1 kJ mol^{-1}. Gutbrod *et al.* ruled out the participation of the carbene as an intermediate in the ozonolysis of alkenes [GSKC96], while Chen *et al.* and Lakshmanan and colleagues found that the *as* conformer is an intermediate in the reaction of methylene with oxygen on a singlet surface [CAHK02, LPMH18], but it is featured as an intermediate by Womack *et al.* although it was not detected in their fast-flow reactor study [WMBFM15].

3.7.6.1. Species data.

1	1.706 623	−0.405 848	0.000 000
6	1.168 510	0.551 803	0.000 000
8	0.000 000	0.655 566	0.000 000
8	−0.866 794	−0.939 908	0.000 000
1	−1.783 333	−0.630 234	0.000 000
B (GHz)	61.916	9.797 6	8.459 0

No.	$\bar{\upsilon}$ (cm^{-1})	x_{ii}	
1	3771.84	−78.92	a'
2	3000.16	−72.69	a'
3	1827.64	−19.57	a'
4	1029.52	−9.27	a''
5	912.51	−12.30	a'
6	407.38	−7.23	a'
7	335.94	−1.22	a'
8	830.01	−3.50	a''
9	161.76	12.70	a''

3.7.6.2. Formation enthalpy, $\Delta_f H(0\ K)$.

Richardson *et al.* placed hydroperoxyl carbene at 52 kJ mol^{-1} above dioxirane, implying $\Delta_f H^o(0\ K) \sim 61$ kJ mol^{-1}. A W3X-L calculation gives $\Delta_f H^o(0\ K) = 68.8$ kJ mol^{-1} (64.5 kJ mol^{-1} at 298.15 K) for this $T_1 = 0.034$ species; W2X and WMS values of 77.8 kJ mol^{-1} and 74.3 kJ mol^{-1} bracket the multi-composite, *sans* G3, of 73.3 ± 4.6 kJ mol^{-1}.

3.7.6.3. Results.

A relaxed potential energy scan of mode no. 9 (C–O–O–H) coupled with anharmonic frequencies is employed *here*.

T (K)	$S^o(T)$	$C_p^o(T)$	$H^o(T) - H^o(0)$
298.15	268.84	60.77	13.81
300.	269.22	60.92	13.92
400.	287.78	68.18	20.39
500.	303.64	73.94	27.51
600.	317.54	78.55	35.14
700.	329.94	82.36	43.19
800.	341.16	85.61	51.59
900.	351.41	88.44	60.30
1000.	360.86	90.91	69.27
1100.	369.63	93.07	78.47
1200.	377.81	94.92	87.87
1300.	385.47	96.49	97.44
1400.	392.67	97.81	107.16
1500.	399.45	98.91	116.99
1600.	405.87	99.81	126.93
1800.	417.71	101.16	147.03
2000.	428.42	102.08	167.36

References for hydroperoxycarbene; hydroperoxymethylene.

OM06 K. Ohno and S. Maeda, "Global reaction route mapping on potential energy surfaces of formaldehyde, formic acid, and their metal-substituted analogues," J. Phys. Chem. A **110**(28), 8933–8941 (2006).

RRS99 N. A. Richardson, J. C. Rienstra-Kiracofe, and H. F. Schaefer, "Examining trends in the tetravalent character of group 14 elements (C, Si, Ge, Sn, Pb) with acids and hydroperoxides," J. Am. Chem. Soc. **121**(46), 10813–10819 (1999).

GSKC96 R. Gutbrod, R. N. Schindler, E. Kraka, and D. Cremer, "formation of OH radicals in the gas phase ozonolysis of alkenes: The unexpected role of carbonyl oxides," Chem. Phys. Lett. **252**(3), 221–229 (1996).

CAHK02 B.-Z. Chen, J. M. Anglada, M.-B. Huang, and F. Kong, "The reaction of CH_2 ($X\ ^3B_1$) with O_2 ($X\ ^3$): A theoretical CASSCF/CASPT2 investigation," J. Phys. Chem. A **106**(9), 1877–1884 (2002).

LPMH18 S. Lakshmanan, S. Pratihar, F. B. C. Machado, and W. L. Hase, "Direct dynamics simulation of the thermal $^3CH_2 + {}^3O_2$ reaction. Rate constant and product branching ratios," J. Phys. Chem. A **122**(21), 4808–4818 (2018).

WMBFM15 C. C. Womack, M.-A. Martin-Drumel, G. G. Brown, R. W. Field, and M. C. McCarthy, "Observation of the simplest Criegee intermediate CH_2OO in the gas-phase ozonolysis of ethylene," Sci. Adv. **1**(2), e1400105 (2015).

3.8. $C_1H_2O_3$

3.8.1. Carbonic acid

$^1A_1$ g = 1 C_{2v} σ = 2 M_0 = 62.0251

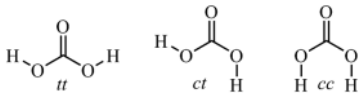

In contrast to many of the other species mentioned *here*, carbonic acid has been widely studied in solution and in the solid state because of its key role in life processes. However, it has until recently been quite difficult to prepare and characterize spectroscopically in the gas-phase despite its importance in ocean acidification [B16], for example, or the continuing unsuccessful efforts to detect it in the atmosphere of the Earth and other planets [GH16].

Of the three possible conformers, the one in which both O=C–O–H dihedrals are *trans* lies much higher in energy than the lowest *cis/cis*. The *cis/trans* conformer lies 6.49 kJ mol^{-1} above the *cc* with a rotational barrier of 39.7 kJ mol^{-1} separating them [RWS14]; experiments [BSKL10] show a 10:1 ratio at 210 K.

3.8.1.1. Species data.

6	0.000 000	0.000 000	0.101 910
8	0.000 000	0.000 000	1.304 449
8	0.000 000	1.088 341	−0.679 517
8	0.000 000	−1.088 341	−0.679 517
1	0.000 000	1.851 216	−0.087 392
1	0.000 000	−1.851 216	−0.087 392
B (GHz)	11.996 4	11.280 9	5.813 8

No.	$\bar{\upsilon}$ (cm^{-1})	x_{ii}	
1	3797.00	−40.90	a_1
2	1835.81	−8.82	a_1
3	1293.38	−4.89	a_1
4	977.59	−1.25	a_1
5	546.61	0.18	a_1
6	528.99	−2.70	a_2
7	801.48	0.22	b_1
8	598.79	−6.79	b_1
9	3794.20	−40.66	b_2
10	1463.67	−5.40	b_2
11	1153.27	−4.02	b_2
12	602.34	0.43	b_2

3.8.1.2. Formation enthalpy, $\Delta_f H$(0 K).

An isodesmic reaction

$$O = C(OH)_2 + O = CH_2 = 2HC(O)OH$$

has an averaged reaction enthalpy of −33.36 ± 0.26 kJ mol^{-1}, which coupled with the reference values for formaldehyde (−105.32 ± 0.11 kJ mol^{-1}) and *syn* formic acid (−371.12 ± 0.22 kJ mol^{-1}) yields $\Delta_f H^o$(0 K) = −603.6 ± 0.4 kJ mol^{-1}, which is in very good agreement with the ATcT value of −602.78 ± 0.79 kJ mol^{-1}; however, the self-same reaction is employed in ATcT (albeit with different approaches to calculating the reaction enthalpies), which contributes approximately 13% toward the final outcome and so the agreement cannot be regarded as totally independent.

Multi-composite atomization gives $\Delta_f H^o$(0 K) = −605.4 ± 4.0 kJ mol^{-1}, and W3X-L returns $\Delta_f H^o$(0 K) = −605.5 kJ mol^{-1} (−614.9 kJ mol^{-1} at 298.15 K).

3.8.1.3. Results.

Hindered rotor analysis identifies mode nos. 6 and 8, with the former having a higher impact near room temperature. Starting from the lowest energy conformer, *cc*, a relaxed potential energy scan reveals a barrier of 44 kJ mol^{-1} leading to the *ct* at +6.3 kJ mol^{-1}.

T (K)	$S^o(T)$	$C_p^o(T)$	$H^o(T) - H^o(0)$
298.15	267.36	66.23	13.10
300.	267.77	66.51	13.23
400.	288.72	79.04	20.54
500.	307.39	88.10	28.92
600.	324.08	94.97	38.09
700.	339.15	100.37	47.86
800.	352.85	104.72	58.13
900.	365.39	108.24	68.78
1000.	376.95	111.12	79.75
1100.	387.66	113.47	90.99
1200.	397.62	115.39	102.43
1300.	406.92	116.96	114.05
1400.	415.64	118.26	125.82
1500.	423.83	119.33	137.70
1600.	431.56	120.21	149.68
1800.	445.81	121.57	173.86
2000.	458.67	122.54	198.28

References for carbonic acid.

B16 J. M. Buth, "Ocean acidification: Investigation and presentation of the effects of elevated carbon dioxide levels on seawater chemistry and calcareous organisms," J. Chem. Educ. **93**(4), 718–721 (2016).

GH16 S. Ghoshal and M. K. Hazra, "Impact of OH radical-initiated H_2CO_3 degradation in the Earth's atmosphere via proton-coupled electron transfer mechanism," J. Phys. Chem. A **120**(4), 562–575 (2016).

RWS14 H. P. Reisenauer, J. P. Wagner, and P. R. Schreiner, "Gas-phase preparation of carbonic acid and its monomethyl ester," Angew. Chem., Int. Ed. **53**(44), 11766–11771 (2014).

BSKL10 J. Bernard, M. Seidl, I. Kohl, K. R. Liedl, E. Mayer, O. Gálvez, H. Grothe, and T. Loerting, "Spectroscopic observation of matrix-isolated carbonic acid trapped from the gas phase," Angew. Chem., Int. Ed. **49**, 1939 (2010).

3.8.2. *Dioxiranol; hydroxydioxirane* syn/anti

^{1}A g = 1 C_S σ = 1 M_0 = 62.0251

It has been suggested that a dioxirane is a possible intermediate in the chemistry of peroxy acids even though there is no experimental or theoretical evidence for such a claim [PYP00]. The HOCH *anti* conformer is more stable than the *syn* by some 16.71 kJ mol^{-1}, and a relaxed scan faces a barrier of 27.3 kJ mol^{-1}.

3.8.2.1. Species data.

	anti				*syn*		
1	−1.574 959	0.585 854	0.000 000	1	0.635 261	1.995 738	0.000 000
8	−0.788 415	1.149 035	0.000 000	8	0.854 846	1.059 615	0.000 000
6	0.303 245	0.354 947	0.000 000	6	−0.284 805	0.319 609	0.000 000
8	0.303 245	−0.803 563	0.757 833	8	−0.284 805	−0.830 485	0.757 590
8	0.303 245	−0.803 563	−0.757 833	8	−0.284 805	−0.830 485	−0.757 590
1	1.210 880	0.949 188	0.000 000	1	−1.208 317	0.897 444	0.000 000
B (GHz)	20.240	8.090 5	6.807 3	*B* (GHz)	20.809	8.012 9	6.693 3

	anti				*syn*		
No.	$\bar{\upsilon}$ (cm^{-1})	x_{ii}		No.	$\bar{\upsilon}$ (cm^{-1})	x_{ii}	
1	3762.26	−82.28	a'	1	3842.00	−82.12	a'
2	3158.56	−58.11	a'	2	3092.42	−62.01	a'
3	1467.39	−9.18	a'	3	1492.63	−1.98	a'
4	1318.36	−3.46	a'	4	1348.85	−2.06	a'
5	1303.99	−3.87	a'	5	1235.05	−7.24	a'
6	1101.90	−3.09	a'	6	1107.35	−2.79	a'
7	819.26	−2.79	a'	7	817.66	−2.68	a'
8	555.65	0.79	a'	8	576.46	0.29	a'
9	1177.52	−5.55	a''	9	1172.75	−6.18	a''
10	845.53	−1.13	a''	10	874.49	−1.67	a''
11	546.11	−6.44	a''	11	495.60	−0.64	a''
12	375.12	−0.02	a''	12	128.01	101.56	a''

3.8.2.2. Formation enthalpy, $\Delta_f H$(0 K). An isodesmic reaction

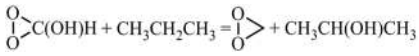

provides a reaction enthalpy of 59.41 ± 1.03 kJ mol^{-1}, which allied with reference ATcT values for propane (−82.75 ± 0.19 kJ mol^{-1}), dioxirane (9.41 ± 0.54 kJ mol^{-1}), and 2-propanol (−248.77 ± 0.36 kJ mol^{-1}) yields $\Delta_f H°$(0 K) = −216.0 ± 1.3 kJ mol^{-1} (−226.2 kJ mol^{-1} at 298.15 K). The direct comparison *anti syn* then gives $\Delta_f H°$(0 K) = −216.0 + 16.7 = −199.3 kJ mol^{-1} for the *syn* conformer (−209.4 kJ mol^{-1} at 298.15 K). An ANL0 value has been reported of −216.0 kJ mol^{-1} presumably for the *anti* conformer [KHR17].

3.8.2.3. Results. The highly anharmonic mode no. 12 for the *syn* is replaced by a hindered rotor treatment via a relaxed potential energy scan of the HOCH dihedral, as is also the case for the *anti*.

	anti			*syn*		
T (K)	$S°(T)$	$C_p°(T)$	$H°(T) - H°(0)$	$S°(T)$	$C_p°(T)$	$H°(T) - H°(0)$
298.15	268.25	58.82	12.31	268.39	58.84	12.34
300.	268.61	59.09	12.42	268.75	59.11	12.44
400.	287.62	73.52	19.06	287.75	73.44	19.08
500.	305.39	85.75	27.05	305.50	85.59	27.06
600.	321.89	94.98	36.11	321.95	94.75	36.10
700.	337.05	101.58	45.95	337.08	101.27	45.92
800.	350.94	106.27	56.36	350.92	105.89	56.29
900.	363.66	109.71	67.17	363.60	109.25	67.05
1000.	375.37	112.35	78.27	375.25	111.80	78.11
1100.	386.18	114.47	89.62	386.00	113.82	89.39
1200.	396.21	116.25	101.15	395.98	115.50	100.86
1300.	405.58	117.80	112.86	405.28	116.92	112.48
1400.	414.36	119.17	124.70	413.99	118.17	124.23
1500.	422.63	120.42	136.68	422.18	119.26	136.10
1600.	430.44	121.55	148.78	429.91	120.25	148.08
1800.	444.87	123.54	173.29	444.17	121.93	172.30
2000.	457.98	125.23	198.17	457.09	123.33	196.83

References for dioxiranol; hydroxydioxirane *syn/anti*.

PYP00 N. A. Porter, H. Yin, and D. A. Pratt, "The peroxy acid dioxirane equilibrium: Base-promoted exchange of peroxy acid oxygens," J. Am. Chem. Soc. **122**(45), 11272–11273 (2000).

KHR17 S. J. Klippenstein, L. B. Harding, and B. Ruscic, "*Ab initio* computations and active thermochemical tables hand in hand: Heats of formation of core combustion species," J. Phys. Chem. A **121**(35), 6580–6602 (2017).

3.8.3. Dioxyhydroxymethyl

$^1A'$ g = 1 C_S σ = 1 M_0 = 62.0251

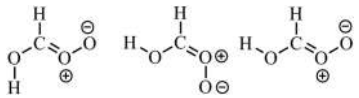

Three conformers exist of this dipolar compound [YYKY97] of which the *anti/anti* (dihedrals HOCH/OCOO) is the ground state with the *ss* at +8.1 kJ mol^{-1} and the *sa* at +12.0 kJ mol^{-1}. Attempts to optimize the *anti/syn* results in a facile H-atom transfer to form peroxyformic acid instead,

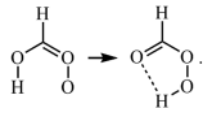

3.8.3.1. Species data.

1	−1.882 858	0.672 140	0.000 000
8	−1.125 024	1.278 111	0.000 000
8	−0.009 205	−0.653 519	0.000 000
6	0.000 000	0.591 060	0.000 000
1	0.927 960	1.147 442	0.000 000
8	1.253 591	−1.295 334	0.000 000
B (GHz)	62.607	4.703 1	4.3745

No.	$\bar{\upsilon}$ (cm^{-1})	x_{ii}	
1	3726.46	−83.27	a'
2	3213.04	−55.07	a'
3	1615.57	−9.64	a'
4	1377.76	−4.12	a'
5	1315.10	−3.09	a'
6	1159.50	−3.39	a'
7	841.09	−6.16	a'
8	573.49	−0.70	a'
9	324.35	−0.31	a'
10	971.51	−5.79	a''
11	585.48	−20.01	a''
12	245.37	−1.81	a''

3.8.3.2. Formation enthalpy, $\Delta_f H$(0 K). The isodesmic reaction

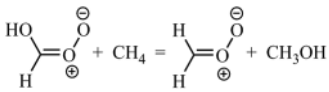

has a reaction enthalpy of 84.5 ± 2.9 kJ mol^{-1}, which leads to $\Delta_f H^o$(0 K) = −96.0 ± 2.9 kJ mol^{-1} based on ATcT reference chaperones methane (−66.550 ± 0.057 kJ mol^{-1}), dioxymethyl (111.90 ± 0.63 kJ mol^{-1}), and methanol (−189.95 ± 0.15 kJ mol^{-1}). This is in very good agreement with a direct atomization W3X-L value of −97.6 kJ mol^{-1}, which, in turn, is in agreement with a multi-composite value of −97.5 ± 2.9 kJ mol^{-1}. Summarizing the values of $\Delta_f H^o$(0 K) = −97.2 ± 1.4 kJ mol^{-1} (−106.1 kJ mol^{-1} at 208.15 K) can be framed.

3.8.3.3. Results. Hindered rotor analysis identifies two modes, nos. 12 and 11, whose reduced barrier height (V/RT) values are 28.7 and 17.3, respectively, impacting on the calculation of thermochemical parameters—neither has any significant impact. In addition, a relaxed scan about OCOO results in structural changes that vitiate the scan.

T (K)	$S^o(T)$	$C_p^o(T)$	$H^o(T) - H^o(0)$
298.15	275.87	63.99	13.67
300.	276.27	64.21	13.79
400.	296.31	75.37	20.78
500.	314.17	84.75	28.80
600.	330.33	92.44	37.67
700.	345.07	98.78	47.24
800.	358.61	104.05	57.39
900.	371.13	108.44	68.02
1000.	382.75	112.08	79.05
1100.	393.58	115.10	90.41
1200.	403.70	117.60	102.05
1300.	413.20	119.66	113.91
1400.	422.13	121.35	125.97
1500.	430.55	122.75	138.17
1600.	438.51	123.90	150.51
1800.	453.21	125.60	175.46
2000.	466.50	126.69	200.70

References for dioxyhydroxymethyl.

YYKY97 Y. Yoshioka, D. Yamaki, S. Kubo, M. Nishino, K. Yamaguchi, K. Mizuno, and I. Saito, "Theoretical study on electronic structures of oxygenated dipoles and mechanisms of ozonolysis reaction," Electron. J. Theor. Chem. **2**, 236–252 (1997).

3.8.4. Hydroxyhydroperoxycarbene

^{1}A′ g = 1 C_S σ = 1 M_0 = 62.0251

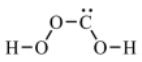

The *asa* conformer (dihedrals HOOC, OOCO, and OCOH in sequence) is the lowest singlet ground state.

3.8.4.1. Species data.

6	−0.974 814	0.173 094	0.000 000
8	0.000 000	0.915 494	0.000 000
8	−0.802 625	−1.126 629	0.000 000
1	−1.670 833	−1.547 267	0.000 000
8	1.494 811	0.151 442	0.000 000
1	1.982 232	0.986 245	0.000 000
B (GHz)	19.054	6.692 1	4.942 7

No.	$\bar{\nu}$ (cm^{-1})	x_{ii}	
1	3800.12	−77.78	a'
2	3785.04	−73.74	a'
3	1598.63	−30.29	a'
4	1283.49	−11.22	a'
5	1193.48	−5.90	a'
6	1100.01	−6.36	a'
7	694.81	−1.57	a'
8	411.82	−1.31	a'
9	231.40	−0.03	a'
10	651.69	−8.71	a''
11	469.81	−2.01	a''
12	183.09	27.55	a''

3.8.4.2. Formation enthalpy, $\Delta_f H$(0 K). A W3X-L atomization calculation gives $\Delta_f H^o$(0 K) = −144.6 kJ mol^{-1} (−151.5 kJ mol^{-1} at 298.15 K), which is in accord with the −142.3 ± 2.1 kJ mol^{-1} computed from a W3X-L reaction enthalpy of 54.12 kJ mol^{-1} for the isodesmic reaction

$$:C(OH)(OOH) + H^{\cdot} = :C(H)(OH) + {}^{\cdot}OOH$$

with an assumed uncertainty of ±2 kJ mol^{-1} for the reaction enthalpy and reference values for H-atom (216.034 kJ mol^{-1}), *anti*-hydroxymethylene (112.7 ± 0.28 kJ mol^{-1}), and the hydroperoxyl radical (15.12 ± 0.12 kJ mol^{-1}).

3.8.4.3. Results. Hindered rotor analysis identifies three modes impacting on the computed properties with mode no. 12 having the greater role. Our results are based on replacing mode no. 12 with a hindered rotor and anharmonic vibrations.

T (K)	$S^o(T)$	$C_p^o(T)$	$H^o(T) - H^o(0)$
298.15	290.78	74.42	15.64
300.	291.24	74.62	15.78
400.	314.02	83.63	23.72
500.	333.42	90.21	32.43
600.	350.33	95.25	41.71
700.	365.33	99.28	51.44
800.	378.81	102.65	61.54
900.	391.07	105.56	71.95
1000.	402.33	108.14	82.64
1100.	412.75	110.47	93.57
1200.	422.45	112.57	104.72
1300.	431.54	114.50	116.08
1400.	440.09	116.27	127.62
1500.	448.17	117.90	139.33
1600.	455.83	119.41	151.19
1800.	470.05	122.11	175.35
2000.	483.04	124.46	200.01

3.8.5. Methylenetrioxygen

$^1A_1$ g = 1 C_{2v} σ = 2 M_0 = 62.0251

This species is mentioned as an intermediate (**IM2**) in a theoretical study [LLWA01] of the reaction O_3 + : CH_2 but is otherwise unknown.

3.8.5.1. Species data.

6	0.000 000	0.000 000	1.283 021
8	0.000 000	0.000 000	−0.011 380
1	0.000 000	0.973 517	1.737 792
1	0.000 000	−0.973 517	1.737 792
8	0.000 000	1.176 033	−0.692 667
8	0.000 000	−1.176 033	−0.692 667
B (GHz)	12.326	10.950	5.798 7

No.	$\bar{\upsilon}$ (cm^{-1})	x_{ii}	
1	3188.30	−26.48	a_1
2	1432.96	−7.23	a_1
3	1334.54	−7.37	a_1
4	812.35	−2.70	a_1
5	495.85	−1.47	a_1
6	506.37	−0.90	a_2
7	755.34	6.85	b_1
8	570.50	−1.35	b_1
9	3364.60	−30.61	b_2
10	1219.39	0.39	b_2
11	775.93	0.40	b_2
12	506.64	0.42	b_2

3.8.5.2. Formation enthalpy, $\Delta_f H(0\ K)$. A 0 K value of 421.0 kJ mol^{-1} can be extracted from the G3B3 calculations [LLWA01], which is in accord with a G4(0 K) of 422.1 kJ mol^{-1}; large changes in geometry are apparent during the multiple optimizations in the CBS-APNO and G3 methods, which result in considerable scatter in the final multi-composite approach 420.2 ± 9.9 kJ mol^{-1}. A W3X-L result of $\Delta_f H^o$(0 K) = 423.0 kJ mol^{-1} (413.3 kJ mol^{-1} at 298.15 K) represents probably the best value for this species with a T_1 of 0.055; WMS concurs with 423.7 kJ mol^{-1}.

A C–H bond dissociation energy of 487 kJ mol^{-1} can be estimated, which is somewhat stronger than the corresponding bond in ethylene [L07] of 464 kJ mol^{-1}.

3.8.5.3. Results. Hindered mode no. 12 with a reduced barrier height V/RT of 33.6 has very little impact on the computed thermochemical quantities, which is fortunate since potential energy scans are compromised.

T (K)	$S^o(T)$	$C_p^o(T)$	$H^o(T) - H^o(0)$
298.15	266.48	63.83	12.88
300.	266.88	64.10	13.00
400.	287.15	76.80	20.07
500.	305.35	86.25	28.25
600.	321.74	93.33	37.25
700.	336.55	98.81	46.86
800.	350.05	103.20	56.97
900.	362.42	106.83	67.48
1000.	373.84	109.90	78.32
1100.	384.44	112.52	89.44
1200.	394.33	114.78	100.81
1300.	403.60	116.74	112.39
1400.	412.31	118.46	124.15
1500.	420.54	119.96	136.07
1600.	428.33	121.28	148.14
1800.	442.75	123.49	172.62
2000.	455.85	125.25	197.50

References for methylenetrioxygen.

LLWA01 L.-C. Li, X.-W. Liao, X. Wang, and .-M. ATian, "*Ab initio* investigation on reaction of ozone with singlet carbene," Huaxue Xuebao **59**(4), 516–519 (2001).

L07 Y. R. Luo, *Comprehensive Handbook of Chemical Bond Energies* (CRC Press, Boca Raton, USA, 2007).

3.8.6. "Oxo formic acid"

^1A g = 1 C_1 σ = 1 M_0 = 62.0251

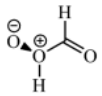

In an automated reaction discovery of the unimolecular decomposition pathways of a γ-keto-hydroperoxide, Grambow *et al.* [GJLG18] reported the formation of a zwitterionic species as a product at B3LYP/6-31+G* (but see also the work of Maeda and Harabuchi [MH19]):

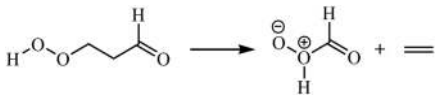

Although probably not a kinetically significant route for this, technically a γ-aldo-hydroperoxide, it is interesting and novel that ethene is being eliminated from non-terminal carbon-atom positions.

Convergence at B3LYP/6-31+G* or a number of other basis sets could not be achieved *here*, but using the functional M06-2X, convergence [MH19] at cc-pVTZ + d was possible and that is reported *here*.

3.8.6.1. Species data.

8	−1.597 380	−0.011 195	−0.292 633
8	0.513 718	0.572 035	0.276 432
6	−0.619 285	−0.285 355	0.295 358
1	−0.357 435	−1.147 509	0.904 229
8	1.545 038	−0.359 302	−0.266 764
1	0.382 137	1.247 339	−0.412 657
B (GHz)	29.852	5.407 3	5.070 0

No.	$\bar{\upsilon}$ (cm^{-1})	x_{ii}
1	3719.29	−71.03
2	3197.67	2.40
3	1932.35	−8.41
4	1365.46	−5.46
5	1208.10	−7.00
6	1051.25	−6.17
7	999.24	0.97
8	869.33	−21.36
9	810.27	−5.04
10	565.26	0.30
11	370.39	−1.97
12	59.34	2.10

3.8.6.2. Formation enthalpy, $\Delta_f H$(0 K). A formation enthalpy of $\Delta_f H^\circ$(0 K) = −54.3 kJ mol^{-1} (−63.1 kJ mol^{-1} at 298.15 K) based on the M06-2X geometry is calculated by W3X-L, in agreement with a WMS of −54.2 kJ mol^{-1}. All of the usual composite methods fail, except for CBS-APNO.

3.8.6.3. Results. A standard RR anharmonic treatment is employed using scaled, by 0.98, M06-2X/cc-pVTZ + d frequencies. A hindered rotor analysis suggests little impact from mode no. 2, rotation about OO–CH, reinforced by the fact that a scan fails.

T (K)	$S^\circ(T)$	$C_p^\circ(T)$	$H^\circ(T) - H^\circ(0)$
298.15	290.06	60.76	13.76
300.	290.44	60.97	13.87
400.	309.49	71.74	20.52
500.	326.49	80.67	28.16
600.	341.85	87.80	36.59
700.	355.84	93.57	45.67
800.	368.65	98.35	55.27
900.	380.48	102.39	65.31
1000.	391.45	105.89	75.73
1100.	401.69	108.95	86.48
1200.	411.29	111.66	97.51
1300.	420.32	114.06	108.80
1400.	428.85	116.21	120.31
1500.	436.94	118.13	132.03
1600.	444.62	119.84	143.93
1800.	458.91	122.71	168.19
2000.	471.96	124.96	192.96

References for "oxo formic acid".

GJLG18 C. A. Grambow, A. Jamal, Y.-P. Li, W. H. Green, J. Zádor, and Y. V. Suleimanov, "Unimolecular reaction pathways of a γ-ketohydroperoxide from combined application of automated reaction discovery methods," J. Am. Chem. Soc. **140**(3), 1035–1048 (2018).

MH19 S. Maeda and Y. Harabuchi, "On benchmarking of automated methods for performing exhaustive reaction path search," J. Chem. Theor. Comput. **15**(4), 2111–2115 (2019).

3.8.7. Peroxyformic acid; methaneperoxoic acid

$^1A'$ g = 1 C_S σ = 1 M_0 = 62.0251

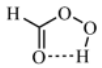

Peroxyformic or performic acid is of atmospheric interest as well as being a well-known disinfectant and bleaching agent [IKS14]. Its electronic photochemistry has been comprehensively studied [IKS14]. Structurally, the lowest energy conformer is characterized by a strong internal H-bond.

3.8.7.1. Species data.

8	−0.914 215	−0.0876 44	0.000 000
8	1.188 085	0.714 684	0.000 000
6	0.000 000	0.891 224	0.000 000
1	−0.523 429	1.853 020	0.000 000
8	−0.290 744	−1.385 282	0.000 000
1	0.658 423	−1.134 430	0.000 000
B (GHz)	20.517	7.583 0	5.536 7

No.	$\bar{\upsilon}$ (cm^{-1})	x_{ii}	
1	3517.97	−103.93	a'
2	3067.40	−60.88	a'
3	1788.45	−9.41	a'
4	1490.07	−9.03	a'
5	1360.26	−6.98	a'
6	1150.46	−8.84	a'
7	896.28	−2.18	a'
8	847.57	−0.95	a'
9	342.75	−1.09	a'
10	1005.31	−2.87	a''
11	486.64	−19.28	a''
12	372.74	−7.69	a''

3.8.7.2. Formation enthalpy, $\Delta_f H(0\ K)$. The isodesmic reactions

$$HC(O)OOH + HOH = HC(O)OH + HOOH, \quad (1)$$

$$HC(O)OOH + CH_3OH = HC(O)OH + CH_3OOH \quad (2)$$

with reaction enthalpies of +18.30 ± 1.12 kJ mol^{-1} and −16.81 ± 1.27 kJ mol^{-1}, respectively, were used together with ATcT values for water (−238.931 ± 0.027 kJ mol^{-1}), *syn* formic acid (−371.12 ± 0.22 kJ mol^{-1}), hydrogen peroxide (−129.47 ± 0.06 kJ mol^{-1}), methanol (−189.83 ± 0.16 kJ mol^{-1}), and methyl hydroperoxide (−114.9 ± 0.74 kJ mol^{-1}) to yield −280.0 ± 1.2 kJ mol^{-1} and −279.4 ± 1.5 kJ mol^{-1} from which a weighted average of $\Delta_f H^o(0\ K)$ = −279.8 ± 0.9 kJ mol^{-1} results together with a 298.15 K value of −290.4 kJ mol^{-1} W2X, W3X-L, and WMS atomization calculations return −281.6 kJ mol^{-1}, −283.1 kJ mol^{-1}, and −283.9 kJ mol^{-1}, respectively, which match the multiple composite values of −281.5 ± 4.5 kJ mol^{-1}.

Feller and co-workers [FDF03] determined $\Delta_f H^o(0\ K)$ = −275.7 ± 2.5 kJ mol^{-1} from extensive coupled cluster calculations, while Villano *et al.* [VEWE10] reported a value of −282.4 ± 3.8 kJ mol^{-1} at 0 K and −289.1 ± 3.8 kJ mol^{-1} at 298.15 K from G3MP2B3 calculations and, noting the disagreement with the Feller values, queried whether the same conformer was being considered. Goldsmith *et al.* [GMG12] reported −289.1 ± 3.8 kJ mol^{-1} at 298.15 K from RQCISD(T)/cc-pV∞QZ levels of theory, and Kieninger *et al.* deduced −291 ± 5 kJ mol^{-1} from isodesmic and composite G3 and CBS-APNO calculations [KSV09]. Atomization energies obtained from coupled cluster calculations augmented with explicitly correlated perturbation theory [KRTBW09] reported a total atomization energy of 2148.9 kJ mol^{-1}, which equates to a formation enthalpy of −264.8 kJ mol^{-1}. The composite method ANL0 shows corrections [KHR17] of 0.6 to the ATcT value, which implies a formation enthalpy of −279.2 kJ mol^{-1}.

In summary, all the determinations with the exception of two [FDF03, KRTBW09] are in agreement that the formation enthalpy of the ground state *syn/syn* O=COO/COOH conformer is $\Delta_f H^o(0\ K)$ = −281.6 ± 0.6 kJ mol^{-1} (−291.0 kJ mol^{-1} at 298.15 K), assuming not unreasonable uncertainties for the atomization calculations. ATcT v1.122d has $\Delta_f H^o(0\ K)$ = −279.8 ± 1.1 kJ mol^{-1} (−289.1 kJ mol^{-1} at 298.15 K) in substantial agreement.

3.8.7.3. Results. A hindered rotor analysis identifies mode no. 11, rotation of the C–O–O–H dihedral, as a possible case but discounts its effects. Comparison with the work of Goldsmith *et al.* [GMG12] reveals some disagreement; for example, they reported $S^o(298.15\ K)$ = 281.2 ± 5.0 J K^{-1} mol^{-1} and $C_p^o(300\ K)$ = 72.0 ± 4.2 J K^{-1} mol^{-1} in comparison to our hindered rotor anharmonic treatment.

T (K)	$S^o(T)$	$C_p^o(T)$	$H^o(T) - H^o(0)$
298.15	277.22	66.88	13.74
300.	277.63	67.14	13.87
400.	298.78	79.86	21.25
500.	317.62	88.79	29.71
600.	334.40	95.10	38.92
700.	349.44	99.96	48.68
800.	363.05	103.97	58.88
900.	375.50	107.36	69.45
1000.	386.96	110.22	80.33
1100.	397.58	112.61	91.47
1200.	407.47	114.58	102.84
1300.	416.71	116.19	114.38
1400.	425.37	117.50	126.06
1500.	433.51	118.56	137.87
1600.	441.19	119.42	149.76
1800.	455.34	120.72	173.78
2000.	468.11	121.64	198.02

References for peroxyformic acid; methaneperoxoic acid.

IKS14 Y. N. Indulkar, M. K. Louie, and A. Sinha, "UV photochemistry of peroxyformic acid (HC(O)OOH): An experimental and computational study investigating 355 nm photolysis," J. Phys. Chem. A **118**(31), 5939–5949 (2014).

FDF03 D. Feller, D. A. Dixon, and J. S. Francisco, "Coupled cluster theory determination of the heats of formation of combustion-related Compounds: CO, HCO, CO_2, HCO_2, HOCO, HC(O)OH, and HC(O)OOH," J. Phys. Chem. A **107**(10), 1604–1617 (2003).

VEWE10 S. M. Villano, N. Eyet, S. W. Wren, G. B. Ellison, V. M. Bierbaum, and W. C. Lineberger, "Photoelectron spectroscopy and thermochemistry of the peroxyformate anion," J. Phys. Chem. A **114**(1), 191–200 (2010).

GMG12 C. F. Goldsmith, G. R. Magoon, and W. H. Green, "Database of small molecule thermochemistry for combustion," J. Phys. Chem. A **116**(36), 9033–9057 (2012).

KSV09 M. Kieninger, P. Saenz Méndez, and O. N. Ventura, "On the experimental structure of monoperoxocarbonic acid and the enthalpy of formation of carbonic acid, peroxyformic acid and monoperoxocarbonic acid in gas phase," Chem. Phys. Lett. **480**(1), 52–56 (2009).

KRTBW09 W. Klopper, B. Ruscic, D. P. Tew, F. A. Bischoff, and S. Wolfsegger, "Atomization energies from coupled-cluster calculations augmented with explicitly-correlated perturbation theory," Chem. Phys. **356**(1), 14–24 (2009).

KHR17 S. J. Klippenstein, L. B. Harding, and B. Ruscic, "*Ab initio* computations and active thermochemical tables hand in hand: Heats of formation of core combustion species," J. Phys. Chem. A **121**(35), 6580–6602 (2017).

3.8.8. Trioxetane

$^1A'$ g = 1 C_S σ = 1 M_0 = 62.0251

This species is mentioned as an intermediate (**IM1**) in a theoretical study [LLWT01] of the reaction O_3 + :CH_2.

3.8.8.1. Species data.

6	−0.115 390	0.936 229	0.000 000
8	−0.115 390	−0.046 258	1.031 664
8	0.342 356	−0.995 466	0.000 000
8	−0.115 390	−0.046 258	−1.031 664
1	0.808 994	1.524 680	0.000 000
1	−1.009 254	1.561 799	0.000 000
B (GHz)	14.344	13.837	7.565 0

No.	$\bar{\upsilon}$ (cm^{-1})	x_{ii}	
1	3081.76	−51.67	a'
2	2994.55	−49.79	a'
3	1543.69	−0.68	a'
4	1155.65	−1.93	a'
5	1088.22	−3.13	a'
6	932.48	−3.23	a'
7	830.90	−1.60	a'
8	222.57	−23.23	a'
9	1385.13	−9.43	a''
10	1146.08	−6.83	a''
11	1007.80	−6.95	a''
12	843.64	−4.16	a''

3.8.8.2. Formation enthalpy, $\Delta_f H$(0 K). An isodesmic reaction featuring dioxirane (9.45 ± 0.55 kJ mol^{-1}), cyclopropane (70.77 ± 0.47 kJ mol^{-1}), and oxetane

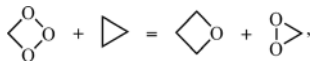

has a reaction enthalpy of −227.07 ± 1.84 kJ mol^{-1}, which together with an assumed value −60.5 kJ mol^{-1} for oxetane based on a 298.15 K formation enthalpy [PP65] of −80.54 ± 0.63 kJ mol^{-1} and thermochemistry [D92] yields $\Delta_f H^o$(0 K) = 105.3 ± 2.2 kJ mol^{-1}; a multi-composite approach yields $\Delta_f H^o$(0 K) = 99.85 ± 5.85 kJ mol^{-1}. Confirmation is obtained from

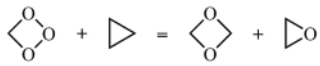

where a reaction enthalpy of −406.0 ± 2.4 kJ mol^{-1} yields $\Delta_f H^o$(0 K) = 104.0 ± 3.2 kJ mol^{-1} based on ATcT reference values for cyclopropane (70.77 ± 0.47 kJ mol^{-1}) and oxirane (−40.01 ± 0.38 kJ mol^{-1}) and a W3X-L of −191.2 kJ mol^{-1} for D_{2h} 1,3-dioxetane. A direct W3X-L atomization calculation yields $\Delta_f H^o$(0 K) = 101.7 kJ mol^{-1} with a final recommendation of $\Delta_f H^o$(0 K) = 102.9 ± 1.8 kJ mol^{-1} (92.7 kJ mol^{-1} at 298.15 K).

3.8.8.3. Results. A standard RR anharmonic treatment is used as no hindered rotor corrections apply.

T (K)	$S^o(T)$	$C_p^o(T)$	$H^o(T) - H^o(0)$
298.15	270.26	50.53	12.32
300.	270.58	50.71	12.42
400.	286.57	61.11	18.00
500.	301.29	70.94	24.62
600.	314.98	79.16	32.14
700.	327.71	85.86	40.40
800.	339.54	91.36	49.27
900.	350.57	95.91	58.64
1000.	360.88	99.72	68.42
1100.	370.54	102.95	78.56
1200.	379.62	105.69	89.00
1300.	388.18	108.04	99.69
1400.	396.26	110.07	110.59
1500.	403.92	111.83	121.69
1600.	411.19	113.37	132.95
1800.	424.69	115.93	155.89
2000.	437.02	117.96	179.29

References for trioxetane.

LLWT01 L.-C. Li, X.-W. Liao, X. Wang, and A.-M. Tian, "*Ab initio* investigation on reaction of ozone with singlet carbene," Huaxue Xuebao **59**(4), 516–519 (2001).

PP65 A. S. Pell and G. Pilcher, "Measurements of heats of combustion by flame calorimetry. Part 3. Ethylene oxide, trimethylene oxide, tetrahydrofuran and tetrahydropyran," Trans. Faraday Soc. **61**, 71–77 (1965).

D92 O. V. Dorofeeva, "Ideal gas thermodynamic properties of oxygen heterocyclic compounds Part 1. Three-membered, four-membered and five-membered rings," Thermochim. Acta **194**(Supplement C), 9–46 (1992).

3.9. $C_1H_2O_4$

3.9.1. Bis-dioxymethylene

^1A g = 1 C_2 σ = 2 M_0 = 78.0245

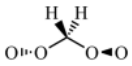

This is one of the many intermediates (**^{1}IM4**) encountered in a theoretical study of the $CH_2O + O_3$ reaction by Wang *et al.* [WSSJ10].

3.9.1.1. Species data.

6	0.000 000	0.000 000	0.733 472
1	−0.760 860	0.518 807	1.308 931
1	0.760 860	−0.518 807	1.308 931
8	0.604 567	0.896 787	−0.184 002
8	−0.604 567	−0.896 787	−0.184 002
8	0.000 000	2.056 499	−0.254 667
8	0.000 000	−2.056 499	−0.254 667
B (GHz)	21.039	2.897 5	2.865 6

No.	$\bar{\upsilon}$ (cm^{-1})	x_{ii}	
1	3089.94	−28.09	*a*
2	1463.03	−0.17	*a*
3	1263.63	−1.81	*a*
4	1187.69	−2.66	*a*
5	988.64	−3.08	*a*
6	498.81	1.04	*a*
7	409.99	−0.92	*a*
8	170.93	−0.46	*a*
9	3187.65	−32.32	*b*
10	1346.67	−4.81	*b*
11	1190.84	−1.36	*b*
12	1018.91	−1.31	*b*
13	791.42	−8.35	*b*
14	572.35	−1.95	*b*
15	105.47	−2.13	*b*

3.9.1.2. Formation enthalpy, $\Delta_f H$(0 K). At the BMC-CCSD level of theory, Wang *et al.* placed this compound at 120 kJ mol^{-1} above $H_2CO + O_3$, thus implying a formation enthalpy of $\Delta_f H^\circ$(0 K) ≈ 159 kJ mol^{-1} that is not in accord with our W3X-L value of $\Delta_f H^\circ$(0 K) = 93.2 kJ mol^{-1} (82.6 kJ mol^{-1} at 298.15 K); however, it does suffer from a T_1 of 0.039. The post-CCSD(T) contribution is substantial, given W2X and WMS values of 126.8 kJ mol^{-1} and 127.4 kJ mol^{-1}, respectively.

3.9.1.3. Results. A rigid-rotor anharmonic treatment is employed, as the relaxed potential energy scans are problematic.

T (K)	$S^\circ(T)$	$C_p^\circ(T)$	$H^\circ(T) - H^\circ(0)$
298.15	299.71	77.50	16.23
300.	300.19	77.78	16.38
400.	324.45	90.96	24.84
500.	345.87	100.94	34.46
600.	364.97	108.49	44.94
700.	382.15	114.40	56.10
800.	397.75	119.20	67.79
900.	412.03	123.20	79.91
1000.	425.19	126.60	92.40
1100.	437.40	129.52	105.21
1200.	448.78	132.04	118.29
1300.	459.44	134.25	131.61
1400.	469.46	136.18	145.13
1500.	478.91	137.90	158.83
1600.	487.86	139.42	172.70
1800.	504.44	142.03	200.85
2000.	519.52	144.20	229.48

References for bis-dioxymethylene.

WSSJ10 F. Wang, H. Sun, J. Sun, X. Jia, Y. Zhang, Y. Tang, X. Pan, Z. Su, L. Hao, and R. Wang, "Mechanistic and kinetic study of $CH_2O + O_3$ reaction," J. Phys. Chem. A **114**(10), 3516–3522 (2010).

3.9.2. Bis-hydroperoxymethylene

$^1A'$ g = 1 C_S σ = 1 M_0 = 78.0245

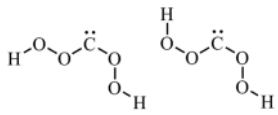

This species has been encountered during a study of singlet and triplet potential energy surfaces by Wang *et al.* of the reaction between methanol and ozone [WSSJ10]. Three distinct singlet conformers were identified (**IM9–IM11**) with approximately the same energy with the **IM11** lowest. The *aasa* ≡ *asaa* conformer (HOOC/OOCO/OCCC/COOH) or **IM11** is the ground state at B3LYP/cc-pVTZ + d with the *sasa* ≡ *asas* some 5 kJ mol^{-1} higher.

3.9.2.1. Species data.

6	0.000 000	0.796 343	0.000 000
8	0.765 187	−0.247 780	0.000 000
8	2.163 181	0.189 161	0.000 000
8	−1.222 875	0.609 645	0.000 000
8	−1.697 403	−0.967 328	0.000 000
1	−2.641 831	−0.759 963	0.000 000
1	2.577 114	−0.687 682	0.000 000
B (GHz)	17.574	2.967 7	2.539 0

No.	$\bar{\upsilon}$ (cm^{-1})	x_{ii}	
1	3782.83	−78.96	a'
2	3743.77	−79.99	a'
3	1524.94	−25.59	a'
4	1445.13	−9.96	a'
5	1175.74	−10.44	a'
6	1126.64	−4.48	a'
7	947.44	−4.55	a'
8	649.96	−2.23	a'
9	457.94	−1.37	a'
10	392.60	−0.55	a'
11	189.56	−1.02	a'
12	490.85	−1.67	a''
13	221.21	−0.71	a''
14	163.06	3.15	a''
15	91.59	−81.78	a''

3.9.2.2. Formation enthalpy, $\Delta_f H(0\ K)$. W3X-L returns a value of $\Delta_f H^o(0\ K) = -38.2$ kJ mol^{-1} (−45.7 kJ mol^{-1} at 298.15 K).

3.9.2.3. Results. A hindered rotor analysis identifies mode nos. 15, 14, 12, and 9 for *aasa* with minimal overall impact, ≤ 0.3 J K^{-1} mol^{-1}, but the highly anharmonic mode no. 15 is replaced.

T (K)	$S^o(T)$	$C_p^o(T)$	$H^o(T) - H^o(0)$
298.15	327.33	87.87	19.11
300.	327.88	88.08	19.27
400.	354.72	98.67	28.63
500.	377.68	107.12	38.93
600.	397.82	113.76	49.99
700.	415.77	119.04	61.64
800.	431.96	123.37	73.76
900.	446.70	127.03	86.28
1000.	460.26	130.22	99.15
1100.	472.80	133.05	112.31
1200.	484.49	135.59	125.75
1300.	495.44	137.89	139.42
1400.	505.73	139.98	153.31
1500.	515.46	141.88	167.41
1600.	524.67	143.61	181.68
1800.	541.76	146.59	210.71
2000.	557.34	149.02	240.28

References for bis-hydroperoxymethylene.

WSSJ10 F. Wang, H. Sun, J. Sun, X. Jia, Y. Zhang, Y. Tang, X. Pan, Z. Su, L. Hao, and R. Wang, "Mechanistic and kinetic study of $CH_2O + O_3$ reaction," J. Phys. Chem. A **114**(10), 3516–3522 (2010).

3.9.3. Carbonoperoxoic acid

$^1A'$ g = 1 C_S σ = 1 M_0 = 78.0245

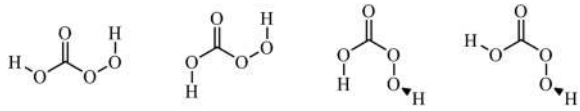

Illustrated on the left is the *sss* conformer classified regarding the dihedrals HOC=O, O=C–O–O, and C–O–O–H, which Kieninger *et al.* reported [KSV09] as the ground state (**M1**), a conclusion reinforced in a related study [SEV09] with which we agree. Of the eight possible conformers only four (**M1–M3**, **M5**) are significant, namely, *sss*, *ass*, *aaa*, and *saa*, with the latter two more properly described as *aag* and *sag* since the peroxylic hydrogens are out of plane.

	sss	*ass*	*aag*	*sag*
Relative energy (kJ mol^{-1})	0	+4.0	+12.5	+17.7

3.9.3.1. Species data.

1	−0.402 507	2.284 687	0.000 000
8	−0.894 929	1.452 991	0.000 000
8	1.201 479	0.573 349	0.000 000
6	0.000 000	0.466 650	0.000 000
8	−0.663 232	−0.699 633	0.000 000
8	0.266 558	−1.797 552	0.000 000
1	1.123 502	−1.317 830	0.000 000
B (GHz)	11.721	4.572 2	3.289 1

No.	$\bar{\upsilon}$ (cm^{-1})	x_{ii}	
1	3787.92	−80.06	a'
2	3512.62	103.50	a'
3	1811.86	−8.88	a'
4	1502.22	−9.06	a'
5	1429.71	−5.91	a'
6	1189.75	−6.56	a'
7	1060.73	−3.65	a'
8	922.78	−2.00	a'
9	692.73	−0.66	a'
10	521.49	−0.09	a'
11	346.85	−0.42	a'
12	783.15	0.03	a''
13	494.97	−7.15	a''
14	425.08	−31.03	a''
15	188.79	0.83	a''

3.9.3.2. Formation enthalpy, $\Delta_f H(0\ K)$. Keininger *et al.* used the isodesmic reaction

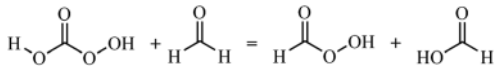

to calculate $\Delta_f H^o(298.15\ K) = -509.3 \pm 1.3$ kJ mol^{-1} from G2(MP2), G3, and CBS-APNO based on the literature values for formaldehyde and formic acid and their determination for peroxyformic acid of -290.7 ± 1.5 kJ mol^{-1}.

Our multi-composite treatment gives $\Delta_f H^o(0\ K) = -42.65 \pm 0.49$ kJ mol^{-1} for the above-mentioned isodesmic reaction, which in conjunction with the reference values for methanal (-105.32 ± 0.11 kJ mol^{-1}) and formic acid (-371.06 ± 0.22 kJ mol^{-1}) and our computed value for peroxyformic acid of -281.6 kJ mol^{-1} (see above) gives $\Delta_f H^o(0\ K) = -504.7 \pm 1.1$ kJ mol^{-1} (-516.1 kJ mol^{-1} at 298.15 K).

3.9.3.3. Results. A hindered rotor analysis shows little impact on the computed properties, given the reduced barrier height (V/RT) values of 12.3 and 14.2, respectively. A scan about the OO–CO dihedral is not well-behaved.

T (K)	$S^o(T)$	$C_p^o(T)$	$H^o(T) - H^o(0)$
298.15	296.50	78.23	15.48
300.	296.98	78.52	15.62
400.	321.54	92.10	24.19
500.	343.19	101.77	33.91
600.	362.40	108.81	44.45
700.	379.59	114.21	55.61
800.	395.14	118.58	67.26
900.	409.32	122.27	79.30
1000.	422.37	125.47	91.69
1100.	434.47	128.30	104.38
1200.	445.74	130.83	117.34
1300.	456.31	133.09	130.54
1400.	466.24	135.12	143.95
1500.	475.63	136.95	157.55
1600.	484.52	138.57	171.33
1800.	501.01	141.29	199.32
2000.	516.01	143.39	227.80

References for carbonoperoxoic acid.

KSV09 M. Kieninger, P. Saenz Méndez, and O. N. Ventura, "On the experimental structure of monoperoxocarbonic acid and the enthalpy of formation of carbonic acid, peroxyformic acid and monoperoxocarbonic acid in gas phase," Chem. Phys. Lett. **480**(1), 52–56 (2009).

SEV09 P. Saenz Méndez, L. A. Eriksson, and O. N. Ventura, "Theoretical study of the structure of neutral, radical and anionic monoperoxo carbonic acid," J. Mol. Struct.: THEOCHEM **913**(1), 131–138 (2009).

3.9.4. Dioxiranediol

$^1A_1$ g = 1 C_{2v} σ = 2 M_0 = 78.0245

Dioxirane derivatives are important oxidants for the epoxidation of olefins [GR01]. The *anti/anti* conformer, as regards the H–O–C–O(H) dihedrals, appears to be the ground state with the *as* and *gg′* at 3.8 kJ mol^{-1} and 24.8 kJ mol^{-1}, respectively.

3.9.4.1. Species data.

6	0.000 000	0.000 000	0.139 397
8	0.763 619	0.000 000	−1.021 278
8	−0.763 619	0.000 000	−1.021 278
8	0.000 000	1.093 802	0.924 976
1	0.000 000	1.869 871	0.352 221
8	0.000 000	−1.093 802	0.924 976
1	0.000 000	−1.869 871	0.352 221
B (GHz)	7.899 8	6.327 8	4.743 9

No.	$\bar{\upsilon}$ (cm^{-1})	x_{ii}	
1	3811.81	−40.87	a_1
2	1474.64	−4.28	a_1
3	1202.06	−2.41	a_1
4	973.27	−1.54	a_1
5	767.21	−1.55	a_1
6	504.24	0.40	a_1
7	437.01	−0.97	a_2
8	246.46	9.68	a_2
9	859.65	−2.06	b_1
10	598.52	−1.10	b_1
11	416.80	−7.46	b_1
12	3811.01	−40.62	b_2
13	1457.03	−4.94	b_2
14	1156.88	−4.29	b_2
15	538.73	0.31	b_2

3.9.4.2. Formation enthalpy, $\Delta_f H(0\ K)$. The isodesmic reaction

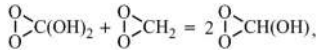

which uses our value for *anti* dioxiranol of 216.0 ± 1.3 kJ mol^{-1}, has a reaction enthalpy of -20.07 ± 0.36 kJ mol^{-1}, which implies a $\Delta_f H^o(0\ K)$ of -421.4 ± 2.0 kJ mol^{-1} for the *anti/anti* diol. This is reinforced by considering

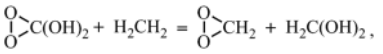

where methane (−66.550 ± 0.057 kJ mol^{-1}), methanediol (−379.2 ± 1.1 kJ mol^{-1}), and dioxirane (9.45 ± 0.55 kJ mol^{-1}) are now the chaperones. A reaction enthalpy of 120.22 ± 2.16 kJ mol^{-1} results in −423.4 ± 2.5 kJ mol^{-1} and, in turn, in a final weighted average of $\Delta_f H^\circ$(0 K) = −422.2 ± 1.6 kJ mol^{-1} (−432.3 kJ mol^{-1} at 298.15 K).

3.9.4.3. Results. Hindered rotor analysis considers mode nos. 8 and 11 ascribing similar impact with the reduced barrier heights (*V*/*RT*)s of 2.2 and 4.7, respectively. These are both replaced by the same relaxed potential energy scan although, in reality, these are symmetric and antisymmetric coupled HOCO(H) rotors and a more appropriate treatment requires an application such as Q2DTor [FCTF18]. In this particular case, if the effect is small, coupling decreases the computed entropy by 1.5 J K^{-1} mol^{-1} at 300 K and by 4.6 J K^{-1} mol^{-1} at 2000 K. Here, we adopt a scheme of two hindered rotors and anharmonic modes.

T (K)	$S^\circ(T)$	$C_p^\circ(T)$	$H^\circ(T) - H^\circ(0)$
298.15	295.60	85.18	16.75
300.	296.12	85.45	16.90
400.	322.54	98.19	26.12
500.	345.51	107.48	36.42
600.	365.72	114.13	47.52
700.	383.70	118.99	59.19
800.	399.84	122.71	71.28
900.	414.47	125.70	83.70
1000.	427.85	128.21	96.40
1100.	440.17	130.36	109.33
1200.	451.60	132.26	122.46
1300.	462.25	133.93	135.77
1400.	472.24	135.43	149.24
1500.	481.63	136.78	162.85
1600.	490.49	137.99	176.59
1800.	506.87	140.07	204.40
2000.	521.72	141.78	232.59

References for dioxiranediol.

GR01 P. Gisdakis and N. Rösch, "Olefin epoxidation by dioxiranes and percarboxylic acids: An analysis of activation energies calculated by a density functional method," J. Phys. Org. Chem. **14**(6), 328–332 (2001).

FCTF18 D. Ferro-Costas, M. N. D. S. Cordeiro, D. G. Truhlar, and A. Fernández-Ramos, "Q2DTor: A program to treat torsional anharmonicity through coupled pair torsions in flexible molecules," Comput. Phys. Commun. **232**, 190–205 (2018).

3.9.5. Dioxydihydroxymethyl

$^1A'$ g = 1 C_S σ = 1 M_0 = 78.0245

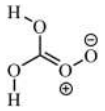

Yoshioka *et al.* discussed the effect of substituents on the Criegee-type oxygenated dipoles [YYKN97] $H_2C{=}O^+{-}O^-$.

3.9.5.1. Species data.

1	−1.521 399	1.485 105	0.000 000
8	−0.557 959	1.585 261	0.000 000
8	−0.720 969	−0.636 842	0.000 000
6	0.000 000	0.376 284	0.000 000
8	−0.040 755	−1.911 861	0.000 000
8	1.303 643	0.340 112	0.000 000
1	1.649 717	1.243 825	0.000 000
B (GHz)	11.094	4.495 8	3.199 3

No.	$\bar{\nu}$ (cm^{-1})	x_{ii}	
1	3768.78	−82.23	a'
2	3750.19	−83.04	a'
3	1729.88	−8.07	a'
4	1502.46	−6.71	a'
5	1233.28	−4.56	a'
6	1213.13	−4.16	a'
7	996.79	−1.92	a'
8	811.63	−4.05	a'
9	607.32	−0.39	a'
10	480.27	0.13	a'
11	276.68	−0.04	a'
12	678.10	−1.53	a''
13	530.49	−10.20	a''
14	465.71	−2.12	a''
15	214.54	−1.44	a''

3.9.5.2. Formation enthalpy, $\Delta_f H$(0 K). An isodesmic reaction

$$(HO)_2COO + H_2C(H)_2 = (H)_2COO + H_2C(OH)_2$$

with methane (−66.550 ± 0.057 kJ mol^{-1}), dioxymethyl (111.90 ± 0.63 kJ mol^{-1}), and methanediol (−379.2 ± 1.1 kJ mol^{-1}) as chaperones leads to a reaction enthalpy of 101.34 ± 2.97 kJ mol^{-1} and, in turn, to a $\Delta_f H^\circ$(0 K) of −302.1 ± 3.2 kJ mol^{-1} (−315.0 kJ mol^{-1} at 218.15 K), in very good agreement with a direct WMS calculation of −303.2 kJ mol^{-1}.

3.9.5.3. Results. Hindered rotor analysis identifies three modes (nos. 1, 3, and 5) as contributing although reduced barrier height (*V*/*RT*) values in excess of 12 limit their impact. Only a relaxed potential energy scan about the HO–CO dihedral (parallel to the O–O

bond) succeeds revealing a barrier of 35 kJ mol^{-1} and leading to a well at +34 kJ mol^{-1}, while a scan about the other O–C dihedral fails as the H-atom undergoes internal transfer to the dioxy oxygen atom. The scan about C=O also fails with the dioxy moiety transforming into a dioxirane-type structure; hence, a simplistic anharmonic treatment is applied.

T (K)	$S^o(T)$	$C_p^o(T)$	$H^o(T) - H^o(0)$
298.15	297.14	78.99	15.56
300.	297.63	79.28	15.71
400.	322.46	93.38	24.37
500.	344.52	104.26	34.27
600.	364.30	112.69	45.14
700.	382.19	119.37	56.75
800.	398.50	124.84	68.97
900.	413.48	129.48	81.69
1000.	427.33	133.51	94.84
1100.	440.23	137.06	108.37
1200.	452.29	140.22	122.24
1300.	463.63	143.01	136.40
1400.	474.32	145.46	150.83
1500.	484.43	147.59	165.48
1600.	494.01	149.41	180.33
1800.	511.78	152.23	210.51
2000.	527.93	154.10	241.15

References for dioxydihydroxymethyl.

YYKN97 Y. Yoshioka, D. Yamaki, S. Kubo, M. Nishino, K. Yamaguchi, K. Mizuno, and I. Saito, "Theoretical study on electronic structures of oxygenated dipoles and mechanisms of ozonolysis reaction," Electron. J. Theor. Chem. **2**, 236–252 (1997).

3.9.6. Dioxyhydroperoxymethyl

^{1}A g = 1 C_S σ = 1 M_0 = 78.0245

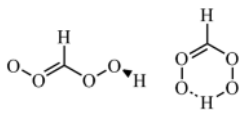

A dipolar intermediate (**^{1}IM5**) on the singlet surface of the $CH_2O + O_3$ reaction [WSSJ10]; however, the ground state is not the *aag* **IM5** reported and shown on the left but rather the H-bonded six-membered ring *sss* conformer which lies some 62 kJ mol^{-1} lower.

3.9.6.1. Species data.

8	1.146 206	0.513 733	0.000 000
8	−1.152 411	0.486 558	0.000 000
6	0.000 000	1.037 992	0.000 000
1	−0.025 779	2.122 822	0.000 000
8	1.216 577	−0.934 835	0.000 000
8	−1.194 766	−0.964 617	0.000 000
1	−0.099 065	−1.157 479	0.000 000
B (GHz)	9.079 5	5.691 9	3.498 6

No.	$\bar{\upsilon}$ (cm^{-1})	x_{ii}	
1	3181.44	−56.28	a'
2	1967.90	−32.96	a'
3	1712.41	−13.00	a'
4	1358.36	−4.08	a'
5	1290.18	−19.20	a'
6	1164.99	−1220.18	a'
7	890.15	−9.78	a'
8	819.37	−3.85	a'
9	775.73	−2.43	a'
10	428.17	−3.93	a'
11	364.06	−128.09	a'
12	1078.31	−7.35	a''
13	932.66	−3.22	a''
14	496.99	−0.27	a''
15	60.35	11.75	a''

3.9.6.2. Formation enthalpy, Δ_fH(0 K). An isodesmic reaction featuring ATcT values for methane (−66.550 ± 0.057 kJ mol^{-1}), methanol oxide (111.90 ± 0.63 kJ mol^{-1}), and methyl hydroperoxide (−115.03 ± 0.76 kJ mol^{-1})

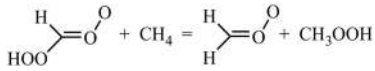

has a reaction enthalpy of 105.03 ± 3.59 kJ mol^{-1}, which leads to $\Delta_f H^o$(0 K) = −41.6 ± 3.7 kJ mol^{-1}.

The direct atomization W3X-L method gives −45.7 kJ mol^{-1} (−57.2 kJ mol^{-1} at 298.15 K), whereas the multi-composite approach has −42.9 ± 5.9 kJ mol^{-1}. In summary, $\Delta_f H^o$(0 K) = −44.6 ± 1.7 kJ mol^{-1} (−56.1 kJ mol^{-1} at 298.15 K) since the *aag* conformer lies some 62 kJ mol^{-1} *higher* that implies $\Delta_f H^o$(0 K) = 17 kJ mol^{-1}, which can be compared with a value extracted from the literature [WSSJ10] (18.8 kJ mol^{-1}).

3.9.6.3. Results. A hindered rotor analysis shows that none is needed and since an anharmonic treatment is compromised with mode nos. 6 and 11 highly anharmonic, a standard RRHO procedure is used.

T (K)	$S°(T)$	$C_p°(T)$	$H°(T) - H°(0)$
298.15	301.38	72.74	15.23
300.	301.83	73.04	15.37
400.	324.94	87.90	23.43
500.	345.92	100.20	32.86
600.	365.09	109.97	43.39
700.	382.64	117.68	54.78
800.	398.77	123.80	66.87
900.	413.65	128.70	79.50
1000.	427.42	132.69	92.58
1100.	440.23	135.96	106.01
1200.	452.18	138.67	119.75
1300.	463.37	140.93	133.73
1400.	473.88	142.84	147.92
1500.	483.79	144.46	162.28
1600.	493.16	145.84	176.80
1800.	510.47	148.06	206.20
2000.	526.17	149.74	235.98

References for dioxyhydroperoxymethyl.

WSSJ10 F. Wang, H. Sun, J. Sun, X. Jia, Y. Zhang, Y. Tang, X. Pan, Z. Su, L. Hao, and R. Wang, "Mechanistic and kKinetic sStudy of $CH_2O + O_3$ rReaction," J. Phys. Chem. A **114**(10), 3516–3522 (2010).

3.9.7. Formyl hydrotrioxide

^1A g = 1 C_1 σ = 1 M_0 = 78.0245

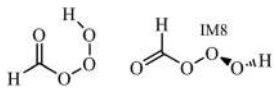

There are several conformers for this formyl hydrotrioxide compound. The lowest energy structure has O=C–O–O, C–O–O–O, and O–O–O–H dihedrals of ~−5°, 70°, and −85° summarized as *cgg′* with an internal H-bond forming a six-membered ring with the next lowest at +7.0 kJ mol^{-1}.

It occurs as an intermediate in the reaction of formaldehyde with ozone [WSSJ10, VKJ09]; the structure shown by Wang *et al.* [WSSJ10] (**^{1}IM8**) is not similar to that found here—our *cgg′* agrees with the more folded structure found by Voukides *et al.* [VKJ09].

3.9.7.1. Species data.

6	1.228 033	−0.196 190	−0.147 258
8	1.230 806	0.945 237	0.209 068
8	0.174 502	−1.040 176	−0.151 744
8	−0.992 057	−0.417 202	0.490 024
8	−1.481 122	0.585 989	−0.354 071
1	−0.909 834	1.335 681	−0.104 653
1	2.084 606	−0.749 321	−0.558 022
B (GHz)	10.099	4.746 9	3.570 3

No.	$\bar{\upsilon}$ (cm−1)	x_{ii}
1	3633.85	−91.06
2	3019.28	−62.89
3	1805.89	−10.68
4	1449.21	−11.44
5	1370.95	−8.58
6	1082.97	−8.03
7	1022.24	−2.55
8	946.02	−3.79
9	845.83	−0.88
10	728.80	−4.61
11	600.62	−13.00
12	501.91	−1.69
13	326.65	−0.38
14	275.03	−0.79
15	159.96	−3.82

3.9.7.2. Formation enthalpy, $\Delta_f H$(0 K). An isodesmic reaction that relates this species to our value for peroxyformic acid (−281.6 ± 0.6 kJ mol^{-1}) and reference values for water (−238.931 ± 0.027 kJ mol^{-1}) and hydrogen peroxide (−129.472 ± 0.064 kJ mol^{-1})

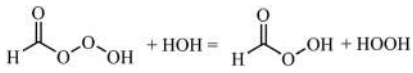

seems sensible. The reaction enthalpy of 51.17 ± 0.94 kJ mol^{-1} leads to $\Delta_f H°$(0 K) = −223.3 ± 1.1 kJ mol^{-1} (−226.3 kJ mol^{-1} at 298.15 K), which is in moderate agreement with the value of −217.1 kJ mol^{-1} implied from CCSD(T)//M062X/6-311+G(d,p) calculations by Voukides *et al.* [VKJ09] and in good agreement with a WMS of −223.4 kJ mol^{-1}.

3.9.7.3. Results. Hindered rotor analysis identifies mode nos. 11 and 15; the impact on the entropy is small, of the order of +0.4 J K^{-1} mol^{-1} at room temperature, rising to +3.7 kJ mol^{-1} at 2000 K. Nevertheless, scans about CO–OO and OO–OH are well-behaved and incorporated in the anharmonic treatment.

T (K)	$S^\circ(T)$	$C_p^\circ(T)$	$H^\circ(T) - H^\circ(0)$
298.15	303.80	86.05	16.66
300.	304.33	86.41	16.82
400.	331.69	103.69	26.37
500.	356.18	115.47	37.37
600.	377.96	123.13	49.32
700.	397.36	128.39	61.91
800.	414.77	132.27	74.95
900.	430.53	135.32	88.34
1000.	444.92	137.80	102.00
1100.	458.15	139.87	115.88
1200.	470.40	141.63	129.96
1300.	481.80	143.13	144.20
1400.	492.46	144.43	158.57
1500.	502.46	145.56	173.07
1600.	511.89	146.56	187.68
1800.	529.25	148.25	217.16
2000.	544.94	149.64	246.95

References for formyl hydrotrioxide.

WSSJ10 F. Wang, H. Sun, J. Sun, X. Jia, Y. Zhang, Y. Tang, X. Pan, Z. Su, L. Hao, and R. Wang, "Mechanistic and kKinetic sStudy of $CH_2O + O_3$ rReaction," J. Phys. Chem. A **114**(10), 3516–3522 (2010).

VKJ09 A. C. Voukides, K. M. Konrad, and R. P. Johnson, "Competing mMechanistic cChannels in the oOxidation of aAldehydes by oOzone," J. Org. Chem. **74**(5), 2108–2113 (2009).

3.9.8. Oxodioxiranol

^{1}A g = 1 C_1 σ = 1 M_0 = 78.0245

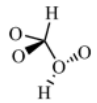

Probably best viewed as a dioxirane derivative, this singlet species featured as an intermediate (^{1}**IM7**) in the $CH_2O + O_3$ reaction [ZTPS10]. A scan about the HCOH dihedral reveals two other conformers at −68° and +14 kJ mol^{-1} and at +52° and +36.5 kJ mol^{-1} above the −165° ground state.

3.9.8.1. Species data.

6	−0.323 906	−0.052 296	0.436 990
1	−0.065 034	0.079 781	1.478 196
8	−0.999 314	0.894 750	−0.260 371
8	−1.544 213	−0.501 882	0.024 574
8	0.789 871	−0.635 771	−0.215 144
1	0.670 801	−0.553 418	−1.178 560
8	1.920 865	0.341 330	0.085 745
B (GHz)	15.156	3.810 3	3.360 9

No.	$\bar{\upsilon}$ (cm^{-1})	x_{ii}
1	3668.07	−88.30
2	3219.47	−55.29
3	1443.90	−4.86
4	1306.61	−2.91
5	1208.46	−7.21
6	1152.02	−6.31
7	1010.14	−6.63
8	918.24	−3.01
9	840.52	−7.64
10	786.79	−4.35
11	736.00	−1.33
12	499.73	0.17
13	454.58	−0.86
14	240.87	−0.44
15	119.28	−0.86

3.9.8.2. Formation enthalpy, $\Delta_f H(0\ K)$. A multi-composite treatment yields $\Delta_f H^\circ(0\ K) = 86.5 \pm 5.8$ kJ mol^{-1} (75.1 kJ mol^{-1} at 298.15 K) as against the value of 93.9 kJ mol^{-1} deduced from BMC-CCSD calculations [ZTPS10]. WMS atomization returns $\Delta_f H^\circ(0\ K) = 86.7$ kJ mol^{-1}.

3.9.8.3. Results. A relaxed potential energy scan about the HCOH dihedral is well-behaved and is included in a RR anharmonic treatment to account for the thermochemical properties. At room temperature, the thermochemical values are largely unaffected in comparison to a purely vibrational approach and do not differ by more than 5 J K^{-1} mol^{-1} at 2000 K.

T (K)	$S^{o}(T)$	$C_{p}^{o}(T)$	$H^{o}(T) - H^{o}(0)$
298.15	299.07	76.88	15.55
300.	299.55	77.21	15.70
400.	324.06	93.41	24.26
500.	346.31	105.85	34.25
600.	366.46	115.03	45.31
700.	384.74	121.96	57.18
800.	401.39	127.39	69.65
900.	416.66	131.77	82.62
1000.	430.74	135.37	95.98
1100.	443.78	138.38	109.67
1200.	455.93	140.91	123.64
1300.	467.30	143.05	137.84
1400.	477.97	144.87	152.23
1500.	488.02	146.44	166.80
1600.	497.52	147.80	181.51
1800.	515.06	150.03	211.30
2000.	530.96	151.79	241.49

References for oxodioxiranol.

ZTPS10 Zhang, Y. Tang, X. Pan, Z. Su, L. Hao, and R. Wang, "Mechanistic and kinetic study of $CH_2O + O_3$ reaction," J. Phys. Chem. A **114**(10), 3516–3522 (2010).

3.9.9. Oxyoxoniumyl methyldioxy

^{1}A g = 1 C_1 σ = 1 M_0 = 78.0245 optical isomers = 2

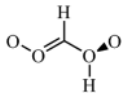

This is one of a number of rather odd intermediates (dipolar **^{1}IM6**) on the singlet surface of the $CH_2O + O_3$ reaction [WSSJ10]; it is not cataloged by SciFinder.

3.9.9.1. Species data.

8	−0.975 396	0.269 504	−0.314 657
8	1.171 167	0.620 654	0.159 597
6	−0.033 811	0.028 333	0.454 385
1	−0.059 631	−0.585 371	1.338 644
8	−2.209 436	−0.302 010	−0.032 329
8	1.908 177	−0.675 566	−0.235 606
1	1.106 403	1.114 715	−0.680 994
B (GHz)	19.965	2.774 7	2.623 5

No.	$\bar{\upsilon}$ (cm^{-1})	x_{ii}
1	3631.89	−89.18
2	3277.06	−53.35
3	1565.65	−12.43
4	1278.95	−2.80
5	1260.25	−6.83
6	1093.60	−5.16
7	902.06	−6.35
8	859.00	−8.15
9	800.03	−1.28
10	690.97	−6.13
11	537.57	−0.90
12	343.52	−2.03
13	279.17	−1.70
14	241.98	−1.34
15	110.74	−2.53

3.9.9.2. Formation enthalpy, Δ_fH(0 K). A T_1 of 0.049 indicates that single-reference methods may be inadequate although WMS, perhaps fortuitously, at $\Delta_f H^{o}$(0 K) = 246.6 kJ mol^{-1} agrees with a W3X-L $\Delta_f H^{o}$(0 K) = 247.3 kJ mol^{-1} (237.7 kJ mol^{-1} at 298.15 K). The multi-composite treatment, excluding G3 that converges to a *different* structure at the second optimization, yields 246.5 ± 6.2 kJ mol^{-1} as against the value of 259 kJ mol^{-1} deduced from the Wang *et al.* data [WSSJ10].

3.9.9.3. Results. A hindered rotor analysis discounts any significant impact of treating mode no. 14 as hindered since the reduced barrier height V/RT = 23.6, and so a default RR anharmonic approach is used with "optical isomers = 2."

T (K)	$S°(T)$	$C_p°(T)$	$H°(T) - H°(0)$
298.15	316.33	84.62	17.23
300.	316.85	84.89	17.39
400.	343.11	97.57	26.55
500.	365.91	106.56	36.78
600.	385.95	113.21	47.78
700.	403.81	118.42	59.37
800.	419.91	122.72	71.43
900.	434.58	126.40	83.89
1000.	448.07	129.62	96.70
1100.	460.56	132.49	109.80
1200.	472.20	135.08	123.18
1300.	483.11	137.45	136.81
1400.	493.38	139.62	150.66
1500.	503.08	141.64	164.73
1600.	512.28	143.53	178.98
1800.	529.39	146.94	208.04
2000.	545.03	149.93	237.73

References for oxyoxoniumyl methyldioxy.

WSSJ10 F. Wang, H. Sun, J. Sun, X. Jia, Y. Zhang, Y. Tang, X. Pan, Z. Su, L. Hao, and R. Wang, "Mechanistic and kinetic study of $CH_2O + O_3$ reaction," J. Phys. Chem. A **114**(10), 3516–3522 (2010).

3.9.10. Tetroxolane

^1A g = 1 C_2 σ = 2 M_0 = 78.0245

This is an intermediate in the oxidation of aldehydes by ozone [WSSJ10, VKJ09].

3.9.10.1. Species data.

6	1.160 854	−0.000 004	0.000 050
8	0.305 030	1.133 345	−0.176 182
8	−0.960 695	−0.630 805	−0.304 294
8	0.305 011	−1.133 355	0.176 176
8	−0.960 698	0.630 818	0.304 241
1	1.762 790	0.068 463	0.906 879
1	1.762 897	−0.068 465	−0.906 709
B (GHz)	8.502 1	8.368 4	4.653 2

No.	$\bar{\upsilon}$ (cm^{-1})	x_{ii}	
1	3038.37	−29.58	*a*
2	1531.27	−0.48	*a*
3	1178.25	−2.39	*a*
4	1018.50	−3.78	*a*
5	950.53	−1.77	*a*
6	757.81	−0.63	*a*
7	670.15	−4.57	*a*
8	494.30	−2.84	*a*
9	3102.80	−35.12	*b*
10	1373.61	−6.46	*b*
11	1133.58	−1.75	*b*
12	958.65	−4.90	*b*
13	827.85	−2.18	*b*
14	700.38	−4.92	*b*
15	62.36	1.63	*b*

3.9.10.2. Formation enthalpy, $\Delta_f H$(0 K). Isodesmics utilizing cyclopropane (70.77 ± 0.47 kJ mol^{-1}) and oxetane (−60.5 ± 2.0 kJ mol^{-1}) together with trioxetane (104.9 ± 1.8 kJ mol^{-1}) and 1,3-dioxetane (−191.2 ± 2.0 kJ mol^{-1}) have reaction enthalpies of −99.96 ± 2.73 kJ mol^{-1}and −522.6 ± 3.6 kJ mol^{-1} leading to $\Delta_f H°$(0 K) of 73.6 ± 3.9 kJ mol^{-1}and 69.4 ± 4.6 kJ mol^{-1}, respectively,

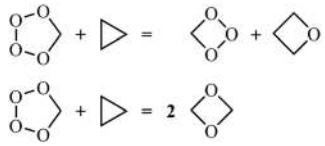

and a grand weighted average of $\Delta_f H°$(0 K) = 71.9 ± 3.0 kJ mol^{-1}. A value of 87.6 kJ mol^{-1} can be extracted from the CCSD(T)//M05-2X/6-311+G(d,p) calculations of Voukides *et al.*, [VKJ09] and that of 41.5 kJ mol^{-1} can be from the BMC-CCSD study of Wang *et al.* [WSSJ10] Finally, W2X and W3X-L values of 70.9 kJ mol^{-1} and 68.1 kJ mol^{-1} reinforce our isodesmic results, but WMS at 63.9 kJ mol^{-1} seems anomalous. A summary result of $\Delta_f H°$(0 K) = 69.9 ± 1.3 kJ mol^{-1} (57.0 kJ mol^{-1} at 298.15 K) best represents these data.

3.9.10.3. Results. The many ring-puckering modes are ignored in favor of a rigid rotor anharmonic oscillator approach.

T (K)	$S^\circ(T)$	$C_p^\circ(T)$	$H^\circ(T) - H^\circ(0)$
298.15	285.30	66.46	13.94
300.	285.72	66.78	14.07
400.	307.22	83.01	21.58
500.	327.20	96.06	30.56
600.	345.65	106.12	40.69
700.	362.62	113.94	51.71
800.	378.25	120.14	63.42
900.	392.71	125.18	75.70
1000.	406.12	129.35	88.43
1100.	418.62	132.83	101.54
1200.	430.30	135.79	114.98
1300.	441.28	138.31	128.68
1400.	451.61	140.49	142.63
1500.	461.37	142.39	156.77
1600.	470.61	144.05	171.09
1800.	487.75	146.82	200.19
2000.	503.33	149.06	229.78

References for tetroxolane.

WSSJ10 F. Wang, H. Sun, J. Sun, X. Jia, Y. Zhang, Y. Tang, X. Pan, Z. Su, L. Hao, and R. Wang, "Mechanistic and kinetic study of $CH_2O + O_3$ reaction," J. Phys. Chem. A **114**(10), 3516–3522 (2010).

VKJ09 A. C. Voukides, K. M. Konrad, and R. P. Johnson, "Competing mechanistic channels in the oxidation of aldehydes by ozone," J. Org. Chem. **74**(5), 2108–2113 (2009).

3.10. $C_1H_2O_5$

3.10.1. Carbonodiperoxoic acid

saas $^1A_1$ g = 1 C_{2v} σ = 2 M_0 = 94.0239;

sasg ^1A g = 1 C_1 σ = 1 M_0 = 94.0239

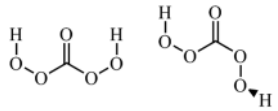

Two principal conformers can be classified as *saas* and *sasg* with regard to the HOOC/OOCO/OCOO/COOH dihedrals in sequence with the latter some 8.2 kJ mol^{-1} above the ground state.

3.10.1.1. Species data.

	saas				*sasg*		
6	0.000 000	0.000 000	0.014 759	6	0.066 781	0.467 072	−0.001 690
8	0.000 000	1.081 402	−0.768 407	8	0.500 067	−0.800 076	−0.001 173
8	0.000 000	2.279 143	0.033 055	8	1.941 573	−0.815 764	0.009 039
8	0.000 000	−1.081 402	−0.768 407	8	−1.277 515	0.586 953	0.002 285
8	0.000 000	−2.279 143	0.033 055	8	−1.953 211	−0.689 446	−0.108 083
1	0.000 000	−1.910 192	0.941 692	1	−2.352 421	−0.748 795	0.772 918
1	0.000 000	1.910 192	0.941 692	1	2.142 674	0.145 891	0.001 346
8	0.000 000	0.000 000	1.224 212	8	0.765 219	1.443 392	0.002 417
B (GHz)	11.319	2.395 9	1.977 4	B (GHz)	7.093 6	2.940 5	2.091 9

	saas				*sasg*		
No.	$\bar{\upsilon}$ (cm^{-1})	x_{ii}		No.	$\bar{\upsilon}$ (cm^{-1})	x_{ii}
1	3549.32	−47.51	a_1	1	3740.75	−82.78
2	1790.31	−8.16	a_1	2	3507.48	−103.54
3	1504.66	−4.49	a_1	3	1818.37	−10.01
4	1089.75	−2.71	a_1	4	1495.64	−8.96
5	975.65	−1.01	a_1	5	1418.25	−9.92
6	503.46	−0.26	a_1	6	1291.40	−6.40
7	262.75	−0.04	a_1	7	1036.94	−3.11
8	380.51	−18.33	a_2	8	981.03	−2.21
9	122.51	−8.30	a_2	9	902.36	−1.46
10	765.32	0.00	b_1	10	759.26	−0.21
11	354.99	−14.44	b_1	11	668.23	−0.49
12	139.87	−0.42	b_1	12	556.34	−0.21
13	3537.55	−48.73	b_2	13	420.12	−35.42
14	1489.24	−4.37	b_2	14	382.15	−0.64
15	1330.94	−7.79	b_2	15	261.71	−0.51
16	932.31	−2.68	b_2	16	221.19	−1.76
17	748.61	−0.35	b_2	17	161.82	−1.40
18	405.42	−0.65	b_2	18	118.27	3.81

3.10.1.2. Formation enthalpy, $\Delta_f H(0\ K)$. In light of the fact that *saas* fails at G3, the *sasg* conformer is used as the basis for the computation of formation enthalpy. The isodesmic reaction

$$O=C(OOH)_2 + O=C(H)_2 \rightarrow 2O=C(H)(OOH)$$

has a reaction enthalpy of −69.49 ± 1.92 kJ mol^{-1}, which together with a reference value for formaldehyde (−105.32 ± 0.11 kJ mol^{-1}) and our peroxyformic acid result of −281.6 ± 0.6 kJ mol^{-1} yields $\Delta_f H^o$(0 K) = −388.4 ± 2.1 kJ mol^{-1} (−398.8 kJ mol^{-1} at 298.15 K) for the *sasg* conformer, in agreement with a WMS of −386.7 kJ mol^{-1}. The *saas* conformer, thus, lies at −396.6 kJ mol^{-1} (−408.8 kJ mol^{-1} at 298.15 K), in comparison to a WMS of −394.9 kJ mol^{-1}.

An O–H bond dissociation energy of 218.0 kJ mol^{-1} + (−222.1 kJ mol^{-1}) − (−408.8 kJ mol^{-1}) = 405 kJ mol^{-1} is similar to that recorded [L07] for benzeneperoxy carboxylic acid, $C_6H_5C(O)OO$–H, of 404 kJ mol^{-1}.

3.10.1.3. Results. Hindered rotor analysis reveals a quite complex picture for the *saas* conformer; mode nos. 11 and 8 are symmetric and asymmetric COOH rotors, respectively, while mode nos. 9 and 12 are asymmetric and symmetric O=COO rotors, respectively. The major contribution to changes in the thermochemistry is made by replacing mode no. 9. The relaxed potential energy scans are unsatisfactory, so a default anharmonic treatment is employed.

For the *sasg* conformer that has C_1 symmetry but 2 "optical isomers," only mode no. 17 is important for which a well-behaved scan is possible. The rotation of this "free" COOH rotor interconverts the optical isomers, thus negating their contribution.

References for carbonodiperoxoic acid.

L07 Y. R. Luo, *Comprehensive Handbook of Chemical Bond Energies* (CRC Press, Boca Raton, USA, 2007).

3.10.2. Formylhydrotetroxide

^{1}A g = 1 C_1 σ = 1 M_0 = 94.0239

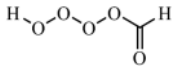

3.10.2.1. Species data.

3.10.2.2. Formation enthalpy, $\Delta_f H(0\ K)$. An isodesmic reaction featuring water (−238.931 ± 0.027 kJ mol^{-1}), formic acid (−371.12 ± 0.22 kJ mol^{-1}), and tetraoxidane (−33.6 ± 2.4 kJ mol^{-1})

$$H(O)_4CHO + HOH = H(O)CHO + H(O)_4H$$

has a reaction enthalpy of −0.17 ± 0.96 kJ mol^{-1}, which leads to $\Delta_f H^o$(0 K) = −165.6 ± 2.6 kJ mol^{-1} (−176.3 kJ mol^{-1} at 298.15 K) in reasonable agreement with a WMS atomization of −167.4 kJ mol^{-1}.

3.10.2.3. Results. Four potential hindered rotors are identified all with reduced barrier heights (*V*/*RT*)s in excess of 9.3 for mode nos. 14 and 16–18. The relaxed potential energy scans are not entirely satisfactory, so an approximate treatment consisting of the two most

saas				*sasg*			
T (K)	$S^o(T)$	$C_p^o(T)$	$H^o(T) - H^o(0)$	T (K)	$S^o(T)$	$C_p^o(T)$	$H^o(T) - H^o(0)$
298.15	323.98	91.96	19.06	298.15	336.00	95.15	19.24
300.	324.55	92.25	19.23	300.	336.59	95.45	19.41
400.	353.20	107.18	29.22	400.	366.01	109.01	29.67
500.	378.43	118.77	40.55	500.	391.45	118.79	41.09
600.	400.85	126.86	52.86	600.	413.78	126.14	53.35
700.	420.84	132.35	65.84	700.	433.68	131.95	66.26
800.	438.78	136.18	79.27	800.	451.62	136.74	79.70
900.	454.99	139.04	93.04	900.	467.97	140.82	93.58
1000.	469.76	141.31	107.06	1000.	482.99	144.36	107.85
1100.	483.32	143.21	121.28	1100.	496.90	147.48	122.44
1200.	495.85	144.88	135.69	1200.	509.85	150.22	137.33
1300.	507.51	146.37	150.25	1300.	521.98	152.64	152.47
1400.	518.41	147.72	164.95	1400.	533.37	154.75	167.84
1500.	528.64	148.97	179.79	1500.	544.11	156.58	183.41
1600.	538.29	150.11	194.74	1600.	554.26	158.16	199.14
1800.	556.10	152.16	224.97	1800.	573.04	160.66	231.04
2000.	572.22	153.91	255.58	2000.	590.07	162.45	263.36

important rotors, mode nos. 18 and 14, and anharmonic frequencies is employed.

6	−1.601 911	0.197 899	−0.195 953
8	−2.590 291	−0.458 366	−0.189 388
8	−0.530 371	−0.164 237	0.590 638
8	0.550 228	0.800 721	0.409 064
8	1.391 543	0.303 621	−0.583 196
8	2.323 988	−0.589 660	0.021 279
1	1.856 443	−1.437 805	−0.044 917
1	−1.405 747	1.113 788	−0.766 548
B (GHz)	12.592	1.769 5	1.711 8

No.	$\bar{\upsilon}$ (cm^{-1})	x_{ii}	No.	$\bar{\upsilon}$ (cm^{-1})	x_{ii}
1	3707.41	−84.29	10	686.25	−2.02
2	3041.76	−62.31	11	628.17	−3.09
3	1856.53	−10.48	12	584.11	−2.82
4	1410.27	−11.77	13	470.45	−1.76
5	1373.06	−9.57	14	382.98	−10.26
6	1083.40	−8.13	15	319.76	−0.66
7	1032.99	−2.77	16	182.37	−0.22
8	947.80	−2.09	17	145.53	−1.07
9	864.02	−3.98	18	75.59	1.63

T (K)	$S^{o}(T)$	$C_{p}^{o}(T)$	$H^{o}(T) - H^{o}(0)$
298.15	344.79	100.76	20.55
300.	345.41	101.09	20.74
400.	376.77	116.96	31.67
500.	404.21	128.88	43.99
600.	428.53	137.76	57.34
700.	450.30	144.56	71.47
800.	469.97	149.96	86.21
900.	487.90	154.34	101.43
1000.	504.35	157.94	117.05
1100.	519.55	160.89	132.99
1200.	533.65	163.30	149.20
1300.	546.80	165.26	165.63
1400.	559.11	166.85	182.24
1500.	570.67	168.14	198.99
1600.	581.55	169.17	215.86
1800.	601.57	170.72	249.85
2000.	619.62	171.80	284.11

3.10.3. Pentoxane

$^{1}A'$ g = 1 C_S σ = 1 M_0 = 94.0239

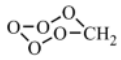

This compound features as an intermediate in a study of the reaction between the Criegee CH_2OO and ozone [VRNB15]. The "chair" form of pentoxane lies some 43 kJ mol^{-1} below the "twist-boat" form of this heterocyclic species [D92].

3.10.3.1. Species data.

6	−0.702 003	1.084 445	0.000 000
8	0.006 753	0.701 276	1.161 930
8	0.006 753	−0.742 013	1.126 015
8	0.801 964	−1.083 118	0.000 000
8	0.006 753	−0.742 013	−1.126 015
8	0.006 753	0.701 276	−1.161 930
1	−0.723 191	2.173 026	0.000 000
1	−1.696 602	0.637 038	0.000 000
B (GHz)	5.564 0	5.448 7	3.053 6

No.	$\bar{\upsilon}$ (cm^{-1})	x_{ii}		No.	$\bar{\upsilon}$ (cm^{-1})	x_{ii}	
1	3133.86	−38.42	a'	10	556.27	−0.23	a'
2	3053.49	−36.24	a'	11	368.21	−0.78	a'
3	1461.08	−0.82	a'	12	1392.03	−8.70	a''
4	1161.39	−1.54	a'	13	1294.51	−3.90	a''
5	1008.74	−3.74	a'	14	952.01	−5.14	a''
6	925.85	−1.42	a'	15	848.95	−1.88	a''
7	825.86	−2.24	a'	16	523.79	−3.68	a''
8	763.49	−1.37	a'	17	498.74	−0.53	a''
9	580.17	−1.09	a'	18	348.42	−0.42	a''

3.10.3.2. Formation enthalpy, $\Delta_f H$(0 K). An isodesmic reaction

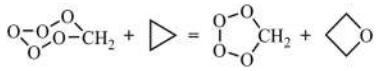

whose reaction enthalpy of −156.46 ± 1.53 kJ mol^{-1} yields a $\Delta_f H^{o}$(0 K) of 97.1 ± 3.9 kJ mol^{-1} based on a reference for cyclopropane (70.77 ± 0.47 kJ mol^{-1}), our value for tetroxolane of 71.85 ± 2.97 kJ mol^{-1}, and Dorofeeva's result for oxetane [VRNB15] of −60.5 ± 2.0 kJ mol^{-1}. A multi-composite, *sans* CBS-QB3, which is aberrant, returns 93.8 ± 5.1 kJ mol^{-1}, and direct atomization calculations give W2X 95.7 kJ mol^{-1} and WMS 86.7 kJ mol^{-1}. A final value of $\Delta_f H^{o}$(0 K) = 95.8 ± 2.0 kJ mol^{-1} (79.5 kJ mol^{-1} at 298.15 K) best summarizes these results.

3.10.3.3. Results. The ring puckering modes are treated as anharmonic oscillators.

T (K)	$S^o(T)$	$C_p^o(T)$	$H^o(T) - H^o(0)$
298.15	298.90	81.88	14.94
300.	299.41	82.29	15.09
400.	325.96	102.44	24.37
500.	350.55	117.78	35.42
600.	373.09	129.30	47.80
700.	393.71	138.10	61.18
800.	412.62	145.01	75.35
900.	430.04	150.56	90.14
1000.	446.14	155.12	105.43
1100.	461.11	158.92	121.13
1200.	475.08	162.12	137.19
1300.	488.17	164.85	153.54
1400.	500.47	167.20	170.14
1500.	512.08	169.24	186.96
1600.	523.06	171.03	203.98
1800.	543.38	174.01	238.49
2000.	561.84	176.40	273.53

References for pentoxane.

VRNB15 L. Vereecken, A. R. Rickard, M. J. Newland, and W. J. Bloss, "Theoretical study of the reactions of Criegee intermediates with ozone, alkylhydroperoxides, and carbon monoxide," Phys. Chem. Chem. Phys. **17**(37), 23847–23858 (2015).

D92 O. V. Dorofeeva, "Ideal gas thermodynamic properties of oxygen heterocyclic compounds. Part 1. Three-membered, four-membered and five-membered rings," Thermochim. Acta **194**, 9–46 (1992).

3.11. $C_2H_1O_1$

3.11.1. Ethynyloxy; oxoethynyl; ketenyl

$^2A''$ g = 2 C_S σ = 1 M_0 = 41.0293

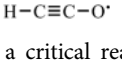

The ketenyl radical is a critical reaction intermediate in hydrocarbon combustion with the oxidation of acetylene dominated by the reaction $O(^3P) + HC{\equiv}CH \rightarrow HC{\equiv}CO^{\bullet} + H^{\bullet}$, a characteristic of all flames [BMR99, KMH02]. It is also of considerable astrophysical interest [ACG15, WLHR15].

3.11.1.1. Species data.

6	−0.378 461	1.178 274	0.000 000
6	0.000 000	−0.019 459	0.000 000
1	−0.636 929	2.206 164	0.000 000
8	0.363 462	−1.144 882	0.000 000
B (GHz)	1165.52	10.955 8	10.853 8

No.	$\bar{\upsilon}$ (cm^{-1})	x_{ii}	
1	3342.47	−63.64	a'
2	2083.13	−13.76	a'
3	1264.61	−4.50	a'
4	566.67	−4.21	a'
5	476.58	−32.80	a'
6	503.60	−1.97	a''

3.11.1.2. Formation enthalpy, $\Delta_f H$(0 K). The ATcT value of 176.85 ± 0.60 kJ mol^{-1} is largely based on high-level work by Szalay *et al.* [STS05]; it is in good accord with the value of 175.5 kJ mol^{-1} (176.5 kJ mol^{-1} at 298.15 K) computed via W3X-L and indeed with multi-composite 175.8 ± 2.0 kJ mol^{-1}. Various ANL composites [KHR17] suggest slight reductions in the ATcT value of 0.2–0.3 kJ mol^{-1}.

3.11.1.3. Results. Good agreement with our anharmonic rigid rotor treatment is obtained with the tabulated data, S^o = 246.41 J K^{-1} mol^{-1} and C_p^o = 49.98 J K^{-1} mol^{-1}, in the Extended Third Millennium Ideal Gas and Condensed Phase Thermochemical Database and with the Small Molecule database [GMG12] S^o(298.15 K) = 246.0 ± 2.5 J K^{-1} mol^{-1} and C_p^o(300 K) = 50.2 ± 1.7 J K^{-1} mol^{-1}.

T (K)	$S^o(T)$	$C_p^o(T)$	$H^o(T) - H^o(0)$
298.15	247.38	51.65	11.93
300.	247.70	51.78	12.03
400.	263.39	57.09	17.49
500.	276.50	60.28	23.37
600.	287.67	62.22	29.51
700.	297.37	63.57	35.80
800.	305.93	64.67	42.21
900.	313.61	65.64	48.73
1000.	320.57	66.55	55.34
1100.	326.95	67.40	62.03
1200.	332.85	68.19	68.81
1300.	338.34	68.94	75.67
1400.	343.48	69.62	82.60
1500.	348.30	70.26	89.59
1600.	352.85	70.85	96.65
1800.	361.26	71.90	110.92
2000.	368.89	72.82	125.40

References for ethynyloxy; oxoethynyl; ketenyl.

BMR99 L. R. Brock, B. Mischler, and E. A. Rohlfing, "Laser-induced fluorescence spectroscopy of the B $^2\Pi$–X $^2A''$ band system of HCCO and DCCO," J. Chem. Phys. **110**, 6773–6781 (1999).

KMH02 S. J. Klippenstein, J. A. Miller, and L. B. Harding, "Resolving the mystery of prompt CO_2: The HCCO + O_2 reaction," Proc. Combust. Inst. **29**, 1209 (2002).

ACG15 M. Agúndez, J. Cernicharo and M. Guélin Discovery of interstellar ketenyl (HCCO), a surprisingly abundant radical. Astron. Astrophys., **577**, L5 (2015).

WLHR15 V. Wakelam, J.-C. Loison, K. M. Hickson, and M. Ruaud, "A proposed chemical scheme for HCCO formation in cold dense clouds," Mon. Not. R. Astron. Soc. Lett. **453**, L48–L52 (2015).

STS05 P. G. Szalay, A. Tajti, and J. F. Stanton, "*Ab initio* determination of the heat of formation of ketenyl (HCCO) and ethynyl (CCH) radicals," Mol. Phys. **103**(15-16), 2159–2168 (2005).

KHR17 S. J. Klippenstein, L. B. Harding, and B. Ruscic, "*Ab initio* computations and active thermochemical tables hand in hand: Heats of formation of core combustion species," J. Phys. Chem. A **121**(35), 6580–6602 (2017).

GMG12 C. F. Goldsmith, G. R. Magoon, and W. H. Green, "Database of small molecule thermochemistry for combustion," J. Phys. Chem. A **116**(36), 9033–9057 (2012).

3.11.2. Hydroxyethynyl

^2A g = 2 C_1 σ = 1 M_0 = 41.0293

The iso-ketenyl radical was noted as an intermediate in a combined experimental and theoretical study of the reaction between the ethynyl radical and nitrous oxide [NEPC12]. Zeng *et al.* used general multiconfigurational perturbation theory to explore the ground (C_S, $^2A''$) and excited state of hydroxyethynyl [ZDSA15]. Sattelmeyer *et al.* showed that (**2d**), energetically at least, the floppy nature of the torsional angle renders C_1 and C_S symmetry structures quite similar [SYS04].

3.11.2.1. Species data.

6	1.481 819	0.020 056	−0.021 139
6	0.203 169	0.003 003	0.041 510
8	−1.074 773	−0.111 886	−0.013 569
1	−1.511 744	0.756 739	−0.013 676
B (GHz)	657.27	10.6112	10.4551

No.	$\bar{\upsilon}$ (cm^{-1})	x_{ii}
1	3650.55	−96.89
2	1998.10	−45.12
3	1257.33	−14.71
4	1071.31	−2.33
5	325.51	−4.28
6	141.82	−762.37

3.11.2.2. Formation enthalpy, $\Delta_f H$(0 K).

Relative to the reactants, HCC$^\bullet$ + N_2O, hydroxyethynyl lies 232 kJ mol^{-1} below [NEPC12]; this transforms into a $\Delta_f H^\circ$(0 K) of 418.1 kJ mol^{-1}. Sattelmeyer *et al.* [SYS04] placed it at +229 kJ mol^{-1} above ketenyl from EOMIP-CCSD/cc-pVQZ calculations, which can be interpreted as a value of $\Delta_f H^\circ$(0 K) = 406.2 kJ mol^{-1}. Multi-composite computations suggest 408.5 ± 2.8 kJ mol^{-1}. Our highest level W3X-L returns $\Delta_f H^\circ$(0 K) = 408.1 kJ mol^{-1} (410.3 at 298.15 K).

3.11.2.3. Results.

There is only moderate agreement with the CCSD(T)/cc-pVTZ frequencies of the Sattelmeyer study [SYS04], which did not report any anharmonicities. Mode no. 6 is highly anharmonic, and hence, a simplified RRHO treatment is used.

T (K)	$S^\circ(T)$	$C_p^\circ(T)$	$H^\circ(T) - H^\circ(0)$
298.15	258.16	50.21	12.79
300.	258.47	50.27	12.89
400.	273.43	53.92	18.10
500.	285.84	57.33	23.66
600.	296.56	60.31	29.55
700.	306.06	62.88	35.71
800.	314.60	65.09	42.11
900.	322.38	67.00	48.72
1000.	329.53	68.66	55.50
1100.	336.14	70.12	62.44
1200.	342.30	71.39	69.52
1300.	348.06	72.52	76.71
1400.	353.47	73.50	84.01
1500.	358.57	74.38	91.41
1600.	363.40	75.15	98.88
1800.	372.33	76.44	114.05
2000.	380.43	77.46	129.44

References for hydroxyethynyl.

NEPC12 V. S. Nguyen, R. M. I. Elsamra, J. Peeters, S. A. Carl, and M. T. Nguyen, "Experimental and theoretical study of the reaction of the ethynyl radical with nitrous oxide, C_2H + N_2O," Phys. Chem. Chem. Phys. **14**(20), 7456–7470 (2012).

ZDSA15 T. Zeng, D. Danovich, S. Shaik, N. Ananth, anmann, "Tuning the ground state symmetry of acetylenyl radicals," ACS Cent. Sci. **1**(5), 270–278 (2015).

SYS04 K. W. Sattelmeyer, Y. Yamaguchi, and H. F. Schaefer III, "Energetics of the low-lying isomers of HCCO," Chem. Phys. Lett. **383**, 266–269 (2004).

3.11.3. Oxirenyl

$^2A''$ g = 2 C_S σ = 1 M_0 = 41.0293

In a study of the low-lying isomers of HCCO, Sattelmeyer *et al.* computed the geometry and frequencies of this bridged oxiryl radical, which they found to be highest in relative energy compared to the

ketenyl radical [SYS04]. Oxirenyl is an intermediate in the reaction of ethynyl, HC≡C•, and O(^{3}P)-atom [ZZLL07].

3.11.3.1. Species data.

6	0.000 000	0.639 199	0.000 000
6	0.978 630	−0.287 124	0.000 000
8	−0.690 603	−0.471 730	0.000 000
1	−0.346 954	1.661 387	0.000 000
B (GHz)	42.307	25.968	16.091

No.	$\bar{\upsilon}$ (cm^{-1})	x_{ii}	
1	3228.01	−61.52	a'
2	1555.22	−7.84	a'
3	1295.67	−14.65	a'
4	1036.97	−3.57	a'
5	315.34	0.01	a'
6	819.25	−7.64	a''

3.11.3.2. Formation enthalpy, $\Delta_f H$(0 K). Relative to ketenyl, Sattelmeyer [SYS04] placed oxirenyl at +220 kJ mol^{-1}, which therefore implies $\Delta_f H^\circ$(0 K) = 397 kJ mol^{-1}; this is in good agreement with W3X-L of $\Delta_f H^\circ$(0 K) = 398.1 kJ mol^{-1} (398.7 kJ mol^{-1} at 298.15 K).

3.11.3.3. Results. There is very good agreement with the CCSD(T)/cc-pVTZ frequencies of the Sattelmeyer study.

T (K)	$S^\circ(T)$	$C_p^\circ(T)$	$H^\circ(T) - H^\circ(0)$
298.15	253.40	45.26	11.30
300.	253.68	45.36	11.38
400.	267.50	50.94	16.20
500.	279.42	55.88	21.55
600.	289.98	59.96	27.35
700.	299.48	63.30	33.51
800.	308.12	66.05	39.99
900.	316.03	68.35	46.71
1000.	323.34	70.30	53.64
1100.	330.12	71.96	60.76
1200.	336.44	73.39	68.03
1300.	342.37	74.63	75.43
1400.	347.94	75.71	82.94
1500.	353.19	76.67	90.56
1600.	358.17	77.51	98.27
1800.	367.38	78.94	113.92
2000.	375.76	80.11	129.83

References for oxirenyl.

SYS04 K. W. Sattelmeyer, Y. Yamaguchi, and H. F. Schaefer III, "Energetics of the low-lying isomers of HCCO," Chem. Phys. Lett. **383**, 266–269 (2004).

ZZLL07 X.-l. Zhao, J.-x. Zhang, J.-y. Liu, X.-t. Li, and Z.-s. Li, "Theoretical study on the mechanism of the C_2H + O reaction," Chem. Phys. Lett. **436**, 41–46 (2007).

3.11.4. Oxoethylidyne

$^4A''$ g = 4 C_S σ = 1 M_0 = 41.0293

This has been encountered in a BHandHYLP/aug-cc-pVDZ theoretical study of the reaction between the methylidyne radical, CH ($^2\Pi$), with formaldehyde [NNNV14]. Attempts to optimize the doublet structure at B3LYP/cc-pVDZ + d results in the oxirenyl-type structure with a CCO bond angle of ~80°, shown previously above, and in fact, this is what was reported by Nguyen *et al.* as **P4**. An estimate can be made of its formation enthalpy, from the relative energies given in that work, of 408 kJ mol^{-1}, which is close to our result of 398.1 kJ mol^{-1} for oxirenyl above. Thus, oxoethylidyne has been mis-classified as featuring in the work of Nguyen *et al.* It apparently occurs as an intermediate in a study of conversion of ethanol on PtSn catalytic surfaces but is called formylmethylidene [ASHS05].

However, a quartet state $^4A''$ readily exists, ∠CCO ~ 125°, and is featured *here*.

3.11.4.1. Species data.

6	1.359 251	−0.203 453	0.000 000
8	−1.018 312	−0.294 728	0.000 000
6	0.000 000	0.353 594	0.000 000
1	−0.009 013	1.456 977	0.000 000
B (GHz)	93.411	13.018 0	11.4247

No.	$\bar{\upsilon}$ (cm^{-1})	x_{ii}	
1	2921.87	−77.59	a'
2	1639.19	−16.10	a'
3	1258.28	−10.94	a'
4	977.71	−11.92	a'
5	583.37	−0.26	a'
6	902.05	−3.30	a''

3.11.4.2. Formation enthalpy, $\Delta_f H$(0 K). A W3X-L atomization calculation returns $\Delta_f H^\circ$(0 K) = 510.1 kJ mol^{-1} (510.1 kJ mol^{-1} at 298.15 K) with W2X and WMS at 518.6 kJ mol^{-1} and 517.3 kJ mol^{-1}, respectively.

3.11.4.3. Results. A standard rigid rotor anharmonic approach is used.

T (K)	$S^o(T)$	$C_p^o(T)$	$H^o(T) - H^o(0)$
298.15	256.46	42.64	10.66
300.	256.73	42.76	10.74
400.	269.92	49.14	15.34
500.	281.49	54.64	20.54
600.	291.87	59.16	26.24
700.	301.28	62.86	32.34
800.	309.87	65.90	38.79
900.	317.78	68.42	45.51
1000.	325.11	70.53	52.45
1100.	331.91	72.32	59.60
1200.	338.27	73.84	66.91
1300.	344.24	75.15	74.36
1400.	349.85	76.28	81.93
1500.	355.15	77.27	89.61
1600.	360.16	78.14	97.38
1800.	369.45	79.62	113.16
2000.	377.91	80.83	129.21

References for oxoethylidyne.

NNNV14 H. M. T. Nguyen, H. T. Nguyen, T.-N. Nguyen, H. Van Hoang, and L. Vereecken, "Theoretical study on the reaction of the methylidyne radical, CH($X^2\Pi$), with formaldehyde CH2O," J. Phys. Chem. A **118**(38), 8861–8871 (2014).

ASHS05 R. Alcala, J. W. Shabaker, G. W. Huber, M. A. Sanchez-Castillo, and J. A. Dumesic, "Experimental and DFT studies of the conversion of ethanol and acetic acid on PtSn-based catalysts," J. Phys. Chem. B **109**, 2074 (2005).

3.12. $C_2H_1O_2$

3.12.1. *Carboxymethylidyne* syn/anti

$^2A''$ g = 2 C_S σ = 1 M_0 = 57.0287

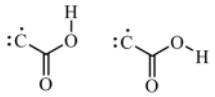

This is one of a number of species that cropped up as an intermediate, no. **8**, in a theoretical study of the HC≡C$^\bullet$ + O_2 reaction [SPN98]. The authors illustrate the *syn* HOCO conformer although we find the *anti* to be only slightly less stable but the difference is small, ~ 2 kJ mol^{-1}. Paradoxically, a more recent study of the self-same reaction only illustrates the *anti* conformer, their species **M4** [BBTS18].

3.12.1.1. Species data.

	syn				*anti*		
1	1.689 126	−0.710 601	0.000 000	1	1.414 514	1.325 495	0.000 000
8	1.314 245	0.184 808	0.000 000	8	1.285 836	0.367 114	0.000 000
6	0.000 000	0.102 949	0.000 000	6	0.000 000	0.087 538	0.000 000
6	−1.072 611	0.991 096	0.000 000	6	−1.279 120	0.616 994	0.000 000
8	−0.720 927	−0.916 516	0.000 000	8	−0.503 310	−1.061 200	0.000 000
B (GHz)	19.153	9.611 3	6.399 7	B (GHz)	21.048 7	9.243 9	6.423 1

	syn				*anti*		
No.	$\bar{\upsilon}$ (cm^{-1})	x_{ii}		No.	$\bar{\upsilon}$ (cm^{-1})	x_{ii}	
1	3713.08	−85.22	a'	1	3770.05	−82.94	a'
2	1665.56	−8.94	a'	2	1696.83	−7.93	a'
3	1506.45	−6.05	a'	3	1460.63	−6.26	a'
4	1165.16	−6.33	a'	4	1171.04	−5.43	a'
5	947.42	−3.07	a'	5	949.52	−3.02	a'
6	511.72	0.10	a'	6	517.11	−0.24	a'
7	250.23	0.06	a'	7	288.20	−1.07	a'
8	608.73	−2.05	a''	8	561.27	0.32	a''
9	482.77	−5.34	a''	9	488.77	−15.42	a''

3.12.1.2. Formation enthalpy, $\Delta_f H(0\ K)$. W3X-L returns $\Delta_f H^o(0\ K) = 176.9\ kJ\ mol^{-1}$ ($175.9\ kJ\ mol^{-1}$ at 298.15 K) for the *syn*, which is only in moderate agreement with the value of $185.3\ kJ\ mol^{-1}$ that can be extracted for the *syn* conformer [SPN98] but close to an ANL0 value [KHR17] of $179.5\ kJ\ mol^{-1}$. Recent high-level work [BBTS18] can be interpreted as implying a $\Delta_f H^o(0\ K)$ of $182.5\ kJ\ mol^{-1}$ for the *anti*, which is in excellent agreement with our W3X-L of $\Delta_f H^o(0\ K) = 181.0\ kJ\ mol^{-1}$ ($179.9\ kJ\ mol^{-1}$ at 298.15 K).

At multiple composite atomization levels of theory, the *syn* is $179.6 \pm 3.3\ kJ\ mol^{-1}$ and the *anti* is adjudged to be $181.7 \pm 2.8\ kJ\ mol^{-1}$.

3.12.1.3. Results. Hindered rotor correction for mode no. 8 is minimal at 300 K, $< 0.4\ J\ K^{-1}\ mol^{-1}$, but is nevertheless included in a full treatment.

References for carboxymethylidyne *syn/anti*.

SPN98 R. Sumathi, J. Peeters, and M. T. Nguyen, "Theoretical studies on the $C_2H + O_2$ reaction: Mechanism for HCO + CO, HC≡CO + O and CH + CO_2 formation," Chem. Phys. Lett. **287**(1-2), 109–118 (1998).

BBTS18 M. C. Bowman, A. D. Burke, J. M. Turney and H. F. Schaefer Mechanisms of the ethynyl radical reaction with molecular oxygen. J. Phys. Chem. A, **122**, 9498–9511 (2018).

KHR17 S. J. Klippenstein, L. B. Harding, and B. Ruscic, "*Ab initio* computations and active thermochemical tables hand in hand: Heats of formation of core combustion species," J. Phys. Chem. A **121**(35), 6580–6602 (2017).

3.12.2. Dioxyethenylidene anti/syn

$^2A''$ g = 2 C_S σ = 1 M_0 = 57.0287

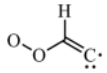

This is yet another intermediate species, no. **6**, in a theoretical study of the $HC{\equiv}C^{\bullet} + O_2$ reaction [BBTS18]. The *syn* conformer is higher in energy by $1.5\ kJ\ mol^{-1}$, as shown by multiple composite atomization computations.

3.12.2.1. Species data.

	syn			*anti*		
T (K)	$S^o(T)$	$C_p^o(T)$	$H^o(T) - H^o(0)$	$S^o(T)$	$C_p^o(T)$	$H^o(T) - H^o(0)$
298.15	281.74	63.48	13.84	280.98	63.94	13.80
300.	282.13	63.63	13.95	281.37	64.10	13.92
400.	301.53	71.28	20.71	300.94	72.03	20.74
500.	318.13	77.51	28.16	317.74	78.62	28.28
600.	332.72	82.58	36.17	332.58	84.16	36.43
700.	345.77	86.64	44.64	345.91	88.70	45.08
800.	357.56	89.89	53.47	358.00	92.30	54.14
900.	368.30	92.49	62.60	369.03	95.05	63.51
1000.	378.16	94.59	71.95	379.16	97.05	73.12
1100.	387.26	96.31	81.50	388.48	98.47	82.90
1200.	395.70	97.74	91.20	397.09	99.42	92.79
1300.	403.57	98.95	101.04	405.08	100.04	102.77
1400.	410.95	99.99	110.99	412.50	100.41	112.79
1500.	417.88	100.90	121.03	419.44	100.61	122.84
1600.	424.41	101.70	131.16	425.94	100.70	132.91
1800.	436.47	103.05	151.64	437.80	100.70	153.05
2000.	447.39	104.13	172.36	448.40	100.61	173.18

OOCC *anti*				OOCC *syn*			
6	1.501 969	−1.237 505	0.000 000	6	−0.599 119	−1.559 567	0.000 000
6	0.324 644	−0.648 981	0.000 000	6	−0.812 412	−0.257 900	0.000 000
8	0.000 000	0.685 296	0.000 000	8	0.000 000	0.841 385	0.000 000
8	−1.308 481	0.901 555	0.000 000	8	1.293 748	0.525 081	0.000 000
1	−0.491 830	−1.375 887	0.000 000	1	−1.880 794	−0.026 919	0.000 000

	anti				*syn*	
B (GHz)	66.840	5.363 9	4.965 4	*B* (GHz)	26.028	7.344 9	5.728 5

	anti			*syn*		
No.	$\bar{\upsilon}$ (cm^{-1})	x_{ii}		$\bar{\upsilon}$ (cm^{-1})	x_{ii}	
1	3081.92	−69.96	a'	3088.80	−68.85	a'
2	1665.18	−12.52	a'	1654.54	−13.63	a'
3	1142.12	−3.67	a'	1160.73	−5.51	a'
4	1079.64	−4.55	a'	1038.23	−3.30	a'
5	884.08	−4.85	a'	946.52	−8.62	a'
6	516.07	−0.51	a'	584.13	−6.02	a'
7	257.63	−2.27	a'	180.26	−3.97	a'
8	675.84	−4.47	a''	683.09	−6.90	a''
9	116.48	−4.18	a''	203.70	−6.64	a''

3.12.2.2. Formation enthalpy, $\Delta_f H(0\ K)$. A high level W3X-L value of $\Delta_f H^o(0\ K) = 549.2$ kJ mol^{-1} (549.2 kJ mol^{-1} at 298.15 K) is found for the *anti* species whose T_1 of 0.038 indicates some multi-reference character. The most recent high-level work of Bowman *et al.* [BBTS18] has 550.3 kJ mol^{-1} for the *anti*-conformer, which they label **M7**, in excellent agreement with our W3X-L result.

A $\Delta_f H^o(0\ K)$ of 542 kJ mol^{-1} emerges from the study of Sumathi *et al.*; [SPN98] an averaged multi-composite atomization value of 551.2 ± 3.3 kJ mol^{-1} (552.7 ± 2.1 kJ mol^{-1} at 298.15 K) is in moderate agreement. The agreement is not as good for the *syn* conformer, **M8**, literature [BBTS18] value of 557.1 kJ mol^{-1} as against our $\Delta_f H^o(0\ K) =$ 551.8 kJ mol^{-1} (552.1 kJ mol^{-1} at 298.15 K).

3.12.2.3. Results. An anharmonic hindered rotor treatment is employed here.

	anti			*syn*		
T (K)	$S^o(T)$	$C_p^o(T)$	$H^o(T) - H^o(0)$	$S^o(T)$	$C_p^o(T)$	$H^o(T) - H^o(0)$
298.15	290.48	66.64	15.04	295.00	67.87	15.30
300.	290.89	66.80	15.16	295.42	68.04	15.43
400.	311.14	73.96	22.22	316.17	76.16	22.66
500.	328.25	79.32	29.89	333.81	81.80	30.58
600.	343.09	83.43	38.04	349.07	85.42	38.95
700.	356.21	86.73	46.55	362.42	87.72	47.61
800.	367.97	89.47	55.36	374.24	89.25	56.47
900.	378.65	91.81	64.43	384.82	90.38	65.45
1000.	388.43	93.85	73.71	394.39	91.28	74.53
1100.	397.46	95.65	83.19	403.13	92.06	83.70
1200.	405.85	97.23	92.83	411.17	92.75	92.94
1300.	413.69	98.63	102.63	418.62	93.39	102.25
1400.	421.05	99.84	112.55	425.56	94.00	111.62
1500.	427.97	100.88	122.59	432.07	94.57	121.04
1600.	434.51	101.77	132.72	438.19	95.13	130.53
1800.	446.58	103.12	153.22	449.46	96.20	149.66
2000.	457.49	103.99	173.93	459.65	97.24	169.00

References for dioxyethenylidene *anti/syn*.

SPN98 R. Sumathi, J. Peeters, and M. T. Nguyen, "Theoretical studies on the $C_2H + O_2$ reaction: Mechanism for HCO + CO, HC≡CO + O and CH + CO_2 formation," Chem. Phys. Lett. **287**(1-2), 109–118 (1998).

BBTS18 M. C. Bowman, A. D. Burke, J. M. Turney and H. F. Schaefer Mechanisms of the ethynyl radical reaction with molecular oxygen. J. Phys. Chem. A, **122**, 9498–9511 (2018).

3.12.3. 1,2-Dioxet-3-yl; dioxetenyl

$^2A'$ g = 2 C_S σ = 1 M_0 = 57.0287

This is yet another intermediate species, no. **4**, in a theoretical study of the $HC{\equiv}C^{\bullet} + O_2$ reaction [SPN98], which is also to be found in the more recent work of Bowman *et al.* (**S3**) [BBTS18].

3.12.3.1. Species data.

6	0.994 070	−0.091 556	0.000 000
6	0.031 945	−1.000 421	0.000 000
8	−1.025 655	−0.135 176	0.000 000
8	0.000 000	0.943 235	0.000 000
1	2.049 149	0.087 391	0.000 000
B (GHz)	19.065 1	15.319 5	8.494 2

No.	$\bar{\upsilon}$ (cm^{-1})	x_{ii}	
1	3335.59	−53.79	a'
2	1598.71	−11.44	a'
3	1180.78	−4.65	a'
4	1133.04	−3.79	a'
5	980.02	−1.97	a'
6	865.01	−6.07	a'
7	741.13	−15.44	a'
8	606.17	−3.29	a''
9	329.12	−43.49	a''

3.12.3.2. Formation enthalpy, $\Delta_f H(0\ K)$. A literature value [BBTS18] of $\Delta_f H^o(0\ K)$ = 422.6 kJ mol^{-1} exists for this species, which is in excellent agreement with our W3X-L of 421.9 kJ mol^{-1} (419.3 kJ mol^{-1} at 298.15 K).

3.12.3.3. Results. A standard anharmonic treatment is employed, neglecting the impact of ring-puckering modes.

T (K)	$S^o(T)$	$C_p^o(T)$	$H^o(T) - H^o(0)$
298.15	271.85	52.69	12.42
300.	272.18	52.83	12.51
400.	288.45	60.53	18.19
500.	302.70	67.23	24.59
600.	315.46	72.65	31.59
700.	327.00	76.98	39.08
800.	337.52	80.49	46.96
900.	347.17	83.41	55.16
1000.	356.09	85.87	63.63
1100.	364.38	88.00	72.32
1200.	372.12	89.85	81.22
1300.	379.38	91.49	90.29
1400.	386.22	92.94	99.51
1500.	392.67	94.23	108.87
1600.	398.79	95.38	118.35
1800.	410.14	97.27	137.63
2000.	420.47	98.72	157.23

References for 1,2-dioxet-3-yl; dioxetenyl.

SPN98 R. Sumathi, J. Peeters, and M. T. Nguyen, "Theoretical studies on the $C_2H + O_2$ reaction: Mechanism for HCO + CO, HC≡CO + O and CH + CO_2 formation," Chem. Phys. Lett. **287**(1-2), 109–118 (1998).

BBTS18 M. C. Bowman, A. D. Burke, J. M. Turney, and H. F. Schaefer, "Mechanisms of the ethynyl radical reaction with molecular oxygen," J. Phys. Chem. A, **122**, 9498–9511 (2018).

3.12.4. Ethynylhydroperoxide radical

$^2A''$ g = 2 C_S σ = 1 M_0 = 57.0287

·C≡C−OOH

This little-known isomer of ethynylperoxy (see below) is said to be highly unstable [SBB02] and readily dissociates as follows:

$$HOOC{\equiv}\dot{C} \longrightarrow H\dot{O} + O{=}C{=}C{:}$$

3.12.4.1. Species data.

6	−1.622 362	−1.225 555	0.000 000
6	−0.745 251	−0.270 798	0.000 000
8	0.000 000	0.702 583	0.000 000
8	1.537 259	0.273 292	0.000 000
1	1.907 608	1.171 115	0.000 000
B (GHz)	45.004	5.168 8	4.636 3

No.	$\bar{\upsilon}$ (cm^{-1})	x_{ii}	
1	3733.05	−78.90	a'
2	1896.18	−18.16	a'
3	1280.26	−19.77	a'
4	1097.35	−1.97	a'
5	590.50	−12.95	a'
6	316.51	−525.88	a'
7	186.04	0.52	a'
8	297.26	7.42	a''
9	176.93	−29.43	a''

3.12.4.2. Formation enthalpy, $\Delta_f H$(0 K). W2X and WMS coupled cluster CBS atomization methods give $\Delta_f H^\circ$(0 K) of 484.3 kJ mol^{-1} and 481.9 kJ mol^{-1} with W3X-L at 476.2 kJ mol^{-1} (477.1 kJ mol^{-1} at 298.15 K) for this T_1 = 0.032 species.

3.12.4.3. Results. A strongly anharmonic mode no. 6 and a failed potential energy scan about the O–O bond, which leads to dissociation and reformation of HOCCO$^\bullet$, mean that a simplistic RRHO treatment is employed.

T (K)	$S^\circ(T)$	$C_p^\circ(T)$	$H^\circ(T) - H^\circ(0)$
298.15	295.82	69.28	15.76
300.	296.25	69.40	15.89
400.	317.03	75.17	23.13
500.	334.32	79.81	30.89
600.	349.22	83.55	39.06
700.	362.33	86.59	47.57
800.	374.07	89.11	56.36
900.	384.69	91.22	65.38
1000.	394.39	93.01	74.59
1100.	403.33	94.56	83.97
1200.	411.62	95.91	93.49
1300.	419.34	97.08	103.14
1400.	426.58	98.11	112.90
1500.	433.38	99.02	122.76
1600.	439.79	99.82	132.70
1800.	451.63	101.15	152.80
2000.	462.34	102.21	173.14

References for ethynylhydroperoxide radical.

SBB02 N. Sebbar, H. Bockhorn, and J. W. Bozzelli, "Structures, thermochemical properties (enthalpy, entropy and heat capaci-ty), rotation barriers, and peroxide bond energies of vinyl, allyl, ethynyl and phenyl hydroperoxides," Phys. Chem. Chem. Phys. **4**, 3691–3703 (2002).

3.12.5. Ethynylperoxy; ethynyldioxy radical

$^2A''$ g = 2 C_1 σ = 1 M_0 = 57.0287

This species, no. **1**, has been encountered [SPN98] in the reaction between ethynyl radicals and molecular oxygen, the chemically activated product dissociating to HC≡CO$^\bullet$ + O or else to the thermodynamically most stable products HCO$^\bullet$ + CO. A much more recent and detailed study by Bowman *et al.* shows that the ground electronic state is $^2A''$ and concludes [BBTS18] that it lies −200.7 kJ mol^{-1} *below* the reactants HC≡C$^\bullet$ + $O_2(^3\Sigma_g^-)$, which gives rise to a $\Delta_f H^\circ$(0 K) of 363.2 kJ mol^{-1}.

3.12.5.1. Species data.

6	−0.504 378	1.716 931	0.000 000
6	0.000 000	0.631 149	0.000 000
1	−0.968 856	2.670 581	0.000 000
8	0.652 984	−0.505 084	0.000 000
8	−0.153 594	−1.589 799	0.000 000
B (GHz)	58.034	5.365 0	4.911 0

No.	$\bar{\upsilon}$ (cm^{-1})	x_{ii}	
1	3477.20	−50.50	a'
2	2208.96	−8.98	a'
3	1066.89	−9.98	a'
4	989.91	−3.93	a'
5	677.53	−3.46	a'
6	612.61	−0.48	a'
7	233.88	0.46	a'
8	603.62	−2.13	a''
9	395.17	−1.95	a''

3.12.5.2. Formation enthalpy, $\Delta_f H$(0 K). Sebbar *et al.* reported [SBB02] a value of 351.9 ± 1.5 kJ mol^{-1} at 298.15 K from a series of isodesmic reactions at B3LYP/6-311G(d,p).

We have used the isodesmic reaction

$$HCCOO^\cdot + CH_4 = CH_3OO^\cdot + HCCH$$

for which a reaction enthalpy of −45.01 ± 2.40 kJ mol^{-1} is obtained; this together with reference values for methane, methyl peroxy, and ethyne leads to $\Delta_f H^\circ$(0 K) = 362.7 ± 2.5 kJ mol^{-1} (361.1 kJ mol^{-1} at 298.15 K).

A T_1 of 0.031 indicates some multi-reference character with W2X predicting 366.9 kJ mol^{-1}, whereas W3X-L predicts 364.0 kJ mol^{-1} (362.4 kJ mol^{-1} at 298.15 K); the latest result [BBTS18] of $\Delta_f H^o$(0 K) = 363.2 kJ mol^{-1}, which uses correlation methods up to CCSDT(Q) and basis sets as large as cc-pV6Z, is neatly bracketed by our values.

3.12.5.3. Results. A straightforward rigid rotor–anharmonic oscillator treatment is applied here.

T (K)	$S^o(T)$	$C_p^o(T)$	$H^o(T) - H^o(0)$
298.15	278.46	62.32	13.42
300.	278.85	62.51	13.54
400.	298.09	71.17	20.25
500.	314.67	77.33	27.69
600.	329.19	81.91	35.66
700.	342.10	85.51	44.03
800.	353.72	88.45	52.74
900.	364.28	90.93	61.71
1000.	373.98	93.06	70.91
1100.	382.93	94.90	80.31
1200.	391.26	96.51	89.88
1300.	399.04	97.92	99.60
1400.	406.35	99.17	109.46
1500.	413.23	100.28	119.43
1600.	419.73	101.27	129.51
1800.	431.76	102.97	149.93
2000.	442.68	104.39	170.67

References for ethynylperoxy; ethynyldioxy radical.

SPN98 R. Sumathi, J. Peeters, and M. T. Nguyen, "Theoretical studies on the $C_2H + O_2$ reaction: Mechanism for HCO + CO, HC≡CO + O and CH + CO_2 formation," Chem. Phys. Lett. **287**(1-2), 109–118 (1998).

BBTS18 M. C. Bowman, A. D. Burke, J. M. Turney, and H. F. Schaefer, "Mechanisms of the ethynyl radical reaction with molecular oxygen," J. Phys. Chem. A, **122**, 9498–9511 (2018).

SBB02 N. Sebbar, H. Bockhorn, and J. W. Bozzelli, "Structures, thermochemical properties (enthalpy, entropy and heat capacity), rotation barriers, and peroxide bond energies of vinyl, allyl, ethynyl and phenyl hydroperoxides," Phys. Chem. Chem. Phys. **4**(15), 3691–3703 (2002).

3.12.6. Formyloxymethylidyne; formoxycarbyne

$^2A'$ g = 2 C_S σ = 1 M_0 = 57.0287

The *anti* OCOC conformer was adjudged to be the most stable, in a study of carbynes [KSS82], with a $^2A'$ ground state. Sumathi and colleagues [SPN98] reported on the *syn* conformer, no. **9**.

3.12.6.1. Species data.

8	−1.022 058	1.243 627	0.000 000
6	0.000 000	0.680 238	0.000 000
1	1.036 341	1.044 694	0.000 000
8	0.030 219	−0.829 730	0.000 000
6	1.149 729	−1.406 217	0.000 000
B (GHz)	66.651	5.482 5	5.068 4

No.	$\bar{\upsilon}$ (cm^{-1})	x_{ii}	
1	3016.31	−68.83	a'
2	1928.95	−11.88	a'
3	1384.04	−10.56	a'
4	1285.39	−9.00	a'
5	723.68	−12.90	a'
6	394.78	−29.83	a'
7	362.50	−56.00	a'
8	932.05	−20.23	a''
9	90.91	−4.77	a''

3.12.6.2. Formation enthalpy, $\Delta_f H$(0 K). A $\Delta_f H^o$(0 K) of 161 kJ mol^{-1} can be extracted from relative energy data [SPN98] for the *syn* conformer with $\Delta_f H^o$(0 K) = 156.1 ± 3.8 kJ mol^{-1} for the *anti* conformer. Multiple composite atomization returns 116.8 ± 3.1 kJ mol^{-1}, which is in excellent agreement with a W3X-L value of 118.9 kJ mol^{-1} (118.6 kJ mol^{-1} at 298.15 K).

3.12.6.3. Results. A straightforward rigid rotor–anharmonic oscillator treatment is applied here. At issue is the very low frequency hindered rotor that gives rise to a problematic relaxed potential energy scan. Values of S^o = 293.3 ± 4.6 J K^{-1} mol^{-1} and C_p^o = 72.0 ± 4.2 J K^{-1} mol^{-1} have been reported [SPN98].

T (K)	$S^o(T)$	$C_p^o(T)$	$H^o(T) - H^o(0)$
298.15	292.44	56.98	14.70
300.	292.80	57.04	14.81
400.	309.62	60.04	20.66
500.	323.31	62.66	26.80
600.	334.95	65.01	33.19
700.	345.13	67.21	39.80
800.	354.24	69.27	46.62
900.	362.51	71.18	53.65
1000.	370.11	72.93	60.85
1100.	377.13	74.54	68.23
1200.	383.68	76.03	75.75
1300.	389.82	77.40	83.43
1400.	395.61	78.67	91.23
1500.	401.08	79.86	99.16
1600.	406.27	80.95	107.20
1800.	415.92	82.89	123.58
2000.	424.74	84.48	140.33

References for formyloxymethylidyne; formoxycarbyne.

KSS82 K. S. Kim, S. P. So, and H. F. Schaefer, "Structure and energetics of realistic carbynes: (Carbohydroxy)carbyne (HOCOCC:)," J. Am. Chem. Soc. **104**, 1457–1461 (1982).

SPN98 R. Sumathi, J. Peeters, and M. T. Nguyen, "Theoretical studies on the $C_2H + O_2$ reaction: Mechanism for HCO + CO, HC≡CO + O and CH + CO_2 formation," Chem. Phys. Lett. **287**(1-2), 109–118 (1998).

3.12.7. Hydroxyoxirenyl

^2A g = 2 C_1 σ = 1 M_0 = 57.0287

This oxirenyl derivative is little known. It does, however, feature in very recent work on the ethynyl plus O_2 reaction where it is categorized as species **M5** with a ^2A ground state of C_1 symmetry [BBTS18] from a CCSD(T)/ANO2 geometry and CCSD(T)/ANO1 frequencies. At our chosen DFT and basis set, convergence fails but instead results in *syn*-carboxymethylidyne (**M4**) (see above). *Here*, we show results based on the Bowman *et al.* geometry and frequencies [BBTS18].

3.12.7.1. Species data.

6	0.195 719 5	0.181 719 8	−0.393 690 4
6	−1.046 756 4	0.704 877 1	0.155 826 5
8	1.399 397 4	−0.081 935 5	0.143 264 7
1	1.942 208 1	0.709 823 3	0.060 550 4
8	−0.883 293 6	−0.627 948 9	0.031 374 6
B (GHz)	320.27	7.932	6.784

No.	$\bar{\nu}$ (cm^{-1})
1	3817
2	1473
3	1277
4	1176
5	904
6	658
7	436
8	327
9	236

3.12.7.2. Formation enthalpy, $\Delta_f H$(0 K). Bowman *et al.* reported $\Delta_f H^\circ$(0 K) = 255.5 kJ mol^{-1} in excellent agreement with our W3X-L value of 256.1 kJ mol^{-1} (254.6 kJ mol^{-1} at 298.15 K), which is, however, based on their CCSD(T)/ANO2 geometry and with a zero-point energy from their ANO1 frequencies. Of our lower-level composite methods, only CBS-APNO optimizes to the "correct" structure with an atomization result of 256.7 kJ mol^{-1}.

3.12.7.3. Results. A simple rigid rotor treatment is used adopting the unscaled frequencies and rotational constants from Bowman *et al.*

References for hydroxyoxirenyl.

BBTS18 M. C. Bowman, A. D. Burke, J. M. Turney, and H. F. Schaefer, "Mechanisms of the ethynyl radical reaction with molecular oxygen," J. Phys. Chem. A **122**, 9498–9511 (2018).

T (K)	$S^\circ(T)$	$C_p^\circ(T)$	$H^\circ(T) - H^\circ(0)$
298.15	279.19	61.16	13.56
300.	279.57	61.32	13.68
400.	298.38	69.53	20.23
500.	314.62	76.07	27.52
600.	328.96	81.10	35.39
700.	341.76	84.96	43.70
800.	353.31	87.98	52.36
900.	363.82	90.41	61.28
1000.	373.45	92.40	70.42
1100.	382.34	94.08	79.75
1200.	390.59	95.50	89.23
1300.	398.28	96.74	98.84
1400.	405.49	97.81	108.57
1500.	412.27	98.74	118.39
1600.	418.67	99.57	128.31
1800.	430.48	100.94	148.36
2000.	441.17	102.03	168.66

3.12.8. Hydroxyoxoethenyl; 1-hydroxylketenyl

$^2A''$ g = 2 C_S σ = 1 M_0 = 57.0287

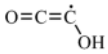

This species, no. **7**, has been encountered [SPN98] This little-known isomer of ethynylperoxy and molecular oxygen [SPN98, BBTS18].

3.12.8.1. Species data.

6	−0.414 733	−0.556 666	0.000 000
8	−1.079 386	−1.522 268	0.000 000
6	0.000 000	0.687 793	0.000 000
8	1.240 659	1.158 615	0.000 000
1	1.198 216	2.122 464	0.000 000
B (GHz)	143.674	4.371 1	4.242 1

No.	$\bar{\upsilon}$ (cm^{-1})	x_{ii}	
1	3768.35	−91.59	a'
2	2108.51	−13.29	a'
3	1515.02	−9.31	a'
4	1277.95	−11.80	a'
5	918.98	−4.47	a'
6	570.01	−1.60	a'
7	264.82	−2.35	a'
8	570.96	−1.63	a''
9	364.67	0.01	a''

3.12.8.2. Formation enthalpy, $\Delta_f H$(0 K). The most recent study [BBTS18] can be interpreted to yield a $\Delta_f H^o$(0 K) of 34.7 kJ mol^{-1} for the $^2A''$ ground state (**M6**), which is in moderate agreement with the $\Delta_f H^o$(0 K) = 31.3 kJ mol^{-1} (29.5 kJ mol^{-1} at 298.15 K) from our W3X-L calculation. Both W2X and WMS composites are in agreement at 34.3 kJ mol^{-1} and 34.9 kJ mol^{-1}, respectively, neither of which include post-CCSD(T) corrections.

A value of 10.4 kJ mol^{-1} can be extracted from Sumathi *et al.* [SPN98], one of 22.1 ± 3.8 kJ mol^{-1} at 298.15 K from the small combustion database [GMG12] and 21.3 kJ mol^{-1} from an ANL0 calculation [KHR17]. The last two are in agreement with a multiple composite atomization value of 19.9 ± 1.5 kJ mol^{-1} (19.9 ± 1.4 kJ mol^{-1} at 298.15 K) for this species with a T_1 of 0.027.

The reasons for this disagreement are unclear; very similar geometries and frequencies are encountered between the ANL0 and our work with bond lengths within 2 pm and bond angles ≤2.8°. The maximum deviation between wavenumbers is 4%, for mode no. 9, 350.6 vs 364.7 cm^{-1}, with others at ≤2%. Changing the input geometry to that of reported [KHR17] by Klippenstein *et al.* only changes the final WMS result by 0.2 kJ mol^{-1}.

3.12.8.3. Results. Good agreement for entropy, S^o = 274.9 J K^{-1} mol^{-1}, and C_p^o = 59.83 J K^{-1} mol^{-1} with the literature [GMG12] is obtained from our rigid rotor–anharmonic treatment dictated by the failure of a potential energy scan.

T (K)	$S^o(T)$	$C_p^o(T)$	$H^o(T) - H^o(0)$
298.15	275.12	59.62	13.21
300.	275.49	59.78	13.32
400.	293.78	67.45	19.70
500.	309.52	73.62	26.76
600.	323.40	78.67	34.38
700.	335.85	82.84	42.46
800.	347.15	86.37	50.93
900.	357.50	89.39	59.72
1000.	367.06	92.02	68.79
1100.	375.94	94.33	78.11
1200.	384.24	96.38	87.65
1300.	392.02	98.18	97.38
1400.	399.36	99.77	107.27
1500.	406.29	101.15	117.32
1600.	412.86	102.34	127.50
1800.	425.03	104.21	148.16
2000.	436.08	105.52	169.14

References for hydroxyoxoethenyl; 1-hydroxylketenyl.

SPN98 R. Sumathi, J. Peeters, and M. T. Nguyen, "Theoretical studies on the $C_2H + O_2$ reaction: Mechanism for HCO + CO, HC≡CO + O and CH + CO_2 formation," Chem. Phys. Lett. **287**(1-2), 109–118 (1998).

BBTS18 M. C. Bowman, A. D. Burke, J. M. Turney, and H. F. Schaefer, "Mechanisms of the ethynyl radical reaction with molecular oxygen," J. Phys. Chem. A **122**, 9498–9511 (2018).

GMG12 C. F. Goldsmith, G. R. Magoon, and W. H. Green, "Database of small molecule thermochemistry for combustion," J. Phys. Chem. A **116**(36), 9033–9057 (2012).

KHR17 S. J. Klippenstein, L. B. Harding, and B. Ruscic, "*Ab initio* computations and active thermochemical tables hand in hand: Heats of formation of core combustion species," J. Phys. Chem. A **121**(35), 6580–6602 (2017).

3.12.9. Methylenedioxiranyl

$^2A'$ g = 2 C_S σ = 1 M_0 = 57.0287

This species crops up as an intermediate, no. **2**, characterized in a theoretical study of the reaction of the ethynyl radical, HC≡C•, with molecular oxygen [SPN98, BBTS18].

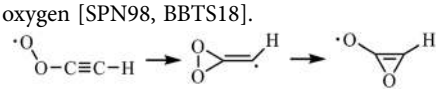

3.12.9.1. Species data.

6	0.000 000	0.271 450	0.000 000
8	−0.717 509	−0.877 453	0.000 000
8	0.818 918	−0.796 886	0.000 000
6	−0.032 443	1.553 342	0.000 000
1	−0.616 610	2.445 959	0.000 000
B(GHz)	26.329 3	8.654 7	6.513 6

No.	$\bar{\upsilon}$ (cm^{-1})	x_{ii}	
1	3377.79	−59.26	a'
2	1859.26	−6.89	a'
3	1101.37	−1.69	a'
4	897.84	−14.05	a'
5	725.52	−4.26	a'
6	593.94	−41.89	a'
7	393.08	−2.00	a'
8	531.09	−0.18	a''
9	410.29	10.44	a''

3.12.9.2. Formation enthalpy, $\Delta_f H(0\ K)$. A W3X-L calculation returns $\Delta_f H^o(0\ K)$ = 374.7 kJ mol^{-1} (372.8 kJ mol^{-1} at 298.15 K), in excellent agreement with the value of 373.3 kJ mol^{-1} extracted from the recent study of Bowman *et al.* (their compound **S1**) [BBTS18]; a value of 392 kJ mol^{-1} can be deduced from the work of Sumathi [SPN98] from their B3LYP/6-311++G(d,p) computations. Composite methods that have two optimization steps, such as CBS-APNO and G3, struggle to converge.

3.12.9.3. Results.

T (K)	$S^o(T)$	$C_p^o(T)$	$H^o(T) - H^o(0)$
298.15	276.06	63.20	13.15
300.	276.46	63.42	13.27
400.	296.14	73.33	20.13
500.	313.28	80.05	27.82
600.	328.29	84.41	36.06
700.	341.53	87.26	44.65
800.	353.32	89.21	53.48
900.	363.91	90.63	62.48
1000.	373.52	91.76	71.60
1100.	382.31	92.70	80.82
1200.	390.41	93.51	90.13
1300.	397.93	94.25	99.52
1400.	404.94	94.92	108.97
1500.	411.51	95.54	118.50
1600.	417.69	96.12	128.08
1800.	429.07	97.20	147.41
2000.	439.37	98.19	166.95

Ring puckering and hindered rotors are neglected in favor of a rigid rotor anharmonic oscillator approach, as a relaxed potential energy scan is problematic.

References for methylenedioxiranyl.

SPN98 R. Sumathi, J. Peeters, and M. T. Nguyen, "Theoretical studies on the $C_2H + O_2$ reaction: Mechanism for HCO + CO, HCCO + O and CH + CO_2 formation," Chem. Phys. Lett. **287**(1-2), 109–118 (1998).

BBTS18 M. C. Bowman, A. D. Burke, J. M. Turney, and H. F. Schaefer, "Mechanisms of the ethynyl radical reaction with molecular oxygen," J. Phys. Chem. A **122**, 9498–9511 (2018).

3.12.10. Oxirenyloxy

^{2}A g = 2 C_1 σ = 1 M_0 = 57.0287

As for the previous species, the oxirenyloxy radical, no. **3**, is an intermediate in the combination of ethynyl and molecular oxygen and results from a dioxiranyl ring-opening reaction [SPN98]. All attempts to repeat the work at uB3LYP/6-311++G(d,p) with post-Gaussian-94 software were unsuccessful with convergence to oxoethynyloxy O=C$^{\bullet}$–CHO the result.

In recent work [BBTS18], a CCSD(T) geometry and frequencies are given for a ^{2}A ground state (**M2**), which are adopted *here*.

3.12.10.1. Species data.

6	0.329 033 1	0.175 218 0	0.012 964 3
6	−0.924 209 4	0.699 307 3	−0.054 087 6
8	1.480 275 4	−0.044 025 2	0.001 753 1
8	−0.929 964 0	−0.699 094 1	0.006 459 5
1	−1.647 178 5	1.381 019 1	0.359 306 5
B (GHz)	48.666	4.430	4.165

No.	$\bar{\upsilon}$ (cm^{-1})
1	3259
2	2063
3	1180
4	1143
5	920
6	671
7	571
8	505
9	235

3.12.10.2. Formation enthalpy, $\Delta_f H(0\ K)$. A $\Delta_f H^o(0\ K)$ of 38.5 kJ mol^{-1} can be estimated from the relative results presented by Bowman *et al.*; this can be extrapolated to 36.3 kJ mol^{-1} at 298.15 K.

Only the composite CBS-APNO returns the "correct" structure and a value of 39.9 kJ mol^{-1} (38.2 kJ mol^{-1} at 298.15 K).

3.12.10.3. Results. The CCSD(T) geometry and frequencies are used unscaled in a RRHO treatment.

T (K)	$^{So}(T)$	$C_p^o(T)$	$H^o(T) - H^o(0)$
298.15	277.82	58.16	12.85
300.	278.18	58.34	12.96
400.	296.21	67.06	19.25
500.	311.93	73.76	26.30
600.	325.85	78.92	33.95
700.	338.34	83.01	42.05
800.	349.65	86.32	50.52
900.	359.98	89.06	59.29
1000.	369.48	91.35	68.32
1100.	378.28	93.28	77.55
1200.	386.47	94.93	86.96
1300.	394.13	96.34	96.53
1400.	401.31	97.55	106.22
1500.	408.08	98.60	116.03
1600.	414.47	99.51	125.94
1800.	426.28	101.00	145.99
2000.	436.99	102.14	166.31

References for oxirenyloxy.

SPN98 R. Sumathi, J. Peeters, and M. T. Nguyen, "Theoretical studies on the $C_2H + O_2$ reaction: Mechanism for HCO + CO, HC≡CO + O and CH + CO_2 formation," Chem. Phys. Lett. **287**(1-2), 109–118 (1998).

BBTS18 M. C. Bowman, A. D. Burke, J. M. Turney, and H. F. Schaefer, "Mechanisms of the ethynyl radical reaction with molecular oxygen," J. Phys. Chem. A, **122**, 9498–9511 (2018).

3.12.11. Oxoethnyloxy; glyoxalyl

$^2A''$ g = 2 C_S σ = 1 M_0 = 57.0287

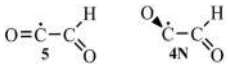

The atmospheric chemistry of this radical produced by the oxidation of glyoxal has been studied [OT01], and the radical itself was comprehensively investigated by Cooksy [C01] at QCISD/6-311G(d,p). In this latter study, two different structures, **4N** and **5**, are shown to vie for the ground state, the principal differences relate to the C–C bond length, which, as it lengthens from 1.40 Å in **5** to 1.52 Å in **4N** the planar arrangement, changes to a OCCO dihedral of 90°. Zero-point corrected electronic energies at the QCISD/cc-pVTZ+d level are virtually identical with **5** more stable than **4N** by only 0.3 kJ mol^{-1}. At B3LYP/cc-pVTZ+d, however, only structure **5** appears to exist, which is featured *here*.

3.12.11.1. Species data.

6	0.599 287	−0.601 653	0.000 000
6	0.000 000	0.650 685	0.000 000
8	−0.114 868	−1.629 001	0.000 000
1	1.695 512	−0.593 197	0.000 000
8	−0.546 537	1.666 376	0.000 000
B (GHz)	56.833	5.059 5	4.645 9

No.	$\bar{\upsilon}$ (cm^{-1})	x_{ii}	
1	3008.91	−70.26	a'
2	2159.33	−12.72	a'
3	1465.89	−8.58	a'
4	1343.67	−4.81	a'
5	990.03	−7.32	a'
6	679.15	−1.76	a'
7	184.31	1.05	a'
8	781.99	−1.90	a''
9	252.17	−15.14	a''

3.12.11.2. Formation enthalpy, $\Delta_f H(0\ K)$. A $\Delta_f H^o(0\ K)$ of −62.3 ± 1.7 kJ mol^{-1} is reported [GMG12], while a value of −75.8 kJ mol^{-1} can be extracted from a study of the HC≡C$^•$ + O_2 reaction [OT01]. Our multiple composite atomization derived value of $\Delta_f H^o(0\ K)$ = −67.4 ± 2.3 kJ mol^{-1} is bracketed by these values. Our high-level W3X-L returns −64.8 kJ mol^{-1}, which is in excellent agreement with the value of −63.8 kJ mol^{-1} extracted from the most recent work (**M3**) [BBTS18] and the −63.2 kJ mol^{-1} of an ANL0 calculation [KHR17]. Summarizing the values of $\Delta_f H^o(0\ K)$ = −64.3 ± 1.0 kJ mol^{-1} (−65.5 kJ mol^{-1} at 298.15 K) is to be recommended.

3.12.11.3. Results. An entropy of 281.2 ± 2.9 K^{-1} mol^{-1} and a $C_p^o(300\ K)$ of 58.2 ± 1.7 J K^{-1} mol^{-1} are known [GMG12]. These are in good agreement with those RR anharmonic values computed here.

T (K)	$S^o(T)$	$C_p^o(T)$	$H^o(T) - H^o(0)$
298.15	283.34	59.45	13.82
300.	283.71	59.57	13.93
400.	301.62	64.95	20.17
500.	316.59	69.26	26.89
600.	329.55	73.00	34.00
700.	341.06	76.31	41.47
800.	351.44	79.21	49.25
900.	360.92	81.73	57.30
1000.	369.65	83.92	65.58
1100.	377.74	85.80	74.07
1200.	385.28	87.44	82.73
1300.	392.33	88.85	91.55
1400.	398.96	90.07	100.50
1500.	405.21	91.14	109.56
1600.	411.13	92.07	118.72
1800.	422.06	93.63	137.29
2000.	431.99	94.86	156.14

References for oxoethnyloxy; glyoxalyl.

OT01 J. J. Orlando and G. S. Tyndall, "The atmospheric chemistry of the HC(O)CO radical," Int. J. Chem. Kinet. **33**(3), 149–156 (2001).

C01 A. L. Cooksy, "Relocalization in floppy free radicals: The OCNO and OCCHO isoelectronic series," J. Am. Chem. Soc. **123**(17), 4003–4013 (2001).

GMG12 C. F. Goldsmith, G. R. Magoon, and W. H. Green, "Database of small molecule thermochemistry for combustion," J. Phys. Chem. A **116**(36), 9033–9057 (2012).

BBTS18 M. C. Bowman, A. D. Burke, J. M. Turney, and H. F. Schaefer, "Mechanisms of the ethynyl radical reaction with molecular oxygen," J. Phys. Chem. A, **122**, 9498–9511 (2018).

KHR17 S. J. Klippenstein, L. B. Harding, and B. Ruscic, "*Ab initio* computations and active thermochemical tables hand in hand: Heats of formation of core combustion species," J. Phys. Chem. A **121**(35), 6580–6602 (2017).

6	0.000 000	0.050 583	0.000 000
6	1.226 564	0.783 151	0.000 000
1	2.245 731	0.425 853	0.000 000
8	−1.171 563	0.535 081	0.000 000
8	−0.029 077	−1.213 614	0.000 000
B (GHz)	14.514 7	11.008 8	6.260 5

No.	$\bar{\upsilon}$ (cm^{-1})	x_{ii}	
1	3225.18	−57.64	a'
2	1488.56	−7.32	a'
3	1115.48	−11.76	a'
4	992.79	−5.80	a'
5	874.43	−11.08	a'
6	564.75	−9.59	a'
7	382.08	0.69	a'
8	629.83	4.19	a''
9	467.14	−6.52	a''

3.12.12. 2-Oxo-2-oxy-ethylidene

$^4A''$ g = 4 C_S σ = 1 M_0 = 57.0287

This species (**Q1**) features in a study of the reactions between ethynyl radicals and oxygen [BBTS18]. The doublet state (**S2**: C_S, $^2A'$) does not optimize at our chosen DFT and basis set combination, and so here we present our data on the quartet and the derived thermodata for the doublet.

3.12.12.1. Species data.

3.12.12.2. Formation enthalpy, $\Delta_f H$(0 K). The quartet, which lies 52.1 kJ mol^{-1} *below* the $^2A'$ doublet, has a $\Delta_f H^\circ$(0 K) of 274.2 kJ mol^{-1} as extracted from the literature [BBTS18], with a corresponding 298.15 K value of 271.9 kJ mol^{-1}. A multi-composite treatment yields 272.1 ± 1.7 kJ mol^{-1} (271.4 kJ mol^{-1} at 298.15 K), in good agreement with the W2X and WMS values of 270.2 kJ mol^{-1} and 268.5 kJ mol^{-1}, respectively.

However, W3X-L indicates a substantially different value of $\Delta_f H^\circ$(0 K) = 261.1 kJ mol^{-1} (258.8 kJ mol^{-1} at 298.15 K).

3.12.12.3. Results. A standard rigid rotor anharmonic treatment is applied for the $^4A''$ state and a RRHO protocol for the $^2A'$ state where the CASSCF(13,9)/cc-pVDZ frequencies and the CASPT2(11,9)/cc-pVQZ geometry obtained by Bowman *et al.* are employed [B18].

	$^4A''$			$^2A'$		
T (K)	$S^\circ(T)$	$C_p^\circ(T)$	$H^\circ(T) - H^\circ(0)$	$S^\circ(T)$	$C_p^\circ(T)$	$H^\circ(T) - H^\circ(0)$
298.15	281.27	59.80	12.70	272.22	50.88	11.41
300.	281.64	60.02	12.81	272.54	51.08	11.50
400.	300.36	70.11	19.34	288.65	61.14	17.13
500.	316.86	77.63	26.74	303.20	69.23	23.66
600.	331.54	83.28	34.80	316.40	75.53	30.91
700.	344.72	87.64	43.36	328.43	80.43	38.72
800.	356.66	91.15	52.30	339.43	84.30	46.96
900.	367.57	94.08	61.57	349.55	87.43	55.56
1000.	377.62	96.59	71.10	358.90	89.99	64.43
1100.	386.93	98.80	80.88	367.58	92.13	73.54
1200.	395.62	100.78	90.86	375.67	93.92	82.84
1300.	403.75	102.56	101.03	383.25	95.45	92.31
1400.	411.41	104.14	111.36	390.37	96.76	101.92
1500.	418.65	105.56	121.85	397.09	97.88	111.65
1600.	425.50	106.80	132.47	403.44	98.86	121.49
1800.	438.21	108.77	154.04	415.18	100.45	141.43
2000.	449.74	110.11	175.94	425.83	101.68	161.64

References for 2-oxo-2-oxy-ethylidene.

BBTS18 M. C. Bowman, A. D. Burke, J. M. Turney, and H. F. Schaefer, "Mechanisms of the ethynyl radical reaction with molecular oxygen," J. Phys. Chem. A **122**, 9498–9511 (2018).

B18 M. C. Bowman (Private communication, University of Georgia, Athens, GA, USA, 23 November 2018).

3.13. $C_2H_1O_3$

3.13.1. Carboxyoxomethyl

^{2}A g = 2 C_1 σ = 1 M_0 = 73.0281

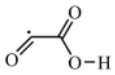

This is a radical derived from oxoacetic or glyoxylic acid, cognate to the dioxoethoxy radical below, and which features as an intermediate (**INT 8**), in the reaction between the ketenyl radical and molecular oxygen [DWFL04]. The lowest energy conformer exhibits *syn* HOCO and *gauche* O=CC=O with the *anti* HOCO lying 15.7 ± 2.5 kJ mol^{-1} above.

3.13.1.1. Species data.

1	−2.061 337	−0.868 018	−0.170 476
8	−1.118 403	−1.057 029	−0.041 504
8	−0.966 194	1.209 258	−0.044 423
6	−0.473 488	0.117 106	0.025 012
6	0.969 853	−0.084 368	0.398 190
8	1.969 991	−0.068 280	−0.210 165
B (GHz)	11.232	4.284 2	3.207 7

No.	$\bar{\upsilon}$ (cm^{-1})	x_{ii}	No.	$\bar{\upsilon}$ (cm^{-1})	x_{ii}
1	3720.85	−83.85	7	749.16	−4.87
2	1974.90	−13.48	8	558.03	−12.91
3	1790.06	−11.88	9	494.99	−0.86
4	1342.85	−7.02	10	437.93	−1.60
5	1127.59	−6.45	11	253.11	−0.78
6	761.82	−1.80	12	135.94	−1.27

3.13.1.2. Formation enthalpy, $\Delta_f H$(0 K). Ding *et al.* placed this species as −474.53 kJ mol^{-1} below ketenyl + O_2; thus, a $\Delta_f H^\circ$(0 K) of −297.6 kJ mol^{-1} can be extracted from G3B3 calculations [DWFL04]. A multi-composite approach has $\Delta_f H^\circ$(0 K) = −306.8 ± 1.7 kJ mol^{-1} (−310.6 kJ mol^{-1} at 298.15 K), in good agreement with a WMS of −305.0 kJ mol^{-1}.

3.13.1.3. Results. A hindered rotor analysis suggests that mode no. 12, rotation about the C–C bond for which reduced barrier height (*V*/*RT*) = 3.00, has a much larger effect than that due to mode no. 8, H–O–C=O, where (*V*/*RT*)=15.5. Both relaxed scans are well-behaved so a complete anharmonic treatment is possible.

T (K)	$S^\circ(T)$	$C_p^\circ(T)$	$H^\circ(T) - H^\circ(0)$
298.15	310.29	75.38	15.61
300.	310.75	75.63	15.75
400.	334.25	87.89	23.95
500.	354.95	97.52	33.24
600.	373.40	104.73	43.37
700.	389.96	110.00	54.12
800.	404.91	113.80	65.32
900.	418.48	116.56	76.84
1000.	430.88	118.59	88.60
1100.	442.25	120.11	100.54
1200.	452.76	121.28	112.61
1300.	462.50	122.21	124.78
1400.	471.59	122.96	137.04
1500.	480.09	123.60	149.37
1600.	488.09	124.15	161.76
1800.	502.77	125.09	186.68
2000.	515.99	125.88	211.78

References for carboxyoxomethyl.

DWFL04 Y.-Q. Ding, C. Wang, D.-C. Fang, and R.-Z. Liu, "Theoretical study on the doublet-state potential energy surface of the reactions between HCCO (^{2}A″) and O_2 ($^3\Sigma_g^-$)," Huaxue Xuebao **62**(15), 1373–1378 (2004).

3.13.2. Dioxiranyloxomethyl

^{2}A′ g = 2 C_S σ = 1 M_0 = 73.0281

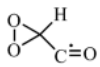

This is a radical found (**INT 5**) in a theoretical study [DWFL04] of the reaction between HCCO (^{2}A″) and O_2 ($^3\Sigma_g^-$). In agreement with that work, we find that a dihedral, HCC=O, of zero represents the lowest energy conformer, but the gauche forms, ± 69°, do lie close with a difference of only 1.3 kJ mol^{-1} at W1BD.

3.13.2.1. Species data.

6	0.367 636	0.326 124	0.000 000
8	−0.279 739	1.291 967	0.746 538
8	−0.279 739	1.291 967	−0.746 538
1	1.458 890	0.337 551	0.000 000
6	−0.279 739	−1.059 411	0.000 000
8	0.311 194	−2.076 163	0.000 000
B(GHz)	20.624	3.463 1	3.217 1

No.	$\bar{\upsilon}$ (cm^{-1})	x_{ii}	
1	3066.68	−64.41	a'
2	1933.57	−11.78	a'
3	1369.68	−6.33	a'
4	1279.23	−2.79	a'
5	916.56	−16.64	a'
6	821.02	−2.87	a'
7	471.95	−1.01	a'
8	328.69	0.29	a'
9	1131.12	−5.31	a''
10	890.12	−1.80	a''
11	430.77	−2.39	a''
12	53.14	8.13	a''

3.13.2.2. Formation enthalpy, $\Delta_f H(0\ K)$. Ding *et al.* placed this species 93.63 kJ mol^{-1} *below* reactants from G3B3 data, which translates to a $\Delta_f H^o(0\ K)$ of ~84 kJ mol^{-1}. A multi-composite approach yields $\Delta_f H^o(0\ K) = 71.7 \pm 4.5$ kJ mol^{-1} (68.7 kJ mol^{-1} at 298.15 K), which agrees with 73.8 ± 2.9 kJ mol^{-1} from the isodesmic reaction

$$R - C\cdot = O + H_2C = O = R - CHO + HC\cdot = O,$$

where R represents the dioxiranyl ring and literature values for formyl (41.426 ± 0.099 kJ mol^{-1}) and formaldehyde (−105.32 ± 0.11 kJ mol^{-1}) have been used as well as our previous value for dioxiranecarboxaldehyde of −94.4 kJ mol^{-1}. An additional isodesmic reaction

$$R - C\cdot = O + CH_4 = R - H + CH_3C\cdot = O,$$

which uses reference ATcT values for the chaperones methane (−66.550 ± 0.057 kJ mol^{-1}), dioxirane (9.45 ± 0.55 kJ mol^{-1}), and acetyl (−3.37 ± 0.36 kJ mol^{-1}), yields 75.80 ± 1.63 kJ mol^{-1} for a grand weighted mean of $\Delta_f H^o(0\ K) = 75.3 \pm 1.4$ kJ mol^{-1} (71.3 kJ mol^{-1} at 298.15 K).

3.13.2.3. Results. A relaxed potential energy scan about the C–C bond is used to replace the vibrational contribution from mode no. 12.

T (K)	$S^o(T)$	$C_p^o(T)$	$H^o(T) - H^o(0)$
298.15	309.44	67.52	15.31
300.	309.86	67.74	15.44
400.	330.87	78.56	22.76
500.	349.40	87.48	31.08
600.	366.00	94.58	40.20
700.	381.02	100.23	49.95
800.	394.71	104.79	60.21
900.	407.28	108.52	70.88
1000.	418.88	111.61	81.89
1100.	429.64	114.20	93.18
1200.	439.67	116.40	104.71
1300.	449.07	118.29	116.45
1400.	457.89	119.94	128.36
1500.	466.22	121.39	140.43
1600.	474.10	122.68	152.63
1800.	488.68	124.91	177.39
2000.	501.94	126.77	202.56

References for dioxiranyloxomethyl.

DWFL04 Y.-Q. Ding, C. Wang, D.-C. Fang, and R.-Z. Liu, "Theoretical study on the doublet-state potential energy surface of the reactions between HCCO ($^2A''$) and O_2 ($^3\Sigma_g^-$)," Huaxue Xuebao **62**(15), 1373–1378 (2004).

3.13.3. Dioxoethoxy

$^2A'$ g = 2 C_S σ = 1 M_0 = 73.0281

A radical derived from oxoacetic acid, dioxoethoxy, is one of the many species encountered during a computational study of key intermediates in the oxidation of benzene by Merle and Hadad [MH04] and in the reactions [WHSS04] of the ketenyl radical with O_2.

3.13.3.1. Species data.

6	−0.588 882	−0.898 255	0.000 000
6	0.000 000	0.511 157	0.000 000
1	−1.692 582	−0.928 844	0.000 000
8	0.112 316	−1.867 370	0.000 000
8	−0.698 784	1.538 644	0.000 000
8	1.239 703	0.735 154	0.000 000
B(GHz)	12.776 5	4.356 3	3.248 6

No.	$\bar{\upsilon}$ (cm^{-1})	x_{ii}	
1	2950.47	−66.64	a'
2	1818.99	−10.20	a'
3	1559.55	−6.32	a'
4	1363.74	−9.70	a'
5	1108.47	−6.84	a'
6	863.95	−5.27	a'
7	651.89	−13.36	a'
8	478.41	−0.04	a'
9	198.37	0.30	a'
10	1007.69	−1.65	a''
11	515.96	0.32	a''
12	109.72	1.22	a''

3.13.3.2. Formation enthalpy, $\Delta_f H(0\ K)$. Direct atomization formation enthalpies are WMS $\Delta_f H^o(0\ K) = -107.3$ kJ mol^{-1} and W2X $\Delta_f H^o(0\ K) = -103.7$ kJ mol^{-1}, in comparison to −231 kJ mol^{-1} that can be gleaned from the work of Wei [WHSS04] for this radical with a T_1 of 0.08. The highest level W3X-L result of $\Delta_f H^o(0\ K) = -117.3$ kJ mol^{-1} (−121.3 kJ mol^{-1} at 298.15 K) is to be preferred.

3.13.3.3. Results. Rotation about the C–C bond, mode no. 12, experiences a barrier of 14.9 kJ mol^{-1} and has little impact on the room temperature entropy, but the relaxed potential energy scan is well-behaved and so a HR–anharmonic treatment is used.

T (K)	$S^o(T)$	$C_p^o(T)$	$H^o(T) - H^o(0)$
298.15	304.73	71.45	15.41
300.	305.17	71.67	15.54
400.	327.35	82.63	23.28
500.	346.75	91.21	31.99
600.	363.99	97.87	41.45
700.	379.49	103.12	51.51
800.	393.54	107.34	62.04
900.	406.39	110.81	72.95
1000.	418.22	113.70	84.18
1100.	429.18	116.16	95.68
1200.	439.38	118.26	107.40
1300.	448.92	120.08	119.32
1400.	457.87	121.64	131.40
1500.	466.31	122.99	143.64
1600.	474.29	124.14	155.99
1800.	489.02	125.95	181.01
2000.	502.36	127.19	206.33

References for dioxoethoxy.

MH04 J. K. Merle and C. M. Hadad, "Computational study of the oxygen initiated decomposition of 2-oxepinoxy radical: A key intermediate in the oxidation of benzene," J. Phys. Chem. A **108**(40), 8419–8433 (2004).

WHSS04 Z.-G. Wei, X.-R. Huang, Y.-B. Sun, and C.-C. Sun, "Theoretical study on the potential energy surface of the reaction of ketenyl radical (HCCO•) with oxygen (O_2)," Gaodeng Xuexiao Huaxue Xuebao **25**(8), 1504–1506 (2004).

3.13.4. Formyloxy oxomethyl

$^2A'$ g = 2 C_S σ = 1 M_0 = 73.0281

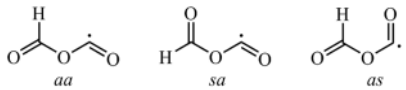

aa *sa* *as*

The *sa* conformer of the radical of formic acid anhydride is slightly more stable, 0.39 ± 0.39 kJ mol^{-1}, than the *aa* with the *as* considerably less so at +7 kJ mol^{-1} [PT05].

3.13.4.1. Species data.

		sa				*aa*	
8	0.000 000	−0.711 862	0.000 000	8	2.257 120	0.275 607	0.000 000
8	−1.658 469	0.871 606	0.000 000	6	1.204 510	−0.242 261	0.000 000
6	−1.311 652	−0.260 349	0.000 000	8	0.000 000	0.389 584	0.000 000
1	−1.956 903	−1.145 022	0.000 000	6	−1.125 104	−0.436 113	0.000 000
6	0.994 198	0.239 793	0.000 000	8	−2.209 389	0.031 004	0.000 000
8	2.141 172	−0.001 200	0.000 000	1	−0.858 287	−1.499 324	0.000 000
B (GHz)	23.414	3.258 0		*B* (GHz)	62.921	2.608 5	2.504 6
			2.860 0				

sa				*aa*			
No.	$\bar{\upsilon}$ (cm^{-1})	x_{ii}		No.	$\bar{\upsilon}$ (cm^{-1})	x_{ii}	
1	3063.31	−60.45	a'	1	3042.97	−62.76	a'
2	1914.53	−12.27	a'	2	1933.28	−7.05	a'
3	1851.22	−9.71	a'	3	1855.94	−5.89	a'
4	1393.52	−9.28	a'	4	1381.62	−9.90	a'
5	1039.09	−8.23	a'	5	1083.24	−3.85	a'
6	942.69	−12.22	a'	6	997.89	−13.78	a'
7	778.02	−2.42	a'	7	684.23	−0.53	a'
8	515.69	−0.08	a'	8	518.79	−2.16	a'
9	218.69	0.04	a'	9	255.14	−0.64	a'
10	1031.35	−2.29	a''	10	1032.27	−2.76	a''
11	227.65	−0.64	a''	11	250.99	−2.17	a''
12	127.58	6.43	a''	12	129.63	0.79	a''

3.13.4.2. Formation enthalpy, $\Delta_f H$(0 K). Ponomarev and Takhistov [PT05] estimated $\Delta_f H^o$(0 K) of some −270 kJ mol^{-1} from IR correlations, which is in modest agreement with a multi-composite $\Delta_f H^o$(0 K) = −285.2 ± 3.1 kJ mol^{-1}.

High-level W3X-L returns $\Delta_f H^o$(0 K) = −282.9 kJ mol^{-1} (−285.8 kJ mol^{-1} at 298.15 K) for the *aa* with values ~0.4 kJ mol^{-1} lower for the *sa* at $\Delta_f H^o$(0 K) = −283.3 kJ mol^{-1} (−286.0 kJ mol^{-1} at 298.15 K). WMS concurs with the *sa* at −282.7 kJ mol^{-1} and the *aa* at −281.9 kJ mol^{-1}.

The computed BDE(C–H) of (218.0 − 289.9 + 474.5) = 403 kJ mol^{-1} is similar to the corresponding values for formic and acetic acids [L07].

3.13.4.3. Results. Two modes, nos. 12 and 11, for the *sa* impinge upon the computed thermochemistry with the reduced barrier heights (*V*/*RT*)s of 2.9 and 7.4, respectively. Two modes, nos. 2 and 11, are identified with (*V*/*RT*)s of 6.3 and 8.0, respectively, for the *aa* whose total impact is small. Since the relaxed potential energy scans are well behaved, they are used to replace pure vibrational modes.

sa				*aa*			
T (K)	$S^o(T)$	$C_p^o(T)$	$H^o(T) - H^o(0)$	T (K)	$S^o(T)$	$C_p^o(T)$	$H^o(T) - H^o(0)$
298.15	314.70	74.73	16.65	298.15	309.87	74.03	16.46
300.	315.16	74.96	16.79	300.	310.33	74.23	16.60
400.	338.35	86.36	24.87	400.	333.12	84.44	24.54
500.	358.60	95.06	33.96	500.	352.91	93.00	33.43
600.	376.52	101.35	43.80	600.	370.51	99.94	43.09
700.	392.50	105.92	54.18	700.	386.34	105.40	53.37
800.	406.88	109.35	64.95	800.	400.70	109.65	64.13
900.	419.92	112.00	76.02	900.	413.82	112.94	75.26
1000.	431.83	114.11	87.33	1000.	425.85	115.50	86.69
1100.	442.79	115.82	98.82	1100.	436.96	117.51	98.34
1200.	452.93	117.24	110.48	1200.	447.26	119.11	110.17
1300.	462.37	118.43	122.26	1300.	456.84	120.41	122.15
1400.	471.18	119.46	134.16	1400.	465.81	121.48	134.25
1500.	479.45	120.35	146.15	1500.	474.22	122.38	146.44
1600.	487.25	121.13	158.22	1600.	482.14	123.14	158.71
1800.	501.59	122.45	182.58	1800.	496.72	124.41	183.47
2000.	514.55	123.54	207.18	2000.	509.89	125.44	208.46

References for formyloxy oxomethyl.

PT05 D. Ponomarev and V. Takhistov, "Thermochemistry of organic and hetero-organic species. Part XVI. Application of IR sSpectra of unsaturated aliphatic molecules to the thermochemistry of vinylic and allylic free radicals," Int. J. Mol. Des.Internet J. Mol. Design **4**, 367–380 (2005).

L07 Y.-R. Luo, *Comprehensive Handbook of Chemical Bond Energies* (CRC Press, Boca Raton, USA, 2007).

3.13.5. Hydroperoxyketenyl; hydroperoxyoxoethenyl

$^2A''$ g = 2 C_S σ = 1 M_0 = 73.0281

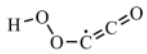

These species (**INT 6** and **INT 7**) have been encountered in a theoretical study of the reaction between the ketenyl radical and ground state oxygen [DWFL04] with the *anti/anti* conformer (CCOO and COOH dihedrals), some 4.7 kJ more stable than the *anti/syn*, a conclusion with which we agree; however, the *syn/anti* conformer is considerably more stable than either by some 18.4 kJ mol^{-1} and is featured *here*.

3.13.5.1. Species data.

8	2.248 641	−0.399 459	0.000 000
6	1.167 329	0.045 951	0.000 000
6	0.082 570	0.763 466	0.000 000
8	−1.156 754	0.705 622	0.000 000
8	−1.698 282	−0.833 170	0.000 000
1	−2.648 227	−0.640 443	0.000 000
B (GHz)	17.412 4	2.940 4	2.515 6

No.	$\bar{\upsilon}$ (cm^{-1})	x_{ii}	
1	3752.34	−78.94	a'
2	2177.47	−13.48	a'
3	1640.58	−19.32	a'
4	1174.06	−33.22	a'
5	920.64	−3.03	a'
6	604.21	−5.34	a'
7	473.65	−16.77	a'
8	348.47	−153.99	a'
9	97.92	−11.04	a'
10	369.76	−0.82	a''
11	304.92	−1.55	a''
12	159.72	−5.59	a''

3.13.5.2. Formation enthalpy, $\Delta_f H(0\ K)$. Direct atomization calculations based on the W3X-L protocol returns $\Delta_f H^o(0\ K)$ = 78.8 kJ mol^{-1} (77.2 kJ mol^{-1} at 298.15 K)

3.13.5.3. Results. A hindered rotor analyses identifies mode nos.12 and 10 as contributing equally to a +3.4 J K^{-1} mol^{-1} change to the room temperature entropy. Conventional relaxed potential

energy scans are complicated by dissociation to O=C=C=O and •OH part way through the scans, so a simple RRHO treatment is presented here since, in particular, mode no. 8 is highly anharmonic.

T (K)	$S°(T)$	$C_p°(T)$	$H°(T) - H°(0)$
298.15	320.84	82.52	17.75
300.	321.35	82.70	17.90
400.	346.34	90.98	26.61
500.	367.34	97.22	36.03
600.	385.51	102.13	46.00
700.	401.57	106.10	56.42
800.	415.95	109.37	67.20
900.	429.0	112.11	78.27
1000.	440.93	114.44	89.60
1100.	451.94	116.43	101.15
1200.	462.14	118.14	112.88
1300.	471.66	119.63	124.77
1400.	480.57	120.92	136.79
1500.	488.95	122.05	148.94
1600.	496.86	123.05	161.20
1800.	511.46	124.69	185.98
2000.	524.66	125.99	211.05

References for hydroperoxyketenyl; hydroperoxyoxoethenyl.

DWFL04 Y.-Q. Ding, C. Wang, D.-C. Fang, and R.-Z. Liu, "Theoretical study on the doublet-state potential energy surface of the reactions between HCCO ($^2A''$) and O_2 ($^3\Sigma_g^-$)," Huaxue Xuebao **62**(15), 1373–1378 (2004).

3.13.6. Hydroxyoxarinonyl

^2A g = 2 C_1 σ = 1 M_0 = 73.0281

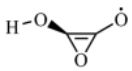

A *gauche* conformer with a dihedral angle HOCC of ~−150° is the ground state with a second *gauche* at +114° lying 2.6 kJ mol^{-1} above.

3.13.6.1. Species data.

6	−0.625 945	−0.023 253	0.413 410
6	0.741 671	−0.090 297	0.074 246
8	0.105 974	1.136 190	−0.108 065
8	1.822 814	−0.530 064	−0.078 392
8	−1.706 593	−0.526 137	−0.177 767
1	−2.471 918	0.041 392	−0.012 136
B (GHz)	15.510	4.204 6	3.438 8

No.	$\bar{\upsilon}$ (cm^{-1})	x_{ii}
1	3756.61	−86.96
2	2042.39	−11.06
3	1393.39	−7.56
4	1214.62	−10.97
5	1064.78	−2.62
6	871.23	−3.28
7	671.92	−2.22
8	575.86	−0.12
9	496.80	−19.37
10	423.18	−12.71
11	277.63	−20.62
12	237.61	−2.69

3.13.6.2. Formation enthalpy, $\Delta_f H$(0 K). A multi-composite atomization calculation returns $\Delta_f H°$(0 K) = −146.3 ± 3.2 kJ mol^{-1} (−149.5 kJ mol^{-1} at 298.15 K), in agreement with −142.4 kJ mol^{-1} from WMS.

3.13.6.3. Results. A relaxed potential energy scan about the HOCC dihedral is used to replace the anharmonic mode no. 11.

T (K)	$S°(T)$	$C_p°(T)$	$H°(T) - H°(0)$
298.15	305.73	76.85	16.17
300.	306.21	77.07	16.31
400.	329.88	87.65	24.56
500.	350.40	96.29	33.77
600.	368.60	103.34	43.77
700.	384.97	108.90	54.39
800.	399.80	113.08	65.50
900.	413.30	116.07	76.96
1000.	425.64	118.06	88.68
1100.	436.95	119.27	100.55
1200.	447.36	119.89	112.51
1300.	456.97	120.08	124.51
1400.	465.86	119.97	136.51
1500.	474.13	119.65	148.49
1600.	481.84	119.20	160.43
1800.	495.81	118.08	184.16
2000.	508.19	116.91	207.66

3.13.7. 4-Oxo-1,2-dioxetan-3-yl

$^2A''$ g = 2 C_S σ = 1 M_0 = 73.0281

This species has been postulated as an intermediate in the reaction of the ketenyl radical, O=C=C•H ($^2A''$), with molecular ground

8	−0.976 548	−0.457 587	0.000 000
8	0.158 648	−1.421 749	0.000 000
6	1.037 505	−0.389 436	0.000 000
6	0.000 000	0.607 971	0.000 000
1	2.116 362	−0.517 762	0.000 000
8	−0.224 774	1.780 155	0.000 000
B (GHz)	15.525 2	5.366 5	3.988 0

No.	$\bar{\upsilon}$ (cm^{-1})	x_{ii}	
1	3282.74	−58.57	a'
2	1890.06	−13.20	a'
3	1358.64	−8.78	a'
4	1159.01	−3.67	a'
5	1034.49	−1.15	a'
6	947.14	−4.79	a'
7	815.09	−3.96	a'
8	725.19	−2.52	a'
9	461.37	−1.50	a'
10	651.69	−0.07	a''
11	435.31	2.21	a''
12	323.88	−1.41	a''

state oxygen [DWFL04]. From G3B3 calculations, they estimated an energy of −175.4 kJ mol^{-1} relative to the initial reactants.

3.13.7.1. Species data.

3.13.7.2. Formation enthalpy, $\Delta_f H$(0 K). Isodesmics featuring 1,2-dioxetan-3-one have averaged reaction enthalpies of 27.16 ± 2.74 kJ mol^{-1} and −13.98 ± 1.53 kJ mol^{-1}, respectively,

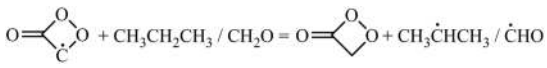

which in conjunction with reference propane (−82.75 ± 0.19 kJ mol^{-1})/iso-propyl (105.28 ± 0.67 kJ mol^{-1}), formaldehyde (−105.32 ± 0.11 kJ mol^{-1})/formyl (41.426 ± 0.099 kJ mol^{-1}) values and our somewhat less well-established value for 1,2-dioxetan-3-one of −167.1 ± 1.6 kJ mol^{-1} yields $\Delta_f H^o$(0 K) = −6.3 ± 1.8 kJ mol^{-1} (−12.1 kJ mol^{-1} at 298.15 K). This is to be compared with an estimated +1.4 kJ mol^{-1} from the study of Ding [DWFL04].

The more symmetric radical, 4-oxo-1,3-dioxetan-2-yl (see below), can be computed at W3X-L, and a back-calculation yields $\Delta_f H^o$(0 K) = −8.3 kJ mol^{-1} (−14.0 kJ mol^{-1} at 298.15 K) for 4-oxo-1,2-dioxetan-3-yl.

3.13.7.3. Results. A rigid-rotor anharmonic treatment ignoring ring puckering modes is used.

T (K)	$S^o(T)$	$C_p^o(T)$	$H^o(T) - H^o(0)$
298.15	287.06	66.37	13.46
300.	287.48	66.64	13.58
400.	308.51	79.66	20.93
500.	327.41	89.66	29.41
600.	344.46	97.27	38.78
700.	359.91	103.15	48.81
800.	374.00	107.79	59.36
900.	386.92	111.53	70.34
1000.	398.84	114.60	81.65
1100.	409.88	117.16	93.24
1200.	420.17	119.31	105.06
1300.	429.80	121.15	117.09
1400.	438.83	122.74	129.28
1500.	447.35	124.12	141.62
1600.	455.40	125.33	154.10
1800.	470.28	127.37	179.37
2000.	483.79	129.02	205.01

References for 4-oxo-1,2-dioxetan-3-yl.

DWFL04 Y.-Q. Ding, C. Wang, D.-C. Fang, and R.-Z. Liu, "Theoretical study on the doublet-state potential energy surface of the reactions between HCCO (^{2}A″) and O_2 ($^3\Sigma_g^-$)," Huaxue Xuebao **62**(15), 1373–1378 (2004).

3.13.8. 4-Oxo-1,3-dioxetan-2-yl

^{2}A′ g = 2 C_S σ = 1 M_0 = 73.0281

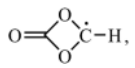

Only the 4-oxo-1,2-dioxetan-3-yl radical features in the chemical literature; this more symmetric radical is unknown.

3.13.8.1. Species data.

6	0.067 639	−1.363 340	0.000 000
6	0.001 838	0.540 591	0.000 000
8	0.007 617	−0.409 278	1.013 029
8	0.007 617	−0.409 278	−1.013 029
1	−0.599 672	−2.218 647	0.000 000
8	0.007 617	1.712 949	0.000 000
B (GHz)	15.202 6	6.058 8	4.363 2

No.	$\bar{\upsilon}$ (cm^{-1})	x_{ii}	
1	3149.11	−66.57	a'
2	1993.30	−10.75	a'
3	1148.76	−3.37	a'
4	1032.73	−1.21	a'
5	942.61	−27.50	a'
6	804.02	−1.44	a'
7	745.83	−0.86	a'
8	313.45	−1.05	a'
9	1294.63	−5.67	a''
10	1060.45	−1.45	a''
11	812.88	−6.47	a''
12	524.47	0.50	a''

3.13.8.2. Formation enthalpy, $\Delta_f H(0\ K)$. A multi-composite calculation of the dissociation energy of this radical, to yield carbon dioxide and formyl radical, gives −125.67 ± 2.56 kJ mol^{-1} from which $\Delta_f H^o(0\ K)$ = −226.0 ± 2.6 kJ mol^{-1} can be computed. A W3X-L calculation returns $\Delta_f H^o(0\ K)$ = −229.1 kJ mol^{-1} (−235.9 kJ mol^{-1} at 298.15 K). The combined results from isodesmic and atomization computations for these two radicals are all in good agreement.

3.13.8.3. Results. A standard anharmonic oscillator, rigid rotor treatment that ignores ring puckering modes is employed here.

T (K)	$S^o(T)$	$C_p^o(T)$	$H^o(T) - H^o(0)$
298.15	281.99	60.51	12.59
300.	282.37	60.79	12.70
400.	301.82	74.73	19.50
500.	319.75	85.84	27.55
600.	336.19	94.41	36.58
700.	351.26	101.08	46.37
800.	365.12	106.38	56.75
900.	377.91	110.69	67.61
1000.	389.76	114.26	78.86
1100.	400.79	117.27	90.44
1200.	411.11	119.83	102.30
1300.	420.79	122.04	114.39
1400.	429.91	123.95	126.69
1500.	438.52	125.60	139.17
1600.	446.67	127.03	151.80
1800.	461.77	129.30	177.45
2000.	475.48	130.95	203.48

3.13.9. *Peroxyketenyls* syn/anti

$^2A''$ g = 2 C_S σ = 1 M_0 = 73.0281

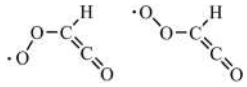

The *anti* and *syn* conformers are considered jointly since they were described in a theoretical study of the ketenyl radical with oxygen by Wei and colleagues [WHSS04] who showed from G2 calculations that the *syn* is more stable than the *anti* by 4.4 kJ mol^{-1}, a conclusion that we agree with a difference of 6.1 ± 0.9 kJ mol^{-1} from CBS-QB3, G4, and W1BD calculations. A ketenylperoxy is tabulated [GMG12], and its formation enthalpy at 298.15 K is reported as 80.3 ± 3.8 kJ mol^{-1}, which probably pertains to the *anti* OOCC conformer.

3.13.9.1. Species data.

	syn				*anti*		
6	1.009 520	0.061 017	0.000 000	6	−1.248 812	−0.058 223	0.000 000
8	1.931 507	−0.633 822	0.000 000	8	−2.351 439	0.293 759	0.000 000
6	0.000 000	0.923 418	0.000 000	6	0.000 000	−0.489 836	0.000 000
1	0.147 955	1.989 348	0.000 000	1	0.251 998	−1.536 627	0.000 000
8	−1.304 393	0.486 748	0.000 000	8	1.031 942	0.441 849	0.000 000
8	−1.402 749	−0.839 922	0.000 000	8	2.224 606	−0.132 486	0.000 000
B (GHz)	14.565	3.839 5	3.038 5	*B* (GHz)	51.979	2.480 6	2.367 6

	syn				*anti*		
No.	$\bar{\upsilon}$ (cm^{-1})	x_{ii}		No.	$\bar{\upsilon}$ (cm^{-1})	x_{ii}	
1	3251.52	−55.52	a'	1	3241.49	−55.97	a'
2	2208.35	−11.17	a'	2	2215.20	−11.08	a'
3	1390.60	−6.81	a'	3	1371.19	−6.10	a'
4	1137.85	−4.25	a'	4	1159.33	−4.24	a'
5	1098.37	−2.27	a'	5	1116.97	−1.39	a'
6	974.35	−5.56	a'	6	1008.63	−7.61	a'
7	753.84	−0.64	a'	7	620.57	−1.28	a'
8	389.83	−0.47	a'	8	473.93	−0.16	a'
9	164.71	0.55	a'	9	190.75	0.31	a'
10	537.63	0.52	a''	10	547.36	2.26	a''
11	471.36	−0.26	a''	11	468.22	−3.31	a''
12	198.71	−3.92	a''	12	44.08	−0.71	a''

3.13.9.2. Formation enthalpy, $\Delta_f H(0\ K)$. An isodesmic reaction O=C=C(H)OO• + CH_4 → O=C=CH_2 + CH_3OO• featuring reference species methane (−66.550 ± 0.057 kJ mol^{-1}), ketene (−45.45 ± 0.13 kJ mol^{-1}), and methyl peroxy radical (22.29 ± 0.49 kJ mol^{-1}) returns a reaction enthalpy of −33.80 ± 1.00, which implies $\Delta_f H^o(0\ K)$ = 77.2 ± 1.2 kJ mol^{-1} (75.2 kJ mol^{-1} at 298.15 K) for the *syn* conformer and corresponding values for the *anti* of $\Delta_f H^o(0\ K)$ = 83.3 kJ mol^{-1} (81.1 kJ mol^{-1} at 298.15 K); the latter is in good agreement with the literature [GMG12] and with a WMS of 81.3 kJ mol^{-1}.

3.13.9.3. Results. Analysis suggests that hindered rotor treatments are unnecessary for the *syn* as a reduced barrier height (*V*/*RT*)=18.6 and for the *anti* as well although *here* we replace mode no. 12 with hindered rotors and treat the remainder as anharmonics.

	syn			*anti*		
T (K)	$S^o(T)$	$C_p^o(T)$	$H^o(T) - H^o(0)$	$S^o(T)$	$C_p^o(T)$	$H^o(T) - H^o(0)$
298.15	315.15	79.31	17.34	310.70	79.83	17.17
300.	315.64	79.47	17.48	311.20	80.00	17.32
400.	339.63	87.38	25.84	335.36	88.04	25.74
500.	359.83	93.72	34.91	355.71	94.33	34.87
600.	377.38	98.78	44.54	373.37	99.34	44.56
700.	392.93	102.89	54.63	389.00	103.42	54.70
800.	406.90	106.29	65.09	403.04	106.82	65.22
900.	419.59	109.15	75.87	415.79	109.69	76.05
1000.	431.21	111.56	86.90	427.47	112.13	87.14
1100.	441.95	113.61	98.16	438.26	114.22	98.46
1200.	451.91	115.37	109.61	448.28	116.03	109.97
1300.	461.20	116.88	121.23	457.63	117.59	121.65
1400.	469.92	118.19	132.98	466.40	118.96	133.48
1500.	478.11	119.33	144.86	474.65	120.16	145.44
1600.	485.84	120.33	156.84	482.44	121.23	157.51
1800.	500.12	121.97	181.08	496.82	123.03	181.94
2000.	513.04	123.27	205.60	509.86	124.52	206.69

Goldsmith *et al.* reported [GMG12] an entropy of 317.1 ± 5.4 J K^{-1} mol^{-1} and C_p^o(300 K)=78.2 ± 2.5 J K^{-1} mol^{-1}, which are more in accord with the *syn* conformer.

References for peroxyketenyls *syn/anti*.

WHSS04 Z.-G. Wei, X.-R. Huang, Y.-B. Sun, and C.-C. Sun, "Theoretical study on the potential energy surface of the reaction of ketenyl radical (HCCO•) with oxygen (O_2)," Gaodeng Xuexiao Huaxue Xuebao **25**(8), 1504–1506 (2004).

GMG12 C. F. Goldsmith, G. R. Magoon, and W. H. Green, "Database of small molecule thermochemistry for combustion," J. Phys. Chem. A **116**(36), 9033–9057 (2012).

3.13.10. 2,3,5-Trioxabicyclo[2.1.0]pentyl

^2A g = 2 C_1 σ = 1 M_0 = 73.0281

3.13.10.1. Species data.

6	0.357 906 000	0.749 392 000	0.315 910 000
6	0.357 471 000	−0.659 836 000	0.516 582 000
8	−0.952 423 000	−0.775 415 000	−0.026 905 000
8	−0.919 428 000	0.716 708 000	−0.244 215 000
1	0.790 297 000	1.673 675 000	0.657 163 000
8	1.236 531 000	−0.217 669 000	−0.435 395 000
B (GHz)	12.008	7.771 5	5.641 9

No.	$\bar{\upsilon}$ (cm^{-1})	x_{ii}	No.	$\bar{\upsilon}$ (cm^{-1})	x_{ii}
1	3263.97	−57.36	7	875.81	−3.12
2	1421.29	−7.45	8	853.13	−2.96
3	1203.11	−3.90	9	659.27	−24.92
4	1072.46	−6.55	10	591.54	−1.16
5	1042.80	−4.47	11	523.56	−5.35
6	934.72	−1.71	12	434.17	−19.73

3.13.10.2. Formation enthalpy, $\Delta_f H$(0 K). This radical fails at CBS-APNO and G3; consequently, we have compared it directly with the isomeric radical 2,4,5-trioxabicyclo[1.1.1]pentyl for which it lies 116.7 ± 3.0 kJ mol^{-1} *higher*; this implies a $\Delta_f H^o$(0 K) = 260.0 ± 5.2 kJ mol^{-1} (253.6 kJ mol^{-1} at 298.15 K).

3.13.10.3. Results. A standard rigid—anharmonic oscillator treatment is employed.

T (K)	$S^o(T)$	$C_p^o(T)$	$H^o(T) - H^o(0)$
298.15	281.91	65.11	12.92
300.	282.31	65.43	13.04
400.	303.39	81.28	20.40
500.	322.90	93.45	29.17
600.	340.76	102.22	38.97
700.	357.01	108.41	49.52
800.	371.79	112.79	60.59
900.	385.26	115.90	72.04
1000.	397.59	118.11	83.74
1100.	408.93	119.68	95.63
1200.	419.39	120.78	107.66
1300.	429.09	121.55	119.78
1400.	438.12	122.08	131.96
1500.	446.56	122.44	144.19
1600.	454.47	122.69	156.44
1800.	468.94	123.00	181.01
2000.	481.91	123.19	205.63

3.13.11. 2,4,5-Trioxabicyclo[1.1.1]pentyl

$^2A_1$ g = 2 C_{3v} σ = 3 M_0 = 73.0281

3.13.11.1. Species data.

6	0.000 000	0.000 000	−0.737 598
8	0.000 000	1.214 526	0.051 114
8	1.051 811	−0.607 263	0.051 114
8	−1.051 811	−0.607 263	0.051 114
1	0.000 000	0.000 000	−1.824 671
6	0.000 000	0.000 000	0.837 255
B (GHz)	9.399 4	9.399 4	7.140 0

No.	$\bar{\upsilon}$ (cm^{-1})	x_{ii}	*g*	
1	3136.71	−64.48	1	a_1
2	1317.02	−0.80	1	a_1
3	962.96	−1.92	1	a_1
4	895.29	−2.28	1	a_1
5	1123.30	8.78	2	*e*
6	927.17	0.68	2	*e*
7	741.98	−0.71	2	*e*
8	210.38	−23.23	2	*e*

3.13.11.2. Formation enthalpy, Δ_fH(0 K). A multi-composite treatment yields $\Delta_f H^o$(0 K) = 146.5 ± 8.0 kJ mol^{-1}, the

larger than normal uncertainty due to an aberrant G3 value. A W3X-L of $\Delta_f H^o(0\ K) = 147.3\ kJ\ mol^{-1}$ ($142.2\ kJ\ mol^{-1}$ at 298.15 K) and a WMS of 148.0 kJ mol^{-1} complete the picture.

A C–H bond dissociation energy of 218.0 + 142.2 − (−110.0) = 470 kJ mol^{-1} follows; interestingly, this is is just as strong as the comparable bond in benzene [L07] of 472.2 ± 2.2 kJ mol^{-1}.

3.13.11.3. Results. A rigid rotor anharmonic treatment is followed.

T (K)	$S^o(T)$	$C_p^o(T)$	$H^o(T) - H^o(0)$
298.15	285.81	57.96	14.25
300.	286.16	58.14	14.35
400.	304.25	68.10	20.66
500.	320.43	77.00	27.93
600.	335.12	83.99	36.00
700.	348.48	89.35	44.67
800.	360.70	93.52	53.83
900.	371.91	96.81	63.35
1000.	382.25	99.47	73.16
1100.	391.84	101.64	83.22
1200.	400.76	103.43	93.48
1300.	409.10	104.94	103.90
1400.	416.93	106.21	114.46
1500.	424.29	107.29	125.13
1600.	431.25	108.22	135.91
1800.	444.09	109.72	157.71
2000.	455.71	110.87	179.77

References for 2,4,5-trioxabicyclo[1.1.1]pentyl. *3.14. $C_2H_1O_4$*

L07 Y.-R. Luo, *Comprehensive Handbook of Chemical Bond Energies* (CRC Press, Boca Raton, USA, 2007).

3.14.1. Carboxyformyl ether radical

$^2A'$ g = 2 C_S σ = 1 M_0 = 89.0275

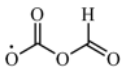

A cognate radical to carboxyoxy oxomethyl has been identified in an EPR study as a planar π-radical [KSAH15]. Two conformers exist categorized as *anti* or *syn* based on the C–O–CH=O dihedral with the *anti* the more stable.

3.14.1.1. Species data.

8	−2.109 043	−0.104 629	0.000 000
8	−0.612 397	−1.594 799	0.000 000
6	−0.884 804	−0.389 169	0.000 000
8	0.000 000	0.620 375	0.000 000
6	1.374 194	0.331 205	0.000 000
8	2.156 176	1.215 111	0.000 000
1	1.585 772	−0.740 679	0.000 000
B (GHz)	12.318 6	2.303 9	1.940 9

No.	$\bar{\upsilon}$ (cm^{-1})	x_{ii}	
1	3083.77	−61.07	a'
2	1882.17	−10.06	a'
3	1535.03	−7.01	a'
4	1390.08	−9.11	a'
5	1185.05	2.02	a'
6	1051.40	−4.76	a'
7	984.49	−4.87	a'
8	647.72	−0.47	a'
9	562.21	−0.83	a'
10	449.34	−1.87	a'
11	205.99	−0.20	a'
12	1023.15	−2.27	a''
13	752.21	0.50	a''
14	121.80	−0.48	a''
15	29.49	34.29	a''

3.14.1.2. Formation enthalpy, $\Delta_f H(0\ K)$. A multi-composite treatment returns $\Delta_f H^o(0\ K) = -452.7 \pm 4.0\ kJ\ mol^{-1}$ ($-458.0\ kJ\ mol^{-1}$ at 298.15 K) for the *anti*, T_1=0.034, which is 65.2 kJ mol^{-1} *less* stable than the carboxyoxy oxomethyl radical discussed above. WMS returns $\Delta_f H^o(0\ K) = -453.2\ kJ\ mol^{-1}$ for the *anti* and $\Delta_f H^o(0\ K) = -446.3\ kJ\ mol^{-1}$ for the *syn*.

3.14.1.3. Results. An anharmonic treatment combined with two hindered rotors for mode nos. 14 and 15 is employed.

T (K)	$S°(T)$	$C_p°(T)$	$H°(T) - H°(0)$
298.15	338.63	82.86	18.37
300.	339.15	83.11	18.52
400.	364.82	95.65	27.48
500.	387.31	105.87	37.57
600.	407.34	113.82	48.57
700.	425.37	119.99	60.27
800.	441.72	124.84	72.52
900.	456.66	128.72	85.21
1000.	470.39	131.86	98.24
1100.	483.08	134.45	111.56
1200.	494.88	136.61	125.11
1300.	505.88	138.42	138.87
1400.	516.20	139.97	152.79
1500.	525.90	141.31	166.85
1600.	535.06	142.46	181.04
1800.	551.96	144.37	209.73
2000.	567.25	145.88	238.76

References for carboxyformyl ether radical.

KSAH15 A. Krivokapic, A. Sanderud, S. G. Aalbergsjoe, E. O. Hole, and E. Sagstuen, "Lithium formate for EPR dosimetry (2): Secondary radicals in X-irradiated crystals," Radiat. Res. **183**(6), 675–683 (2015).

3.14.2. *Carboxyoxomethoxy* syn/anti

$^2A'$ g = 2 C_S σ = 1 M_0 = 89.0275

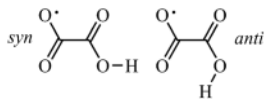

The neutral radical of oxalic acid is catalytically converted into carbon dioxide and formate by oxalate decarboxylase—an enzyme found in fungi and some bacteria [MLCB15]. Otherwise, it rates very little mention in the chemical literature. The two conformers are distinguished by H-bonded interactions with that forming a four-membered ring (*syn* OCOH), the lowest in energy.

3.14.2.1. Species data.

1	1.292 475	2.121 936	0.000 000
8	1.272 902	1.151 916	0.000 000
8	−0.970 033	1.456 646	0.000 000
6	0.000 000	0.755 921	0.000 000
6	−0.115 213	−0.768 358	0.000 000
8	0.857 655	−1.546 731	0.000 000
8	−1.235 674	−1.317 745	0.000 000
B (GHz)	6.518 2	3.582 3	2.311 8

No.	$\bar{\upsilon}$ (cm^{-1})	x_{ii}	
1	3726.84	−82.03	a'
2	1837.79	−9.91	a'
3	1554.91	−7.98	a'
4	1352.26	−5.49	a'
5	1169.13	−6.45	a'
6	1095.12	24.87	a'
7	798.98	−0.40	a'
8	627.46	−0.60	a'
9	525.96	−1.57	a'
10	398.14	−0.47	a'
11	200.85	0.11	a'
12	813.00	−0.15	a''
13	634.50	−5.86	a''
14	408.01	0.51	a''
15	69.37	−0.61	a''

3.14.2.2. Formation enthalpy, Δ_fH(0 K). An isodesmic featuring *syn* formic (−378.38 ± 0.22 kJ mol^{-1}), *syn* acetic (−432.63 ± 0.52 kJ mol^{-1}), and *tTt* oxalic acids (−721.0 ± 1.2 kJ mol^{-1}) as well as formyloxy (−125.57 ± 0.56 kJ mol^{-1}) and acetoxy

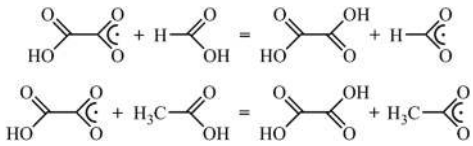

yield reaction enthalpies of −12.5 ± 7.4 kJ mol^{-1} and −25.1 ± 7.1 kJ mol^{-1}, respectively, which transforms into $\Delta_fH°$(0 K) of −463.0 ± 7.8 kJ mol^{-1} and −460.3 ± 7.5 kJ mol^{-1}, giving rise to a final $\Delta_fH°$(0 K) = −461.6 ± 5.3 kJ mol^{-1} (−468.1 kJ mol^{-1} at 298.15 K) where our W3X-L value for acetoxyl of $\Delta_fH°$(0 K) = −182.9 ± 2.0 kJ mol^{-1} has been used.

A multi-composite treatment, *sans* CBS-APNO, yields $\Delta_fH°$(0 K) = −461.1 ± 5.4 kJ mol^{-1} for the *syn*, which is 5.0 kJ mol^{-1} more stable than the *anti* conformer.

An O–H bond energy, using the more appropriate *cTc* conformer of the parent oxalic acid, of 218–468 + (734–17) = 467 kJ mol^{-1}, is in agreement with typical values for carboxylic acids [L07].

3.14.2.3. Results. Hindered rotor analysis ascribes very little impact of the carboxylic rotor, which is confirmed by a relaxed

potential energy scan that has two-fold symmetry and a barrier of 13.9 kJ mol^{-1}. The barrier to internal rotation about the OCOH dihedral amounts to 48.2 kJ mol^{-1}.

T (K)	$S^o(T)$	$C_p^o(T)$	$H^o(T) - H^o(0)$
298.15	323.97	84.96	17.20
300.	324.49	85.25	17.36
400.	351.04	99.28	26.62
500.	374.36	109.63	37.09
600.	395.07	117.32	48.45
700.	413.61	123.14	60.49
800.	430.36	127.67	73.04
900.	445.61	131.29	85.99
1000.	459.60	134.25	99.27
1100.	472.52	136.71	112.82
1200.	484.50	138.79	126.59
1300.	495.68	140.57	140.56
1400.	506.16	142.10	154.70
1500.	516.01	143.45	168.97
1600.	525.31	144.64	183.38
1800.	542.46	146.63	212.51
2000.	558.00	148.27	242.00

References for carboxyoxomethoxy *syn/anti*.

MLCB15 R. W. Molt, A. M. Lecher, T. Clark, R. J. Bartlett, and N. G. J. Richards, "Facile $C_{sp^2} - -C_{sp^2}$ bond cleavage in oxalic acid-derived radicals," J. Am. Chem. Soc. **137**(9), 3248–3252 (2015).

L07 Y.-R. Luo, *Comprehensive Handbook of Chemical Bond Energies* (CRC Press, Boca Raton, USA, 2007).

3.14.3. Carboxyoxy oxomethyl

$^2A'$ g = 2 C_S σ = 1 M_0 = 89.0275

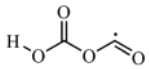

This species is cataloged by SciFinder (791545-05-6), but oddly has no references as of January15, 2020. The *ssa* conformer with HOC=O *syn*, O=C–O–Ċ *syn*, and C–O–Ċ=O *anti* is the more stable by some 6.2 kJ mol^{-1} from *asa*, with *sss* and *saa* higher in energy by 14.0 kJ mol^{-1}and 6.6 kJ mol^{-1}, respectively. The quasi-cyclic *aas* conformer lies much higher at +17.8 kJ mol^{-1}.

3.14.3.1. Species data.

6	−0.721 463	−0.552 875	0.000 000
8	−2.004 990	−0.195 664	0.000 000
1	−2.526 646	−1.010 165	0.000 000
8	−0.273 280	−1.655 380	0.000 000
8	0.000 000	0.623 540	0.000 000
6	1.362 499	0.496 028	0.000 000
8	2.113 324	1.396 410	0.000 000
B (GHz)	11.464	2.326 6	1.934 1

No.	$\bar{\upsilon}$ (cm^{-1})	x_{ii}	
1	3775.89	−80.14	a'
2	1914.67	−12.54	a'
3	1867.25	−9.96	a'
4	1378.85	−6.16	a'
5	1181.06	−5.68	a'
6	1039.18	−11.72	a'
7	970.64	−0.44	a'
8	681.36	−0.10	a'
9	572.59	−0.13	a'
10	455.06	−0.67	a'
11	207.13	−0.11	a'
12	785.68	−0.16	a''
13	571.22	−11.41	a''
14	155.14	1.12	a''
15	104.49	5.20	a''

3.14.3.2. Formation enthalpy, Δ_fH(0 K). A multi-composite approach yields $\Delta_f H^o$(0 K) = −517.9 ± 3.6 kJ mol^{-1} (−523.2 kJ mol^{-1} at 298.15 K); WMS agrees at $\Delta_f H^o$(0 K) = −513.9 kJ mol^{-1} as does W2X at $\Delta_f H^o$(0 K) = −514.4 kJ mol^{-1} for this T_1=0.021 radical.

3.14.3.3. Results. A hindered rotor analysis suggests that only two vibrational modes, nos. 14 and 15, impact sufficiently. The relaxed potential energy scans for these dihedrals are well-behaved, and these are incorporated into an anharmonic treatment.

T (K)	$S^o(T)$	$C_p^o(T)$	$H^o(T) - H^o(0)$
298.15	329.80	92.32	18.41
300.	330.37	92.64	18.58
400.	359.20	107.66	28.64
500.	384.41	118.01	39.95
600.	406.58	124.91	52.12
700.	426.21	129.61	64.86
800.	443.75	133.01	78.00
900.	459.58	135.65	91.43
1000.	473.98	137.81	105.11
1100.	487.21	139.66	118.98
1200.	499.43	141.28	133.03
1300.	510.80	142.70	147.23
1400.	521.42	143.94	161.56
1500.	531.39	145.02	176.01
1600.	540.78	145.94	190.56
1800.	558.05	147.36	219.89
2000.	573.63	148.31	249.46

3.14.4. Dioxirane carboxylic acid radical no. 1

^{2}A g = 2 C_1 σ = 1 M_0 = 89.0275

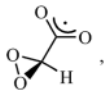

3.14.4.1. Species data.

6	−0.577 580	−0.556 407	−0.182 119
8	−1.532 538	0.332 814	−0.638 248
8	−1.494 350	−0.149 746	0.775 247
1	−0.634 300	−1.588 088	−0.523 917
6	0.825 906	−0.019 562	−0.028 288
8	1.828 797	−0.754 740	−0.022 663
8	1.091 134	1.202 160	0.108 958
B (GHz)	8.775 5	2.881 3	2.539 2

No.	$\bar{\upsilon}$ (cm^{-1})	x_{ii}
1	3114.08	−59.82
2	1584.57	−6.05
3	1403.87	−6.88
4	1285.99	−2.45
5	1161.12	−5.25
6	1126.50	−1.50
7	903.64	−2.37
8	893.09	−3.50
9	831.09	−2.37
10	708.13	−1.13
11	620.10	−8.34
12	451.66	0.67
13	267.98	−0.15
14	212.37	−1.65
15	27.33	−25.61

3.14.4.2. Formation enthalpy, $\Delta_f H$(0 K). The isodesmic reaction

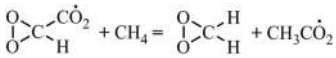

which uses our W3X-L value for acetoxyl of −182.9 ± 2.0 kJ mol^{-1} as well as ATcT references for the chaperones methane (−66.550 ± 0.057 kJ mol^{-1}) and dioxirane (9.41 ± 0.54 kJ mol^{-1}), has a reaction enthalpy of −18.57 ± 1.84 kJ mol^{-1}, leading to $\Delta_f H^o$(0 K) = −88.4 ± 2.8 kJ mol^{-1} (−96.2 kJ mol^{-1} at 298.15 K) [KHR17]. Acetoxyl is itself poorly characterized in the chemical literature, but an ANL0 value of −182.2 kJ mol^{-1} has been reported [KHR17] for it, which lends credence to these results.

A multiple composite atomization calculation returns a value of $\Delta_f H^o$(0 K) = −91.4 ± 7.4 kJ mol^{-1} for this radical with T_1 = 0.028, excluding CBS-APNO and G3 that fail at their second optimization steps.

3.14.4.3. Results. The highly anharmonic mode no. 15 is interpreted as a free rotor ("qro") with a reduced moment of inertia of 24.44 GHz and twofold symmetry since the relaxed potential energy scan is compromised and the reduced barrier height (*V*/*RT*) = 0.58.

T (K)	$S^o(T)$	$C_p^o(T)$	$H^o(T) - H^o(0)$
298.15	330.20	76.29	15.88
300.	330.67	76.59	16.02
400.	354.83	91.68	24.46
500.	376.66	103.90	34.26
600.	396.48	113.41	45.14
700.	414.54	120.81	56.87
800.	431.07	126.68	69.25
900.	446.27	131.42	82.16
1000.	460.33	135.34	95.51
1100.	473.39	138.62	109.21
1200.	485.57	141.40	123.21
1300.	496.98	143.76	137.47
1400.	507.71	145.77	151.95
1500.	517.83	147.47	166.61
1600.	527.39	148.92	181.43
1800.	545.07	151.15	211.45
2000.	561.08	152.68	241.84

References for dioxirane carboxylic acid radical no. 1.

KHR17 S. J. Klippenstein, L. B. Harding, and B. Ruscic, "*Ab initio* computations and active thermochemical tables hand in hand: Heats of formation of core combustion species," J. Phys. Chem. A **121**(35), 6580–6602 (2017).

3.14.5. Dioxirane carboxylic acid radical no. 2; carboxy dioxiranyl

^{2}A g = 2 C_1 σ = 1 M_0 = 89.0275

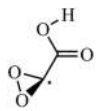

The HOCO *syn* conformer is the ground state.

3.14.5.1. Species data.

6	0.607 736	−0.011 328	0.320 299
8	1.582 160	−0.820 677	−0.116 553
8	1.655 406	0.731 109	−0.052 278
6	−0.815 778	0.126 735	0.027 424
8	−1.365 081	1.195 701	−0.067 719
8	−1.420 323	−1.077 703	−0.008 581
1	−2.369 052	−0.919 881	−0.125 290
B (GHz)	7.977 7	3.051 9	2.238 5

No.	$\bar{\upsilon}$ (cm^{-1})	x_{ii}
1	3745.39	−82.48
2	1774.86	−11.88
3	1604.94	−10.51
4	1336.47	−5.67
5	1137.21	−5.55
6	1003.50	−3.33
7	856.78	−2.85
8	723.56	−3.39
9	689.43	−0.99
10	535.69	−5.84
11	525.55	−1.61
12	449.99	0.29
13	217.82	−5.11
14	193.24	−0.15
15	118.91	−0.37

3.14.5.2. Formation enthalpy, Δ_fH(0 K). A multi-composite atomization value of −146.4 ± 5.8 kJ mol^{-1} is obtained, excluding CBS-APNO that fails at the second optimization step. A direct comparison with the previous radical, which is only possible at CBS-QB3, G4, and W1BD, shows that it is 56.7 ± 1.6 kJ mol^{-1} *more* stable, implying $\Delta_f H^o$(0 K) = −145.1 ± 2.9 kJ mol^{-1} (−151.2 kJ mol^{-1} at 298.15 K).

3.14.5.3. Results. A relaxed potential energy scan about the C–C bond, vibrational mode no. 15, faces a barrier of 26 kJ mol^{-1}, and fails while one about the OC–OH bond, mode no. 10, of 37 kJ mol^{-1} is well-behaved.

T (K)	$S^o(T)$	$C_p^o(T)$	$H^o(T) - H^o(0)$
298.15	330.62	88.16	17.71
300.	331.17	88.49	17.87
400.	358.95	105.05	27.57
500.	383.93	118.74	38.79
600.	406.54	129.09	51.21
700.	427.02	136.33	64.50
800.	445.56	141.11	78.39
900.	462.37	144.16	92.66
1000.	477.66	146.07	107.18
1100.	491.65	147.30	121.85
1200.	504.50	148.13	136.62
1300.	516.38	148.74	151.46
1400.	527.43	149.24	166.36
1500.	537.74	149.70	181.31
1600.	547.41	150.13	196.30
1800.	565.14	150.96	226.41
2000.	581.09	151.71	256.67

3.14.6. 1,2-Dioxoethyldioxy

^{2}A″ g = 2 C_S σ = 1 M_0 = 89.0275

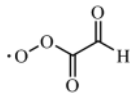

This species is an intermediate in the photochemical oxidation of glyoxal itself as an important trace component in the atmosphere formed from the burning of biomass and from the photo-oxidation of volatile organic compounds [S10]. Conformationally, the lowest is *syn/anti* OOCO/O=CC=O with the *syn/syn*, some 4.3 kJ mol^{-1} less stable; yet another conformer, *gauche/anti*, is close to the *syn/syn* at 3.2 kJ mol^{-1}.

3.14.6.1. Species data.

6	1.490 953	0.121 944	0.000 000
6	0.000 000	0.471 216	0.000 000
8	−0.427 181	1.575 712	0.000 000
8	1.917 471	−0.994 340	0.000 000
8	−0.786 247	−0.704 481	0.000 000
8	−2.087 218	−0.450 331	0.000 000
1	2.119 677	1.028 564	0.000 000
B (GHz)	7.327 5	2.903 0	2.079 3

No.	$\bar{\upsilon}$ (cm^{-1})	x_{ii}	
1	2962.92	−64.49	a'
2	1866.91	−11.78	a'
3	1821.45	−10.11	a'
4	1378.46	−10.14	a'
5	1154.17	−3.59	a'
6	1110.83	−5.30	a'
7	813.33	−3.48	a'
8	671.70	−2.48	a'
9	507.20	−2.25	a'
10	351.87	0.36	a'
11	207.78	0.38	a'
12	1009.89	−1.79	a''
13	531.10	−0.67	a''
14	135.85	0.04	a''
15	78.18	0.68	a''

3.14.6.2. Formation enthalpy, $\Delta_f H$(0 K). da Silva [S10] calculated $\Delta_f H^o$(298.15 K) = −183.7 kJ mol^{-1} for the *syn/anti* in very good agreement with our multi-composite treatment of −182.9 kJ mol^{-1} (−178.2 ± 4.3 kJ mol^{-1} at 0 K) [S10]. WMS values for the *sa* of $\Delta_f H^o$(0 K) = −176.9 kJ mol^{-1} (−181.6 kJ mol^{-1} at 298.15 K) and for the *ss* of −170.9 kJ mol^{-1}, respectively, round out this picture.

3.14.6.3. Results. Hindered rotor analysis identifies mode nos. 15 and 14 as contributing +2 J K^{-1} mol^{-1} to the entropy at room temperature. Key relaxed potential energy scans are problematic, but mode no. 15 has been replaced by an HR term. Literature [S10] values of S^o = 345.9 J K^{-1} mol^{-1} and C_p^o = 80.66 J K^{-1} mol^{-1} have been computed at B3LYP/6-31G(2df,p) for the *syn/anti* conformer using a RRHO approximation but with free rotation about the C–OO bond—it is probably this assumption that accounts for the differences.

T (K)	$S^o(T)$	$C_p^o(T)$	$H^o(T) - H^o(0)$
298.15	335.69	88.68	18.79
300.	336.24	88.92	18.95
400.	363.44	100.32	28.44
500.	386.84	109.36	38.94
600.	407.44	116.59	50.25
700.	425.87	122.42	62.21
800.	442.53	127.18	74.69
900.	457.75	131.08	87.61
1000.	471.73	134.31	100.88
1100.	484.66	137.01	114.45
1200.	496.68	139.28	128.27
1300.	507.91	141.20	142.29
1400.	518.43	142.85	156.50
1500.	528.34	144.27	170.85
1600.	537.69	145.50	185.34
1800.	554.95	147.54	214.65
2000.	570.58	149.15	244.33

References for 1,2-dioxoethyldioxy.

S10 G. da Silva, "Hydroxyl radical regeneration in the photochemical oxidation of glyoxal: Kinetics and mechanism of the HC(O)CO + O_2 reaction," Phys. Chem. Chem. Phys. **12**(25), 6698–6705 (2010).

3.14.7. Formylperoxy oxomethyl

^{2}A g = 2 C_1 σ = 1 M_0 = 89.0275

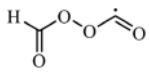

The lowest energy conformer of the radical of diformyl peroxide can be described as *sga* based on O=COO/COOC•/OOC•=O dihedrals with the *aga* lying some 5 kJ mol^{-1} higher.

3.14.7.1. Species data.

8	−0.715 821	0.994 663	0.120 611
8	0.478 617	0.511 026	−0.548 605
6	1.328 445	−0.029 202	0.354 930
6	−1.676 387	0.017 456	0.190 559
1	−2.549 419	0.516 391	0.635 376
8	2.394 209	−0.448 167	0.086 072
8	−1.577 371	−1.113 261	−0.146 618
B (GHz)	9.880 0	2.377 2	2.037 4

No.	$\bar{\upsilon}$ (cm^{-1})	x_{ii}
1	3022.04	−62.01
2	1880.25	−12.21
3	1857.62	−9.25
4	1362.42	−8.41
5	1014.43	−2.31
6	1006.47	−3.37
7	993.80	−8.74
8	874.20	−5.51
9	826.54	−1.80
10	567.52	−0.33
11	430.27	−2.05
12	315.21	−0.73
13	241.26	−0.68
14	231.16	0.37
15	44.93	−4.77

3.14.7.2. Formation enthalpy, Δ_fH(0 K). A multi-composite value of $\Delta_f H^o$(0 K) = −209.5 ± 5.1 kJ mol^{-1} is buttressed by an isodesmically derived result from

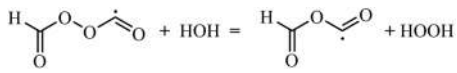

whose reaction enthalpy of 34.51 ± 1.46 kJ mol^{-1}, in conjunction with reference values for water (−238.931 ± 0.027 kJ mol^{-1}) and hydrogen peroxide (−129.472 ± 0.064 kJ mol^{-1}) as well as our high-level value for formyloxy oxomethyl (−282.9 ± 2.0 kJ mol^{-1}), yields $\Delta_f H^o$(0 K) = −208.0 ± 2.5 kJ mol^{-1} (−214.4 kJ mol^{-1} at 298.15 K).

3.14.7.3. Results. Three hindered rotors are identified (mode nos. 15, 14, and 11) with the first having the greatest impact. A scan about the OOC•O dihedral leads to dissociation, while that about the OOCH dihedral encounters a barrier in excess of 58 kJ mol^{-1} and so only mode no. 15 is treated as a hindered rotor together with anharmonic frequencies.

T (K)	$S^o(T)$	$C_p^o(T)$	$H^o(T) - H^o(0)$
298.15	336.45	81.39	17.30
300.	336.96	81.65	17.45
400.	362.31	94.82	26.30
500.	384.66	105.48	36.33
600.	404.67	113.99	47.32
700.	422.77	120.79	59.07
800.	439.28	126.27	71.43
900.	454.41	130.74	84.29
1000.	468.39	134.40	97.55
1100.	481.34	137.45	111.15
1200.	493.41	140.00	125.02
1300.	504.71	142.15	139.13
1400.	515.31	144.00	153.44
1500.	525.30	145.60	167.92
1600.	534.74	146.99	182.55
1800.	552.20	149.31	212.18
2000.	568.03	151.19	242.24

3.14.8. 2-Hydroperoxy-1,2-dioxoethyl

^{2}A g = 2 C_1 σ = 1 M_0 = 89.0275

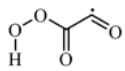

This species is yet another intermediate in the photochemical oxidation of glyoxal itself as an important trace component in the atmosphere formed from the burning of biomass and from the photo-oxidation of volatile organic compounds [S10]. The most stable conformer has HOOC(O)C planar, influenced by the hydrogen bond H···O=C, with the C•=O bond out-of-plane, which makes the species "optically active" according to MultiWell. da Silva [S10] illustrated a different conformer *gg*, ~planar OOC(O)C backbone, and *gauche* H and O, encountered during the reaction of the glyoxal radical HC(O)C•=O with O_2.

3.14.8.1. Species data.

6	1.449 140	−0.109 853	0.399 145
6	0.032 632	0.271 645	0.051 862
8	−0.341 139	1.412 255	−0.039 623
8	2.391 595	−0.346 536	−0.250 506
8	−0.753 654	−0.810 858	0.034 625
8	−2.147 633	−0.442 837	−0.065 228
1	−2.083 986	0.533 061	−0.140 185
B (GHz)	9.745 0	2.420 0	1.985 5

No.	$\bar{\upsilon}$ (cm^{-1})	x_{ii}
1	3539.42	−101.32
2	1973.09	−13.24
3	1765.22	−13.41
4	1479.41	−9.64
5	1145.42	−12.00
6	927.92	−4.04
7	904.07	−2.58
8	745.42	−3.26
9	517.49	−5.25
10	421.32	−2.60
11	400.97	−18.35
12	323.76	−3.73
13	300.49	−1.26
14	131.90	−0.67
15	99.94	−0.50

3.14.8.2. Formation enthalpy, $\Delta_f H(0\ \mathrm{K})$. Our multi-composite atomization approach yields $\Delta_f H^\circ(0\ \mathrm{K}) = -207.4 \pm 3.6$ kJ mol^{-1} (−210.9 kJ mol^{-1} at 298.15 K), in good agreement with a WMS of $\Delta_f H^\circ(0\ \mathrm{K}) = -208.1$ kJ mol^{-1}. For the *gg* conformer, a formation enthalpy of $\Delta_f H^\circ(298.15\ \mathrm{K}) = -205.4$ kJ mol^{-1} has been estimated [S10], which accords with our multi-composite of $\Delta_f H^\circ(298.15\ \mathrm{K}) = -204.3$ kJ mol^{-1}.

3.14.8.3 Results. A hindered rotor treatment for mode nos. 15 (C–C) and 11 (O–O) and incorporating anharmonicity is employed; this HR approach negates the "optical activity" of the molecule.

T (K)	$S^\circ(T)$	$C_p^\circ(T)$	$H^\circ(T) - H^\circ(0)$
298.15	346.24	98.32	20.04
300.	346.85	98.56	20.22
400.	376.72	108.83	30.63
500.	401.80	115.87	41.88
600.	423.43	121.41	53.76
700.	442.51	126.06	66.13
800.	459.61	130.12	78.95
900.	475.15	133.72	92.14
1000.	489.41	136.95	105.68
1100.	502.60	139.85	119.52
1200.	514.88	142.43	133.63
1300.	526.37	144.70	147.99
1400.	537.17	146.66	162.56
1500.	547.35	148.34	177.31
1600.	556.97	149.74	192.21
1800.	574.73	151.86	222.38
2000.	590.81	153.23	252.90

References for 2-hydroperoxy-1,2-dioxoethyl.

S10 G. da Silva, "Hydroxyl radical regeneration in the photochemical oxidation of glyoxal: Kinetics and mechanism of the HC(O)CO + O_2 reaction," Phys. Chem. Chem. Phys. **12**(25), 6698–6705 (2010).

3.15. $C_2H_1O_5$

3.15.1. 2-Carboxyl peroxoic acid radical

$^2A'$ g = 2 C_S σ = 1 M_0 = 105.0269

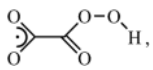

This is the other possible radical formed from 2-hydroperoxy-2-oxoacetic acid but an alkoxy radical, RO$^\bullet$, the lowest energy conformer of which adopts a quasi-cyclic structure.

3.15.1.1. Species data.

6	0.000 000	0.401 122	0.000 000
6	−0.845 211	−0.868 717	0.000 000
8	−2.090 550	−0.792 137	0.000 000
8	−0.467 851	1.507 211	0.000 000
8	−0.387 371	−2.026 405	0.000 000
8	1.300 457	0.111 151	0.000 000
8	2.102 347	1.300 666	0.000 000
1	1.415 013	2.001 691	0.000 000
B (GHz)	6.128 4	1.974 5	1.493 4

No.	$\bar{\upsilon}$ (cm^{-1})	x_{ii}		No.	$\bar{\upsilon}$ (cm^{-1})	x_{ii}	
1	3525.96	−101.22	a'	10	503.61	−1.03	a'
2	1811.85	−9.95	a'	11	394.05	−0.34	a'
3	1543.99	−7.06	a'	12	342.22	−0.54	a'
4	1491.63	−8.48	a'	13	167.19	0.20	a'
5	1238.31	−7.95	a'	14	790.86	0.22	a''
6	1084.32	27.32	a'	15	516.03	−1.63	a''
7	955.45	−3.81	a'	16	392.79	−22.10	a''
8	922.40	−1.48	a'	17	170.29	−0.51	a''
9	688.59	−2.10	a'	18	55.33	−0.41	a''

3.15.1.2. Formation enthalpy, $\Delta_f H(0\ K)$. An isodesmic reaction

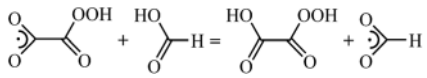

yields a reaction enthalpy of 2.9 ± 2.5 kJ mol^{-1}, which together with ATcT reference values for formic acid (−378.38 ± 0.22 kJ mol^{-1}) and formyloxy (−125.57 ± 0.56 kJ mol^{-1}) and our estimate q.v. for 2-hydroperoxy-2-oxoacetic acid of −611.0 ± 3.2 kJ mol^{-1} gives rise to $\Delta_f H^o(0\ K)$ = −368.5 ± 4.1 kJ mol^{-1} (−374.9 kJ mol^{-1} at 298.15 K), which is in accord with a multi-composite atomization result, *sans* CBS-APNO, of $\Delta_f H^o(0\ K)$ = −364.6 ± 8.6 kJ mol^{-1}.

In a direct comparison with the previous isomeric peroxy radical, this species is less stable in accord with the general findings that, for example, $HOCH_2CH_2OO\bullet$ is more stable than $\bullet OCH_2CH_2OOH$ [KDSP07, ZFGM09].

3.15.1.3. Results. Hindered rotor analysis identifies mode nos. 18 and 16 with the reduced barrier heights (*V*/*RT*)s of 4.6 and 11.3, respectively, as significant; a hindered rotor and anharmonic treatment is employed here.

T (K)	$S^o(T)$	$C_p^o(T)$	$H^o(T) - H^o(0)$
298.15	362.66	110.17	21.49
300.	363.34	110.49	21.70
400.	397.24	124.98	33.51
500.	426.35	135.88	46.57
600.	451.94	144.82	60.62
700.	474.82	151.98	75.48
800.	495.49	157.46	90.96
900.	514.28	161.48	106.92
1000.	531.45	164.36	123.21
1100.	547.22	166.39	139.76
1200.	561.76	167.83	156.47
1300.	575.24	168.86	173.31
1400.	587.78	169.61	190.23
1500.	599.50	170.16	207.22
1600.	610.50	170.58	224.25
1800.	630.63	171.19	258.43
2000.	648.69	171.61	292.71

3.15.2. Dicarbonic acid radical

$^2A'$ g = 2 C_S σ = 1 M_0 = 105.0269

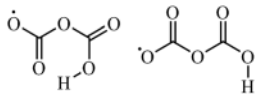

The lowest energy conformer exhibits a six-membered ring structure with an *anti* carboxylic configuration. However, there is another conformer, generated by rotation about the O_2CO–C(O)OH dihedral, which is very close, within 0.4 kJ mol^{-1}, in energy,

3.15.2.1. Species data.

6	−1.172 333	0.123 216	0.000 000
8	−1.368 736	−1.091 056	0.000 000
8	−2.201 593	0.878 557	0.000 000
8	0.000 000	0.752 749	0.000 000
6	1.273 681	0.073 579	0.000 000
8	2.240 919	0.746 222	0.000 000
8	1.217 323	−1.238 917	0.000 000
1	0.288 596	−1.561 218	0.000 000
B(GHz)	6.613 8	2.040 0	1.559 1

No.	$\bar{\upsilon}$(cm^{-1})	x_{ii}		No.	$\bar{\upsilon}$(cm^{-1})	x_{ii}	
1	3398.98	−180.53	a'	10	576.21	−0.07	a'
2	1941.57	−12.62	a'	11	467.00	−0.10	a'
3	1539.55	−13.31	a'	12	385.90	−1.79	a'
4	1404.15	−23.49	a'	13	250.31	−0.98	a'
5	1292.99	−6.45	a'	14	779.24	−1.23	a''
6	1167.64	−4.14	a'	15	755.48	0.03	a''
7	1030.62	−4.58	a'	16	672.40	−16.49	a''
8	807.24	−3.25	a'	17	115.33	−0.35	a''
9	668.13	−1.51	a'	18	65.52	0.07	a''

3.15.2.2. Formation enthalpy, $\Delta_f H(0\ K)$. A multi-composite treatment returns $\Delta_f H^o(0\ K) = -678.2 \pm 4.2$ kJ mol^{-1} (−686.3 kJ mol^{-1} at 298.15 K), in reasonable agreement with a WMS value of $\Delta_f H^o(0\ K) = -674.6$ kJ mol^{-1}.

3.15.2.3. Results. A hindered rotor analysis identifies the dihedrals O_2C–OC, CO–CO, and OC–OH with the vibrational mode nos. 18, 17, and 16; the overall impact on the computed entropy is small, particularly for the OH rotor, mode no. 16. Our treatment employs HRs for nos. 18 and 17 and anharmonic frequencies.

T (K)	$S^o(T)$	$C_p^o(T)$	$H^o(T) - H^o(0)$
298.15	350.81	95.60	19.93
300.	351.41	95.96	20.10
400.	381.50	113.43	30.60
500.	408.34	127.07	42.66
600.	432.47	137.47	55.91
700.	454.29	145.44	70.07
800.	474.13	151.63	84.93
900.	492.28	156.53	100.35
1000.	508.99	160.49	116.21
1100.	524.44	163.74	132.42
1200.	538.81	166.43	148.93
1300.	552.22	168.68	165.69
1400.	564.79	170.57	182.65
1500.	576.62	172.16	199.79
1600.	587.77	173.50	217.07
1800.	608.33	175.60	251.99
2000.	626.92	177.14	287.27

References for dicarbonic acid radical.

KDSP07 K. T. Kuwata, T. S. Dibble, E. Sliz, and E. B. Petersen, "Computational studies of intramolecular hydrogen atom transfers in the β-hydroxyethylperoxy and β-hydroxyethoxy radicals," J. Phys. Chem. A **111**(23), 5032–5042 (2007).

ZFGM09 J. Zádor, R. X. Fernandes, Y. Georgievskii, G. Meloni, C. A. Taatjes, and J. A. Miller, "The reaction of hydroxyethyl radicals with O_2: A theoretical analysis and experimental product study," Proc. Combust. Inst. **32**(1), 271–277 (2009).

3.15.3. Diformyl trioxide radical

^{2}A g = 2 C_1 σ = 1 M_0 = 105.0269

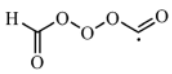

The *agga* conformer (O=COO/COOO/OOOC•/OOC•=O) of the diformyl trioxide radical is the ground state.

3.15.3.1. Species data.

8	1.021 410	0.247 460	0.571 331
8	2.977 953	−0.685 028	0.010 654
6	2.016 190	−0.080 445	−0.291 547
8	0.019 680	1.042 392	−0.121 214
8	−0.941 209	0.133 414	−0.634 374
6	−1.970 730	−0.028 629	0.290 017
8	−2.887 741	−0.725 890	0.024 663
1	−1.793 509	0.555 656	1.200 707
B(GHz)	10.042 5	1.203 2	1.149 4

No.	$\bar{\upsilon}$(cm^{-1})	x_{ii}	No.	$\bar{\upsilon}$(cm^{-1})	x_{ii}
1	3049.10	−61.61	10	656.52	−0.94
2	1886.53	−9.81	11	611.02	−2.27
3	1873.29	−7.38	12	433.43	−0.87
4	1365.03	−9.10	13	406.46	−1.49
5	1053.75	−6.88	14	289.83	−0.22
6	1026.73	−2.46	15	237.79	1.34
7	984.07	−5.25	16	181.64	−0.84
8	934.16	−5.36	17	109.78	−1.77
9	739.98	−7.52	18	55.51	0.32

3.15.3.2. Formation enthalpy, $\Delta_f H(0\ K)$. An isodemic reaction featuring water (−238.931 ± 0.027 kJ mol^{-1}) and trioxidane (−81.71 ± 0.72 kJ mol^{-1}) as references and our high-level value for formyloxy oxomethyl (−282.9 ± 2.0 kJ mol^{-1})

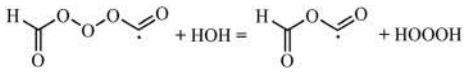

has a reaction enthalpy of 20.87 ± 1.97 kJ mol^{-1}, which translates to $\Delta_f H^o(0\ K) = -146.6 \pm 2.9$ kJ mol^{-1} (−153.5 kJ mol^{-1} at 298.15 K). Multi-composites of −149.2 ± 7.8 kJ mol^{-1} and a WMS of −149.1 kJ mol^{-1} are within agreement, resulting in a final value of $\Delta_f H^o(0\ K) = -148.3 \pm 1.6$ kJ mol^{-1} (−155.2 kJ mol^{-1} at 298.15 K).

3.15.3.3. Results. Four vibrational modes, nos. 1–4, are classified as hindered rotors; however, all have reduced barrier heights (V/RT)s in excess of 7.8, and moreover, potential energy scans lead to dissociation, except for that about the HCOO dihedral. Hence, a simpler treatment is indicated.

T (K)	$S^o(T)$	$C_p^o(T)$	$H^o(T) - H^o(0)$
298.15	364.83	104.34	21.14
300.	365.48	104.68	21.34
400.	397.87	120.47	32.63
500.	426.04	131.77	45.28
600.	450.81	139.80	58.87
700.	472.83	145.71	73.16
800.	492.60	150.28	87.97
900.	510.51	153.94	103.19
1000.	526.90	156.96	118.73
1100.	541.98	159.52	134.56
1200.	555.96	161.72	150.62
1300.	568.98	163.64	166.89
1400.	581.17	165.34	183.34
1500.	592.63	166.85	199.95
1600.	603.44	168.21	216.70
1800.	623.39	170.54	250.58
2000.	641.46	172.44	284.88

3.15.4. 2-Oxo-2-peroxyl-2-ethanoic acid radical

^{2}A g = 2 C_1 σ = 1 M_0 = 105.0269

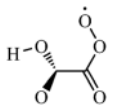

This is one of the possible radicals, ROO•, formed from 2-hydroperoxy-2-oxoacetic acid; the lowest energy conformer can be classified as *syn/gauche/anti* for the HOCO/O=CC=O/OOCO dihedrals.

3.15.4.1. Species data.

6	0.510 118	0.632 418	−0.018 743
6	−0.892 305	0.026 222	0.120 321
8	−1.415 966	−0.115 793	1.184 950
8	0.776 944	1.780 835	−0.068 390
8	−1.436 370	−0.202 358	−1.076 900
1	−2.339 239	−0.532 443	−0.939 639
8	1.560 895	−0.323 983	−0.009 989
8	1.093 542	−1.566 125	0.011 601
B (GHz)	3.619 1	2.615 6	2.032 4

No.	$\bar{\upsilon}$ (cm^{-1})	x_{ii}	No.	$\bar{\upsilon}$ (cm^{-1})	x_{ii}
1	3711.73	−82.86	10	713.90	−1.78
2	1908.88	−11.27	11	616.18	−4.46
3	1839.90	−9.76	12	581.34	−1.03
4	1375.13	−6.04	13	452.74	−0.43
5	1185.71	−5.10	14	357.18	0.00
6	1148.42	−4.99	15	239.24	0.27
7	1035.37	−3.68	16	184.35	0.09
8	792.62	−0.43	17	151.53	−1.34
9	745.02	−1.28	18	57.10	−0.80

3.15.4.2. Formation enthalpy, $\Delta_f H$(0 K). A multi-composite treatment for the *sga* conformer yields $\Delta_f H^o$(0 K) = −432.6 ± 4.8 kJ mol^{-1} (−440.1 kJ mol^{-1} at 298.15 K) as against the $\Delta_f H^o$(0 K) = −427.9 kJ mol^{-1} in a WMS calculation.

3.15.4.3. Results. A hindered rotor analysis identifies three vibrational modes (nos. 1, 2, and 8) with reduced barrier heights (V/RT)s of 4.3, 15.1, and 19.1, respectively, the first of which, OC–CO, has the largest impact.

T (K)	$S^o(T)$	$C_p^o(T)$	$H^o(T) - H^o(0)$
298.15	358.74	101.83	20.57
300.	359.37	102.13	20.76
400.	390.77	116.12	31.71
500.	417.86	126.60	43.87
600.	441.70	134.88	56.95
700.	463.02	141.57	70.79
800.	482.29	147.01	85.22
900.	499.87	151.41	100.15
1000.	516.01	154.94	115.47
1100.	530.91	157.74	131.11
1200.	544.74	159.95	147.00
1300.	557.61	161.69	163.08
1400.	569.65	163.06	179.32
1500.	580.93	164.14	195.68
1600.	591.56	165.00	212.14
1800.	611.07	166.26	245.27
2000.	628.63	167.14	278.61

3.16. $C_2H_1O_6$

3.16.1. Diformyltetroxide radical

^{2}A g = 2 C_1 σ = 1 M_0 = 121.0263

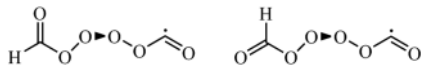

The *sgGga* conformer, classified according to O=COO/COOO/OOOO/OOOĊ/OOĊ=O dihedrals, is the ground state with the *agGga* lying some 3.3 ± 0.7 kJ mol^{-1} above.

3.16.1.1. Species data.

6	−2.425 124	−0.206 305	0.196 215
8	−3.517 359	0.225 045	0.085 335
8	−1.407 536	0.040 116	−0.635 854
8	−0.201 981	−0.741 303	−0.170 241
8	0.439 184	−0.017 237	0.754 199
8	1.323 136	0.946 964	0.074 042
6	2.543 451	0.382 422	−0.209 008
8	2.884 093	−0.735 101	−0.015 701
1	3.133 745	1.195 418	−0.657 489
B (GHz)	9.370 8	0.886 6	0.858 4

No.	$\bar{\upsilon}$(cm^{-1})	x_{ii}	No.	$\bar{\upsilon}$(cm^{-1})	x_{ii}	No.	$\bar{\upsilon}$(cm^{-1})	x_{ii}
1	3042.12	−61.73	8	949.93	−3.77	15	334.78	−6.92
2	1875.99	−11.76	9	791.47	−5.70	16	282.25	−0.71
3	1863.95	−8.62	10	692.13	−1.53	17	233.79	0.99
4	1376.41	−9.82	11	651.43	−1.66	18	171.04	−0.38
5	1070.63	−7.99	12	605.56	−4.49	19	118.02	−1.10
6	1025.66	−2.56	13	522.81	−2.94	20	56.77	−0.04
7	984.94	−11.67	14	426.15	−9.85	21	47.32	−1.07

3.16.1.2. Formation enthalpy, $\Delta_f H$(0 K). An isodesmic reaction

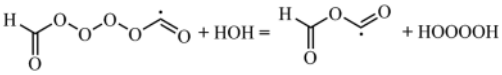

which uses water (−238.931 ± 0.027 kJ mol^{-1}) and tetraoxidane (−33.8 ± 2.4 kJ mol^{-1}) as references and utilizes our high-level result for formyloxy oxomethyl (−282.9 ± 2.0 kJ mol^{-1}), gives 26.20 ± 1.85 kJ mol^{-1} corresponding to $\Delta_f H^o$(0 K) = −104.0 ± 3.6 kJ mol^{-1} (−111.7 kJ mol^{-1} at 298.15 K).

3.16.1.3. Results. Five hindered rotors feature, all apart from no. 21, with reduced barrier heights (*V*/*RT*)s in excess of 7.4; the relaxed scans tend to lead to dissociation; hence, a simplistic treatment is used.

T (K)	$S^o(T)$	$C_p^o(T)$	$H^o(T) - H^o(0)$
298.15	398.23	118.65	24.66
300.	398.97	118.99	24.88
400.	435.58	135.78	37.64
500.	467.40	149.45	51.93
600.	495.66	160.51	67.44
700.	521.09	169.36	83.95
800.	544.18	176.27	101.25
900.	565.26	181.48	119.14
1000.	584.59	185.28	137.49
1100.	602.38	187.94	156.16
1200.	618.81	189.70	175.05
1300.	634.04	190.80	194.07
1400.	648.21	191.42	213.19
1500.	661.43	191.71	232.34
1600.	673.80	191.78	251.52
1800.	696.38	191.59	289.85
2000.	716.55	191.27	328.14

3.16.2. Ethanediperoxoic acid radical

^{2}A g = 2 C_1 σ = 1 M_0 = 121.0263

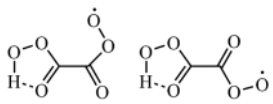

Two principal conformers are listed; the ground state is nonplanar with a ≈90° angle between the ring and the O=COO• group, which is itself in an *anti* configuration. A planar conformer (C_S, ^{2}A″) with a 180° O=C–C=O dihedral is found at +4.3 kJ mol^{-1}.

3.16.2.1. Species data.

8	−1.190 834	−0.073 325	−0.796 412
8	−0.844 786	−0.112 973	1.430 882
6	−0.446 429	−0.191 193	0.302 071
6	0.992 513	−0.572 753	−0.066 714
8	1.873 239	0.529 602	−0.168 959
8	1.233 580	1.685 633	−0.031 853
8	−2.569 304	0.187 706	−0.471 869
1	−2.539 199	0.200 061	0.508 847
8	1.405 942	−1.668 692	−0.201 914
B (GHz)	3.398	1.572 3	1.357 9

No.	$\bar{\upsilon}$ (cm^{-1})	x_{ii}	No.	$\bar{\upsilon}$(cm^{-1})	x_{ii}	No.	$\bar{\upsilon}$ (cm^{-1})	x_{ii}
1	3535.48	−99.73	8	926.04	−2.93	15	356.79	−2.96
2	1906.72	−11.50	9	892.20	−1.22	16	348.99	−1.42
3	1807.90	−10.15	10	775.34	−0.54	17	237.94	−0.72
4	1487.84	−9.56	11	712.79	−0.94	18	196.90	−0.56
5	1262.03	−7.51	12	618.16	−1.73	19	148.14	−0.52
6	1147.18	−5.19	13	498.71	−1.10	20	126.60	0.12
7	1053.28	−3.13	14	396.50	−15.48	21	49.71	−0.32

3.16.2.2. Formation enthalpy, $\Delta_f H(0\ K)$. Multiple composite atomization calculation suggests $\Delta_f H^o(0\ K) = -333.3 \pm 6.8$ kJ mol^{-1} (−342.2 kJ mol^{-1} at 298.15 K) for the non-planar; this would lead to a BDE(OO–H) of 402 kJ mol^{-1} almost identical to the same bond in benzeneperoxy carboxylic acid [DD04].

3.16.2.3. Results. A hindered rotor analysis picks out mode nos. 21, 19, and 14 with reduced barrier heights (*V*/*RT*)s of 4.0, 14.1, and 10.3, respectively, the first, rotation about the C–C bond, having the greatest impact, contributing 1.6 J mol^{-1} K^{-1} to the entropy; however, the scan about the C–C bond is unusable.

T (K)	$S^o(T)$	$C_p^o(T)$	$H^o(T) - H^o(0)$
298.15	383.77	119.15	23.54
300.	384.51	119.55	23.76
400.	421.65	138.83	36.72
500.	454.28	153.40	51.36
600.	483.22	163.75	67.25
700.	509.04	170.91	84.00
800.	532.20	175.89	101.36
900.	553.14	179.48	119.13
1000.	572.19	182.20	137.22
1100.	589.66	184.36	155.55
1200.	605.79	186.17	174.08
1300.	620.75	187.75	192.77
1400.	634.72	189.19	211.62
1500.	647.82	190.52	230.60
1600.	660.15	191.76	249.72
1800.	682.87	194.05	288.30
2000.	703.43	196.08	327.31

References for ethanediperoxoic acid radical.

DD04 T. G. Denisova and E. T. Denisov, "Estimation of the O–H bond dissociation energy from kinetic data for hydroperoxides with functional groups," Pet. Chem. **44**, 278–283 (2004).

3.16.3. Peroxydicarbonic acid radical

^{2}A g = 2 C_1 σ = 1 M_0 = 121.0263

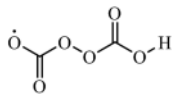

Several conformers of this peroxydicarbonic acid radical exist with the *sgss* (O=C–O–O/CO–OC/OOC=O/O=C–OH) lying approximately 57 kJ mol^{-1} lower than the highest energy conformer (*sgsa*).

3.16.3.1. Species data.

8	0.551 604	0.527 901	−0.738 527
8	−0.643 822	−0.244 061	−0.915 960
6	−1.551 885	0.094 130	0.030 102
6	1.445 811	−0.190 850	0.037 995
8	−1.351 379	0.904 503	0.948 010
8	1.234 463	−1.221 840	0.588 296
8	−2.672 232	−0.443 446	−0.028 183
8	2.560 120	0.538 502	0.022 389
1	3.206 412	0.087 844	0.583 221
B (GHz)	5.426 0	1.293 1	1.266 2

No.	$\bar{\upsilon}$ (cm^{-1})	x_{ii}	No.	$\bar{\upsilon}$ (cm^{-1})	x_{ii}	No.	$\bar{\upsilon}$ (cm^{-1})	x_{ii}
1	3779.07	−80.25	8	949.79	−1.39	15	497.49	−6.47
2	1888.21	−10.36	9	895.71	−3.21	16	416.71	−0.49
3	1515.16	−6.88	10	771.29	0.00	17	335.63	−0.11
4	1374.24	−6.27	11	726.46	−0.99	18	284.09	−0.57
5	1188.37	11.75	12	716.44	−1.15	19	92.27	−0.25
6	1158.07	−5.50	13	633.51	−0.18	20	87.07	0.10
7	1030.71	−5.67	14	556.24	−0.05	21	61.67	−0.30

3.16.3.2. Formation enthalpy, $\Delta_f H(0\ K)$. A multi-composite atomization calculation returns $\Delta_f H^o(0\ K) = -605.4 \pm 9.2$ kJ mol^{-1} (−616.0 kJ mol^{-1} at 298.15 K) excluding CBS-APNO that fails at the second optimization step. The bond dissociation energy for O–H is = −616.0 + 218.0 − (−869.6) = 472 kJ mol^{-1}, which is in good agreement with typical values for carboxylic acids [L07] of 468.6 ± 12.6 kJ mol^{-1}.

3.16.3.3. Results. Four vibrational modes (nos. 21, 20, 19, and 15) are identified but all with reduced barrier heights (V/RT)s in excess of 9.4; the impact on entropy is slight.

T (K)	$S^o(T)$	$C_p^o(T)$	$H^o(T) - H^o(0)$
298.15	374.64	110.70	21.81
300.	375.32	111.13	22.02
400.	410.23	131.77	34.20
500.	441.44	147.83	48.22
600.	469.53	160.06	63.64
700.	494.92	169.27	80.12
800.	518.00	176.19	97.41
900.	539.07	181.41	115.30
1000.	558.40	185.42	133.65
1100.	576.22	188.57	152.35
1200.	592.74	191.10	171.34
1300.	608.13	193.21	190.56
1400.	622.51	194.98	209.97
1500.	636.02	196.51	229.54
1600.	648.74	197.82	249.26
1800.	672.17	199.90	289.04
2000.	693.31	201.36	329.17

References for peroxydicarbonic acid radical.

L07 Y.-R. Luo, *Comprehensive Handbook of Chemical Bond Energies* (CRC Press, Boca Raton, USA, 2007).

3.17. $C_2H_1O_8$

3.17.1. Dicarboxyltetroxide radical

^{2}A g = 2 C_1 σ = 1 M_0 = 153.0251

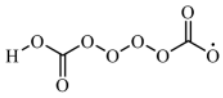

The *sagGg's* conformer, classified according to the dihedrals HOC=O/(H)OCOO/COOO/OOOO/OOOC/OOCO, appears to be the ground state.

3.17.1.1. Species data.

8	−0.455 145	−1.220 684	−0.486 099
8	0.446 335	−1.387 256	0.508 391
8	−1.762 066	−0.895 419	0.145 113
8	1.008 100	−0.100 836	0.862 025
6	2.038 147	0.210 004	−0.011 573
6	−2.074 207	0.394 196	−0.105 014
8	−1.362 620	1.200 281	−0.727 404
8	2.384 601	−0.424 422	−0.954 257
8	−3.170 290	0.812 325	0.312 558
8	2.532 460	1.359 879	0.446 106
1	3.245 358	1.623 855	−0.151 947
B (GHz)	2.706 9	0.819 7	0.714 7

No.	$\bar{\upsilon}$ (cm^{-1})	x_{ii}	No.	$\bar{\upsilon}$ (cm^{-1})	x_{ii}	No.	$\bar{\upsilon}$ (cm^{-1})	x_{ii}
1	3775.96	−80.06	10	845.30	−4.09	19	453.59	−0.61
2	1883.34	−10.78	11	777.24	−0.07	20	402.35	−1.19
3	1505.01	−7.10	12	735.09	0.36	21	280.51	−0.25
4	1370.88	−6.25	13	709.84	−1.13	22	253.58	−0.15
5	1184.50	10.99	14	656.90	−1.39	23	133.95	0.18
6	1156.68	−5.28	15	624.03	−1.53	24	111.84	−0.12
7	999.97	−2.48	16	582.82	−1.06	25	61.70	0.09
8	968.72	−2.97	17	557.07	−1.34	26	53.35	0.95
9	897.94	−4.40	18	505.32	−8.56	27	44.82	0.29

3.17.1.2. Formation enthalpy, Δ_fH(0 K). A multiple composite calculation suggests $\Delta_f H^o(0\ K) = -500.3 \pm 13.5$ kJ mol^{-1}, which is in accord with the $\Delta_f H^o(0\ K) = -500.7 \pm 5.8$ kJ mol^{-1} (−513.5 kJ mol^{-1} at 298.15 K) derived from a reaction enthalpy of −10.7 ± 5.2 kJ mol^{-1} for the isodesmic reaction

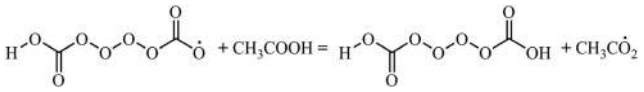

where *cis* acetic acid (−418.51 ± 0.51 kJ mol^{-1}) and acetoxyl (−182.5 ± 1.0 kJ mol^{-1}) and dicarboxyltetroxide (−747.4 ± 2.4 kJ mol^{-1}) have been employed.

3.17.1.3. Results. The relaxed potential energy scans are well-behaved, except for that about the first COOO dihedral, but the hindered rotor analysis minimizes their overall impact with reduced barrier heights (*V*/*RT*)s in excess of 12. A default anharmonic oscillator RR approach is used in light of compromised scans.

T (K)	$S^o(T)$	$C_p^o(T)$	$H^o(T) - H^o(0)$
298.15	426.36	141.52	27.40
300.	427.23	142.05	27.66
400.	471.71	167.12	43.18
500.	511.09	185.54	60.86
600.	546.17	199.01	80.12
700.	577.64	209.04	100.54
800.	606.07	216.70	121.84
900.	631.96	222.71	143.82
1000.	655.68	227.55	166.34
1100.	677.56	231.54	189.30
1200.	697.86	234.88	212.63
1300.	716.77	237.71	236.26
1400.	734.48	240.12	260.15
1500.	751.12	242.17	284.26
1600.	766.80	243.91	308.57
1800.	795.70	246.65	357.63
2000.	821.79	248.60	407.17

3.18. $C_2H_2O_1$

3.18.1. Ethynol; acetylenol

$^1A'$ g = 1 C_S σ = 1 M_0 = 42.0373

H−C≡C−OH

The simplest alkynyl alcohol is an intermediate in the vapor-phase pyrolysis of monolignol compounds themselves derived from the pyrolysis of lignin [FDKH18] and also in the reaction between $O(^3P)$ and vinyl radical [JJKK15].

3.18.1.1 Species data.

6	0.063 969	1.318 541	0.000 000
6	0.000 000	0.123 394	0.000 000
1	0.127 981	2.375 833	0.000 000
8	−0.152 361	−1.176 399	0.000 000
1	0.707 095	−1.616 253	0.000 000
B (GHz)	678.458	9.781 1	9.642 1

No.	$\bar{\upsilon}$ (cm^{-1})	x_{ii}	
1	3765.16	−90.69	a'
2	3489.29	−51.91	a'
3	2282.82	−7.64	a'
4	1256.46	−12.74	a'
5	1084.47	−9.79	a'
6	649.94	−2.34	a'
7	401.58	−0.36	a'
8	545.81	−2.07	a''
9	440.53	0.27	a''

3.18.1.2 Formation enthalpy, $\Delta_f H$(0 K). A W3X-L calculation [SS16] has $\Delta_f H^o$(0 K) = 95.0 kJ mol^{-1} (92.5 kJ mol^{-1} at 298.15 K), in excellent agreement with the value of 94.4–94.6 kJ mol^{-1} of ANL0 and ANL1 calculations [KHR17], with the W2–F12 thermochemical protocol [KT14] at 95.1 kJ mol^{-1}, and indeed with 94.9 ± 1.3 kJ mol^{-1} (92.8 kJ mol^{-1}) in the ATcT whose values are derived from lower level, albeit many, calculations. There is considerable disagreement with the experimental result from Orlov *et al.* [OKMT86] of 41.6 kJ mol^{-1} at 298.15 K, but good agreement with the G4 value of 93.1 kJ mol^{-1} by Rayne and Forrest [RF11].

3.18.1.3 Results. Good agreement with the tabulated values [GMG12] is obtained, viz., S^o(298.15 K) = 247.3 ± 2.9 J mol^{-1} K^{-1} and C_p^o(300 K) = 56.07 ± 2.5 J mol^{-1} K^{-1}.

T (K)	$S^o(T)$	$C_p^o(T)$	$H^o(T) - H^o(0)$
298.15	247.49	56.08	12.42
300.	247.84	56.24	12.53
400.	265.08	63.59	18.54
500.	279.89	69.08	25.18
600.	292.88	73.41	32.32
700.	304.47	77.03	39.84
800.	314.97	80.17	47.70
900.	324.58	82.97	55.86
1000.	333.45	85.50	64.29
1100.	341.71	87.78	72.95
1200.	349.44	89.84	81.83
1300.	356.70	91.70	90.91
1400.	363.56	93.38	100.17
1500.	370.05	94.90	109.58
1600.	376.22	96.27	119.14
1800.	387.70	98.63	138.63
2000.	398.20	100.60	158.56

References for ethynol; acetylenol.

FDKH18 Y. Furutani, Y. Dohara, S. Kudo, J.-I. Hayashi, and K. Norinaga, "Theoretical study on elementary reaction steps in thermal decomposition processes of syringol-type monolignol compounds," J. Phys. Chem. A **122**(3), 822–831 (2018).

JJKK15 S.-H. Jung, S.-C. Jang, J.-W. Kim, J.-W. Kim, and J.-H. Choi, "Theoretical investigation of the radical–radical reaction of $O(^3P)$ + C_2H_3 and comparison with gas-phase crossed-beam experiments," J. Phys. Chem. A **119**(49), 11761–11771 (2015).

SS16 J. M. Simmie and J. N. Sheahan, "Validation of a database of formation enthalpies and of mid-level model chemistries," J. Phys. Chem. A **120**(37), 7370–7384 (2016).

KHR17 S. J. Klippenstein, L. B. Harding, and B. Ruscic, "*Ab initio* computations and active thermochemical tables hand in hand: Heats of formation of core combustion species," J. Phys. Chem. A **121**(35), 6580–6602 (2017).

KT14 A. Karton and D. Talbi, "Pinning the most stable $H_xC_yO_z$ isomers in space by means of high level theoretical procedures," Chem. Phys. **436-437**, 22 (2014).

OKMT86 V. M. Orlov, A. A. Krivoruchko, A. D. Misharev, and V. V. Takhistov, "Enthalpy of formation of ketene, ethynol, and their analogs in the gas phase," Bull. Acad. Sci. USSR, Div. Chem. Sci. **35**, 2404–2405 (1986).

RF11 S. Rayne and K. Forest, "Thermochemistry of mono- and disubstituted acetylenes and polyynes at the Gaussian-4 level of theory," Comput. Theor. Chem. **970**, 15–22 (2011).

GMG12 C. F. Goldsmith, G. R. Magoon, and W. H. Green, "Database of small molecule thermochemistry for combustion," J. Phys. Chem. A **116**(36), 9033–9057 (2012).

3.18.2. Ketene, ethenone

$^1A'$ g = 1 C_{2v} σ = 2 M_0 = 42.0373

O=C=CH_2

This species is very well-known and plays a central role in the combustion of hydrocarbons but also features prominently in the

synthesis of olefins from syngas [JLPX16] as well as further afield in the interstellar medium [EGDA18].

3.18.2.1 Species data.

1	0.000 000	0.936 802	−1.738 899
6	0.000 000	0.000 000	−1.205 598
6	0.000 000	0.000 000	0.102 038
1	0.000 000	−0.936 802	−1.738 899
8	0.000 000	0.000 000	1.262 394
B (GHz)	285.698	10.341 5	9.980 2

No.	$\bar{\upsilon}$ (cm^{-1})	x_{ii}	
1	3180.42	−26.10	a_1
2	2221.73	−10.70	a_1
3	1412.77	−6.46	a_1
4	1171.46	−1.09	a_1
5	593.98	−1.46	b_1
6	552.39	−0.14	b_1
7	3272.35	−30.50	b_2
8	990.74	−1.14	b_2
9	442.75	0.15	b_2

3.18.2.2 Formation enthalpy, $\Delta_f H(0\ K)$. Experimental values for the formation enthalpy at 298.15 K vary widely with −61.84 kJ mol^{-1}, −47.7 ± 1.6 kJ mol^{-1}, and −87.24 kJ mol^{-1} being reported [RG34, NLK71, OKMT86]. Of these the most direct was obtained in an adiabatic solution calorimeter by Nuttall *et al.* in which the enthalpy of the ketene gas reacting with aqueous sodium hydroxide was measured [NLK71]. This is probably the most reliable experimental value as also concluded by others [RLA99, SMC08].

A multiple composite atomization value of $\Delta_f H^o(0\ K) = -46.28 \pm 0.95$ kJ mol^{-1} is in very good agreement with a W3X-L result of −45.9 kJ mol^{-1} (−49.1 kJ mol^{-1} at 298.15 K) and indeed with ATcT v1.122d of −45.37 ± 0.13 kJ mol^{-1}. The latter, oddly, does not include the Nuttall result among its principal contributors.

High-level ANL1 values [KHR17] of $\Delta_f H^o(0\ K) = -45.7$ kJ mol^{-1} round out the good agreement. The difference between the formation enthalpies of ethenone and ethynol (|(−45.9) − (95.0)| = 140.9 kJ mol^{-1}) exactly matches the difference computed by Karton and Talbi [KT14] using their high-level W2-F12 thermochemical protocol. The W3X-L values usefully summarizes these results and confirms the essential correctness of the Nuttall experiment.

3.18.2.3. Results. Straightforward rigid rotor–anharmonic treatment yields results in good agreement with the literature [ER97],[11] for example, S = 241.204 J K^{-1} mol^{-1} and C_p (300 K) = 51.75 J K^{-1} mol^{-1}; and S(298.15 K) = 241.0 ± 2.5 J K^{-1} mol^{-1}and C_p (300 K) = 51.5 ± 2.5 J K^{-1} mol^{-1}.

T (K)	$S^o(T)$	$C_p^o(T)$	$H^o(T) - H^o(0)$
298.15	241.40	51.21	11.72
300.	241.72	51.37	11.82
400.	257.57	58.91	17.34
500.	271.40	65.05	23.55
600.	283.72	70.13	30.32
700.	294.86	74.46	37.55
800.	305.06	78.21	45.19
900.	314.46	81.49	53.17
1000.	323.20	84.39	61.47
1100.	331.36	86.93	70.04
1200.	339.03	89.17	78.84
1300.	346.24	91.13	87.86
1400.	353.06	92.87	97.06
1500.	359.52	94.39	106.42
1600.	365.66	95.74	115.93
1800.	377.07	97.99	135.31
2000.	387.49	99.78	155.09

References for ketene; ethenone.

JLPX16 F. Jiao, J. Li, X. Pan, J. Xiao, H. Li, H. Ma, M. Wei, Y. Pan, Z. Zhou, M. Li, S. Miao, J. Li, Y. Zhu, D. Xiao, T. He, J. Yang, F. Qi, Q. Fu, and X. Bao, "Selective conversion of syngas to light olefins," Science **351**(6277), 1065–1068 (2016).EGDA18 E. E. Etim, P. Gorai, A. Das, and E. Arunan, "Theoretical investigation of interstellar C–C–O and C–O–C bonding backbone molecules," Astrophys. Space Sci. **363**(1), 6 (2018).

RG34 F. O. Rice and J. Greenberg, "Ketene. III. Heat of formation and heat of reaction with alcohols," J. Am. Chem. Soc. **56**, 2268–2270 (1934).

NLK71 R. L. Nuttall, A. H. Laufer, and M. V. Kilday, "The enthalpy of formation of ketene," J. Chem. Thermodyn. **3**, 167–174 (1971).

OKMT86 V. M. Orlov, A. A. Krivoruchko, A. D. Misharev, and V. V. Takhistov, "Enthalpy of formation of ketene, ethynol, and their analogs in the gas phase," Bull. Acad. Sci. USSR, Div. Chem. Sci. **35**, 2404–2405 (1986).

RLA99 B. Ruscic, M. Litorja, and R. L. Asher, "Ionization energy of methylene revisited: Improved values for the enthalpy of formation of CH_2 and the bond dissociation energy of CH_3 via simultaneous solution of the local thermochemical network," J. Phys. Chem. A **103**, 8625–8633 (1999);B. Ruscic, M. Litorja, and R. L. Asher, J. Phys. Chem. A **104**, 8600 (2000).

SMC08 J. M. Simmie, W. K. Metcalfe, and H. J. Curran, "Ketene thermochemistry," ChemPhysChem. **9**, 700–702 (2008).

KHR17 S. J. Klippenstein, L. B. Harding, and B. Ruscic, "*Ab initio* computations and active thermochemical tables hand in hand: Heats of formation of core combustion species," J. Phys. Chem. A **121**(35), 6580–6602 (2017).

KT14 A. Karton and D. Talbi, "Pinning the most stable $H_xC_yO_z$ isomers in space by means of high-level theoretical procedures," Chem. Phys. **436-437**, 22–28 (2014).

ER97 A. L. L. East and L. Radom, "*Ab initio* statistical thermodynamical models for the computation of third-law entropies," J. Chem. Phys. **106**(16), 6655–6674 (1997).

3.18.3. 2-Oxiranylidene

$^1A'$ g = 1 C_S σ = 1 M_0 = 42.0373

This cyclic species crops up in a number of studies [GC03, DJL02] including those of O (^{1}D/^{3}P) + 1HC≡CH and isomerization to ketene.

3.18.3.1 Species data.

6	0.547 520	−0.595 821	0.000 000
6	−0.889 127	−0.147 973	0.000 000
8	0.000 000	0.775 961	0.000 000
1	1.024 822	−0.872 466	0.928 563
1	1.024 822	−0.872 466	−0.928 563
B (GHz)	38.771	23.883 4	16.451 5

No.	$\bar{\upsilon}$ (cm^{-1})	x_{ii}	
1	3130.94	−29.80	a'
2	1528.00	−1.69	a'
3	1418.43	−2.99	a'
4	1096.11	−8.82	a'
5	836.12	−6.25	a'
6	827.17	−1.48	a'
7	3240.83	−35.42	a''
8	1117.94	−1.30	a''
9	884.79	−2.38	a''

3.18.3.2 Formation enthalpy, $\Delta_f H$(0 K). A high-level W3X-L calculation gives $\Delta_f H^o$(0 K) = 213.6 kJ mol^{-1} (209.3 kJ mol^{-1} at 298.15 K), which is in excellent agreement with a multiple composite atomization value of $\Delta_f H^o$(0 K) = 213.1 ± 1.1 kJ mol^{-1} (210.0 ± 1.1 kJ mol^{-1} at 298.15 K) for the singlet state; the triplet state lies some 243 kJ mol^{-1} higher in energy. These are in moderate accord with the values of 206 kJ mol^{-1} and 201 kJ mol^{-1} extracted from relative energies [GC03, DJL02].

3.18.3.3 Results. An anharmonic treatment is employed.

T (K)	$S^o(T)$	$C_p^o(T)$	$H^o(T) - H^o(0)$
298.15	244.46	43.68	10.61
300.	244.73	43.86	10.69
400.	258.63	53.17	15.54
500.	271.40	61.35	21.28
600.	283.20	68.03	27.76
700.	294.11	73.47	34.84
800.	304.22	77.95	42.42
900.	313.63	81.72	50.41
1000.	322.41	84.92	58.74
1100.	330.63	87.66	67.37
1200.	338.37	90.03	76.26
1300.	345.65	92.09	85.37
1400.	352.55	93.88	94.67
1500.	359.08	95.46	104.14
1600.	365.28	96.84	113.75
1800.	376.83	99.16	133.36
2000.	387.38	101.00	153.38

References for 2-oxiranylidene.

GC03 Y. Girard and P. Chaquin, "Addition reactions of ^{1}D and ^{3}P atomic oxygen with acetylene. Potential energy surfaces and stability of the primary products. Is oxirene only a triplet molecule? A theoretical study," J. Phys. Chem. A **107**(48), 10462–10470 (2003).

DJL02 C. Delamere, C. Jakins, and E. Lewars, "Reactions of oxiranylidene and dimethyloxiranylidene, and their generation by retro diels-alder-type reactions: A computational study," J. Mol. Struct.: THEOCHEM **593**, 79–91 (2002).

3.18.4. Oxirene

^{1}A g = 1 C_2 σ = 2 M_0 = 42.0373

This species has a long and checkered history [L11], suffice it to say is that it does not appear to converge to a real symmetric structure with the B3LYP functional irrespective of the basis sets employed. Accordingly, and exceptionally, an MP2/cc-pVTZ + d structure is reported.

3.18.4.1 Species data.

6	0.000 000	0.636 192	−0.464 488
6	0.000 000	−0.636 192	−0.464 488
8	0.000 000	0.000 000	0.896 211
1	−0.000 073	1.650 929	−0.797 918
1	0.000 073	−1.650 929	−0.797 918
B (GHz)	33.232	26.254	14.667

No.	$\bar{\upsilon}$ (cm^{-1})	x_{ii}	
1	3436.65	−27.04	*a*
2	1770.76	−4.21	*a*
3	1092.61	−4.00	*a*
4	886.94	−1.12	*a*
5	616.21	15.85	*a*
6	3364.64	−27.22	*b*
7	968.52	−0.89	*b*
8	511.26	2.51	*b*
9	139.12	38.03	*b*

3.18.4.2 Formation enthalpy, $\Delta_f H$(0 K). A W3X-L calculation based on a CCSD(T)/aVTZ geometry, not the prescribed B3LYP/cc-pVTZ + d, yields $\Delta_f H^\circ$(0 K) = 271.8 kJ mol^{-1} (270.0 kJ mol^{-1} at 298.15 K) in very good agreement with an ANL1 [KHR17] of 271.3 kJ mol^{-1} and with the $\Delta_f H^\circ$(0 K) = 272.85 ± 0.98 kJ mol^{-1} present in the ATcT, which is based largely on W4 calculations by Karton *et al.* [KDM11]

3.18.4.3 Results. A conventional RR anharmonic treatment is used; agreement with the literature [D92] is reasonable, viz., at 298.15 K, S° = 245.6 J K^{-1} mol^{-1} and C_p° = 54.4 J K^{-1} mol^{-1}.

T (K)	$S^\circ(T)$	$C_p^\circ(T)$	$H^\circ(T) - H^\circ(0)$
298.15	248.92	52.81	12.27
300.	249.24	52.97	12.36
400.	265.55	60.48	18.05
500.	279.71	66.34	24.40
600.	292.23	70.91	31.28
700.	303.44	74.59	38.56
800.	313.61	77.68	46.17
900.	322.92	80.34	54.08
1000.	331.51	82.66	62.23
1100.	339.49	84.71	70.60
1200.	346.94	86.51	79.17
1300.	353.93	88.10	87.90
1400.	360.51	89.51	96.78
1500.	366.73	90.76	105.80
1600.	372.62	91.86	114.93
1800.	383.56	93.70	133.49
2000.	393.51	95.16	152.38

References for oxirene.

L11 E. G. Lewars, *Computational Chemistry*, 2nd ed. (Springer, New York, NY, 2011) ISBN: 978-90-481-3861-6.

KHR17 S. J. Klippenstein, L. B. Harding, and B. Ruscic, "*Ab initio* computations and active thermochemical tables hand in hand: Heats of formation of core combustion species," J. Phys. Chem. A **121**(35), 6580–6602 (2017).

KDM11 A. Karton, S. Daon, and J. M. L. Martin, "W4-11: A high-confidence benchmark dataset for computational thermochemistry derived from first-principles W4 data," Chem. Phys. Lett. **510**, 165–178 (2011).

D92 O. V. Dorofeeva, "Ideal gas thermodynamic properties of oxygen heterocyclic compounds. Part 1. Three-membered, four-membered and five-membered rings," Thermochim. Acta **194**, 9–46 (1992).

3.18.5. 1-Oxo-1,2-ethanediyl

$^3A''$ g = 3 C_S σ = 1 M_0 = 42.0373

This radical has been detected during the ultrafast photodissociation of acetone and probably arises from acetyl radical decomposition [FSR00]; it is not currently included in combustion models.

3.18.5.1 Species data.

6	0.000 000	0.455 308	0.000 000
8	−1.176 060	0.242 489	0.000 000
6	1.074 215	−0.493 242	0.000 000
1	0.865 348	−1.559 822	0.000 000
1	2.097 844	−0.152 481	0.000 000
B (GHz)	112.90	11.169	10.164

No.	$\bar{\upsilon}$ (cm^{-1})	x_{ii}	
1	3245.95	−42.87	*a*′
2	3093.15	−43.83	*a*′
3	1779.15	−15.90	*a*′
4	1440.27	−9.10	*a*′
5	1062.98	−5.46	*a*′
6	991.85	−5.07	*a*′
7	463.66	0.38	*a*′
8	801.05	7.68	*a*″
9	393.62	−2.38	*a*″

3.18.5.2 Formation enthalpy, $\Delta_f H$(0 K). A multi-composite treatment gives $\Delta_f H^\circ$(0 K) = 181.2 ± 1.8 kJ mol^{-1} (178.1 kJ mol^{-1} at 298.15 K) for this species with a T_1 of 0.036; a W3X-L calculation returns $\Delta_f H^\circ$(0 K) = 180.7 kJ mol^{-1} (177.6 kJ mol^{-1} at 298.15 K).

3.18.5.3 Results. A relaxed potential energy scan of the C–C bond reveals a large barrier, which has little effect on the computed thermochemistry but is nonetheless included together with anharmonicities.

T (K)	$S^\circ(T)$	$C_p^\circ(T)$	$H^\circ(T) - H^\circ(0)$
298.15	259.91	51.07	11.83
300.	260.23	51.23	11.93
400.	276.09	59.23	17.46
500.	290.05	65.95	23.73
600.	302.58	71.52	30.61
700.	313.97	76.23	38.00
800.	324.42	80.27	45.83
900.	334.08	83.74	54.04
1000.	343.07	86.73	62.57
1100.	351.45	89.30	71.37
1200.	359.32	91.49	80.41
1300.	366.72	93.35	89.65
1400.	373.70	94.94	99.07
1500.	380.29	96.29	108.63
1600.	386.55	97.44	118.32
1800.	398.13	99.26	138.00
2000.	408.67	100.61	157.99

References for 1-oxo-1,2-ethanediyl.

FSR00 P. Farmanara, V. Stert, and W. Radloff, "Ultrafast photodissociation dynamics of acetone excited by femtosecond 155 nm laser pulses," Chem. Phys. Lett. **320**(5), 697–702 (2000).

3.18.6. Oxybismethylene

^{1}A g = 1 C_2 σ = 2 M_0 = 42.0373

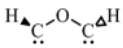

This species was partially investigated in a theoretical study of the C_2H_2O singlet potential energy surface. Apart from a comment that the *anti/anti* conformer is the ground state, its high energy relative to ketene precluded further study [BNRW82]. At our chosen level, the geometry of the ground singlet state is best described as quasi-linear with a C–O–C bond angle of 165° and dihedrals of 135°—quite far from C_{2V} *anti/anti*.

3.18.6.1 Species data.

8	0.000 000	0.000 000	0.038 419
6	0.000 000	1.258 449	−0.123 728
1	−0.745 563	1.657 908	0.588 690
6	0.000 000	−1.258 449	−0.123 728
1	0.745 563	−1.657 908	0.588 690
B (GHz)	248.75	11.313 8	11.292 9

No.	$\bar{\upsilon}$ (cm^{-1})	x_{ii}	
1	2922.85	−35.47	*a*
2	1267.71	−7.38	*a*
3	1057.69	−4.30	*a*
4	985.78	−2.35	*a*
5	372.88	−1.38	*a*
6	2920.05	−35.65	*b*
7	1599.90	−10.89	*b*
8	1198.72	−6.33	*b*
9	355.03	−1.21	*b*

3.18.6.2 Formation enthalpy, $\Delta_f H$(0 K). A multi-composite treatment, *sans* CBS-APNO and G3 that optimize to a different *aa* C_{2V} structure, returns $\Delta_f H^\circ$(0 K) = 503.2 ± 5.6 kJ mol^{-1} (500.3 kJ mol^{-1} at 298.15 K), which is in remarkable agreement with the 502 kJ mol^{-1} estimate of Bouma *et al.* [GKS11]

Higher-level composite WMS gives $\Delta_f H^\circ$(0 K) = 508.5 kJ mol^{-1} and W3X-L $\Delta_f H^\circ$(0 K) = 500.1 kJ mol^{-1} (497.2 kJ mol^{-1} at 298.15 K); the difference is unsurprising as this species has a T_1 of 0.050.

3.18.6.3 Results. Both a hindered rotor analysis and a relaxed potential energy scan of the H–C–O–C fail, so only an approximate treatment is possible. Mode no. 4 at 985 cm^{-1} is primarily responsible for rotation of the H–C···C–H dihedral and so is unlikely to contribute to changes in the anharmonic rigid-rotor treatment espoused *here*.

T (K)	$S^\circ(T)$	$C_p^\circ(T)$	$H^\circ(T) - H^\circ(0)$
298.15	243.27	51.24	12.03
300.	243.58	51.38	12.13
400.	259.43	59.06	17.65
500.	273.37	65.97	23.91
600.	285.93	71.84	30.81
700.	297.39	76.78	38.25
800.	307.92	80.97	46.14
900.	317.67	84.54	54.42
1000.	326.74	87.59	63.03
1100.	335.21	90.22	71.92
1200.	343.16	92.48	81.06
1300.	350.64	94.45	90.40
1400.	357.71	96.17	99.94
1500.	364.40	97.67	109.63
1600.	370.74	99.00	119.46
1800.	382.54	101.22	139.49
2000.	393.30	103.01	159.92

References for oxybismethylene.

BNRW82 W. J. Bouma, R. H. Nobes, L. Radom, and C. Woodward, "On the existence of stable structural isomers of ketene. A theoretical study of the C_2H_2O potential energy surface," J. Org. Chem. **47**, 1869–1875 (1982).

3.18.7. 2-Oxyethenyl anti/syn

$^3A''$ g = 3 C_S σ = 1 M_0 = 42.0373

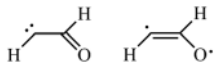

This species has been proposed as intermediate in the Wolff rearrangement [GRHA16] and in the reaction [GRSL13] of ethyne + $HO_2^{\bullet}$. Guan *et al.* [PSGW19] carried out theoretical studies of both the *anti* HCCH triplet ground state and the first excited state ^1A. Their best estimate for the singlet–triplet gap amounts to 8.4 kJ mol^{-1}.

Pokhilko *et al.* explored the spin-forbidden channels in the reactions of unsaturated hydrocarbons with O-atoms [PSGW19] as in HC≡CH + O → HCCHO—so-called Cvetanović diradicals. They found that the Z or *anti* conformer (HCCH) is slightly more stable than the E or *syn*, a conclusion with which we agree since we find that the *syn* lies +(4.7 ± 0.9 kJ mol^{-1}) above the *anti*. *Here*, both *anti* and *syn* HCCH conformers are considered in their triplet ground states.

3.18.7.1 Species data.

3.18.7.2 Formation enthalpy, $\Delta_f H(0\ K)$. Multi-composite values of $\Delta_f H^o(0\ K) = 260.9 \pm 0.9$ kJ mol^{-1} (257.4 kJ mol^{-1} at 298.15 K) for the ground state *anti* are in moderate agreement with 262.0 kJ mol^{-1} and 261.9 kJ mol^{-1} from W2X and WMS as indeed is ANL0 that puts [KHR17] the *anti* triplet at 261.3 kJ mol^{-1}.

Multi-reference W3X-L calculations return *anti* values of $\Delta_f H^o(0\ K) = 259.5$ kJ mol^{-1} (256.0 kJ mol^{-1} at 298.15 K) for the triplet (T_1 = 0.030), the *syn* lies higher at $\Delta_f H^o(0\ K) = 264.9$ kJ mol^{-1} (261.6 kJ mol^{-1} at 298.15 K) and $\Delta_f H^o(0\ K) = 270.6$ kJ mol^{-1} for the singlet (T_1 = 0.049), respectively. The singlet–triplet gap thus amounts to 11.1 kJ mol^{-1}.

There is strong disagreement with the value of 163.2 kJ mol^{-1} tabulated in the Small Molecule for Combustion database [GMG12].

3.18.7.3 Results. Our anharmonic and hindered rotor treatments are in good agreement with the literature values [KHR17],

	anti			*syn*		
T (K)	$S^o(T)$	$C_p^o(T)$	$H^o(T) - H^o(0)$	$S^o(T)$	$C_p^o(T)$	$H^o(T) - H^o(0)$
298.15	262.33	54.17	12.01	261.65	54.61	12.05
300.	262.67	54.36	12.11	261.99	54.80	12.15
400.	279.60	63.45	18.02	279.06	63.95	18.10
500.	294.56	70.64	24.73	294.14	71.13	24.87
600.	307.96	76.21	32.09	307.62	76.69	32.27
700.	320.04	80.57	39.93	319.78	81.04	40.16
800.	331.04	84.04	48.17	330.83	84.51	48.45
900.	341.11	86.88	56.72	340.96	87.34	57.04
1000.	350.38	89.24	65.53	350.28	89.69	65.90
1100.	358.99	91.23	74.55	358.93	91.66	74.97
1200.	367.00	92.94	83.76	366.98	93.35	84.22
1300.	374.50	94.42	93.13	374.51	94.80	93.63
1400.	381.54	95.72	102.64	381.58	96.07	103.17
1500.	388.19	96.88	112.27	388.25	97.19	112.83
1600.	394.47	97.90	122.01	394.55	98.18	122.60
1800.	406.11	99.68	141.77	406.22	99.89	142.41
2000.	416.69	101.17	161.86	416.82	101.31	162.54

	anti				*syn*		
8	−1.079 523	−0.148 901	0.000 000	8	−1.166 660	−0.038 667	0.000 000
6	0.000 000	0.451 327	0.000 000	6	0.000 000	0.338 658	0.000 000
6	1.204 496	−0.284 935	0.000 000	6	1.148 177	−0.481 423	0.000 000
1	1.363 379	−1.355 918	0.000 000	1	2.206 898	−0.259 775	0.000 000
1	0.045 835	1.548 776	0.000 000	1	0.237 316	1.425 699	0.000 000
B (GHz)	65.871	13.213	11.005	B (GHz)	96.658	11.630	10.381

	anti				*syn*		
No.	$\bar{\upsilon}$ (cm^{-1})	x_{ii}		No.	$\bar{\upsilon}$ (cm^{-1})	x_{ii}	
1	3195.76	−65.95	a'	1	3203.58	−63.86	a'
2	2993.26	−70.77	a'	2	2834.70	−80.36	a'
3	1515.33	−17.02	a'	3	1538.69	−20.68	a'
4	1401.42	1.02	a'	4	1381.41	0.45	a'
5	1145.69	−7.47	a'	5	1117.15	−9.08	a'
6	921.90	−13.63	a'	6	869.74	−10.35	a'
7	437.17	−0.51	a'	7	443.76	0.33	a'
8	965.69	−2.10	a''	8	946.85	−2.65	a''
9	635.74	−9.64	a''	9	491.11	−5.52	a''

viz., for the *anti* S^o(298.15 K) = 262.8 ± 3.3 J mol^{-1} K^{-1} and C_p^o (300 K) = 54.8 ± 3.3 J mol^{-1} K^{-1}.

References for 2-oxyethenyl *anti/syn*.

GKS11 D. J. Goebbert, D. Khuseynov, and A. Sanov, "O$^-$+ acetaldehyde reaction products: Search for singlet formylmethylene, a wolff rearrangement intermediate," J. Phys. Chem. A **115**(15), 3208–3217 (2011).

GRHA16 J. Gimenez-Lopez, C. T. Rasmussen, H. Hashemi, M. U. Alzueta, Y. Gao, P. Marshall, C. F. Goldsmith, and P. Glarborg, "Experimental and kinetic modeling study of C_2H_2 oxidation at high pressure," Int. J. Chem. Kinet. **48**(11), 724–738 (2016).

GRSL13 J. Guan, K. R. Randall, H. F. Schaefer, and H. Li, "Formylmethylene: The triplet ground state and the lowest singlet state," J. Phys. Chem. A **117**(10), 2152–2159 (2013).

PSGW19 P. Pokhilko, R. Shannon, D. Glowacki, H. Wang, and A. I. Krylov, "Spin-Forbidden channels in reactions of unsaturated hydrocarbons with O(3P)," J. Phys. Chem. A **123**(2), 482–491 (2019).

KHR17 S. J. Klippenstein, L. B. Harding, and B. Ruscic, "*Ab initio* computations and active thermochemical tables hand in hand: Heats of formation of core combustion species," J. Phys. Chem. A **121**(35), 6580–6602 (2017).

GMG12 C. F. Goldsmith, G. R. Magoon, and W. H. Green, "Database of small molecule thermochemistry for combustion," J. Phys. Chem. A **116**(36), 9033–9057 (2012).

3.19. $C_2H_2O_2$

Some of the species treated here range from the well-known such as glyoxal through to compounds with only a single appearance in current databases. Vijay and Sastry [VS05] used hybrid density functional theory and post-SCF methods to explore these isomers and located a total of 10 minima. In general terms, we agree with their ordering of the relative energies of these species and also with their structures, except for 1,3-dioxetane-2,4-diyl for which we report C_S symmetry *versus* their C_{2v}.

References for $C_2H_2O_2$

VS05 D. Vijay and G. N. Sastry, "Relative energies of $C_2O_2H_2$ isomers and their ionized counterparts: Possibility of bond stretch isomerism," J. Mol. Struct.: THEOCHEM **714**, 199–207 (2005).

3.19.1. Carboxymethylene

$^3A''$ g = 3 C_S σ = 1 M_0 = 58.0367

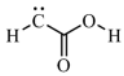

This carbene is not included in the work of Vijay and Sastry; the *syn/syn* HCC = O/HOCO conformer is the lowest lying triplet state with the lowest singlet state some 15.8 kJ mol^{-1} to 19.7 kJ mol^{-1} above [SPR01, XS96]. The other conformers lie higher in energy as per G4 calculations:

Conformer: HCC = O/HOCO	*syn/syn*	*syn/anti*	*anti/syn*	*anti/anti*
Relative energy (kJ mol^{-1})	0.0	7.4	11.1	24.8

3.19.1.1 Species data.

6	1.373 896	0.453 960	0.000 000
6	0.000 000	0.061 392	0.000 000
1	1.787 156	1.451 186	0.000 000
8	−0.902 582	0.880 033	0.000 000
8	−0.205 705	−1.271 552	0.000 000
1	−1.164 234	−1.411 147	0.000 000
B (GHz)	12.916 7	10.820 2	5.887 9

No.	$\bar{\upsilon}$ (cm^{-1})	x_{ii}	
1	3745.24	−81.65	*a′*
2	3230.75	−57.54	*a′*
3	1672.76	−13.52	*a′*
4	1398.91	−6.73	*a′*
5	1191.36	−6.40	*a′*
6	975.13	−4.03	*a′*
7	879.26	−7.04	*a′*
8	744.78	1.42	*a′*
9	574.21	0.37	*a′*
10	554.50	−5.95	*a″*
11	496.51	−5.25	*a″*
12	408.56	0.54	*a″*

3.19.1.2 Formation enthalpy, $\Delta_f H$(0 K). An isodesmic reaction featuring ethanal (−154.97 ± 0.28) and *syn*-ethanoic acid (−418.38 ± 0.54)

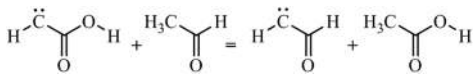

can avail of our value for *anti* formylmethylene of 259.5 ± 2.0 kJ mol^{-1}, which in conjunction with a reaction enthalpy of −17.01 ± 1.63 kJ mol^{-1} yields $\Delta_f H^o$(0 K) = 13.1 ± 2.7 kJ mol^{-1} (+7.0 kJ mol^{-1} at 298.15 K) in good agreement with $\Delta_f H^o$(0 K) = 15.7 kJ mol^{-1} from WMS.

3.19.1.3 Results. A hindered rotor anharmonic oscillator treatment yields the values tabulated; there is no literature with which to compare these.

T (K)	$S^o(T)$	$C_p^o(T)$	$H^o(T) - H^o(0)$
298.15	281.80	67.69	13.19
300.	282.22	68.02	13.32
400.	304.04	83.66	20.94
500.	323.98	94.74	29.90
600.	341.96	102.20	39.77
700.	358.12	107.24	50.26
800.	372.69	110.78	61.17
900.	385.89	113.37	72.38
1000.	397.95	115.35	83.82
1100.	409.02	116.91	95.44
1200.	419.25	118.18	107.19
1300.	428.75	119.23	119.07
1400.	437.62	120.10	131.03
1500.	445.93	120.85	143.08
1600.	453.76	121.49	155.20
1800.	468.13	122.55	179.61
2000.	481.09	123.38	204.21

References for carboxymethylene.

SPR01 A. P. Scott, M. S. Platz, and L. Radom, "Singlet-triplet splittings and barriers to Wolff rearrangement for carbonyl carbenes," J. Am. Chem. Soc. **123**(25), 6069–6076 (2001).

XS96 Y. Xie and H. F. Schaefer, "Singlet-triplet splitting of carbohydroxycarbene," Mol. Phys. **87**(2), 389–397 (1996).

3.19.2. Dihydroxyethenylidene

^{1}A g = 1 C_2 σ = 2 M_0 = 58.0367

There is only a single reference to this species in the literature. Apeloig and Schreiber [AS78] concluded that the ground electronic state is a singlet and our calculations support this. Conformationally, this molecule is quite complex with the *gauche/gauche′* conformer, C–C–O–H of ≈ −112°, having the lowest energy at the multi-composite level, and the next lowest at +2.2 can be described as *cis/gauche*, angle −106°, while a *g′g′* conformer with dihedrals of ≈27° lies at +3.1 kJ mol^{-1}.

3.19.2.1 Species data.

1	−0.842 829	1.278 438	−0.973 919
8	0.000 000	1.177 619	−0.509 637
6	0.000 000	0.000 000	0.178 130
6	0.000 000	0.000 000	1.505 543
8	0.000 000	−1.177 619	−0.509 637
1	0.842 829	−1.278 438	−0.973 919
B (GHz)	12.936 3	10.295 1	5.911 2

No.	$\bar{\upsilon}$ (cm^{-1})	x_{ii}	
1	3735.47	−45.74	*a*
2	1733.	−8.66	*a*
3	1191.20	−5.55	*a*
4	922.08	−1.64	*a*
5	514.49	−2.07	*a*
6	285.59	−14.57	*a*
7	3731.20	−45.76	*b*
8	1295.90	−5.39	*b*
9	1198.01	−7.08	*b*
10	525.57	0.55	*b*
11	356.32	−9.37	*b*
12	132.65	12.44	*b*

3.19.2.2 Formation enthalpy, $\Delta_f H$(0 K). A W3X-L calculation gives a value of $\Delta_f H^o$(0 K) = 138.9 kJ mol^{-1} (135.0 kJ mol^{-1} at 298.15 K), which is close to the 140.5 kJ mol^{-1} of W2X and in very good agreement with a multi-composite value of 139.7 ± 2.6 kJ mol^{-1}. An ANL0 value of $\Delta_f H^o$(0 K) = 141.6 kJ mol^{-1} has been reported [KHR17].

3.19.2.3 Results. Given the paucity of information for this system, there are no possible comparisons to be made. There are problems with the relaxed potential energy scans of the hindered C–C–O–H rotors, mode nos. 6 and 11, and so treatment defaults to consideration as anharmonic modes.

T (K)	$S^o(T)$	$C_p^o(T)$	$H^o(T) - H^o(0)$
298.15	281.35	71.31	15.23
300.	281.79	71.51	15.36
400.	303.71	80.83	23.00
500.	322.51	87.51	31.44
600.	338.92	92.43	40.45
700.	353.47	96.17	49.89
800.	366.51	99.05	59.65
900.	378.31	101.29	69.67
1000.	389.08	103.03	79.89
1100.	398.96	104.41	90.27
1200.	408.10	105.52	100.77
1300.	416.58	106.43	111.37
1400.	424.50	107.20	122.05
1500.	431.92	107.86	132.80
1600.	438.90	108.44	143.62
1800.	451.73	109.42	165.41
2000.	463.31	110.23	187.37

References for dihydroxyethenylidene.

AS78 Y. Apeloig and R. Schreiber, "Theoretical *ab initio* investigation of substituted alkylidene carbenes," Tetrahedron Lett. **19**, 4555–4558 (1978).

KHR17 S. J. Klippenstein, L. B. Harding, and B. Ruscic, "*Ab initio* computations and active thermochemical tables hand in hand: Heats of formation of core combustion species," J. Phys. Chem. A **121**(35), 6580–6602 (2017).

3.19.3. 1,2-Dioxetan-3-ylidene

$^1A'$ g = 1 C_S σ = 1 M_0 = 58.0367

An intermediate postulated during a study of the reactions of the electronically excited vinylidene radicals with molecular oxygen [FL87],

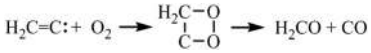

although no actual structure was discerned. The triplet state lies well above, ≥ 200 kJ mol^{-1}, the singlet ground state.

3.19.3.1 Species data.

6	0.463 818	0.977 981	0.000 291
8	1.003 568	−0.174 515	−0.000 102
8	−0.308 439	−0.989 596	0.000 078
6	−0.895 105	0.382 937	−0.000 001
1	−1.487 829	0.573 501	0.895 838
1	−1.485 478	0.573 879	−0.897 388
B (GHz)	16.300	13.885	7.876 7

No.	$\bar{\upsilon}$ (cm^{-1})	x_{ii}		No.	$\bar{\upsilon}$ (cm^{-1})	x_{ii}	
1	3054.51	−28.01	a'	7	886.35	−6.86	a'
2	1437.96	−1.33	a'	8	473.42	−48.76	a'
3	1334.17	−17.61	a'	9	3108.92	−32.77	a''
4	1300.46	−7.31	a'	10	1102.76	−2.41	a''
5	1023.84	−3.98	a'	11	867.86	−1.94	a''
6	928.18	−2.68	a'	12	337.54	3.35	a''

3.19.3.2 Formation enthalpy, $\Delta_f H$(0 K). A multi-composite approach yields $\Delta_f H^\circ$(0 K) = 260.9 ± 3.0 kJ mol^{-1} in agreement with W3X-L $\Delta_f H^\circ$(0 K) = 258.3 kJ mol^{-1} (251.7 kJ mol^{-1} at 298.15 K) for this singlet species whose T_1 is 0.031.

3.19.3.3 Results. A standard RR anharmonic treatment is indicated.

T (K)	$S^\circ(T)$	$C_p^\circ(T)$	$H^\circ(T) - H^\circ(0)$
298.15	267.75	58.94	12.66
300.	268.12	59.16	12.77
400.	286.69	70.07	19.25
500.	303.29	78.64	26.71
600.	318.24	85.33	34.92
700.	331.81	90.68	43.73
800.	344.22	95.09	53.02
900.	355.64	98.79	62.72
1000.	366.22	101.93	72.76
1100.	376.06	104.62	83.09
1200.	385.27	106.95	93.67
1300.	393.91	108.96	104.47
1400.	402.05	110.71	115.46
1500.	409.74	112.25	126.61
1600.	417.03	113.60	137.90
1800.	430.55	115.85	160.85
2000.	442.85	117.66	184.21

References for 1,2-dioxetan-3-ylidene.

FL87 A. Fahr and A. H. Laufer, "The reactions of electronically excited vinylidene radicals with molecular oxygen," J. Am. Chem. Soc. **109**(13), 3843–3846 (1987).

3.19.4. 1,3-Dioxetane-2,4-diyl

$^1A'$ g = 1 C_S σ = 1 M_0 = 58.0367

In agreement with both Kakkar *et al.* [KCR03] and Vijay and Sastry [VS05], we find that the singlet is more stable than the triplet. The latter reported C_{2h} symmetries at B3LYP and MP2 with a cc-pVTZ basis set as well as at B3LYP/6-31G*. Our computations do not agree for B3LYP/cc-pVTZ, which we do not find is a stationary point. At B3LYP/cc-pVTZ + d, our default functional/basis set combination, we find a similar C···C interatomic distance of 1.896 Å as against their 1.883 Å, the C–O bond lengths differ considerably 1.312 Å and 1.439 Å *versus* 1.364 Å required of C_{2h} symmetry as indeed do the H–C···C angles of 156.7° and 124.4° as against the expected 139.7° of a C_{2h} structure. A T_1 diagnostic of 0.030 is indicative of some multi-reference character.

3.19.4.1 Species data.

8	−0.004 890	0.030 278	0.993 584
6	−0.004 890	0.886 851	0.000 000
6	0.086 030	−1.006 595	0.000 000
8	−0.004 890	0.030 278	−0.993 584
1	0.374 186	1.897 818	0.000 000
1	−0.782 795	−1.663 799	0.000 000
B (GHz)	17.492 8	15.600 8	8.471 3

No.	$\bar{\upsilon}$ (cm^{-1})	x_{ii}		No.	$\bar{\upsilon}$ (cm^{-1})	x_{ii}	
1	3221.29	−60.35	a'	7	672.35	−5.60	a'
2	3094.87	−73.74	a'	8	187.07	−123.67	a'
3	1348.52	−13.79	a'	9	1445.10	−43.19	a''
4	1121.63	−5.70	a'	10	1207.01	−1.75	a''
5	1077.43	−5.30	a'	11	1128.51	−2.30	a''
6	840.00	−27.78	a'	12	847.29	−109.22	a''

3.19.4.2 Formation enthalpy, $\Delta_f H(0\ K)$. W2X and W3X-L atomization calculations return values of $\Delta_f H^o(0\ K) = 58.2$ kJ mol^{-1} and 57.3 kJ mol^{-1}, respectively. At 298.15 K, these translate to 51.3 kJ mol^{-1} and 50.6 kJ mol^{-1}.

From a direct comparison at multiple composite methods,

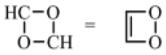

the reaction enthalpy is 84.4 ± 4.7 kJ mol^{-1} so that a value of $\Delta_f H^o(0\ K) = 55.0 \pm 5.0$ kJ mol^{-1} ensues based on 139.4 ± 1.7 kJ mol^{-1} for 1,2-dioxete. The 10% scatter in reaction enthalpies is unusual and probably is due to the differences in multi-reference character between the dioxetane and the more normal dioxete whose T_1 is less than 0.02.

3.19.4.3 Results. Literature values of 266.6 J mol^{-1} K^{-1} and 53.25 J mol^{-1} K^{-1} for the entropy and for the specific heat at constant pressure have been reported [KCR03], which are in moderate agreement with those found here, which are based on an RRHO treatment, given the highly anharmonic vibrational modes.

T (K)	$S^o(T)$	$C_p^o(T)$	$H^o(T) - H^o(0)$
298.15	267.10	55.14	12.43
300.	267.44	55.37	12.53
400.	285.07	67.66	18.69
500.	301.35	78.26	26.01
600.	316.40	86.71	34.27
700.	330.29	93.39	43.29
800.	343.12	98.75	52.90
900.	355.02	103.14	63.01
1000.	366.08	106.79	73.51
1100.	376.41	109.86	84.34
1200.	386.08	112.46	95.46
1300.	395.17	114.68	106.82
1400.	403.74	116.58	118.39
1500.	411.85	118.22	130.13
1600.	419.52	119.65	142.03
1800.	433.76	121.98	166.20
2000.	446.71	123.77	190.78

References for 1,3-dioxetane-2,4-diyl.

KCR03 R. Kakkar, P. Chadha, and P. Rajni, "Density functional (DFT) study of acyloxy carbene-carbene rearrangements," J. Mol. Struct.: THEOCHEM **626**, 187–194 (2003).

VS05 D. Vijay and G. N. Sastry, "Relative energies of $C_2O_2H_2$ isomers and their ionized counterparts: Possibility of bond stretch isomerism," J. Mol. Struct.: THEOCHEM **714**, 199–207 (2005).

3.19.5. 2,4-Dioxabicyclo[1.1.0]butane

$^1A_1$ g = 1 C_{2v} σ = 2 M_0 = 58.0367

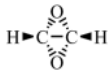

3.19.5.1 Species data.

6	0.000 000	0.675 828	0.336 332
6	0.000 000	−0.675 828	0.336 332
1	0.000 000	1.588 061	0.900 587
1	0.000 000	−1.588 061	0.900 587
8	1.077 271	0.000 000	−0.364 823
8	−1.077 271	0.000 000	−0.364 823
B (GHz)	20.545 7	11.064 2	9.505 0

No.	$\bar{\upsilon}$ (cm^{-1})	x_{ii}	
1	3325.37	−27.23	a_1
2	1597.78	−7.75	a_1
3	991.10	−1.88	a_1
4	751.46	−3.42	a_1
5	701.18	−0.66	a_1
6	1039.67	−1.42	a_2
7	172.77	−171.38	a_2
8	1181.91	−4.60	b_1
9	892.92	−0.39	b_1
10	3288.59	−27.50	b_2
11	931.76	−3.61	b_2
12	698.79	−1.12	b_2

3.19.5.2 Formation enthalpy, $\Delta_f H$(0 K). Vijay and Sastry [VS05] found that this cyclobutane was some 325–335 kJ mol^{-1} less stable than the most stable $C_2H_2O_2$ species, namely, *trans* glyoxal, at MP2/cc-pV5Z and CCSD(T)/cc-pVTZ, respectively, with both assuming a B3LYP/cc-pVTZ geometry. This implies $\Delta_f H^o$(0 K) ~ 103–118 kJ mol^{-1}. An averaged multi-composite atomization calculation returns $\Delta_f H^o$(0 K) = 105.1 ± 3.8 kJ mol^{-1} (98.9 kJ mol^{-1} at 298.15 K).

The isodesmic reaction, employing the chaperones propane (−82.74 ± 0.19 kJ mol^{-1}) and dimethyl ether (−166.50 ± 0.44 kJ mol^{-1}), both of which are ATcT references, has an enthalpy of −34.68 ± 1.16 kJ mol^{-1},

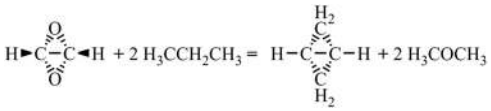

This allied to the Wiberg and Fenoglio [WF68] 1968 calorimetric measurement of 217.1 ± 0.8 kJ mol^{-1} at 298.15 K (which extrapolates to 234.2 kJ mol^{-1} at 0 K) for bicyclo[1.1.0]butane suggests $\Delta_f H^o$(0 K) = 101.3 ± 1.0 kJ mol^{-1}, which is just in agreement, if somewhat on the low side.

Indeed, direct high-level methods such as WMS/W2X/W3X-L predict $\Delta_f H^o$(0 K) = 242.3 kJ mol^{-1}/238.6 kJ mol^{-1}/240.8 kJ mol^{-1} for bicyclo[1.1.0]butane and $\Delta_f H^o$(0 K) = 106.8 kJ mol^{-1}/105.8 kJ mol^{-1}/106.2 kJ mol^{-1} for 2,4-dioxabicyclo[1.1.0]butane. It is probably the case that a modest revision of the bicyclo[1.1.0]butane value would bring all the results for 2,4-dioxabicyclo[1.1.0]butane into alignment. Very recent work suggests that such a revision is overdue for bicyclo [1.1.0]butane with Bakowies [B20] arguing from ATOMIC(hc) calculations for $\Delta_f H^o$(298.15 K) = 225.9 kJ mol^{-1}, which implies $\Delta_f H^o$(0 K) = 243.0 kJ mol^{-1}; this is now more in accord with our direct atomization calculations.

Here, we adopt our W3X-L value for bicyclobutane of 240.8 kJ mol^{-1} and incorporate it into the isodesmic calculation to yield $\Delta_f H^o$(0 K) = 107.9 kJ mol^{-1} (101.7 kJ mol^{-1} at 298.15 K), which now agrees with the direct W3X-L of 106.2 kJ mol^{-1}.

3.19.5.3 Results. The lowest frequency vibration no. 7, which can be described as a C–C bond rocking puckering mode, is highly anharmonic. Hence, the results are based exclusively on a harmonic oscillator basis.

T (K)	$S^o(T)$	$C_p^o(T)$	$H^o(T) - H^o(0)$
298.15	264.01	59.76	12.90
300.	264.38	60.02	13.01
400.	283.48	72.97	19.68
500.	300.90	83.10	27.51
600.	316.76	90.76	36.22
700.	331.22	96.65	45.60
800.	344.44	101.34	55.51
900.	356.60	105.18	65.84
1000.	367.86	108.39	76.52
1100.	378.32	111.11	87.50
1200.	388.09	113.44	98.72
1300.	397.25	115.46	110.17
1400.	405.87	117.20	121.81
1500.	414.01	118.72	133.60
1600.	421.72	120.05	145.54
1800.	435.99	122.24	169.78
2000.	448.96	123.95	194.40

References for 2,4-dioxabicyclo[1.1.0]butane.

VS05 D. Vijay and G. N. Sastry, "Relative energies of $C_2O_2H_2$ isomers and their ionized counterparts: Possibility of bond stretch isomerism," J. Mol. Struct.: THEOCHEM **714**, 199–207 (2005).

WF68 K. B. Wiberg and R. A. Fenoglio, "Heats of formation of C_4H_6 hydrocarbons," J. Am. Chem. Soc. **90**, 3395–3397 (1968).

B20 D. Bakowies, "Estimating systematic error and uncertainty in *ab initio* thermochemistry: II. ATOMIC(hc) enthalpies of formation for a large set of hydrocarbons," J. Chem. Theory Comput. **16**, 399–426 (2020).

3.19.6. 1,2-Dioxete

$^1A_1$ g = 1 C_{2v} σ = 2 M_0 = 58.0367

Also known as *dioxetene*, it has been implicated as an intermediate in the oxidation of acetylenes [TH78].

3.19.6.1 Species data.

6	0.000 000	0.663 605	0.704 664
8	0.000 000	0.732 619	−0.695 124
8	0.000 000	−0.732 619	−0.695 124
6	0.000 000	−0.663 605	0.704 664
1	0.000 000	1.533 172	1.333 008
1	0.000 000	−1.533 172	1.333 008
B (GHz)	16.389 089	15.561 22	7.982 22

No.	$\bar{\upsilon}$ (cm^{-1})	x_{ii}	
1	3319.21	−25.60	a_1
2	1648.82	−7.21	a_1
3	1221.86	−3.13	a_1
4	1071.71	−0.89	a_1
5	878.06	−3.33	a_1
6	707.26	4.19	a_2
7	601.19	−0.76	a_2
8	691.47	0.22	b_1
9	3283.72	−26.09	b_2
10	1253.07	−2.64	b_2
11	1005.56	−1.54	b_2
12	893.16	0.18	b_2

3.19.6.2 Formation enthalpy, $\Delta_f H$(0 K). WMS and W2X atomization calculations return values of $\Delta_f H^o$(0 K) = 137.6 kJ mol^{-1} and 140.5 kJ mol^{-1}, respectively.

An approximate value based on the isodesmic reaction

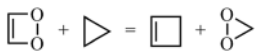

for which a reaction enthalpy at 0 K of −25.29 ± 1.22 kJ mol^{-1} can be calculated from the unweighted average of CBS-QB3, CBS-APNO, G3, G4, and W1BD computations, together with well-established values [RB16] for the companion species (cyclopropane (70.77 ± 0.47 kJ mol^{-1}), cyclobutene (176.79 ± 0.93 kJ mol^{-1}), and dioxirane (9.45 ± 0.55 kJ mol^{-1}), yields $\Delta_f H^o$(0 K) = 140.7 ± 1.7 kJ mol^{-1} (132.9 kJ mol^{-1} at 298.15 K). The W3X-L results of $\Delta_f H^o$(0 K) = 139.4 kJ mol^{-1} (131.6 kJ mol^{-1} at 298.15 K) thus neatly encapsulate all the data.

3.19.6.3 Results. There is good agreement with calculations from the semi-empirical molecular orbital method PM3 by the Bozzelli group [LYTB97] for entropy, S^o = 256.7 J K^{-1} mol^{-1}, and specific heat, C_p^o = 53.60 J K^{-1} mol^{-1}, but not for the 298.15 K formation enthalpy for which they reported 104.9 kJ mol^{-1}.

T (K)	$S^o(T)$	$C_p^o(T)$	$H^o(T) - H^o(0)$
298.15	254.90	53.42	11.47
300.	255.24	53.69	11.57
400.	272.59	67.25	17.64
500.	288.83	78.24	24.94
600.	303.88	86.73	33.20
700.	317.77	93.34	42.22
800.	330.59	98.63	51.83
900.	342.47	102.95	61.91
1000.	353.51	106.56	72.39
1100.	363.81	109.61	83.21
1200.	373.47	112.22	94.30
1300.	382.54	114.46	105.64
1400.	391.10	116.40	117.18
1500.	399.19	118.08	128.91
1600.	406.86	119.56	140.79
1800.	421.09	121.99	164.96
2000.	434.04	123.90	189.56

References for 1,2-dioxete.

TH78 C. Trindle and E. A. Halevi, "Spin-forbidden reaction pathways in the interaction of singlet and triplet molecular oxygen with acetylene," Int. J. Quantum Chem. **14**, 281–290 (1978).

RB16 B. Ruscic and D. H. Bross, Active Thermochemical Tables (ATcT) values based on version 1.122 of the Thermochemical Network, 2016, available at https://ATcT.anl.gov.

LYTB97 T. H. Lay, T. Yamada, P.-L. Tsai, and J. W. Bozzelli, "Thermodynamic parameters and group additivity ring corrections for three- to six-membered oxygen heterocyclic hydrocarbons," J. Phys. Chem. A **101**(13), 2471–2477 (1997).

3.19.7. 1,2-Ethynediol; dihydroxyacetylene

^{1}A g = 1 C_2 σ = 2 M_0 = 58.0367

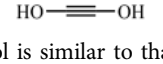

Structurally, this diol is similar to that studied by Lewars and Bonnycastle in MNDO and MP2 calculations [LB97].

3.19.7.1 Species data.

6	−0.051 790	0.595 031	0.002 431
6	0.051 790	−0.595 031	0.002 431
8	0.051 790	−1.913 556	−0.068 779
1	0.712 285	−2.273 410	0.535 645
8	−0.051 790	1.913 556	−0.068 779
1	−0.712 285	2.273 410	0.535 645
B (GHz)	336.320	3.685 1	3.682 9

No.	$\bar{\upsilon}$ (cm^{-1})	x_{ii}	
1	3758.34	−46.32	*a*
2	2457.71	−9.32	*a*
3	1272.52	−6.75	*a*
4	812.79	−1.45	*a*
5	381.94	2.41	*a*
6	327.30	−17.72	*a*
7	243.03	−0.92	*a*
8	3757.39	−45.63	*b*
9	1382.72	−1.42	*b*
10	1231.32	−5.50	*b*
11	374.90	3.55	*b*
12	240.82	−0.77	*b*

3.19.7.2 Formation enthalpy, $\Delta_f H$(0 K). The isodesmic reaction

HOC ≡ COH + HC ≡ CH = HOC ≡ CH + HC ≡ COH

has a reaction enthalpy at 0 K of −19.64 ± 1.01 kJ mol^{-1} based on the averaged series of CBS-QB3, CBS-APNO, G3, G4, and W1BD calculations.

Together with known values [RB16] for the chaperones, ethyne of 228.84 ± 0.14 kJ mol^{-1} and 94.9 ± 1.3 kJ mol^{-1} for ethynol, the resultant $\Delta_f H^o$(0 K) is −19.4 ± 2.1 kJ mol^{-1} (−22.8 kJ mol^{-1} at 298.15 K). The former is in excellent agreement with an ANL0 value [KHR17] of −19.3 kJ mol^{-1}, and the latter is in good agreement with the −21.3 ± 3.8 kJ mol^{-1} computed by Goldsmith *et al.* [GMG12]

3.19.7.3 Results. A relaxed potential energy about the C–C–O–H dihedral is problematic, simply because of the linearity of the C–C–O portion. A scan effectively bypassing the C≡C bond is well behaved, however, with a barrier of ca. 8.1 kJ mol^{-1}. This potential has been used to replace a vibrational mode (no. 6).

There is good to moderate agreement with the literature data [GMG12], for example, S^o(298.15 K) = 282.0 ± 3.8 J mol^{-1} K^{-1} and C_p^o (300 K) = 72.4 ± 2.1 J mol^{-1} K^{-1}.

T (K)	$S^o(T)$	$C_p^o(T)$	$H^o(T) - H^o(0)$
298.15	282.55	72.39	15.83
300.	282.99	72.54	15.96
400.	304.84	79.41	23.57
500.	323.18	85.02	31.80
600.	339.11	89.69	40.54
700.	353.24	93.67	49.71
800.	365.98	97.13	59.25
900.	377.60	100.20	69.12
1000.	388.30	102.96	79.28
1100.	398.23	105.44	89.70
1200.	407.51	107.68	100.36
1300.	416.21	109.71	111.23
1400.	424.40	111.54	122.29
1500.	432.16	113.20	133.53
1600.	439.51	114.71	144.93
1800.	453.18	117.34	168.14
2000.	465.66	119.57	191.83

References for 1,2-ethynediol; dihydroxyacetylene.

LB97 E. Lewars and I. Bonnycastle, "The effect of substituents on the thermodynamic and kinetic stabilities of alkynols: A semiempirical and *ab initio* survey of the effect of H, Li, BeH, BH_2, CH_3, NH_2, OH and F," J. Mol. Struct.: THEOCHEM **418**(1), 17–33 (1997).

RB16 B. Ruscic and D. H. Bross, Active Thermochemical Tables (ATcT) values based on version 1.122 of the Thermochemical Network, 2016, available at https://ATcT.anl.gov.

KHR17 S. J. Klippenstein, L. B. Harding, and B. Ruscic, "*Ab initio* computations and active thermochemical tables hand in hand: Heats of formation of core combustion species," J. Phys. Chem. A **121**(35), 6580–6602 (2017).

GMG12 C. F. Goldsmith, G. R. Magoon, and W. H. Green, "Database of small molecule thermochemistry for combustion," J. Phys. Chem. A **116**(36), 9033–9057 (2012).

3.19.8. Ethynylhydroperoxide

^{1}A g = 1 C_1 σ = 1 M_0 = 58.0367

Alkyl hydroperoxides and peroxy radicals, in general, are important intermediates in atmospheric chemistry and in combustion processes at low temperatures [SBCH08].

3.19.8.1 Species data.

6	−1.823 843	−0.240 959	0.015 284
6	−0.689 145	0.150 326	0.001 000
1	−2.829 304	−0.575 675	0.019 304
8	0.502 157	0.649 058	−0.010 726
8	1.497 957	−0.463 120	−0.100 579
1	1.906 317	−0.368 023	0.773 431
B (GHz)	41.018 3	5.156 02	4.641 79

No.	$\bar{\upsilon}$ (cm^{-1})	x_{ii}
1	3740.57	−81.18
2	3484.02	−50.67
3	2214.65	−8.27
4	1343.30	−11.19
5	1067.78	−4.90
6	778.53	−7.82
7	699.29	−1.83
8	570.60	−0.20
9	514.51	−0.08
10	421.12	1.58
11	229.61	0.30
12	155.31	−3.29

3.19.8.2 Formation enthalpy, $\Delta_f H(0\ K)$. The isodesmic reaction

$$HC \equiv COOH + H_3CCH_3 = HC \equiv C - CH_3 + CH_3OOH$$

has a reaction enthalpy of −49.69 ± 0.67 kJ mol^{-1}, which together with reference values [RB16] for the chaperones ethane (−68.29 ± 0.14 kJ mol^{-1}), propyne (192.80 ± 0.25 kJ mol^{-1}), and methyl hydroperoxide (−114.90 ± 0.74 kJ mol^{-1}) leads to $\Delta_f H^o(0\ K)$ = 195.9 ± 1.0 kJ mol^{-1} (191.6 kJ mol^{-1} at 298.15 K), which is in close agreement with an atomization result, over the same set of composite methods, of 196.1 ± 3.0 kJ mol^{-1} and of a WMS of 194.8 kJ mol^{-1}.

Vijay and Sastry [VS05] reported that this species lies 412 kJ mol^{-1} above *trans* glyoxal, which implies a formation enthalpy of ~205 kJ mol^{-1}. Sebbar *et al.* [SBB04] reported $\Delta_f H^o(0\ K)$ = 172.84 ± 3.01 kJ mol^{-1} at 298.15 K from a number of isodesmic reactions with reaction enthalpies determined at a B3LYP/6-311G(d,p) level of theory. Earlier [SBB04], they found 176.8 ± 0.54 kJ mol^{-1} from a similar procedure.

3.19.8.3 Results. Our computed entropy differs considerably from the literature [SBB02] value of 267.7 J mol^{-1} K^{-1} as does a C_p^o(300 K) of 57.8 J mol^{-1} K^{-1}.

T (K)	$S^o(T)$	$C_p^o(T)$	$H^o(T) - H^o(0)$
298.15	291.61	70.97	15.13
300.	292.05	71.18	15.26
400.	313.93	80.78	22.88
500.	332.73	87.63	31.32
600.	349.18	92.77	40.35
700.	363.79	96.86	49.84
800.	376.96	100.30	59.70
900.	388.95	103.27	69.88
1000.	399.97	105.89	80.34
1100.	410.17	108.22	91.05
1200.	419.68	110.30	101.97
1300.	428.58	112.16	113.10
1400.	436.95	113.83	124.40
1500.	444.86	115.33	135.85
1600.	452.35	116.68	147.45
1800.	466.23	119.00	171.03
2000.	478.87	120.92	195.02

References for ethynylhydroperoxide.

SBCH08 J. M. Simmie, G. Black, H. J. Curran, and J. P. Hinde, "Enthalpies of formation and bond dissociation energies of lower alkyl hydroperoxides and related hydroperoxy and alkoxy radicals," J. Phys. Chem. A **112**(22), 5010–5016 (2008).

RB16 B. Ruscic and D. H. Bross, Active Thermochemical Tables (ATcT) values based on version 1.122 of the Thermochemical Network, 2016, available at https://ATcT.anl.gov.

VS05 D. Vijay and G. N. Sastry, "Relative energies of $C_2O_2H_2$ isomers and their ionized counterparts: Possibility of bond stretch isomerism," J. Mol. Struct.: THEOCHEM **714**, 199–207 (2005).

SBB04 N. Sebbar, J. W. Bozzelli, and H. Bockhorn, "Thermochemical properties, rotation barriers, bond energies, and group additivity for vinyl, phenyl, ethynyl, and allyl peroxides," J. Phys. Chem. A **108**, 8353–8366 (2004).

SBB02 N. Sebbar, H. Bockhorn, and J. W. Bozzelli, "Structures, thermochemical properties (enthalpy, entropy and heat capacity), rotation barriers, and peroxide bond energies of vinyl, allyl, ethynyl and phenyl hydroperoxides," Phys. Chem. Chem. Phys. **4**, 3691–3703 (2002).

3.19.9. Formyloxy methylene

$^1A'$ g = 1 C_S σ = 1 M_0 = 58.0367

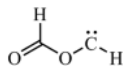

This species appeared in a study of acyloxy carbene to carbene rearrangements [KCR03]. The singlet *anti/anti* ground state lies well below the triplet; other singlet conformers include *as*, *ss*, and *ga* at +18.3 kJ mol^{-1}, +21.5 kJ mol^{-1}, and +20.5 kJ mol^{-1}, respectively, at the G4 level.

3.19.9.1 Species data.

6	1.095 251	−1.316 726	0.000 000
8	−0.076 021	−0.725 011	0.000 000
8	−0.980 042	1.355 838	0.000 000
6	0.000 000	0.705 748	0.000 000
1	1.054 536	1.010 857	0.000 000
1	0.822 464	−2.391 606	0.000 000
B (GHz)	62.342	5.328 6	4.909 0

No.	$\bar{\upsilon}$ (cm^{-1})	x_{ii}	
1	3037.75	−62.38	a'
2	2897.93	−67.49	a'
3	1902.78	−10.62	a'
4	1405.27	−0.83	a'
5	1332.42	−5.07	a'
6	1282.79	−6.47	a'
7	902.80	−11.06	a'
8	618.77	−2.17	a'
9	407.68	−0.97	a'
10	1055.39	−2.72	a''
11	683.14	−4.58	a''
12	143.90	−2.23	a''

3.19.9.2 Formation enthalpy, $\Delta_f H(0\ K)$. A multi-composite treatment gives, remarkably, for the singlet *aa* $\Delta_f H^o(0\ K) = 2.0 \pm 2.1$ kJ mol^{-1} in line with W3X-L of $\Delta_f H^o(0\ K) = 3.4$ kJ mol^{-1} (−2.3 kJ mol^{-1} at 298.15 K).

3.19.9.3 Results. Vibrational mode nos. 12 and 11 impact on the computed thermochemistry but to a limited extent; a relaxed potential energy scan about the O–carbene dihedral displays a large barrier, in excess of 80 kJ mol^{-1}, and is therefore unlikely to contribute. The scan about O=C–O–C is well-behaved and connects the ground state *aa* to a *ga* conformer (barrier of 25 kJ mol^{-1}) at 22 kJ mol^{-1}.

T (K)	$S^o(T)$	$C_p^o(T)$	$H^o(T) - H^o(0)$
298.15	274.98	61.50	13.54
300.	275.36	61.71	13.65
400.	294.71	73.25	20.40
500.	312.19	83.58	28.26
600.	328.22	92.14	37.06
700.	342.95	98.93	46.62
800.	356.52	104.23	56.79
900.	369.05	108.38	67.43
1000.	380.64	111.67	78.44
1100.	391.42	114.32	89.74
1200.	401.46	116.51	101.28
1300.	410.86	118.34	113.03
1400.	419.69	119.90	124.94
1500.	428.01	121.26	137.00
1600.	435.87	122.45	149.18
1800.	450.41	124.46	173.88
2000.	463.62	126.12	198.94

References for formyloxy methylene.

KCR03 R. Kakkar, P. Chadha, and P. Rajni, "Density functional (DFT) study of acyloxy carbene–carbene rearrangements," J. Mol. Struct.: THEOCHEM **626**(1), 187–194 (2003).

3.19.10. Glyoxal trans

^1A_g g = 1 C_{2h} σ = 2 M_0 = 58.0367

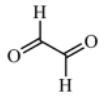

Glyoxal, the smallest dicarbonyl compound, is produced in the atmosphere from the oxidation of many volatile organic compounds in substantial quantities and is implicated in the formation of secondary organic aerosols [FJWB08]. The *trans* conformer of glyoxal or ethanedial is more stable than the *cis* conformer, $\Delta\{\Delta_f H(298.15\ K)\} > 18$ kJ mol^{-1}, and can, therefore, be considered as existing purely as the *trans* form in any experiments conducted at room temperature. A comprehensive test of rotational potentials, all at the same basis set, benchmarked against CCSD(T) shows that B3LYP performs satisfactorily at least as CHO species, and specifically glyoxal, are concerned [TBRL18].

3.19.10.1 Species data.

8	0.648 536	1.600 954	0.000 000
6	0.648 536	0.399 437	0.000 000
1	1.568 648	−0.214 185	0.000 000
6	−0.648 536	−0.399 437	0.000 000
1	−1.568 648	0.214 185	0.000 000
8	−0.648 536	−1.600 954	0.000 000
B (GHz)	56.242 9	4.793 4	4.416 7

No.	$\bar{\upsilon}$ (cm^{-1})	x_{ii}	
1	2935.67	−33.07	a_g
2	1804.00	−5.30	a_g
3	1380.45	−6.12	a_g
4	1065.03	−5.75	a_g
5	552.54	1.17	a_g
6	815.98	−2.26	a_u
7	132.28	−0.56	a_u
8	1081.79	−1.47	b_g
9	2930.74	−33.17	b_u
10	1802.20	−5.56	b_u
11	1337.55	−4.45	b_u
12	337.13	1.37	b_u

3.19.10.2 Formation enthalpy, $\Delta_f H(0\ K)$. Fletcher and Pilcher [FP70] determined −212.0 ± 0.79 kJ mol^{-1} by flame calorimetry at 298.15 K; this is therefore non-specific as it is an

equilibrium mixture of both conformers, but as shown above, this value effectively pertains solely to the *trans* or *anti* conformer. Glyoxal readily polymerizes (even more so than formaldehyde), and this can cause serious practical difficulties in both preparing pure samples and storing them prior to use.

A high-level W4 total atomization energy [KDM11] of 2556 kJ mol^{-1} translates to $\Delta_f H^o$(0 K) = −207.7 kJ mol^{-1}, which is in good agreement with our W3X-L of −208.8 kJ mol^{-1} (−212.6 kJ mol^{-1} at 298.15 K) and indeed with an ANL0 [KHR17] of −207.9 kJ mol^{-1}; the ATcT database concurs at −206.91 ± 0.52 kJ mol^{-1} (−212.55 kJ mol^{-1} at 298.15 K).

3.19.10.3 Results. A purely vibrational mode treatment neglecting anharmonicities and hindered rotors gives excellent agreement with the data in the Burcal database [GBR18], which has S^o = 272.5 J mol^{-1} K^{-1}, C_p^o = 60.41 J mol^{-1} K^{-1}, and $H^o(T) - H^o(0)$ = 13.68 kJ mol^{-1}. Thermodynamic Research Center recommendations [TRC97] have C_p^o = 60.23 J mol^{-1} K^{-1} at 298.15 K and Goldsmith *et al.* [GMG12] reported S^o = 270.3 ± 3.8 J mol^{-1} K^{-1} and C_p^o (300 K) = 60.7 ± 3.3 J mol^{-1} K^{-1}. Our treatment includes both vibrational anharmonicities and a hindered rotor treatment for mode no. 7, which has little impact below 600 K.

T (K)	$S^o(T)$	$C_p^o(T)$	$H^o(T) - H^o(0)$
298.15	271.61	59.78	13.58
300.	271.98	59.97	13.70
400.	290.67	70.50	20.22
500.	307.49	80.42	27.77
600.	322.92	88.84	36.25
700.	337.15	95.61	45.48
800.	350.28	100.95	55.32
900.	362.42	105.15	65.63
1000.	373.68	108.50	76.32
1100.	384.15	111.21	87.31
1200.	393.92	113.43	98.55
1300.	403.08	115.28	109.98
1400.	411.68	116.84	121.59
1500.	419.79	118.16	133.34
1600.	427.45	119.31	145.21
1800.	441.62	121.16	169.27
2000.	454.46	122.60	193.65

References for glyoxal *trans*.

FJWB08 T.-M. Fu, D. J. Jacob, F. Wittrock, J. P. Burrows, M. Vrekoussis, and D. K. Henze, "Global budgets of atmospheric glyoxal and methylglyoxal, and implications for formation of secondary organic aerosols," J. Geophys. Res.: Atmos. **113**, D15303 (2008).

TBRL18 D. N. Tahchieva, D. Bakowies, R. Ramakrishnan, and O. A. von Lilienfeld, "Torsional potentials of glyoxal, oxalyl halides, and their thiocarbonyl derivatives: Challenges for popular density functional approximations," J. Chem. Theory Comput. **14**(9), 4806–4817 (2018).

FP70 R. A. Fletcher and G. Pilcher, "Measurements of heats of combustion by flame calorimetry," Trans. Faraday Soc. **66**, 794–799 (1970).

KDM11 A. Karton, S. Daon, and J. M. L. Martin, "W4-11: A high-confidence benchmark dataset for computational thermochemistry derived from first-principles W4 data," Chem. Phys. Lett. **510**, 165–178 (2011).

KHR17 S. J. Klippenstein, L. B. Harding, and B. Ruscic, "*Ab initio* computations and active thermochemical tables hand in hand: Heats of formation of core combustion species," J. Phys. Chem. A **121**(35), 6580–6602 (2017).

GBR18 A. Goos, A. Burcat, and B. Ruscic, "Extended third Millennium ideal gas and condensed phase thermochemical database for combustion with updates from active thermochemical tables," Mirrored at http://garfield.chem.elte.hu/Burcat/burcat.html; 12 January 2018.

TRC97 Thermodynamics Research Center, *Selected Values of Properties of Chemical Compounds* (Thermodynamics Research Center, Texas A&M University, College Station, Texas, 1997).

GMG12 C. F. Goldsmith, G. R. Magoon, and W. H. Green, "Database of small molecule thermochemistry for combustion," J. Phys. Chem. A **116**, 9033–9057 (2012).

3.19.11. *Glyoxal* cis

$^1A_1$ g = 1 C_{2v} σ = 2 M_0 = 58.0367

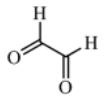

The *cis* conformer of glyoxal or ethanedial is less stable than the *trans* conformer, $\Delta\{\Delta_f H(298.15\ K)\}$ by ≈ 18 kJ mol^{-1}, and glyoxal can therefore be considered as existing purely as the *anti* form in any experiments conducted at room temperature.

3.19.11.1 Species data.

8	0.000 000	1.420 666	−0.536 414
6	0.000 000	0.770 897	0.468 950
1	0.000 000	1.233 910	1.477 612
6	0.000 000	−0.770 897	0.468 950
1	0.000 000	−1.233 910	1.477 612
8	0.000 000	−1.420 666	−0.536 414
B (GHz)	26.973 9	6.171 0	5.022 0

No.	$\bar{\upsilon}$ (cm^{-1})	x_{ii}	
1	2899.19	−31.22	a_1
2	1796.81	−5.84	a_1
3	1394.66	0.20	a_1
4	813.21	−10.29	a_1
5	281.20	0.74	a_1
6	1084.83	−1.54	a_2
7	96.07	2.78	a_2
8	735.57	2.21	b_1
9	2863.37	−33.39	b_2
10	1840.59	−5.17	b_2
11	1393.08	0.67	b_2
12	824.73	−0.20	b_2

3.19.11.2 Formation enthalpy, $\Delta_f H(0\ K)$. A W3X-L atomization calculation gives $\Delta_f H^o(0\ K) = -191.3$ kJ mol^{-1} with a corresponding value at 298.15 K of −196.9 kJ mol^{-1}.

3.19.11.3 Results. There are no reported data for this *cis* conformer.

T (K)	$S^o(T)$	$C_p^o(T)$	$H^o(T) - H^o(0)$
298.15	273.45	59.95	13.64
300.	273.82	60.15	13.75
400.	292.59	70.86	20.30
500.	309.50	80.85	27.89
600.	325.02	89.32	36.41
700.	339.32	96.11	45.70
800.	352.51	101.45	55.59
900.	364.72	105.66	65.95
1000.	376.03	109.01	76.69
1100.	386.55	111.72	87.73
1200.	396.37	113.94	99.01
1300.	405.56	115.80	110.50
1400.	414.20	117.36	122.16
1500.	422.35	118.71	133.96
1600.	430.05	119.88	145.89
1800.	444.28	121.81	170.07
2000.	457.20	123.35	194.59

3.19.12. Hydroxyethenone

^{1}A g = 1 C_1 σ = 1 M_0 = 58.0367

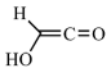

Hydroxyketene is intimately involved in the reactions of the ketenyl radical, HĊ=C=O, which itself is a critical intermediate in the oxidation of all C_2 hydrocarbons [XYLL14].

3.19.12.1 Species data.

1	−0.742 095	1.593 950	0.003 949
6	−0.545 847	0.530 375	0.011 073
6	0.704 490	0.113 329	0.010 283
8	1.813 451	−0.236 651	0.003 072
8	−1.591 341	−0.380 805	−0.113 860
1	−1.986 646	−0.516 530	0.754 215
B (GHz)	49.036	4.688 0	4.333 0

No.	$\bar{\nu}$ (cm^{-1})	x_{ii}
1	3771.21	−92.30
2	3172.98	−60.75
3	2205.27	−11.22
4	1429.86	−9.91
5	1269.36	−7.90
6	1176.87	−3.11
7	1032.31	−3.16
8	689.73	−2.89
9	583.52	−2.54
10	515.33	0.96
11	280.81	−8.47
12	218.57	0.75

3.19.12.2 Formation enthalpy, $\Delta_f H(0\ K)$. An averaged reaction enthalpy of −23.12 ± 0.91 kJ mol^{-1} for the reaction

$$O=C=CH(OH) + CH_4 \rightarrow O=C=CH_2 + CH_3OH$$

in conjunction with reference values [RB16] for methane (−66.550 ± 0.057 kJ mol^{-1}), ketene (−45.45 ± 0.13 kJ mol^{-1}), and methanol (−189.83 ± 0.16 kJ mol^{-1}) yields $\Delta_f H^o(0\ K) = -145.6 \pm 1.0$ kJ mol^{-1} and a corresponding −150.6 kJ mol^{-1} at 298.15 K; the latter is in agreement with the literature [RB16, SG02] value of −151.5 ± 3.8 kJ mol^{-1}. The former agrees with CCSD(T)/CBS calculations [XYLL14] by Xiong *et al.*, which can be interpreted to give $\Delta_f H^o(0\ K) = -143.8$ kJ mol^{-1} and with an ANL0 result [KHR17] of −145.3 kJ mol^{-1}.

3.19.12.3 Results. Hindered rotor analysis identifies mode no. 11 with a reduced barrier height (V/RT) = 6.7 at 300 K as leading to a correction of +0.9 J mol^{-1} K^{-1} to the "harmonic" entropy; the correction diminishes to <0.1 J mol^{-1} K^{-1} at 2000 K. The internal rotation about the CCOH dihedral interconverts between the two "optical isomers" as considered by MultiWell. The inclusion of anharmonicity makes little difference overall, but nevertheless we include a full hindered rotor anharmonic treatment.

Sumathi and Green [SG02] used MP2/6-31G(d′) theory to calculate the thermodynamic properties of this oxygenated ketene within the framework of a rigid-rotor-harmonic-oscillator approximation but with corrections for a hindered rotor. They reported an entropy of 281.6 J mol^{-1} K^{-1} and a C_p^o(300 K) of 64.6 J mol^{-1} K^{-1} in contrast to the small molecule database [GMG12], which has S^o (298.15 K) = 278.7 ± 4.2 J mol^{-1} K^{-1} and C_p^o(300 K) = 66.5 ± 2.9 J mol^{-1} K^{-1}.

T (K)	$S°(T)$	$C°_p(T)$	$H°(T) - H°(0)$
298.15	285.56	66.03	14.25
300.	285.96	66.22	14.37
400.	306.31	75.33	21.46
500.	323.93	82.53	29.37
600.	339.51	88.34	37.92
700.	353.50	93.15	47.00
800.	366.21	97.23	56.52
900.	377.87	100.76	66.43
1000.	388.65	103.83	76.66
1100.	398.67	106.53	87.18
1200.	408.04	108.90	97.95
1300.	416.85	110.99	108.95
1400.	425.14	112.85	120.14
1500.	432.98	114.49	131.51
1600.	440.42	115.95	143.03
1800.	454.23	118.43	166.48
2000.	466.81	120.44	190.37

References for hydroxyethenone.

XYLL14 S.-Z. Xiong, Q. Yao, Z.-R. Li, and X.-Y. Li, "Reaction of ketenyl radical with hydroxyl radical over $C_2H_2O_2$ potential energy surface: A theoretical study," Combust. Flame **161**(4), 885–897 (2014).

RB16 B. Ruscic and D. H. Bross, Active Thermochemical Tables (ATcT) values based on version 1.122 of the Thermochemical Network, 2016, available at https://ATcT.anl.gov.

SG02 R. Sumathi and W. H. Green, "Thermodynamic properties of ketenes: Group additivity values from quantum chemical calculations," J. Phys. Chem. A **106**, 7937–7949 (2002).

KHR17 S. J. Klippenstein, L. B. Harding, and B. Ruscic, "*Ab initio* computations and active thermochemical tables hand in hand: Heats of formation of core combustion species," J. Phys. Chem. A **121**(35), 6580–6602 (2017).

GMG12 C. F. Goldsmith, G. R. Magoon, and W. H. Green, "Database of small molecule thermochemistry for combustion," J. Phys. Chem. A **116**, 9033–9057 (2012).

3.19.13. Methylenedioxirane

^{1}A g = 1 C_{2v} σ = 2 M_0 = 58.0367

Bach and Dimitrenko applied high-level *ab initio* methods to estimate the strain energies of small ring compounds including methylenedioxirane [BD06].

3.19.13.1 Species data.

8	0.000 000	0.773 195	−0.894 125
8	0.000 000	−0.773 195	−0.894 125
6	0.000 000	0.000 000	0.197 146
6	0.000 000	0.000 000	1.506 219
1	0.000 000	0.934 377	2.042 902
1	0.000 000	−0.934 377	2.042 902
B (GHz)	24.199 0	8.231 5	6.142 2

No.	$\bar{\upsilon}$ (cm^{-1})	x_{ii}	
1	3185.70	−25.63	a_1
2	1892.20	−7.03	a_1
3	1428.76	−5.20	a_1
4	1065.70	−1.33	a_1
5	727.50	−1.61	a_1
6	676.94	−4.49	a_2
7	766.76	1.99	b_1
8	526.02	0.61	b_1
9	3282.12	−29.92	b_2
10	1128.09	−1.62	b_2
11	869.96	−7.71	b_2
12	399.12	0.53	b_2

3.19.13.2 Formation enthalpy, $\Delta_f H(0\ K)$. Relative to *trans*-glyoxal, Vijay and Sastry [VS05] placed this isomer at +321 kJ mol^{-1} or $\Delta_f H°(0\ K) \approx 110$ kJ mol^{-1}.

The isodesmic reaction

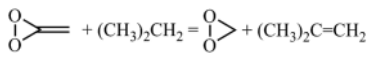

has a 0 K average reaction enthalpy of −15.5 ± 2.3 kJ mol^{-1}, which in conjunction with ATcT values for propane (−82.75 ± 0.19 kJ mol^{-1}), oxirane (9.41 ± 0.54 kJ mol^{-1}), and iso-butene (3.92 ± 0.44 kJ mol^{-1}) chaperones yields $\Delta_f H°(0\ K)$ = 111.6 ± 2.4 kJ mol^{-1} (104.8 kJ mol^{-1} at 298.15 K). The corresponding enthalpy, derived from multi-composite atomization calculations, is 110.3 ± 2.3 kJ mol^{-1}, in very good agreement with a WMS value of 111.2 kJ mol^{-1}.

3.19.13.3 Results. The barrier to rotation about the central C=C bond is very high; thus, it cannot be considered as a hindered rotor but simply as a vibrational mode of 677 cm^{-1}.

T (K)	$S^o(T)$	$C_p^o(T)$	$H^o(T) - H^o(0)$
298.15	261.75	59.58	12.42
300.	262.12	59.84	12.53
400.	281.10	72.23	19.15
500.	298.30	81.87	26.88
600.	313.92	89.37	35.46
700.	328.16	95.34	44.70
800.	341.22	100.23	54.49
900.	353.27	104.31	64.72
1000.	364.44	107.77	75.33
1100.	374.85	110.74	86.25
1200.	384.60	113.29	97.46
1300.	393.76	115.51	108.90
1400.	402.39	117.45	120.55
1500.	410.55	119.14	132.38
1600.	418.29	120.63	144.37
1800.	432.65	123.13	168.75
2000.	445.73	125.12	193.58

1	−2.502 939	−0.519 679	0.093 327
8	−0.452 830	−0.440 977	0.001 309
6	−1.685 192	0.165 705	−0.031 914
6	0.644 270	0.340 183	−0.004 482
8	1.763 220	−0.027 946	0.004 707
1	−1.734 649	1.235 740	0.076 919
B (GHz)	75.872 0	4.996 7	4.690 1

No.	$\bar{\upsilon}$ (cm^{-1})	x_{ii}
1	3331.92	−37.79
2	3171.48	−31.14
3	1877.64	−13.52
4	1453.83	−6.93
5	1220.40	−7.51
6	1165.27	−4.18
7	992.45	−7.41
8	625.79	−0.19
9	329.89	−2.37
10	303.25	−869.42
11	275.90	−5.31
12	221.17	−0.81

References for methylenedioxirane.

BD06 R. D. Bach and O. Dmitrenko, "The effect of carbonyl substitution on the strain energy of small ring compounds and their six-member ring reference compounds," J. Am. Chem. Soc. **128**, 4598 (2006).

VS05 D. Vijay and G. N. Sastry, "Relative energies of $C_2O_2H_2$ isomers and their ionized counterparts: Possibility of bond stretch isomerism," J. Mol. Struct.: THEOCHEM **714**, 199–207 (2005).

3.19.14. Methyleneoxy oxomethyl

^{3}A g = 3 C_1 σ = 1 M_0 = 58.0367

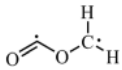

Kovacs and Jackson explored the singlet and triplet surfaces of the $CH_2 + CO_2$ reaction [KJ01]. The *anti* OCOC triplet conformer lies some 2.3 kJ mol^{-1} below the *syn*, as also found previously [KJ01]. The singlet conformers do not exist at B3LYP/cc-pVTZ+d.

3.19.14.1 Species data.

3.19.14.2 Formation enthalpy, $\Delta_f H(0\ K)$. From the G2 calculations of Kovacs and Jackson [KJ01], an estimated $\Delta_f H^o(0\ K)$ of +46.0 kJ mol^{-1} can be deduced for the *anti* triplet; Lee and Bozzelli reported $\Delta_f H^o(298.15\ K)$ = 46.1 kJ mol^{-1} from CBS-Q calculations [LB03]. Our multi-composite treatment returns $\Delta_f H^o(0\ K)$ = 42.8 ± 1.4 kJ mol^{-1} with W3X-L in satisfactory agreement at $\Delta_f H^o(0\ K)$ = 42.1 kJ mol^{-1} (39.0 kJ mol^{-1} at 298.15 K).

3.19.14.3 Results. A hindered rotor analysis identifies mode nos. 11 and 12 and ascribes similar impacts on the derived thermochemistry amounting to some 1.7 J K^{-1} mol^{-1} to the entropy. A VPT2 treatment is compromised by the highly anharmonic "umbrella" mode no. 10. A relaxed scan about the OC–OC is well-behaved as is that about CO–CH. The two modes, nos. 11 and 12, are replaced with the relaxed potential energy scans, and the umbrella mode no. 10 is treated as a pure vibration. Literature [LB03] values for S^o of 302.0 J K^{-1} mol^{-1} and C_p^o of 65.1 J K^{-1} mol^{-1} are not in total accord.

T (K)	$S°(T)$	$C_p°(T)$	$H°(T) - H°(0)$
298.15	303.69	72.27	16.08
300.	304.13	72.43	16.21
400.	326.18	81.08	23.89
500.	345.09	88.50	32.38
600.	361.78	94.56	41.55
700.	376.74	99.46	51.25
800.	390.29	103.45	61.41
900.	402.67	106.72	71.92
1000.	414.06	109.42	82.73
1100.	424.60	111.64	93.78
1200.	434.39	113.48	105.04
1300.	443.54	115.01	116.47
1400.	452.11	116.29	128.03
1500.	460.17	117.35	139.72
1600.	467.77	118.24	151.50
1800.	481.78	119.63	175.29
2000.	494.44	120.64	199.32

References for methyleneoxy oxomethyl.

KJ01 D. Kovacs and J. E. Jackson, "$CH_2 + CO_2 \rightarrow CH_2O + CO$, one-step oxygen atom abstraction or addition/fragmentation via α-lactone?," J. Phys. Chem. A **105**(32), 7579–7587 (2001).

LB03 J. Lee and J. W. Bozzelli, "Thermochemical properties, reaction pathways and kinetics of the formylmethyl radical + O_2 reaction system," J. Phys. Chem. A **107**, 3778–3791 (2003).

3.19.15. 2-Oxiranone; acetolactone; cycloacetate

$^1A'$ g = 1 C_S σ = 1 M_0 = 58.0367

This is an intermediate in the reaction between acetone and the hydroxyl radical in polluted cities with the acetone predominantly coming from ethanol combustion [HLBC16].

3.19.15.1 Species data.

6	0.000 000	0.332 412	0.000 000
6	0.788 716	−0.880 563	0.000 000
8	−0.734 467	−0.775 857	0.000 000
1	1.191 620	−1.278 485	0.922 437
1	1.191 620	−1.278 485	−0.922 437
8	−0.154 975	1.506 591	0.000 000
B (GHz)	25.129 1	8.110 0	6.397 5

No.	$\bar{\upsilon}$ (cm^{-1})	x_{ii}	
1	3116.66	−28.05	a'
2	2007.23	−9.79	a'
3	1483.43	0.11	a'
4	1193.53	−5.12	a'
5	1120.03	−2.06	a'
6	945.17	−5.00	a'
7	717.39	−2.99	a'
8	535.48	−0.48	a'
9	3214.98	−33.28	a''
10	1062.06	−1.67	a''
11	999.66	−1.13	a''
12	494.01	0.56	a''

3.19.15.2 Formation enthalpy, $\Delta_f H$(0 K). On the basis of an isodesmic reaction

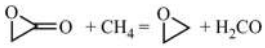

for which a reaction enthalpy of 86.4 ± 2.2 kJ mol^{-1} emerges from CBS-QB3, CBS-APNO, G3, G4, and W1BD calculations in combination with ATcT [RB16] values for the chaperones methane, oxirane, and methanal (−66.550 ± 0.057 kJ mol^{-1}, −40.0 ± 0.38 kJ mol^{-1}, and −105.32 ± 0.11 kJ mol^{-1}, respectively), this gives $\Delta_f H°$(0 K) = −165.1 ± 2.2 kJ mol^{-1}. A similar exercise for

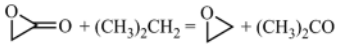

gives $\Delta_r H°$(0 K) of 8.12 ± 1.65 kJ mol^{-1} to yield $\Delta_f H°$(0 K) = −164.8 ± 1.7 kJ mol^{-1} with ATcT assumed values for the chaperones propane (−82.75 ± 0.19 kJ mol^{-1}), oxirane (−40.0 ± 0.38 kJ mol^{-1}), and acetone (−199.45 ± 0.36 kJ mol^{-1}). The combined final weighted average value is therefore $\Delta_f H°$(0 K) = −164.9 ± 1.4 kJ mol^{-1}. Ruscic and Bross [RB16] placed the oxarinone at +40 kJ mol^{-1} compared to *trans* glyoxal, which implies an approximate value of −167 kJ mol^{-1} [VS05].

Our result at 298.15 K is −172.4 ± 1.5 kJ mol^{-1}, which is in very satisfactory agreement with the −171.5 ± 3.8 kJ mol^{-1} of Goldsmith *et al.* [GMG12] and with the −177.9 ± 8 kJ mol^{-1} estimate [GBR18].

3.19.15.3 Results. Our anharmonic treatment is in good agreement with the only literature values available [GMG12, GBR18], viz., $S°$(298.15 K) = 264.0 ± 2.9 J mol^{-1} K^{-1} and $C_p°$(300 K) = 54.8 ± 3.8 J mol^{-1} K^{-1}.

T (K)	$S°(T)$	$C_p°(T)$	$H°(T) - H°(0)$
298.15	263.99	54.05	11.74
300.	264.32	54.29	11.84
400.	281.65	66.48	17.89
500.	297.62	76.71	25.07
600.	312.37	84.96	33.17
700.	325.98	91.64	42.01
800.	338.59	97.14	51.46
900.	350.30	101.74	61.41
1000.	361.23	105.61	71.78
1100.	371.45	108.91	82.51
1200.	381.05	111.73	93.54
1300.	390.10	114.16	104.84
1400.	398.63	116.26	116.36
1500.	406.72	118.09	128.08
1600.	414.39	119.69	139.97
1800.	428.65	122.33	164.18
2000.	441.65	124.41	188.86

References for 2-oxiranone; acetolactone; cycloacetate.

HLBC16 N. U. M. Howes, J. P. A. Lockhart, M. A. Blitz, S. A. Carr, M. T. Baeza-Romero, D. E. Heard, R. J. Shannon, P. W. Seakins, and T. Varga, "Observation of a new channel, the production of CH_3, in the abstraction reaction of OH radicals with acetaldehyde," Phys. Chem. Chem. Phys. **18**(38), 26423–26433 (2016).

RB16 B. Ruscic and D. H. Bross, Active Thermochemical Tables (ATcT) values based on version 1.122 of the Thermochemical Network, 2016, available at https://ATcT.anl.gov.

VS05 D. Vijay and G. N. Sastry, "Relative energies of $C_2O_2H_2$ isomers and their ionized counterparts: Possibility of bond stretch isomerism," J. Mol. Struct.: THEOCHEM **714**, 199–207 (2005).

GMG12 C. F. Goldsmith, G. R. Magoon, and W. H. Green, "Database of small molecule thermochemistry for combustion," J. Phys. Chem. A **116**, 9033–9057 (2012).

GBR18 E. Goos, A. Burcat, and B. Ruscic, "Extended third Millennium ideal gas and condensed phase thermochemical database for combustion with updates from active thermochemical tables," Mirrored at http://garfield.chem.elte.hu/Burcat/burcat.html; 12 January 2018.

3.19.16. 2-Oxo-2-oxoethyl

$^3A_2$ g = 3 C_{2v} σ = 2 M_0 = 58.0367

Dioxatrimethylenemethane has been predicted to have a triplet ground state from uB3LYP, CASPT2, and uCCSD(T) calculations with the aug-cc-pVTZ basis set by Chen *et al.* [CHB17] However, they also reported a very low-lying, open-shell $^1A_2$ excited state at 2.1 kJ mol^{-1} above. It is the only C2 product found in a mechanistic Born–Oppenheimer molecular dynamics study of methylene reacting with carbon dioxide adsorbed on a nickel (110) surface [LS18].

3.19.16.1 Species data.

6	1.395 611	0.000 000	0.000 000
6	−0.037 906	0.000 000	0.000 000
8	−0.750 263	1.045 086	0.000 000
8	−0.750 263	−1.045 086	0.000 000
1	1.928 992	−0.938 671	0.000 000
1	1.928 992	0.938 671	0.000 000
B (GHz)	13.764 7	10.389 0	5.920 5

No.	$\bar{\upsilon}$ (cm^{-1})	x_{ii}	
1	3158.69	−26.75	a_1
2	1550.88	−6.44	a_1
3	1426.81	−5.16	a_1
4	977.75	−1.90	a_1
5	572.70	0.20	a_1
6	384.68	−5.12	a_2
7	739.12	5.98	b_1
8	577.41	0.45	b_1
9	3276.99	−30.87	b_2
10	1135.96	6.56	b_2
11	959.70	−0.18	b_2
12	392.00	0.78	b_2

3.19.16.2 Formation enthalpy, $\Delta_f H(0\ K)$. A direct comparison via multi-composite methods with 2-oxarinone q.v. yields a reaction enthalpy of −181.45 ± 1.63 kJ mol^{-1}, and hence, $\Delta_f H°(0\ K)$ = (−164.9 ± 1.4) − (−181.5 ± 1.6) = 16.6 ± 2.2 kJ mol^{-1} (10.4 kJ mol^{-1} at 298.15 K), which agrees with a W2X value of 15.4 kJ mol^{-1} and indeed with a WMS of 14.4 kJ mol^{-1}. An estimate for the formation enthalpy of ~20 kJ mol^{-1} is available [B19] for this T_1 = 0.026 species.

3.19.16.3 Results. A standard anharmonic rigid rotor treatment is applied since rotation about C–C is essentially barrierless.

T (K)	$S^o(T)$	$C_p^o(T)$	$H^o(T) - H^o(0)$
298.15	276.04	63.30	13.10
300.	276.43	63.55	13.21
400.	296.42	75.50	20.19
500.	314.31	84.83	28.23
600.	330.45	92.08	37.09
700.	345.10	97.85	46.60
800.	358.48	102.57	56.62
900.	370.80	106.55	67.09
1000.	382.21	109.97	77.92
1100.	392.83	112.92	89.06
1200.	402.77	115.50	100.49
1300.	412.11	117.73	112.15
1400.	420.91	119.66	124.03
1500.	429.22	121.32	136.08
1600.	437.10	122.72	148.28
1800.	451.69	124.87	173.05
2000.	464.93	126.31	198.18

References for 2-oxo-2-oxoethyl.

CHB17 B. Chen, D. A. Hrovat, and W. T. Borden, "Calculations of the energies of the low-lying electronic states of dioxatrimethylenemethane (H_2CCO_2) and prediction of the negative ion photoelectron (NIPE) spectrum of its radical anion," J. Phys. Org. Chem. **30**(4), e3594 (2017).

LS18 W. Lin and G. C. Schatz, "Mechanisms of formaldehyde and C_2 formation from methylene reacting with CO_2 adsorbed on Ni (110)," J. Phys. Chem. C **122**, 13827–13833 (2018).

B19 W. T. Borden (personal communication, University of North Texas, Denton, 1 August 2019), see [CHB17].

3.19.17. 1-Oxo-2-oxoethyl

$^3A''$ g = 3 C_S $\sigma = 1$ $M_0 = 58.0367$

This diradical species has been reported in the studies of the ketene + O-atom reaction and the formylmethyl + dioxygen reaction [STWP05, LB03]. Sun *et al.* showed a triplet $^3A''$ state of C_S symmetry (**IM2**) but in the *syn* OCCO conformation [STWP05] for which a formation enthalpy of 85.2 kJ mol^{-1} can be extracted from their QCISD(T) calculations.

3.19.17.1 Species data.

6	0.000 000	0.716 341	0.000 000
8	−1.212 731	1.296 170	0.000 000
1	0.583 215	1.070 090	0.871 835
1	0.583 215	1.070 090	−0.871 835
6	0.046 232	−0.832 866	0.000 000
8	1.0322 53	−1.476 299	0.000 000
B (GHz)	54.972	4.449 9	4.222 0

No.	$\bar{\upsilon}$ (cm^{-1})	x_{ii}		No.	$\bar{\upsilon}$ (cm^{-1})	x_{ii}	
1	2877.26	−36.83	a'	7	513.54	−1.58	a'
2	1924.34	−11.84	a'	8	317.45	0.08	a'
3	1304.27	−5.89	a'	9	2902.86	−42.30	a''
4	1291.85	−6.63	a'	10	1005.62	1.73	a''
5	1095.25	−5.79	a'	11	590.47	27.41	a''
6	792.12	−19.64	a'	12	68.60	9.62	a''

3.19.17.2 Formation enthalpy, $\Delta_f H$(0 K). A high-level W3X-L computation yields $\Delta_f H^o$(0 K) = 83.2 kJ mol^{-1} (78.5 kJ mol^{-1} at 298.15 K), which is in accord with a multi-composite atomization treatment for the *anti* conformer formation enthalpy of 84.5 ± 2.1 kJ mol^{-1} and the *syn* at 85.5 kJ mol^{-1}, which agrees well with the literature [STWP05] 85.2 kJ mol^{-1}.

3.19.17.3 Results. A relaxed potential energy scan shows a barrier of 8.4 kJ mol^{-1} between the *anti* and *syn* forms, which equates to a reduced barrier height (V/RT) of 3.3 at room temperature. A complete hindered rotor and anharmonicity treatment is feasible for this species.

T (K)	$S^o(T)$	$C_p^o(T)$	$H^o(T) - H^o(0)$
298.15	298.75	64.87	14.59
300.	299.15	65.06	14.71
400.	319.19	74.47	21.70
500.	336.68	82.29	29.55
600.	352.27	88.77	38.11
700.	366.38	94.22	47.27
800.	379.27	98.85	56.93
900.	391.15	102.82	67.02
1000.	402.16	106.25	77.47
1100.	412.43	109.22	88.25
1200.	422.05	111.82	99.30
1300.	431.09	114.07	110.60
1400.	439.62	116.04	122.11
1500.	447.68	117.74	133.80
1600.	455.33	119.21	145.64
1800.	469.51	121.54	169.73
2000.	482.41	123.20	194.21

References for 1-oxo-2-oxoethyl.

STWP05 H. Sun, Y.-Z. Tang, Z.-L. Wang, X.-M. Pan, Z.-S. Li, and R.-S. Wang, "DFT investigation of the mechanism ossssf $CH_2CO + O(^3P)$ reaction," Int. J. Quantum Chem. **105**(5), 527–532 (2005).

LB03 J. Lee and J. W. Bozzelli, "Thermochemical and kinetic analysis of sssssssthe formyl methyl radical + O_2 reaction system," J. Phys. Chem. A **107**(19), 3778–3791 (2003).

3.20. $C_2H_2O_3$

3.20.1. Dihydroxyethenone

^1A g = 1 C_2 σ = 2 M_0 = 74.0361

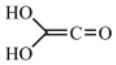

Ketenes are a versatile class of synthetically useful compounds, which Goedecke *et al.* discussed [GLS11] from the viewpoint of carbene carbonylation.

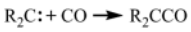

We obtain good agreement with their BP86/def2-TZVP geometries, viz., *d*(HO–C) 1.384 Å, 1.375 Å, ∠OCO 120.0°, 119.6°, and *d*(C–C) 1.328 Å, 1.318 Å.

3.20.1.1 Species data.

6	0.000 000	0.000 000	−0.383 503
6	0.000 000	0.000 000	0.934 077
8	0.000 000	0.000 000	2.101 452
8	0.000 000	1.188 243	−1.074 988
1	0.875 887	1.332 193	−1.457 624
8	0.000 000	−1.188 243	−1.074 988
1	−0.875 887	−1.332 193	−1.457 624
B (GHz)	10.049 1	4.029 0	2.923 5

No.	$\bar{\upsilon}$ (cm^{-1})	x_{ii}	
1	3725.38	−48.02	*a*
2	2221.06	−10.81	*a*
3	1453.12	−4.12	*a*
4	1210.04	−5.00	*a*
5	812.09	−0.90	*a*
6	483.27	−3.13	*a*
7	350.62	0.57	*a*
8	3720.24	−48.32	*b*
9	1321.30	−5.47	*b*
10	1209.27	−4.56	*b*
11	692.32	−3.04	*b*
12	492.31	−5.66	*b*
13	342.15	−5.25	*b*
14	309.04	−0.47	*b*
15	195.29	0.55	*b*

3.20.1.2 Formation enthalpy, $\Delta_f H$(0 K). The isodesmics

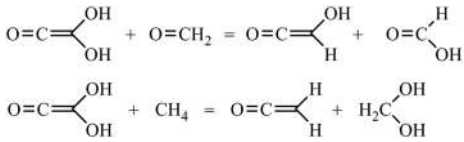

have reaction enthalpies of −110.62 ± 1.61 kJ mol^{-1} and −57.79 ± 1.83 kJ mol^{-1}, respectively, which together with reference values for formaldehyde (−105.32 ± 0.11 kJ mol^{-1}), *syn* formic acid (−371.12 ± 0.22 kJ mol^{-1}), methane (−66.550 ± 0.057 kJ mol^{-1}), and *conrot/gauche*-methanediol (−379.05 ± 0.95 kJ mol^{-1}) yields $\Delta_f H^o$(0 K) = −300.8 ± 1.9 kJ mol^{-1} and −300.2 ± 2.1 kJ mol^{-1}, respectively. A final weighted average value of $\Delta_f H^o$(0 K) = −300.5 ± 1.4 kJ mol^{-1} (−307.6 kJ mol^{-1} at 298.15 K) emerges. Note that the very close agreement observed from both isodesmic reactions validates the result previously obtained for hydroxyethenone.

Sumathi and Green [SG02] reported $\Delta_f H^o$(298.15 K) = −306.4 kJ mol^{-1}, which is in very good agreement with our data.

3.20.1.3 Results. Hindered rotor analysis discounts any substantial corrections, which, given that mode nos. 6 and 12 are identified as internal rotations, is unsurprising. Anharmonic corrections are also slight. An entropy of 293.8 J K^{-1} mol^{-1} and a C_p^o(300 K) of 84.18 J K^{-1} mol^{-1} have been reported [GLS11] in RRHO calculations with internal rotor corrections at the HF/6-31G′ level.

T (K)	$S^o(T)$	$C_p^o(T)$	$H^o(T) - H^o(0)$
298.15	296.76	81.41	16.35
300.	297.27	81.67	16.50
400.	322.52	93.97	25.31
500.	344.57	103.72	35.21
600.	364.20	111.52	45.99
700.	381.89	117.92	57.47
800.	397.99	123.31	69.54
900.	412.79	127.95	82.10
1000.	426.49	131.98	95.10
1100.	439.23	135.48	108.48
1200.	451.16	138.52	122.18
1300.	462.35	141.14	136.17
1400.	472.89	143.39	150.39
1500.	482.85	145.31	164.83
1600.	492.28	146.95	179.44
1800.	509.75	149.55	209.10
2000.	525.61	151.43	239.21

References for dihydroxyethenone.

GLS11 C. Goedecke, M. Leibold, U. Siemeling, and G. Frenking, "When does carbonylation of carbenes yield ketenes? A theoretical study with implications for synthesis," J. Am. Chem. Soc. **133**, 3557 (2011).

SG02 R. Sumathi and W. H. Green, "Thermodynamic properties of ketenes: Group additivity values from quantum chemical calculations," J. Phys. Chem. A **106**(34), 7937–7949 (2002).

3.20.2. 2,4-Dioxabicyclobutanol

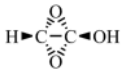

There is only a single mention in the chemical literature [GS12] to this species, but it appears that it refers to a transition state and not the actual molecule [G19]. Thus, attempts to optimize the structure at our chosen protocol were not successful.

References for 2,4-dioxabicyclobutanol.

GS12 R. Gershoni-Poranne and A. Stanger, "An MO-based identification of charge-shift bonds," ChemPhysChem **13**(9), 2377–2381 (2012).

G19 R. Gershoni-Poranne, ETH Zurich (private communication 18 June 2019).

3.20.3. 1,2-Dioxetan-3-one

$^1A'$ g = 1 C_S σ = 1 M_0 = 74.0361

Extensive theoretical work has been carried out particularly on the excited states of this cyclic species, driven by the need to understand the conversion of chemical energy stored in chemical bonds into light as in firefly chemiluminescence [FFLR17].

3.20.3.1 Species data.

8	0.196 633	−1.058 595	0.000 000
8	1.420 119	−0.212 411	0.000 000
6	0.594 386	0.974 136	0.000 000
6	−0.607 102	0.061 750	0.000 000
1	0.723 155	1.572 339	0.901 205
1	0.723 152	1.572 336	−0.901 208
8	−1.788 003	0.101 006	0.000 000
B (GHz)	13.793 0	5.295 9	3.923 9

No.	$\bar{\upsilon}$ (cm^{-1})	x_{ii}	
1	3064.88	−28.01	a'
2	1948.66	−10.41	a'
3	1475.72	−0.73	a'
4	1298.75	−6.69	a'
5	1135.60	−5.73	a'
6	1008.83	−3.48	a'
7	914.79	−2.73	a'
8	877.03	−6.82	a'
9	740.35	−0.14	a'
10	484.09	−0.08	a'
11	3123.92	−32.81	a''
12	1138.27	−2.22	a''
13	1015.04	−1.19	a''
14	509.06	0.62	a''
15	236.94	−0.36	a''

3.20.3.2 Formation enthalpy, $\Delta_f H(0\ K)$. Based on the isodesmic reaction

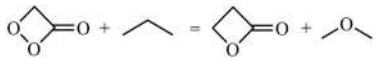

the multi-composite reaction enthalpy is −184.8 ± 1.1 kJ mol^{-1}; using ATcT values for propane (−82.74 ± 0.19 kJ mol^{-1}) and dimethyl ether (−166.50 ± 0.44 kJ mol^{-1}), together with Pedley's 298.15 K value of −282.9 ± 0.9 kJ mol^{-1} for 2-oxetanone, which translated to 0 K is −268.1 ± 1.0 kJ mol^{-1}, yields $\Delta_f H°(0\ K)$ = −167.1 ± 1.6 kJ mol^{-1} (−177.4 kJ mol^{-1} at 298.15 K), in excellent agreement with $\Delta_f H°(0\ K)$ = −167.6 kJ mol^{-1} from a WMS atomization calculation.

3.20.3.3 Results. The puckering modes are treated as conventional anharmonic frequencies here.

T (K)	$S^{o}(T)$	$C_{p}^{o}(T)$	$H^{o}(T) - H^{o}(0)$
298.15	282.18	65.08	13.34
300.	282.58	65.38	13.46
400.	303.55	80.78	20.79
500.	323.00	93.59	29.53
600.	341.00	103.79	39.42
700.	357.63	111.93	50.22
800.	373.03	118.52	61.75
900.	387.31	123.93	73.88
1000.	400.61	128.44	86.50
1100.	413.03	132.22	99.54
1200.	424.68	135.43	112.93
1300.	435.63	138.17	126.61
1400.	445.96	140.53	140.55
1500.	455.72	142.57	154.70
1600.	464.98	144.35	169.05
1800.	482.16	147.29	198.22
2000.	497.80	149.60	227.92

References for 1,2-dioxetan-3-one.

FFLR17 A. Francés-Monerris, I. Fdez Galván, R. Lindh, and D. Roca-Sanjuán, "Triplet versus singlet chemiexcitation mechanism in dioxetanone: A CASSCF/CASPT2 study," Theor. Chem. Acc. **136**, 70 (2017).

3.20.4. 1,3-Dioxetan-2-one

$^{1}A_{1}$ g = 1 C_{2v} σ = 2 M_{0} = 74.0361

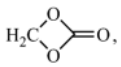

3.20.4.1 Species data.

6	0.000 000	0.000 000	−1.355 978
8	0.000 000	1.018 264	−0.343 750
6	0.000 000	0.000 000	0.580 966
8	0.000 000	−1.018 264	−0.343 750
1	0.910 429	0.000 000	−1.951 260
1	−0.910 429	0.000 000	−1.951 260
8	0.000 000	0.000 000	1.756 573
B (GHz)	14.506	5.717 6	4.215 4

No.	$\bar{\upsilon}$ (cm^{-1})	x_{ii}	
1	3073.70	−28.22	a_1
2	1986.85	−10.34	a_1
3	1540.05	−0.03	a_1
4	1080.53	−2.64	a_1
5	1029.58	−0.80	a_1
6	822.90	−0.83	a_1
7	1108.04	−1.95	a_2
8	3146.37	−33.29	b_1
9	1151.46	−1.65	b_1
10	763.74	−0.95	b_1
11	272.09	−0.21	b_1
12	1386.00	−6.73	b_2
13	1097.37	−0.82	b_2
14	873.08	−5.42	b_2
15	533.29	−0.47	b_2

3.20.4.2 Formation enthalpy, $\Delta_{f}H(0\ K)$. A direct comparison, via the multiple composites method, with 1,2-dioxetan-3-one (see above, −167.1 ± 1.6 kJ mol^{-1}) yields a reaction enthalpy of 264.91 ± 0.67 kJ mol^{-1} from which $\Delta_{f}H^{o}(0\ K)$ = −432.0 ± 1.7 kJ mol^{-1} emerges (−442.9 kJ mol^{-1} at 298.15 K), in good agreement with $\Delta_{f}H^{o}(0\ K)$ = −435.0 kJ mol^{-1} from W3X-L and $\Delta_{f}H^{o}(0\ K)$ = −433.8 kJ mol^{-1} from WMS.

3.20.4.3 Results. There are no literature values available for validation purposes.

T (K)	$S°(T)$	$C_p°(T)$	$H°(T) - H°(0)$
298.15	271.66	60.21	12.61
300.	272.03	60.51	12.72
400.	291.60	76.04	19.56
500.	310.05	89.38	27.85
600.	327.33	100.17	37.35
700.	343.45	108.83	47.81
800.	358.45	115.85	59.06
900.	372.44	121.61	70.94
1000.	385.51	126.39	83.35
1100.	397.75	130.40	96.19
1200.	409.24	133.79	109.40
1300.	420.07	136.68	122.93
1400.	430.29	139.15	136.72
1500.	439.97	141.29	150.75
1600.	449.15	143.14	164.97
1800.	466.19	146.18	193.91
2000.	481.72	148.55	223.39

3.20.5. Dioxiranecarboxaldehyde

^{1}A g = 1 C_S σ = 1 M_0 = 74.0361

This species has been found in an extensive exploration of the acetylene + ozone potential energy surface by Cremer *et al.* [CCA01],

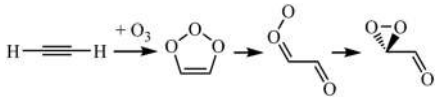

The lowest energy conformer has an HCCH dihedral of 180° and lies some 20 kJ mol^{-1} below that with HCCH = 0°, as reported in the literature [CCA01]. However, we find that the *cis* conformer is not a stationary point at B3LYP/cc-pVTZ+d.

3.20.5.1 Species data.

2	2–30.407 564	0.339 847	0.000 000
8	0.253 085	1.311 665	0.744 946
8	0.253 085	1.311 665	−0.744 946
1	−1.494 986	0.359 164	0.000 000
6	0.253 085	−1.015 956	0.000 000
8	−0.373 116	−2.039 849	0.000 000
1	1.357 417	−0.970 360	0.000 000
B (GHz)	18.826 0	3.424 33	3.234 52

No.	$\bar{\upsilon}$ (cm^{-1})	x_{ii}	
1	3123.64	−59.42	a'
2	2942.95	−65.25	a'
3	1819.98	−9.66	a'
4	1430.33	−6.82	a'
5	1338.97	−3.97	a'
6	1266.09	−2.36	a'
7	1092.34	−5.47	a'
8	839.01	−2.98	a'
9	494.91	−0.99	a'
10	322.54	1.04	a'
11	1168.04	−4.56	a''
12	996.66	−1.57	a''
13	867.17	−0.72	a''
14	380.98	−0.78	a''
15	111.10	−0.43	a''

3.20.5.2 Formation enthalpy, $\Delta_f H$(0 K). A $\Delta_f H°$ = −90.0 kJ mol^{-1} has been reported [CCA01] at 298.15 K from restricted B3LYP/6-311+G(2d,2p) calculations, which can be compared to the value obtained from the isodesmic reaction

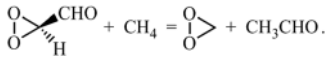

whose 0 K reaction enthalpy of 14.92 ± 1.51 kJ mol^{-1} leads to $\Delta_f H°$(0 K) = −93.9 ± 1.6 kJ mol^{-1} (−102.5 kJ mol^{-1} at 298.15 K) where reference values for methane (−66.550 ± 0.057 kJ mol^{-1}), dioxirane (9.41 ± 0.54 kJ mol^{-1}), and ethanal (−154.97 ± 0.28 kJ mol^{-1}) are employed.

WMS and W2X concur at −95.3 kJ mol^{-1} and −93.5 kJ mol^{-1}, while high-level W3X-L atomization values of −94.4 kJ mol^{-1} (−103.0 kJ mol^{-1} at 298.15 K) are in excellent agreement.

3.20.5.3 Results. An entropy of 295.8 J K^{-1} mol^{-1} resulted from B3LYP/6-311+G(2d,2p) calculations [CCA01]. This compares favorably with the value obtained here of 294.8 J K^{-1} mol^{-1} based on anharmonic frequencies and a hindered rotor treatment for mode no. 15—rotation about the C–C bond.

T (K)	$S^o(T)$	$C_p^o(T)$	$H^o(T) - H^o(0)$
298.15	294.81	71.02	14.92
300.	295.25	71.30	15.06
400.	317.87	86.57	22.95
500.	338.69	100.09	32.31
600.	357.92	110.80	42.87
700.	375.64	118.87	54.38
800.	391.93	124.90	66.58
900.	406.91	129.47	79.31
1000.	420.75	133.03	92.44
1100.	433.56	135.88	105.89
1200.	445.49	138.21	119.59
1300.	456.63	140.17	133.51
1400.	467.08	141.83	147.61
1500.	476.92	143.26	161.87
1600.	486.20	144.52	176.26
1800.	503.35	146.60	205.37
2000.	518.88	148.26	234.86

References for dioxiranecarboxaldehyde.

CCA01 D. Cremer, R. Crehuet, and J. Anglada, "The ozonolysis of acetylene-A quantum chemical investigation," J. Am. Chem. Soc. **123**, 6127–6141 (2001).

3.20.6. 2,2′-Dioxo-ethan-1-ol

$^3A''$ g = 3 C_S σ = 1 M_0 = 74.0361

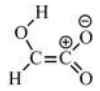

This is an intermediate noted during a photochemical study of glyoxylic acid, one of the most abundant carboxylic acids found in atmospheric aerosols and water samples, which is formed via a beta-hydrogen transfer [HSB19].

3.20.6.1 Species data.

8	−0.082 886	−1.844 006	0.000 000
8	1.263 622	0.557 597	0.000 000
8	−0.504 264	1.702 815	0.000 000
6	−0.743 909	−0.684 810	0.000 000
6	0.000 000	0.529 214	0.000 000
1	−1.819 324	−0.743 455	0.000 000
1	0.871 002	−1.654 215	0.000 000
B (GHz)	12.638	4.267 5	3.190 3

No.	$\bar{\upsilon}$ (cm^{-1})	x_{ii}	
1	3666.62	−95.72	a'
2	3247.45	−54.53	a'
3	1603.80	−6.23	a'
4	1417.28	−4.24	a'
5	1347.21	−4.49	a'
6	1212.27	−1.87	a'
7	1134.61	−3.71	a'
8	950.43	−1.87	a'
9	644.48	−0.16	a'
10	476.54	−4.62	a'
11	227.74	0.86	a'
12	701.97	0.97	a''
13	620.36	2.10	a''
14	493.82	−5.83	a''
15	212.20	−0.50	a''

3.20.6.2 Formation enthalpy, $\Delta_f H$(0 K). A multi-composite approach returns $\Delta_f H^o$(0 K) = −177.2 ± 2.7 kJ mol^{-1}, which is in agreement with the −178.8 kJ mol^{-1} from WMS and the −176.9 kJ mol^{-1} from W2X, but the higher level W3X-L yields $\Delta_f H^o$(0 K) = −181.9 kJ mol^{-1} (−190.0 kJ mol^{-1} at 298.15 K). Harrison *et al.*, in M06-2X/aug-cc-pVTZ calculations, placed this T_1 = 0.050 species some 2.89 eV above glyoxylic acid, which is equivalent to $\Delta_f H^o$(0 K) = −186 kJ mol^{-1}.

3.20.6.3 Results. A hindered rotor analysis identifies mode nos. 15 and 13 with reduced barrier heights (V/RT)s of 32 and 18, respectively; a failed scan about the C–C bond means that only mode no. 13 is treated as a hindered rotor in an otherwise anharmonic approach.

T (K)	$S^\circ(T)$	$C_p^\circ(T)$	$H^\circ(T) - H^\circ(0)$
298.15	305.56	77.93	15.50
300.	306.04	78.24	15.65
400.	330.74	93.78	24.27
500.	353.09	106.46	34.30
600.	373.41	116.31	45.46
700.	391.93	123.82	57.49
800.	408.85	129.58	70.17
900.	424.38	134.06	83.36
1000.	438.70	137.61	96.95
1100.	451.95	140.48	110.85
1200.	464.28	142.86	125.02
1300.	475.80	144.88	139.41
1400.	486.60	146.62	153.99
1500.	496.77	148.15	168.73
1600.	506.38	149.52	183.61
1800.	524.13	151.86	213.75
2000.	540.23	153.79	244.32

References for 2,2′-dioxo-ethan-1-ol.

HSB19 A. W. Harrison, M. F. Shaw, and W. J. De Bruyn, "Theoretical investigation of the atmospheric photochemistry of glyoxylic acid in the gas phase," J. Phys. Chem. A **123**, 8109 (2019).

3.20.7. 1-Dioxy-2-oxoethyl

$^1A'$ g = 1 C_S σ = 1 M_0 = 74.0361

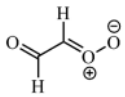

This species is mentioned in a theoretical study of the electronic structures of oxygenated dipoles, in particular, the relative contributions of zwitterionic and biradical characteristics [YYKN97]. We find three other conformers (*as*, *sa*, and *ss*) at +7.9 kJ mol^{-1}, +14.5 kJ mol^{-1}, and +28.7 kJ mol^{-1}, respectively, based on the dihedrals OCCO and CCOO, over the *aa* ground state. In a theoretical study of the atmospheric ozonolysis of formylcinnamaldehyde [LWWL19], the *sa* was reported to lie 12.0 kJ mol^{-1} above the *aa*.

3.20.7.1 Species data.

8	2.313 618	0.020 182	0.000 000
6	1.212 050	−0.478 874	0.000 000
1	1.043 319	−1.569 200	0.000 000
6	0.000 000	0.338 715	0.000 000
8	−1.106 098	−0.287 413	0.000 000
1	−0.004 357	1.422 329	0.000 000
8	−2.246 428	0.390 709	0.000 000
B (GHz)	46.127	2.452 4	2.328 6

No.	$\bar{\upsilon}$ (cm^{-1})	x_{ii}	
1	3185.11	−55.59	a'
2	2956.41	−65.06	a'
3	1756.21	−9.89	a'
4	1489.63	−8.95	a'
5	1381.44	−5.74	a'
6	1319.94	−1.61	a'
7	1124.63	−5.03	a'
8	1065.79	−9.26	a'
9	570.01	0.39	a'
10	501.32	−0.97	a'
11	234.37	0.02	a'
12	1014.15	−1.67	a''
13	892.96	−1.55	a''
14	321.43	−1.28	a''
15	158.10	−0.78	a''

3.20.7.2 Formation enthalpy, $\Delta_f H$(0 K). A multi-composite treatment gives $\Delta_f H^\circ$(0 K) = 2.4 ± 6.7 kJ mol^{-1}, which is in line with a WMS of 1.9 kJ mol^{-1} and the $\Delta_f H^\circ$(0 K) = 3.9 ± 2.8 kJ mol^{-1} (−3.7 kJ mol^{-1} at 298.15 K) computed from the isodesmic

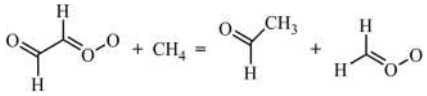

whose reaction enthalpy of 19.63 ± 2.66 kJ mol^{-1} is combined with known chaperones methane (−66.550 ± 0.057 kJ mol^{-1}), ethanal (−154.97 ± 0.28 kJ mol^{-1}), and dioxymethyl (111.9 ± 0.63 kJ mol^{-1}). This particular reaction was chosen in the expectation that the T_1's in excess of 0.035 largely cancel out.

3.20.7.3 Results. A hindered rotor analysis identifies just mode no. 14 with a reduced barrier height (V/RT) of 18.9 and only a small impact on the entropy.

T (K)	$S°(T)$	$C_p°(T)$	$H°(T) - H°(0)$
298.15	301.26	75.	16.08
300.	301.72	75.25	16.22
400.	325.25	88.77	24.43
500.	346.38	100.75	33.92
600.	365.65	110.65	44.51
700.	383.34	118.68	55.99
800.	399.62	125.19	68.19
900.	414.69	130.53	80.98
1000.	428.67	134.93	94.26
1100.	441.71	138.58	107.94
1200.	453.90	141.64	121.96
1300.	465.35	144.21	136.25
1400.	476.12	146.38	150.78
1500.	486.28	148.20	165.51
1600.	495.89	149.72	180.41
1800.	513.67	152.05	210.60
2000.	529.78	153.64	241.17

References for 1-dioxy-2-oxoethyl.

YYKN97 Y. Yoshioka, D. Yamaki, S. Kubo, M. Nishino, K. Yamaguchi, K. Mizuno, and I. Saito, "Theoretical study on electronic structures of oxygenated dipoles and mechanisms of ozonolysis reaction," Electron. J. Theor. Chem. **2**, 236–252 (1997).

LWWL19 Y. Liu, W. Wang, W. Wang, and X. Lei, "Theoretical investigation on the ozonolysis mechanism of (E)-2-formylcinnamaldehyde in the atmosphere," Chem. Phys. Lett. **730**, 165 (2019).

3.20.8. Formic acid anhydride

$^1A'$ g = 1 C_S σ = 1 M_0 = 74.0361

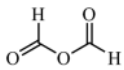

The anhydride of formic acid, sometimes known as formanhydride, is an intermediate in the low temperature oxidation of dimethyl ether [XZWL17] and is produced [V17, CSL19, CE19] during the reaction of a Criegee intermediate, methanal oxide, and formic acid CH_2OO + HCOOH. The *anti/syn* OCOC/COCO conformer is the ground state (called simply *anti* in [CSL19]), and our geometry, frequencies and anharmonicities are in very good agreement with those reported [CSL19].

3.20.8.1 Species data.

8	2.133 078	0.045 972	0.000 000
6	0.989 282	−0.265 062	0.000 000
8	0.000 000	0.712 528	0.000 000
6	−1.316 408	0.324 696	0.000 000
8	−1.718 699	−0.796 602	0.000 000
1	−1.937 406	1.227 179	0.000 000
1	0.585 128	−1.280 158	0.000 000
B (GHz)	22.459 8	3.203 7	2.803 8

No.	$\bar{\nu}$(cm^{-1})	x_{ii}	
1	3087.90	−59.29	a'
2	3054.33	−61.22	a'
3	1869.03	−7.64	a'
4	1818.50	−7.58	a'
5	1408.75	−9.08	a'
6	1383.56	−7.16	a'
7	1108.42	−8.86	a'
8	1008.31	−4.66	a'
9	782.59	−1.36	a'
10	540.02	−0.43	a'
11	253.96	−0.34	a'
12	1048.61	−1.46	a''
13	1036.88	−1.32	a''
14	224.33	−0.59	a''
15	82.84	7.48	a''

3.20.8.2 Formation enthalpy, $\Delta_f H$(0 K). The isodesmic reaction

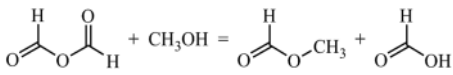

whose reaction enthalpy of −59.03 ± 0.36 kJ mol^{-1} can be combined with reference ATcT values for methanol (−189.83 ± 0.16 kJ mol^{-1}), methyl formate (−344.75 ± 0.58 kJ mol^{-1}), and formic acid (−371.12 ± 0.22 kJ mol^{-1}) to yield $\Delta_f H°$(0 K) = −467.0 ± 0.73 kJ mol^{-1} with a corresponding $\Delta_f H°$(298.15 K) = −474.5 kJ mol^{-1}—this is roughly in accord with an estimated −465 kJ mol^{-1} by Perks and Liebman [PL00] who based their result on an assumed enthalpy change for the dehydration reaction: 2HCOOH → $(HCO)_2O$ + H_2O. A direct atomization calculation using the WMS methodology yields $\Delta_f H°$(0 K) = −469.8 kJ mol^{-1}.

3.20.8.3 Results. Wu *et al.* [WSVG95] showed that a *synperiplanar, antiperiplanar* ground state structure (see above) was the lowest energy conformer, an observation that agreed with electron diffraction, microwave, and IR studies [KHMG79]. Our results show that this is indeed the case with the more symmetrical conformer being strongly disfavored. Structurally, there is very good agreement with the data of Vereecken [V17].

A complete hindered rotor plus anharmonic treatment is thus possible in this case. There is not good agreement with the RRHO study by Kühne *et al.* who reported [KHMG79] 298.15 K values of $S°$ = 302.1 J mol^{-1} K^{-1}, $C_p°$ = 70.81 J mol^{-1} K^{-1}, and $H°(T) - H°(0)$ of 15.65 kJ mol^{-1}, but these are in agreement with our RRHO values.

T (K)	$S^o(T)$	$C_p^o(T)$	$H^o(T) - H^o(0)$
298.15	305.86	74.67	16.07
300.	306.32	74.98	16.21
400.	330.09	90.69	24.51
500.	351.75	103.32	34.24
600.	371.46	112.69	45.06
700.	389.38	119.62	56.69
800.	405.71	124.84	68.93
900.	420.65	128.88	81.62
1000.	434.41	132.09	94.67
1100.	447.12	134.69	108.01
1200.	458.94	136.84	121.59
1300.	469.96	138.63	135.37
1400.	480.29	140.16	149.31
1500.	490.01	141.46	163.39
1600.	499.18	142.60	177.59
1800.	516.09	144.48	206.31
2000.	531.39	145.99	235.35

References for formic acid anhydride.

XZWL17 L.-l. Xing, X.-y. Zhang, Z.-d. Wang, S. Li, and L.-d. Zhang, "New insight into the competition between decomposition pathways of hydroperoxymethyl formate in low temperature DME oxidation," Chin. J. Chem. Phys. **28**, 563–572 (2015).

V17 L. Vereecken, "The reaction of Criegee intermediates with acids and enols," Phys. Chem. Chem. Phys. **19**, 28630–28640 (2017).

CSL19 C.-A. Chung, J. W. Su, and Y.-P. Lee, "Detailed mechanism and kinetics of the reaction of Criegee intermediate CH_2OO with HCOOH investigated via infrared identification of conformers of hydroperoxymethyl formate and formic acid anhydride," Phys. Chem. Chem. Phys. **21**, 21445 (2019).

CE19 C. Cabezas and Y. Endo, "The Criegee intermediate-formic acid reaction explored by rotational spectroscopy," Phys. Chem. Chem. Phys. **21**, 18059 (2019).

PL00 H. M. Perks and J. F. Liebman, "Aspects of the energetics of carboxylic acids and their anhydrides," Struct. Chem. **11**(4), 265–269 (2000).

WSVG95 G. Wu, S. Shlykov, F. S. Van Alseny, H. J. Geise, E. Sluyts, and B. J. Van der Veken, "Formic anhydride in the gas phase, studied by electron diffraction and microwave and infrared spectroscopy, supplemented with *ab initio* calculations of geometries and force fields," J. Phys. Chem. **99**, 8589–8598 (1995).

KHMG79 H. Kühne, T.-K. Ha, R. Meyer, and H. H. Günthard, "Formic acid anhydride. Matrix infrared spectra of five isotopic species, vibrational analysis, empirical and *ab initio* harmonic force field and thermodynamic functions," J. Mol. Spectrosc. **77**, 251–269 (1979).

3.20.9. Hydroperoxyethenone

^1A g = 1 C_1 σ = 1 M_0 = 74.0361

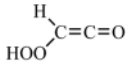

This species rates few mentions in the chemical literature cropping up as an intermediate in a study of the ozonolysis of ethyne [CCA01]. In that study, a formation enthalpy, at 298.15 K, of −98.3 kJ mol^{-1} is reported, which converted to 0 K is −92.4 kJ mol^{-1}.

3.20.9.1 Species data.

1	−0.052 276	1.483 840	0.977 879
6	0.055 063	0.711 595	0.227 395
6	1.211 483	0.067 888	0.092 043
8	2.233 629	−0.446 238	−0.067 136
8	−0.978 946	0.323 721	−0.552 251
8	−1.857 910	−0.613 838	0.259 022
1	−2.721 183	−0.269 902	−0.011 585
B (GHz)	18.726 5	2.763 6	2.594 0

No.	$\bar{\upsilon}$ (cm^{-1})	x_{ii}
1	3756.84	−81.12
2	3165.74	−60.79
3	2201.83	−11.63
4	1384.63	−9.75
5	1308.87	−14.32
6	1175.42	−3.81
7	1061.89	−3.10
8	736.54	−2.48
9	691.46	−0.51
10	626.55	−2.04
11	546.87	1.30
12	392.75	0.19
13	230.85	0.57
14	117.26	37.68
15	107.25	2.75

3.20.9.2 Formation enthalpy, $\Delta_f H$(0 K). The isodesmic reaction

$$O=C=CH(OOH) + CH_3 - H = O=C=CH(H) + CH_3 - OOH$$

has a reaction enthalpy of −18.51 ± 1.36 kJ mol^{-1} at 0 K; taken in conjunction with ATcT reference values for methane (−66.550 ± 0.057 kJ mol^{-1}), ketene (−45.45 ± 0.13 kJ mol^{-1}) and methyl hydroperoxide (−114.90 ± 0.74 kJ mol^{-1}), that implies $\Delta_f H^o$(0 K) = −75.3 ± 1.6 kJ mol^{-1} (−81.3 kJ mol^{-1} at 298.15 K). The more direct high-level atomization protocol W3X-L yields $\Delta_f H^o$(0 K) = −75.9 kJ mol^{-1} (−82.0 kJ mol^{-1} at 298.15 K), which is in excellent agreement with the isodesmic result.

In a theoretical study of the ozonolysis of cinnamaldehyde [LWWL19], a number of $C_2H_2O_3$ species occur as intermediates; the zero-point corrected electronic energies reported, relative to hydroperoxyethenone to dioxiranecarboxylaldehyde to 2-oxoacetic acid, are 0 kJ mol^{-1}:−9 kJ mol^{-1}:−393 kJ mol^{-1}, which very closely match our results.

3.20.9.3 Results. The calculated thermodata include the contribution from two hindered rotors (one of which reduces the number of optical isomers to 1), mode nos. 14 and 15, and anharmonic frequencies, but these differ little at room temperature from a purely harmonic oscillator rigid rotor treatment with two optical isomers, viz., S^o(298.15 K) = 321.79 J K^{-1} mol^{-1} and C_p^o (298.15 K) = 83.44 J K^{-1} mol^{-1}, and H^o(298.15 K) − H^o(0) = 17.68 kJ mol^{-1}.

Cremer *et al.* [CCA01] reported an entropy of 315.0 J mol^{-1} K^{-1} but probably did not include a contribution from "optical isomers," which increases the computed entropy by R × ln 2 or 5.8 J mol^{-1} K^{-1}.

T (K)	$S^o(T)$	$C_p^o(T)$	$H^o(T) - H^o(0)$
298.15	321.32	81.37	17.57
300.	321.82	81.62	17.72
400.	347.05	93.89	26.52
500.	369.09	103.56	36.41
600.	388.66	111.07	47.16
700.	406.24	116.96	58.57
800.	422.18	121.68	70.51
900.	436.74	125.52	82.87
1000.	450.13	128.70	95.59
1100.	462.53	131.37	108.60
1200.	474.06	133.63	121.85
1300.	484.83	135.57	135.31
1400.	494.94	137.24	148.95
1500.	504.46	138.69	162.74
1600.	513.45	139.96	176.68
1800.	530.07	142.07	204.88
2000.	545.12	143.75	233.47

References for hydroperoxyethenone.

CCA01 D. Cremer, R. Crehuet, and J. Anglada, "The ozonolysis of acetylene—A quantum chemical investigation," J. Am. Chem. Soc. **123**, 6127–6141 (2001).

LWWL19 Y. Liu, W. Wang, W. Wang, and X. Lei, "Theoretical investigation on the ozonolysis mechanism of (E)-2-formylcinnamaldehyde in the atmosphere," Chem. Phys. Lett. **730**, 165 (2019).

3.20.10. "2-Hydroxyl acetic acid"

^{1}A g = 1 C_1 σ = 1 M_0 = 74.0361

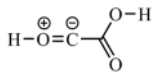

Attempts to optimize dihydroxy oxirene leads to ring opening and the formation of a hydroxyl acetic acid,

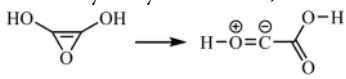

An NBO analysis suggests the Lewis-type structure, as shown, with the hydroxyl OCC angle of 109.5° and an HOCC dihedral of ≈180°. The carboxylic HOC=O *syn* conformer is more stable than the *anti* by some 14.1 kJ mol^{-1}.

3.20.10.1 Species data.

6	0.487 484	0.110 136	0.075 083
6	−0.885 877	−0.050 167	0.622 902
8	0.963 053	1.207 934	−0.083 756
8	−1.750 823	−0.086 342	−0.350 900
8	1.157 609	−1.048 012	−0.056 234
1	2.074 475	−0.827 950	−0.285 498
1	−2.642 834	−0.120 511	0.024 711
B (GHz)	10.356 2	4.360 3	3.350 4

No.	$\bar{\nu}$ (cm^{-1})	x_{ii}
1	3714.92	−84.35
2	3702.76	−94.48
3	1779.26	−10.82
4	1438.03	−6.43
5	1346.54	−4.61
6	1313.27	−6.61
7	1136.95	−6.48
8	851.63	−2.91
9	847.48	−5.20
10	786.62	−2.28
11	589.55	−10.30
12	517.90	−0.26
13	344.82	0.21
14	282.36	0.49
15	111.19	0.30

3.20.10.2 Formation enthalpy, $\Delta_f H(0\ K)$. Multiple composite atomization calculations suggest $\Delta_f H^o(0\ K) = -255.3 \pm 2.4$ kJ mol^{-1} (−263.3 kJ mol^{-1} at 298.15 K), which agrees with a WMS of −252.8 kJ mol^{-1}.

3.20.10.3 Results. Three modes (nos. 15, 11, and 9) are identified with the most impactful, no. 15, having a reduced barrier height (V/RT) of 4.0 and increasing the entropy by 1.6 J K^{-1} mol^{-1} at

T (K)	$S^o(T)$	$C_p^o(T)$	$H^o(T) - H^o(0)$
298.15	305.79	75.74	15.64
300.	306.26	76.02	15.78
400.	330.08	89.85	24.10
500.	351.39	101.13	33.67
600.	370.65	109.95	44.24
700.	388.13	116.82	55.59
800.	404.10	122.26	67.55
900.	418.76	126.68	80.00
1000.	432.31	130.36	92.86
1100.	444.88	133.50	106.06
1200.	456.62	136.23	119.54
1300.	467.62	138.62	133.29
1400.	477.97	140.73	147.26
1500.	487.74	142.59	161.42
1600.	497.00	144.24	175.77
1800.	514.16	146.97	204.90
2000.	529.75	149.04	234.50

300 K. A relaxed scan about the C–C bond is well-behaved and is used to replace mode no. 15.

3.20.11. Hydroxy-2-oxarinone

^{1}A g = 1 C_1 σ = 1 M_0 = 74.0361

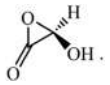

There are two conformers, and we are in agreement with Firth-Clar *et al.* [FRW97] that the one whose dihedral, H–O–C–H, is ~−170° is the more stable by some 5 kJ mol^{-1}.

3.20.11.1 Species data.

6	−0.667 992	0.076 252	0.481 680
6	0.725 782	−0.031 413	0.084 843
8	0.210 877	1.130 619	−0.286 993
1	−0.964 449	0.468 141	1.443 962
8	1.747 063	−0.629 637	−0.022 636
8	−1.705 691	−0.467 524	−0.180 539
1	−1.400 275	−1.004 835	−0.921 753
B (GHz)	12.872 8	4.277 1	3.551 9

No.	$\bar{\upsilon}$ (cm^{-1})	x_{ii}
1	3780.92	−84.40
2	3194.57	−58.30
3	1981.16	−9.60
4	1439.55	−7.60
5	1311.40	−6.23
6	1260.52	−3.50
7	1178.34	−3.96
8	1055.72	−2.28
9	932.94	−4.98
10	732.05	0.01
11	587.01	−3.22
12	538.06	0.09
13	418.86	−8.85
14	381.25	−2.24
15	220.87	0.35

3.20.11.2 Formation enthalpy, $\Delta_f H(0\ K)$. From QCISD(T)(full)/6-311G(2df,p)//MP2(full)/6-311G(d,p) *ab initio* calculations, Firth-Clar *et al.* [FRW97] deduced −377 ± 10 kJ mol^{-1} at 298.15 K for the most stable conformer.

The isodesmic reaction

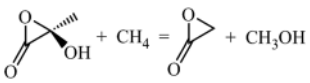

has a reaction enthalpy of +61.64 ± 1.38 kJ mol^{-1}, which together with ATcT values for the chaperones, methane (−66.550 ± 0.057 kJ mol^{-1}) and methanol (−189.83 ± 0.16 kJ mol^{-1}), and our value for 2-oxarinone of −164.9 ± 1.4 kJ mol^{-1} results in $\Delta_f H^o$(0 K) = −349.9 ± 2.0 kJ mol^{-1} (−358.2 kJ mol^{-1} at 298.15 K); WMS returns $\Delta_f H^o$(0 K) = −351.0 kJ mol^{-1}.

Previously, the same isodesmic reaction was used for which a reaction enthalpy change of 62.1 kJ mol^{-1} at 298.15 K was computed [FRW97]—this is in excellent agreement with our $\Delta_r H^o$(298.15 K) = 60.1 ± 1.4 kJ mol^{-1}. The difference in formation enthalpy for the target species is therefore a reflection purely of the differences in the formation enthalpy of 2-oxiranone.

3.20.11.3 Results. The internal rotor, mode no. 13, faces high barriers and has little impact but is included, nonetheless, in the anharmonic treatment.

T (K)	$S^o(T)$	$C_p^o(T)$	$H^o(T) - H^o(0)$
298.15	300.14	76.41	15.33
300.	300.62	76.69	15.47
400.	324.60	90.29	23.84
500.	345.98	101.23	33.44
600.	365.22	109.72	44.00
700.	382.65	116.32	55.32
800.	398.53	121.55	67.22
900.	413.10	125.81	79.59
1000.	426.55	129.35	92.36
1100.	439.02	132.36	105.44
1200.	450.65	134.94	118.81
1300.	461.54	137.19	132.42
1400.	471.78	139.16	146.24
1500.	481.45	140.90	160.24
1600.	490.59	142.46	174.41
1800.	507.53	145.11	203.17
2000.	522.93	147.31	232.42

References for hydroxy-2-oxarinone.

FRW97 S. Firth-Clar, C. F. Rodiquez, and I. H. Williams, "Hydroxyoxiranone: An *ab initio* MO investigation of the structure and stability of a model for a possible α-lactone intermediate in hydrolysis of sialyl glycosides," J. Chem. Soc., Perkin Trans. **2**(10), 1943–1948 (1997).

3.20.12. 2-Oxo-acetic acid; glyoxylic acid

^{1}A′ g = 1 C_S σ = 1 M_0 = 74.0361

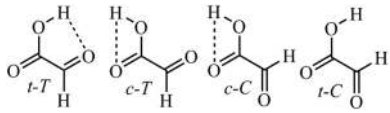

Glyoxylic acid has been proposed as a fundamental prebiotic starting material, and consequently, its identification in the interstellar medium has been important although fruitless so far. However, laboratory experiments in which CO/water ices are irradiated with energetic electrons demonstrated the formation of glyoxylic acid [EBSS19]. It has even been detected in both indoor and outdoor environments [STSZ17].

The lowest energy conformer of 2-oxoacetic acid or glyoxylic acid has a *trans* O=C–C=O configuration, designated *T*, and *trans* HOC=O, *t*, because hydrogen bonding OH···O=C favors the formation of a five-membered ring, *t-T*, over that of a four-membered ring, *c-T*. Those conformers with *cis* O=C–C=O, *c-C* and *t-C*, lie much higher in energy.

Below we compare, relative to *t-T*, zero-point corrected electronic energies obtained in this work from multiple composite chemistries with literature [EBSS19] values for all three conformers.

Conformer	*This* work	[EBSS19]	[B09]
c-T	5.2 ± 0.4	5.4	2.4
t-C	10.0 ± 0.6	10.0	6.1
c-C	33.2 ± 0.7	. . .	32.1

This compound is an intermediate in the ozonolysis of ethyne [CCA01] and results from the rearrangement of dioxiranecarboxaldehyde.

3.20.12.1 Species data.

8	−0.149 414	−1.800 941	0.00 000
6	−0.745 983	−0.755 996	0.000 00
1	−1.843 730	−0.675 476	0.000 00
6	0.000 000	0.582 222	0.000 00
8	−0.580 131	1.630 529	0.000 00
8	1.328 514	0.448 267	0.000 00
1	1.527 877	−0.504 720	0.000 00
1	1.527 877	−0.504 720	0.000 00
B (GHz)	11.017 9	4.602 8	3.246 6

No.	$\bar{\upsilon}$ (cm^{-1})	x_{ii}	
1	3653.82	−97.53	*a′*
2	2994.69	−62.36	*a′*
3	1849.54	−9.28	*a′*
4	1797.36	−10.12	*a′*
5	1374.46	−9.37	*a′*
6	1351.45	−7.45	*a′*
7	1213.90	−3.96	*a′*
8	879.56	−6.31	*a′*
9	687.94	0.10	*a′*
10	500.44	−0.46	*a′*
11	281.13	0.37	*a′*
12	1021.03	−1.71	*a″*
13	688.85	−13.74	*a″*
14	578.12	−1.29	*a″*
15	169.91	0.63	*a″*

3.20.12.2 Formation enthalpy, $\Delta_f H(0\ K)$. The isodesmic reaction for *t-T* 2-oxo-acetic acid

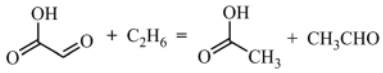

was chosen with reference values for ethane (−68.29 ± 0.14 kJ mol^{-1}), ethanal (−154.96 ± 0.28 kJ mol^{-1}), and *syn* acetic acid (−418.51 ± 0.52 kJ mol^{-1}), which together with an averaged reaction enthalpy of −40.68 ± 0.61 kJ mol^{-1} yields $\Delta_f H°(0\ K)$ = −464.5 ± 0.9 kJ mol^{-1} (−471.1 kJ mol^{-1} at 298.15 K), in moderate agreement with the Cremer *et al.* [CCA01] value of −469 kJ mol^{-1}. WMS, W2X, and W3X-L atomization values of −466.1 kJ mol^{-1}, −465.9 kJ mol^{-1}, and −466.7 kJ mol^{-1} concur. The C(O)–H bond energy is computed at 369 kJ mol^{-1}, which is close to that found in formaldehyde [L07] of 368 kJ mol^{-1}.

3.20.12.3 Results. Two hindered rotors are present, mode nos. 15 and 13, which are associated with the C–C bond and the C–C–O–H dihedral, respectively. A hindered rotor anharmonic treatment is espoused.

T (K)	$S°(T)$	$C_p°(T)$	$H°(T) - H°(0)$
298.15	298.52	78.01	15.81
300.	299.00	78.27	15.95
400.	323.30	90.87	24.43
500.	344.75	101.55	34.06
600.	364.10	110.76	44.69
700.	381.79	118.70	56.17
800.	398.09	125.44	68.38
900.	413.20	131.05	81.22
1000.	427.25	135.62	94.56
1100.	440.36	139.28	108.31
1200.	452.61	142.18	122.38
1300.	464.08	144.46	136.72
1400.	474.85	146.25	151.26
1500.	484.99	147.66	165.96
1600.	494.56	148.77	180.78
1800.	512.18	150.36	210.70
2000.	528.08	151.40	240.88

References for 2-oxo-acetic acid; glyoxylic acid.

EBSS19 A. K. Eckhardt, A. Bergantini, S. K. Singh, P. R. Schreiner, and R. I. Kaiser, "Formation of glyoxylic acid in interstellar ices: A key entry point for prebiotic chemistry," Angew. Chem., Int. Ed. **58**, 5663 (2019).

STSZ17 S. Liu, S. L. Thompson, H. Stark, P. J. Ziemann, and J. L. Jimenez, "Gas-phase carboxylic acids in a university classroom: Abundance, variability, and sources," Environ. Sci. Technol. **51**, 5454 (2017).

B09 G. Buemi, "DFT study of the hydrogen bond strength and IR spectra of formic, oxalic, glyoxylic and pyruvic acids in vacuum, acetone and water solution," J. Phys. Org. Chem. **22**, 933–947 (2009).

CCA01 D. Cremer, R. Crehuet, and J. Anglada, "The ozonolysis of acetylene—A quantum chemical investigation," J. Am. Chem. Soc. **123**, 6127–6141 (2001).

L07 Y.-R. Luo, *Comprehensive Handbook of Chemical Bond Energies* (CRC Press, Boca Raton, USA, 2007), p. 313.

3.20.13. 1,2,3-Trioxolene; 1,2,3-trioxole

$^1A'$ g = 1 C_S σ = 1 M_0 = 74.0361

This species crops up in the reaction of ozone with acetylene and is a primary ozonide intermediate. The reaction is synthetically useful and has been widely studied theoretically with the results being categorized as "unnerving" due to the wide scatter in reported cycloaddition barrier heights [WEH08].

3.20.13.1 Species data.

C	−0.659 017	0.942 232	0.039 412
C	0.659 042	0.942 214	0.039 411
O	−1.168 982	−0.333 575	−0.110 107
H	1.378 082	1.739 278	0.083 673
O	1.168 974	−0.333 605	−0.110 106
O	−0.000 017	−1.180 980	0.140 177
H	−1.378 036	1.739 315	0.083 676
B (GHz)	9.382 2	8.607 0	4.549 7

No.	$\bar{\upsilon}$ (cm^{-1})	x_{ii}	
1	3297.47	−27.22	a'
2	1706.39	−3.57	a'
3	1140.23	−1.11	a'
4	1092.08	−2.25	a'
5	905.22	−2.72	a'
6	711.79	−0.46	a'
7	638.59	3.03	a'
8	183.82	−29.60	a'
9	3272.96	−27.46	a''
10	1299.02	−3.10	a''
11	960.94	−1.05	a''
12	907.80	−0.44	a''
13	798.08	−0.81	a''
14	767.59	−3.40	a''
15	462.76	0.11	a''

3.20.13.2 Formation enthalpy, $\Delta_f H$(0 K). An isodesmic reaction

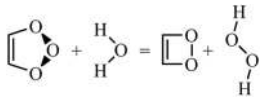

has a reaction enthalpy of 117.98 ± 0.74 kJ mol^{-1}, which allied with reference values for water (−238.931 ± 0.027 kJ mol^{-1}) and hydrogen peroxide (−129.472 ± 0.064 kJ mol^{-1}) together with our computed value for 1,2-dioxete of 140.7 ± 1.7 kJ mol^{-1} yields $\Delta_f H^o$(0 K) = 132.2 ± 1.9 kJ mol^{-1} with a corresponding 121.5 kJ mol^{-1} at 298.15 K.

Multiple composite atomization values of 132.6 ± 5.0 kJ mol^{-1} and a W3X-L of 131.9 kJ mol^{-1} complete a satisfactory picture, which can be summarized as $\Delta_f H^o$(0 K) = 132.0 kJ mol^{-1} (121.3 kJ mol^{-1} at 298.15 K). Formation enthalpies [WEH08] of $\Delta_f H^o$(298.15 K) = 137.2 kJ mol^{-1} and 127.6 kJ mol^{-1} have been reported; only the latter [CCA01] is within reasonable agreement with those from *this work*.

3.20.13.3 Results. Lay *et al.* [LYTB01] reported an entropy of 285.4 J K^{-1} mol^{-1} and a C_p^o(300 K) of 70.88 J K^{-1} mol^{-1} from semi-empirical PM3 calculations; Cremer *et al.* [CCA01] reported S^o = 284.5 J K^{-1} mol^{-1}, which is in good agreement with our standard anharmonic RR treatment. The ring-puckering mode no. 8 is highly anharmonic, and a better approach is indicated.

T (K)	$S^o(T)$	$C_p^o(T)$	$H^o(T) - H^o(0)$
298.15	282.78	62.06	13.11
300.	283.16	62.38	13.22
400.	303.34	78.17	20.27
500.	322.19	90.69	28.74
600.	339.61	100.21	38.31
700.	355.64	107.56	48.71
800.	370.39	113.36	59.77
900.	384.03	118.08	71.35
1000.	396.68	121.99	83.36
1100.	408.47	125.27	95.73
1200.	419.49	128.06	108.40
1300.	429.84	130.45	121.33
1400.	439.58	132.51	134.48
1500.	448.79	134.30	147.82
1600.	457.51	135.86	161.33
1800.	473.67	138.43	188.77
2000.	488.36	140.45	216.66

References for 1,2,3-trioxolene; 1,2,3-trioxolesults.

WEH08 S. E. Wheeler, D. H. Ess, and K. N. Houk, "Thinking out of the black box: Accurate barrier heights of 1,3-dipolar cycloadditions of ozone with acetylene and ethylene," J. Phys. Chem. A **112**(8), 1798–1807 (2008).

LYTB01 T. H. Lay, T. Yamada, P.-L. Tsai, and J. W. Bozzelli, "Thermodynamic parameters and group additivity ring corrections for three- to six-membered oxygen heterocyclic hydrocarbons," J. Phys. Chem. A **101**(13), 2471–2477 (1997).

CCA01 D. Cremer, R. Crehuet, and J. Anglada, "The ozonolysis of acetylene-A quantum chemical investigation," J. Am. Chem. Soc. **123**(25), 6127–6141 (2001).

3.20.14. 2,3,5-Trioxabicyclo[2.1.0]pentane

$^1A'$ g = 1 C_S σ = 1 M_0 = 74.0361

This species, effectively a cyclic version of formic acid anhydride, features as an intermediate in a comprehensive study of the ozonolysis of acetylene [CCA01] at various levels of theory including CCSD(T), CASPT2, and B3LYP–DFT.

3.20.14.1 Species data.

6	−0.220 720	−0.474 259	0.715 199
6	−0.220 720	−0.474 259	−0.715 199
8	−0.220 720	0.948 552	−0.745 646
8	−0.220 720	0.948 552	0.745 646
1	−0.596 050	−1.018 025	1.567 113
1	−0.596 050	−1.018 025	−1.567 113
8	0.921 531	−0.931 209	0.000 000
B (GHz)	11.220	7.532 5	5.488 7

No.	$\bar{\upsilon}$ (cm^{-1})	x_{ii}	
1	3241.48	−28.08	a'
2	1447.32	−6.31	a'
3	1240.17	−2.83	a'
4	1074.54	−3.16	a'
5	1003.40	−1.35	a'
6	893.33	−4.18	a'
7	793.19	−0.88	a'
8	611.43	−0.34	a'
9	3222.81	−28.36	a''
10	1215.22	−1.98	a''
11	1034.55	−1.78	a''
12	936.04	−1.58	a''
13	868.71	−1.27	a''
14	675.10	−0.73	a''
15	481.32	−0.23	a''

3.20.14.2 Formation enthalpy, $\Delta_f H$(0 K).

	(a)	(b)	(c)
H(0 K)	0	114.5 ± 1.4	231.4 ± 1.8
$\Delta_f H^o$(0 K)	−99.6 ± 2.5	15.1 ± 2.8	**132.0 ± 1.9**
$\Delta_f H^o$(298.15 K)	−110.0	3.8	121.3

(a) 2,4,5-trioxabicyclopentane
(b) 2,3,5-trioxabicyclopentane
(c) 1,2,3-trioxolene

A direct comparison via our multi-composite treatment indicates that 2,4,5-trioxabicyclo[1.1.1]pentane is the most stable.

Adoption of the isodesmically derived formation enthalpy for 1,2,3-trioxolene of $\Delta_f H^o$(0 K) = 132.0 ± 1.9 kJ mol^{-1} (see above) then yields the values for the other isomers. A direct W3X-L calculation yields $\Delta_f H^o$(0 K) = 17.7 kJ mol^{-1} (6.4 kJ mol^{-1} at 298.15 K), confirming the isodesmically derived value as does $\Delta_f H^o$(0 K) = 16.7 kJ mol^{-1} from a WMS calculation.

Literature values of 29.3 kJ mol^{-1} and 48.1 kJ mol^{-1} at 298.15 K are available from DFT and CASPT2 calculations, which are not in accord with ours of 4.1 kJ mol^{-1}.

3.20.14.3 Results. Cremer *et al.* reported an entropy of 273.4 J K^{-1} mol^{-1} at 298.15 K, which is in good agreement with our computed values.

T (K)	$S^o(T)$	$C_p^o(T)$	$H^o(T) - H^o(0)$
298.15	273.47	62.04	12.27
300.	273.86	62.40	12.39
400.	294.36	80.50	19.56
500.	313.94	94.85	28.36
600.	332.24	105.70	38.41
700.	349.18	113.95	49.41
800.	364.83	120.40	61.14
900.	379.32	125.57	73.44
1000.	392.78	129.81	86.22
1100.	405.32	133.34	99.38
1200.	417.06	136.31	112.87
1300.	428.07	138.85	126.63
1400.	438.44	141.03	140.62
1500.	448.24	142.91	154.82
1600.	457.51	144.55	169.19
1800.	474.70	147.26	198.38
2000.	490.33	149.38	228.05

References for 2,3,5-trioxabicyclo[2.1.0]pentane.

CCA01 D. Cremer, R. Crehuet, and J. Anglada, "The ozonolysis of acetylene-A quantum chemical investigation," J. Am. Chem. Soc. **123**, 6127–6141 (2001).

3.20.15. 2,4,5-Trioxabicyclo[1.1.1]pentane

$^1A_1$ g = 1 C_{3v} σ = 3 M_0 = 74.0361

Ebrahimi *et al.* studied the structures and relative stabilities of the ground states of [1.1.1] hetero-propellanes including this species [EDR00].

3.20.15.1 Species data.

6	0.000 000	0.000 000	0.811 339
8	0.000 000	1.200 521	−0.000 012
8	−1.039 681	−0.600 260	−0.000 012
8	1.039 681	−0.600 260	−0.000 012
1	0.000 000	0.000 000	1.894 640
6	0.000 000	0.000 000	−0.811 299
1	0.000 000	0.000 000	−1.894 603
B (GHz)	8.772 1	8.772 1	7.307 6

No.	$\bar{\upsilon}$ (cm^{-1})	x_{ii}	g	
1	3198.98	−28.44	1	a_1
2	3191.33	−27.97	1	a_1
3	1311.19	−1.02	1	a_1
4	1006.08	−1.61	1	a_1
5	960.57	−1.37	1	a_1
6	1273.99	−4.53	2	e
7	1121.98	9.27	2	e
8	884.07	0.40	2	e
9	762.07	−0.07	2	e
10	435.81	−71.18	2	e

3.20.15.2 Formation enthalpy, $\Delta_f H$(0 K). As shown above, $\Delta_f H^o$(0 K) = −99.1 ± 2.5 kJ mol^{-1} (−109.5 kJ mol^{-1} at 298.15 K) is indicated, which accords with a W3X-L value of $\Delta_f H^o$(0 K) = −96.6 kJ mol^{-1}.

It is of interest to note that this bicyclopentane, and the previous compound also, has the strongest tertiary C–H bond dissociation energies known, 470 kJ mol^{-1} and 464 kJ mol^{-1}, respectively, rivaling that of the bridgehead C–H in 3-*tert*-butylbicyclo[1.1.1]pentane [RKMD02] of 459 ± 14 kJ mol^{-1} and comfortably exceeding those in bicyclo[2.2.1]heptane, bicyclo[2.2.2]octane, and adamantane [FLTM12].

3.20.15.3 Results. A standard RR anharmonic treatment is used.

T (K)	$S^o(T)$	$C_p^o(T)$	$H^o(T) - H^o(0)$
298.15	270.54	60.36	13.27
300.	270.92	60.59	13.38
400.	290.07	73.14	20.07
500.	307.63	84.25	27.96
600.	323.81	93.17	36.85
700.	338.72	100.20	46.53
800.	352.48	105.83	56.84
900.	365.22	110.42	67.66
1000.	377.06	114.22	78.90
1100.	388.10	117.40	90.48
1200.	398.43	120.10	102.36
1300.	408.14	122.39	114.48
1400.	417.28	124.37	126.82
1500.	425.92	126.07	139.34
1600.	434.11	127.55	152.03
1800.	449.28	129.96	177.79
2000.	463.07	131.84	203.97

References for 2,4,5-trioxabicyclo[1.1.1]pentane.

EDR00 A. Ebrahimi, F. Deyhimi, and H. Roohi, "Investigation of structural properties of heteropropellane compounds by *ab initio* methods," J. Chem. Res. **2000**(2), 93–95.

RKMD02 D. R. Reed, S. R. Kass, K. R. Mondanaro, and W. P. Dailey, "formation of a 1-bicyclo[1.1.1]pentyl anion and an experimental determination of the acidity and C–H bond dissociation energy of 3-tert-Butylbicyclo [1.1.1]pentane," J. Am. Chem. Soc. **124**(11), 2790–2795 (2002).

FLTM12 A. Fattahi, L. Lis, Z. A. Tehrani, S. S. Marimanikkuppam, and S. R. Kass, "Experimental and computational bridgehead C–H bond dissociation enthalpies," J. Org. Chem. **77**(4), 1909–1914 (2012).

3.21. $C_2H_2O_4$

3.21.1. Carboxyformyl ether

$^1A'$ g = 1 C_S σ = 1 M_0 = 90.0355

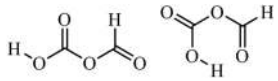

Important conformers include *ssa* and the cyclic *aas* classified according to the HOC=O, O=COC, and COC=O dihedrals. There are no references to this species in the chemical literature.

3.21.1.1 Species data.

	ssa				*aas*		
1	−2.593 768	−0.906 074	0.000 000	8	2.093 153	0.141 789	0.000 000
8	−2.046 551	−0.108 562	0.000 000	6	0.946 669	−0.141 630	0.000 000
8	−0.387 343	−1.642 525	0.000 000	8	0.000 000	0.942 342	0.000 000
6	−0.774 702	−0.508 692	0.000 000	6	1.331 363	0.776 487	0.000 000
8	0.000 000	0.611 130	0.000 000	8	1.925 913	−0.273 105	0.000 000
6	1.380 441	0.438 660	0.000 000	1	1.820 202	1.754 785	0.000 000
8	2.094 940	1.382 644	0.000 000	8	0.419 540	−1.345 436	0.000 000
1	1.670 964	−0.615 224	0.000 000	1	0.565 872	−1.288 656	0.000 000
B (GHz)	10.970 6	2.300 6	1.901 8	*B* (GHz)	9.095 6	2.986 8	2.248 4

	ssa				*aas*		
No.	$\bar{\upsilon}$ (cm^{-1})	x_{ii}			No.	$\bar{\upsilon}$ (cm^{-1})	x_{ii}
1	3775.27	−80.57	a'	1	3347.12	−178.70	a'
2	3083.58	−60.39	a'	2	3078.84	−59.85	a'
3	1876.49	−8.12	a'	3	1942.88	−10.44	a'
4	1831.45	−7.81	a'	4	1761.03	−9.74	a'
5	1398.83	−3.59	a'	5	1458.23	−27.02	a'
6	1374.58	−4.20	a'	6	1403.51	−8.16	a'
7	1191.02	−5.99	a'	7	1229.37	−4.25	a'
8	1059.92	−8.72	a'	8	1127.98	−3.96	a'
9	1012.44	−1.71	a'	9	854.46	−0.90	a'
10	686.70	0.03	a'	10	735.21	−7.20	a'
11	588.24	−0.25	a'	11	578.93	−0.43	a'
12	464.36	−0.38	a'	12	480.05	−0.06	a'
13	239.22	0.05	a'	13	312.65	−1.91	a'
14	1043.78	−3.00	a''	14	1048.86	−2.73	a''
15	795.94	−0.11	a''	15	819.06	−28.75	a''
16	576.01	−11.42	a''	16	768.23	−0.08	a''
17	134.45	−0.87	a''	17	265.08	−2.15	a''
18	99.04	−0.78	a''	18	93.65	−0.52	a''

3.21.1.2 Formation enthalpy, $\Delta_f H(0\ K)$. The isodesmic reaction

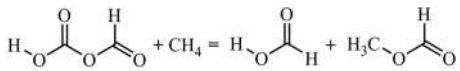

yields a reaction enthalpy of 52.94 ± 1.41 kJ mol^{-1}, which in conjunction with reference values for methane, *syn* formic acid, and *cis* or **Z** methyl formate (−66.550 ± 0.057 kJ mol^{-1}, −371.06 ± 0.22 kJ mol^{-1}, and −344.73 ± 0.59 kJ mol^{-1}, respectively) gives rise to $\Delta_f H^o$(0 K) = −702.2 ± 1.5 kJ mol^{-1} (−712.3 kJ mol^{-1} at 298.15 K) for the *ssa* conformer and $\Delta_f H^o$(0 K) = −697.5 kJ mol^{-1} (−708.5 kJ mol^{-1} at 298.15 K) for the cyclic *aas*.

The high-level atomization methods WMS and W2X return $\Delta_f H^o$(0 K) = −705.4 kJ mol^{-1} and $\Delta_f H^o$(0 K) = −706.9 kJ mol^{-1} for the *ssa*, which indicates that revision of methyl formate, the ATcT reference, might be required—the ATcT value is heavily reliant, to the extent of 96.4%, on just two replicate runs in a combustion calorimeter [HB71] and measurements of the enthalpy of vapourization show some variation [SNV12] as indeed do other estimates [B19] of the formation enthalpy at 298.15 K. Indeed, multi-composite and WMS values for Z-methyl formate are $\Delta_f H^o$(0 K) = −350.4 ± 2.6 kJ mol^{-1} and $\Delta_f H^o$(0 K) = −347.0 kJ mol^{-1}, respectively, suggesting that a downwards revision of some 2.3 kJ mol^{-1} to $\Delta_f H^o$(0 K) = −347.0 ± 1.5 kJ mol^{-1} is necessary with a concomitant change for 298.15 K.

The O–H bond energy of 218.0 + −458.0 − (−712.3) = 472 kJ mol^{-1} is typical of many carboxylic acids, as is the C–H bond energy of 218.0–523.2 − (−712.3) = 407 kJ mol^{-1}.

3.21.1.3 Results. Three hindered rotors are identified for the *ssa* conformer of which just two, mode nos. 18 and 17, impact on the thermochemical properties. The cyclic *aas* by contrast is much less affected since the reduced barrier height (V/RT) = 31.3 for mode no. 17.

	ssa			aas		
T (K)	$S°(T)$	$C°_p(T)$	$H°(T) - H°(0)$	$S°(T)$	$C°_p(T)$	$H°(T) - H°(0)$
298.15	321.72	88.73	17.69	312.11	82.55	16.52
300.	322.27	89.12	17.85	312.62	82.89	16.67
400.	350.70	108.91	27.78	338.88	100.04	25.84
500.	376.75	124.36	39.49	362.81	114.45	36.59
600.	400.46	135.38	52.50	384.76	126.37	48.64
700.	421.94	143.08	66.45	405.01	136.28	61.79
800.	441.43	148.61	81.05	423.76	144.56	75.84
900.	459.18	152.77	96.12	441.20	151.47	90.65
1000.	475.45	156.06	111.57	457.47	157.23	106.10
1100.	490.46	158.78	127.31	472.68	161.98	122.06
1200.	504.37	161.08	143.31	486.95	165.89	138.46
1300.	517.35	163.06	159.51	500.36	169.09	155.21
1400.	529.50	164.77	175.91	512.99	171.69	172.26
1500.	540.92	166.25	192.46	524.91	173.80	189.53
1600.	551.69	167.52	209.14	536.18	175.49	207.00
1800.	571.54	169.51	242.85	557.00	177.95	242.36
2000.	589.48	170.90	276.90	575.84	179.51	278.11

References for carboxyformyl ether.

HB71 H. K. K. Hall, Jr. and J. H. Baldt, "Thermochemistry of strained-ring bridgehead nitriles and esters," J. Am. Chem. Soc. **93**, 140–145 (1971).

SNV12 A. A. Samarov, A. G. Nazmutdinov, and S. P. Verevkin, "Vapour pressures and enthalpies of vaporization of aliphatic esters," Fluid Phase Equilib. **334**, 70–75 (2012).

B19 Thermochemical Data by D. R. Burgess, Jr., in *NIST Chemistry WebBook, NIST Standard Reference Database Number 69*, edited by P. J. Linstrom and W. G. Mallard (National Institute of Standards and Technology, Gaithersburg, MD, 2019) (retrieved October 18, 2019).

3.21.2. Diformyl peroxide

^{1}A g = 1 C_2 σ = 2 M_0 = 90.0355

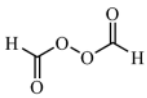

This peroxide has been found during the partial oxidation of methane [FWCK92] and the slow oxidation of ethene [SISK65]. A C_2 structure with a C–O–O–C dihedral of around 90° has been identified as the global minimum [UHTF97], and this is in agreement with our findings.

3.21.2.1 Species data.

8	−0.545 205	−0.473 883	0.869 005
8	0.545 205	0.473 883	0.869 005
6	0.352 296	1.457 446	−0.062 224
1	1.209 679	2.134 017	0.061 219
6	−0.352 296	−1.457 446	−0.062 224
1	−1.209 679	−2.134 017	0.061 219
8	−0.545 205	1.556 799	−0.829 989
8	0.545 205	−1.556 799	−0.829 989
B (GHz)	7.095 4	2.976 0	2.643 4

No.	$\bar{\upsilon}$ (cm^{-1})	x_{ii}		No.	$\bar{\upsilon}$ (cm^{-1})	x_{ii}	
1	3025.51	−31.35	*a*	10	69.66	−2.05	*a*
2	1874.05	−5.13	*a*	11	3025.14	−31.36	*b*
3	1372.82	−4.52	*a*	12	1837.31	−5.07	*b*
4	1027.50	−5.19	*a*	13	1356.80	−4.19	*b*
5	1012.58	−1.33	*a*	14	1026.76	−2.89	*b*
6	867.64	−2.35	*a*	15	1005.63	−1.16	*b*
7	757.72	−1.88	*a*	16	852.57	−2.45	*b*
8	386.80	−0.46	*a*	17	387.06	−0.24	*b*
9	217.24	−0.34	*a*	18	226.92	0.17	*b*

3.21.2.2 Formation enthalpy, $\Delta_f H$ (0 K). The isodesmic reactions

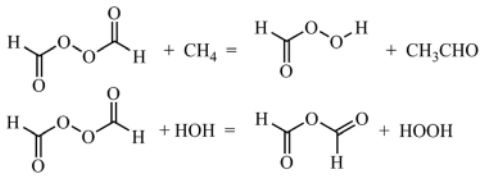

have reaction enthalpies of 40.33 ± 2.76 kJ mol^{-1} and −48.58 ± 1.58 kJ mol^{-1}, respectively. These were used in conjunction with ATcT values for methane (−66.550 ± 0.057 kJ mol^{-1}), peroxyformic acid (−279.8 ± 1.1 kJ mol^{-1}), ethanal (−154.97 ± 0.28 kJ mol^{-1}), water (−238.931 ± 0.027 kJ mol^{-1}), and hydrogen peroxide (−129.47 ± 0.06 kJ mol^{-1}) together with our value for formic acid anhydride (−467.0 ± 0.73 kJ mol^{-1}) to derive $\Delta_f H^o$(0 K) = −406.7 ± 1.5 kJ mol^{-1} (−416.9 kJ mol^{-1} at 298.15 K) based on WMS returns $\Delta_f H^o$(0 K) = −407.5 kJ mol^{-1}, while a multiple composite atomization value of −410.9 ± 5.5 kJ mol^{-1} is just in agreement.

The calculated BDE(O–O) of 2 × (−131.7) − (−417.0) = 154 kJ mol^{-1} is not inconsistent with those cataloged for dialkyl peroxides [L07].

3.21.2.3 Results. Three hindered rotors impinge upon the computed thermodata, namely, rotation about the central O–O bond and about the O–O–C=O dihedrals. Reduced barrier height (V/RT) values of 10 and 22, however, mean that there is little in the way of HR corrections at temperatures below 1000 K.

T (K)	$S^o(T)$	$C_p^o(T)$	$H^o(T) - H^o(0)$
298.15	317.82	82.08	17.73
300.	318.33	82.34	17.88
400.	343.90	95.94	26.80
500.	366.64	108.01	37.02
600.	387.25	118.07	48.33
700.	406.10	126.35	60.57
800.	423.43	133.19	73.56
900.	439.45	138.86	87.16
1000.	454.34	143.61	101.29
1100.	468.22	147.61	115.86
1200.	481.21	151.00	130.79
1300.	493.42	153.90	146.04
1400.	504.91	156.38	161.56
1500.	515.78	158.53	177.30
1600.	526.07	160.39	193.25
1800.	545.15	163.47	225.65
2000.	562.50	165.87	258.58

References for diformyl peroxide.

FWCK92 K. W. Frese, Jr., F. Wang, C. Chen, and K. Krist, "Partial oxidation of methane in aqueous electrochemical systems," Am. Chem. Soc., Div. Pet. Chem. **37**(1), 15–25 (1992).

SISK65 K. Sugino, E. Inoue, K. Shirai, T. Koseki, and T. Gomi, "Slow oxidation of ethylene by silent electric discharge," Nippon Kagaku Zasshi **86**(11), 1200–1201 (1965).

UHTF97 T. Uchimaru, R. Hara, K. Tanabe, and K. Fujimori, "Acyloxyl radical pair intermediate for the initial stage of the thermal decomposition of diacyl peroxide: A density functional study," Chem. Phys. Lett. **267**, 244–250 (1997).

L07 Y.-R. Luo, *Comprehensive Handbook of Chemical Bond Energies* (CRC Press, Boca Raton, USA, 2007), p. 313.

3.21.3. Dioxirane carboxylic acid

^{1}A g = 1 C_1 σ = 1 M_0 = 90.0355

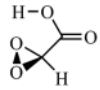

The lowest energy structure is characterized by H–C–C=O and H–O–C=O dihedrals of ~0° and ~180°, as shown above. Apart from a study by Sung [S00] on substituent effects on the stability of dioxiranes, there is no other work reported.

3.21.3.1 Species data.

6	−0.534 021	−0.619 792	−0.174 831
8	−1.509 472	0.253 676	−0.647 442
8	−1.462 196	−0.201 577	0.775 726
1	−0.590 034	−1.654 727	−0.497 569
6	0.875 740	−0.069 191	−0.027 579
8	1.827 291	−0.794 833	−0.012 602
8	0.953 562	1.260 646	0.095 654
1	0.066 237	1.645 334	0.021 337
B (GHz)	7.841 5	2.996 4	2.540 18

No.	$\bar{\upsilon}$ (cm^{-1})	x_{ii}	No.	$\bar{\upsilon}$ (cm^{-1})	x_{ii}
1	3715.80	−89.17	10	883.36	−2.12
2	3148.87	−57.91	11	843.09	−2.52
3	1861.24	−9.16	12	751.77	−0.37
4	1404.09	−6.03	13	652.51	−0.25
5	1357.25	−6.24	14	564.36	−30.78
6	1278.19	−1.99	15	468.27	−0.18
7	1214.37	−3.08	16	288.53	−0.18
8	1165.86	−4.77	17	264.00	0.11
9	887.67	−3.18	18	60.58	−16.68

3.21.3.2 Formation enthalpy, $\Delta_f H$(0 K). The isodesmic reaction

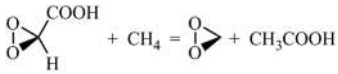

is essentially thermoneutral, as is to be expected, with a reaction enthalpy of −0.30 ± 1.9 kJ mol^{-1} from which $\Delta_f H^o$(0 K) = −342.1 ± 2.1 kJ mol^{-1} (−352.3 kJ mol^{-1} at 298.15 K) emerges based on ATcT values for the chaperones methane (−66.550 ± 0.057 kJ mol^{-1}),

dioxirane (9.45 ± 0.55 kJ mol^{-1}), and *syn* acetic acid (−418.38 ± 0.54 kJ mol^{-1}); WMS concurs at $\Delta_f H^o$(0 K) = −343.1 kJ mol^{-1}.

3.21.3.3 Results. Hindered rotor analysis shows that mode no. 18 is associated with the C–C rotor and no. 14 with H–O–C=O; the first has the ratio of barrier height to thermal energy [(*V*/*RT*)] of 2.2 at room temperature, while the second has (*V*/*RT*) = 16.7; both vibrational modes are replaced by hindered rotors in an overall anharmonic treatment.

T (K)	$S^o(T)$	$C_p^o(T)$	$H^o(T) - H^o(0)$
298.15	323.89	84.01	17.73
300.	324.41	84.33	17.88
400.	350.98	100.81	27.16
500.	375.03	114.88	37.96
600.	397.03	126.39	50.04
700.	417.24	135.68	63.16
800.	435.86	143.14	77.12
900.	453.08	149.11	91.74
1000.	469.05	153.90	106.90
1100.	483.90	157.75	122.48
1200.	497.77	160.86	138.42
1300.	510.74	163.38	154.63
1400.	522.93	165.45	171.08
1500.	534.41	167.16	187.71
1600.	545.24	168.58	204.50
1800.	565.23	170.78	238.44
2000.	583.31	172.39	272.76

References for dioxirane carboxylic acid.

S00 K. Sung, "Substituent effects on stability of oxiranes, oxirenes, and dioxiranes," Can. J. Chem. **78**(5), 562–567 (2000).

3.21.4. Oxalic acid; ethanedioic acid

^1A_g g = 1 C_{2h} σ = 2 M_0 = 90.0355

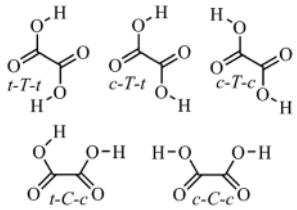

Oxalic acid is one of the many commodity chemicals that can be produced from the catalytic oxidation of carbohydrates in one-pot reactions [ZH18]. It is the most abundant and ubiquitous diacid in atmospheric aerosols [KB16].

There are six low energy conformers for oxalic acid as outlined in the literature [CS00, B09], with the most stable having O=C–C=O *trans* or *anti*, designated *T*, and varying H–O–C=O dihedrals *t*-*T*-*t*, *c*-*T*-*t*, and *c*-*T*-*c*. There are three conformers with *cis* or *syn* O=C–C=O, *C*, namely, *c*-*C*-*c*, *t*-*C*-*c*, and *t*-*C*-*t*, but the latter is non-planar and lies much higher in energy, > 50 kJ mol^{-1}. Relative, to the C_{2h} ground state *t*-*T*-*t*, zero-point corrected electronic energies are (kJ mol^{-1}):

Conformer	Point group	*This* work	[CS00]	[B09]
c-*T*-*t*	C_S	10.7 ± 0.4	7.0	12.0
c-*T*-*c*	C_{2h}	16.7 ± 0.8	8.4	8.3
c-*C*-*c*	C_{2v}	18.9 ± 1.0	9.9	13.3
t-*C*-*c*	C_S	23.3 ± 0.9	17.9	18.5

3.21.4.1 Species data.

1	−1.312 855	1.413 811	0.000 000
8	−0.391 364	1.732 597	0.000 000
8	1.593 339	0.683 246	0.000 000
6	0.391 364	0.664 441	0.000 000
6	−0.391 364	−0.664 441	0.000 000
8	−1.593 339	−0.683 246	0.000 000
8	0.391 364	−1.732 597	0.000 000
1	1.312 855	−1.413 811	0.000 000
B (GHz)	5.812 99	3.831 18	2.309 23

No.	$\bar{\upsilon}$ (cm^{-1})	x_{ii}	
1	3635.19	−50.65	a_g
2	1832.19	−4.79	a_g
3	1439.58	−5.09	a_g
4	1224.58	−2.34	a_g
5	824.44	−1.45	a_g
6	563.33	−0.40	a_g
7	405.28	−0.16	a_g
8	710.56	−9.00	a_u
9	465.27	0.59	a_u
10	125.65	−0.70	a_u
11	838.44	−0.61	b_g
12	708.44	−6.18	b_g
13	3638.49	−49.95	b_u
14	1855.56	−4.79	b_u
15	1336.71	−6.10	b_u
16	1206.20	−2.61	b_u
17	675.55	0.20	b_u
18	261.67	1.60	b_u

3.21.4.2 Formation enthalpy, $\Delta_f H(0\ K)$. Earlier it was shown [SS15] that there was disagreement with ATcT [RB16] values; the order *c-T-c* > *c-T-t* > *t-T-t* was established with 16.7 ± 0.8 kJ mol^{-1} > 10.7 ± 0.4 kJ mol^{-1} > 0 kJ/mol at 298.15 K.

The enthalpy change for the isodesmic reaction:

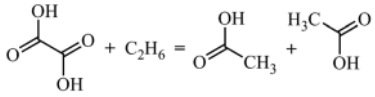

of −44.73 ± 1.14 kJ mol^{-1} yields, in conjunction with reference values for ethane (−68.33 ± 0.13 kJ mol^{-1}) and *syn*-acetic acid (−418.51 ± 0.52 kJ mol^{-1}), $\Delta_f H^o(0\ K) = -724.0 \pm 1.4$ kJ mol^{-1} (−734.3 kJ mol^{-1} at 298.15 K) for the most stable *tTt* conformer. Reaction enthalpies of −44.84 kJ mol^{-1} and −44.39 kJ mol^{-1} are obtained from W2X and W3X-L calculations, respectively, which reinforces the essential correctness of the computed reaction enthalpy.

Atomization calculations are in good agreement, viz., multi-composites yield $\Delta_f H^o(0\ K) = -726.7 \pm 5.3$ kJ mol^{-1}, W2X and W3X-l yields −725.5 kJ mol^{-1} and −726.4 kJ mol^{-1}, and WMS yields −724.3 kJ mol^{-1}; all our results can be summarized as $\Delta_f H^o(0\ K) = -724.9 \pm 1.0$ kJ mol^{-1} and $\Delta_f H^o(298.15\ K) = -735.2$ kJ mol^{-1}.

The agreement with Dorofeeva *et al.* [DNN01] who obtained $\Delta_f H^o(0\ K) = -721.2 \pm 2.0$ kJ mol^{-1} (−731.8 kJ mol^{-1} at 298.15 K), respectively, from rotating bomb calorimetric [WS64] and vapor pressure experiments [BC53], is just within combined uncertainties. This is probably surprising, given that solid oxalic acid exhibits polymorphism and that different saturation vapor pressures and sublimation enthalpies have been reported for the polymorphs [BBBC15].

In a very recent publication [FBR19], Feller *et al.* carried out some very high level FPD calculations and obtained $\Delta_f H^o(0\ K) = -721.8 \pm 4.0$ kJ mol^{-1}, which is again within joint uncertainties. However, the major revision of the ATcT thermochemical network prompted by that work results in a final value of $\Delta_f H^o(0\ K) = -721.0 \pm 1.2$ kJ mol^{-1} (−731.6 kJ mol^{-1} at 298.15 K), which is only marginally in agreement. Their study [FBR19], prompted, in part, by an earlier critique [SS15], in addition offers a complete re-examination of all pertinent experimental and theoretical data.

3.21.4.3 Results. The thermochemical data are not in good agreement with the values determined by Dorofeeva *et al.* [DNN01] For example, see the following table:

T (K)	$S^o(T)$	$C_p^o(T)$	$H^o(T) - H^o(0)$
298.15	320.644	86.176	17.231

At issue here is the difference in the treatment of the hindered rotor about the C–C bond because in all other respects the underlying molecular data (geometry, symmetry, and moments of inertia) are very similar. In their case, a ν_{10} of ~90 cm^{-1} is replaced by a potential energy function whose barrier is 700 cm^{-1} or 8.4 kJ mol^{-1}. We find that the barrier to a relaxed potential energy scan about C–C is >50 kJ mol^{-1} and incorporation of an HR treatment for this mode has little effect. Nevertheless, *here* we replace all three modes with HRs and anharmonic frequencies for the remainder.

Gaussian's own hindered rotor treatment concurs, identifying ν_{10} with the C–C rotor and ν_8 and ν_{12} with H–O–C=O rotors. In all cases, the reduced barrier height (V/RT) ratio is >18.5, and hence, the changes to S^o and C_p^o are minimal if McClurg or Pitzer and Gwinn or Truhlar corrections are applied.

It is instructive to observe how the entropy, S^o/J K^{-1} mol^{-1}, varies according to the level of treatment.

Treatment of vibrational modes	S^o(298.15 K)	S^o(2000 K)
Pure vibrations	307.8	564.0
Anharmonics	304.0	562.0
Anharmonics + hindered rotor no. 1	312.3	580.3
Anharmonics + hindered rotor nos. 1 and 2	311.8	584.2
Anharmonics + hindered rotor nos. 1, 2, and 3	310.5	580.6

Although frequencies and anharmonicities and the potential energy scans reported by various functionals varies, for example, the net effect at room temperature is slight, at least for this set of functionals; even at the higher temperature, the variation in S only amounts to 1%.

	$\bar{\upsilon}$	x_{ii}	S^o(298.15 K)	S^o(2000 K)
B3LYP/Def2TZVP	3624.20	−48.14	311.61	580.38
M06-2X/Def2TZVP	3719.84	−70.06	310.90	575.85
B97XD/Def2TZVP	3707.40	−28.58	311.16	584.58

Dorofeeva and colleagues acknowledged that uncertainties can arise from their adopted vibrational frequencies and the approximate model for internal rotation, and these could reach as much as 10 J K^{-1} mol^{-1} for S^o and 7 J K^{-1} mol^{-1} for C_p^o.

T (K)	$S^o(T)$	$C_p^o(T)$	$H^o(T) - H^o(0)$
298.15	310.50	91.20	17.60
300.	311.06	91.55	17.77
400.	339.79	108.34	27.79
500.	365.44	121.49	39.31
600.	388.53	131.72	51.99
700.	409.47	139.86	65.58
800.	428.60	146.57	79.91
900.	446.20	152.27	94.86
1000.	462.51	157.21	110.34
1100.	477.69	161.50	126.28
1200.	491.91	165.23	142.62
1300.	505.27	168.44	159.30
1400.	517.85	171.15	176.29
1500.	529.74	173.41	193.51
1600.	540.99	175.25	210.95
1800.	561.80	177.90	246.28
2000.	580.63	179.45	282.03

References for oxalic acid; ethanedioic acid.

ZH18 Z. Zhang and G. W. Huber, "Catalytic oxidation of carbohydrates into organic acids and furan chemicals," Chem. Soc. Rev. **47**, 1351 (2018).

KB16 K. Kawamura and S. Bikkina, "A review of dicarboxylic acids and related compounds in atmospheric aerosols: Molecular distributions, sources and transformation," Atmos. Res. **170**, 140 (2016).

CS00 C. Chen and S.-F. Shyu, "Conformers and intramolecular hydrogen bonding of the oxalic acid monomer and its anions," Int. J. Quantum Chem. **76**, 541–551 (2000).

B09 G. Buemi, "DFT study of the hydrogen bond strength and IR spectra of formic, oxalic, glyoxylic and pyruvic acids in vacuum, acetone and water solution," J. Phys. Org. Chem. **22**, 933–947 (2009).

SS15 J. M. Simmie and K. P. Somers, "Benchmarking compound methods (CBS-QB3, CBS-APNO, G3, G4, W1BD) against the active thermochemical tables: A litmus test for cost-effective molecular formation enthalpies," J. Phys. Chem. A **119**(28), 7235–7246 (2015).

RB16 B. Ruscic and D. H. Bross, Active Thermochemical Tables (ATcT) values based on ver. 1.122 of the Thermochemical Network, 2016, available at https://ATcT.anl.gov.

DNN01 O. V. Dorofeeva, V. P. Novikov, and D. B. Neumann, "NIST-JANAF thermochemical tables. I. Ten organic molecules related to atmospheric chemistry," J. Phys. Chem. Ref. Data **30**, 475–513 (2001).

WS64 R. C. Wilhoit and D. Shiao, "Thermochemistry of biologically important compounds. Heats of combustion of solid organic acids," J. Chem. Eng. Data **9**, 595–599 (1964).

BC53 R. S. Bradley and S. Cotson, "The vapour pressure and lattice energy of hydrogen-bonded crystals .Part II. α- and β-Anhydrous oxalic acid and tetragonal pentaerythritol," J. Chem. Soc. **1953**, 1684–1688.

BBBC15 M. Bilde, K. Barsanti, M. Booth, C. D. Cappa, N. M. Donahue, E. U. Emanuelsson, G. McFiggans, U. K. Krieger, C. Marcolli, D. Topping, P. Ziemann, M. Barley, S. Clegg, B. Dennis-Smither, M. Hallquist, Å. M. Hallquist, A. Khlystov, M. Kulmala, D. Mogensen, C. J. Percival, F. Pope, J. P. Reid, M. A. V. Ribeiro da Silva, T. Rosenoern, K. Salo, V. P. Soonsin, T. Yli-Juuti, N. L. Prisle, J. Pagels, J. Rarey, A. A. Zardini, and I. Riipinen, "Saturation vapor pressures and transition enthalpies of low-volatility organic molecules of atmospheric relevance: From dicarboxylic acids to complex mixtures," Chem. Rev. **115**(10), 4115–4156 (2015).

FBR19 D. Feller, D. H. Bross, and B. Ruscic, "Enthalpy of formation of $C_2H_2O_4$ (oxalic acid) from high-level calculations and the active thermochemical tables approach," J. Phys. Chem. A **123**, 3481–3496 (2019).

ZH18 Z. Zhang and G. W. Huber, "Catalytic oxidation of carbohydrates into organic acids and furan chemicals," Chem. Soc. Rev. **47**, 1351 (2018).

KB16 K. Kawamura and S. Bikkina, "A review of dicarboxylic acids and related compounds in atmospheric aerosols: Molecular distributions, sources and transformation," Atmos. Res. **170**, 140 (2016).

CS00 C. Chen and S.-F. Shyu, "Conformers and intramolecular hydrogen bonding of the oxalic acid monomer and its anions," Int. J. Quantum Chem. **76**, 541–551 (2000).

B09 G. Buemi, "DFT study of the hydrogen bond strength and IR spectra of formic, oxalic, glyoxylic and pyruvic acids in vacuum, acetone and water solution," J. Phys. Org. Chem. **22**, 933–947 (2009).

SS15 J. M. Simmie and K. P. Somers, "Benchmarking compound methods (CBS-QB3, CBS-APNO, G3, G4, W1BD) against the active thermochemical tables: A litmus test for cost-effective molecular formation enthalpies," J. Phys. Chem. A **119**(28), 7235–7246 (2015).

RB16 B. Ruscic and D. H. Bross, Active Thermochemical Tables (ATcT) values based on ver. 1.122 of the Thermochemical Network, 2016, available at https://ATcT.anl.gov.

DNN01 O. V. Dorofeeva, V. P. Novikov, and D. B. Neumann, "NIST-JANAF thermochemical tables. I. Ten organic molecules related to atmospheric chemistry," J. Phys. Chem. Ref. Data **30**, 475–513 (2001).

WS64 R. C. Wilhoit and D. Shiao, "Thermochemistry of biologically important compounds. Heats of combustion of solid organic acids," J. Chem. Eng. Data **9**, 595–599 (1964).

BC53 R. S. Bradley and S. Cotson, "The vapour pressure and lattice energy of hydrogen-bonded crystals .Part II. α- and β-Anhydrous oxalic acid and tetragonal pentaerythritol," J. Chem. Soc. **1953**, 1684–1688.

BBBC15 M. Bilde, K. Barsanti, M. Booth, C. D. Cappa, N. M. Donahue, E. U. Emanuelsson, G. McFiggans, U. K. Krieger, C. Marcolli, D. Topping, P. Ziemann, M. Barley, S. Clegg, B. Dennis-Smither, M. Hallquist, Å. M. Hallquist, A. Khlystov, M. Kulmala, D. Mogensen, C. J. Percival, F. Pope, J. P. Reid, M. A. V. Ribeiro da Silva, T. Rosenoern, K. Salo, V. P. Soonsin, T. Yli-Juuti, N. L. Prisle, J. Pagels, J. Rarey, A. A. Zardini, and I. Riipinen, "Saturation vapor pressures and transition enthalpies of low-volatility organic molecules of atmospheric relevance: From dicarboxylic acids to complex mixtures," Chem. Rev. **115**(10), 4115–4156 (2015).

FBR19 D. Feller, D. H. Bross, and B. Ruscic, "Enthalpy of formation of $C_2H_2O_4$ (oxalic acid) from high-level calculations and the active thermochemical tables approach," J. Phys. Chem. A **123**, 3481–3496 (2019).

3.21.5. Peroxyglyoxylic acid; 2-oxo-ethaneperoxoic acid

$^1A'$ g = 1 C_S σ = 1 M_0 = 90.0355

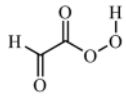

The ground state conformer *aas* (O=CC=O/CCOO/COOH) adopts a *syn* COOH and in common with oxalic acid an *anti* (*trans*) O=CC=O arrangement; the *aaa* conformer lies 10.96 ± 0.84 kJ mol^{-1} above. Peroxyglyoxylic acid features in just three publications [RF13, MBT07, SU04] largely concerned with atmospheric reactions in which it is an intermediate or product. Thus, Maranzana *et al.* showed [MBT07] that it crops up as a product (**B4**) in the reaction of acetyl radical with molecular oxygen, and Rypkema and Francisco [RF13] found that it features in the atmospheric oxidation of peroxyacetic acid, $CH_3C(O)OOH$, in their methyl H abstraction pathway no. 3.

3.21.5.1 Species data.

C	1.525 244	0.260 282	0.000 000
O	2.107 696	−0.782 754	0.000 000
C	0.000 000	0.399 619	0.000 000
H	2.017 618	1.247 867	0.000 000
O	−0.560 365	1.469 399	0.000 000
O	−0.626 360	−0.777 863	0.000 000
O	−2.051 456	−0.606 342	0.000 000
H	−2.125 195	0.373 205	0.000 000
B (GHz)	7.888 1	2.710 2	2.017 1

No.	$\bar{\upsilon}$ (cm^{-1})	x_{ii}	
1	3509.33	−106.38	a'
2	2959.94	−63.40	a'
3	1824.91	−9.86	a'
4	1779.79	−9.29	a'
5	1493.78	−9.54	a'
6	1380.28	1.87	a'
7	1266.41	−7.50	a'
8	983.07	−5.00	a'
9	921.12	−1.46	a'
10	707.80	−0.20	a'
11	505.56	−0.68	a'
12	361.01	−0.72	a'
13	205.82	0.41	a'
14	1018.40	−1.72	a''
15	615.68	−1.20	a''
16	436.05	−28.28	a''
17	205.74	−0.61	a''
18	83.88	−1.30	a''

3.21.5.2 Formation enthalpy, $\Delta_f H(0\ K)$. A value of −694.7 kJ mol^{-1} from CCSD(T) energies at MP2/6-311++G(2df,2p) geometries is reported [MBT07], and the value of −277.9 kJ mol^{-1} can be extracted [SU04] from relative zero-point corrected electronic energies at B3LYP/6-311G(2df,p).

The isodesmic reaction

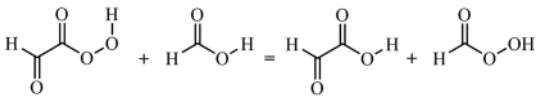

has a reaction enthalpy of −8.81 ± 0.64 kJ mol^{-1}, which translates to $\Delta_f H^o(0\ K)$ = −366.2 ± 1.3 kJ mol^{-1} (−375.4 kJ mol^{-1} at 298.15 K), based on the ATcT reference value for formic (−371.12 ± 0.22 kJ mol^{-1}) and ours for peroxyformic acid (−281.6 ± 0.6 kJ mol^{-1}) and our result for *tT* oxoacetic acid q.v. (−464.50 ± 0.86 kJ mol^{-1}). WMS yields $\Delta_f H^o(0\ K)$ = −365.3 kJ mol^{-1} in good agreement.

The 298.15 K value in conjunction with that for the appropriate radicals q.v. gives a BDE(C–H) of 218.0–210.9 + 375.4 = 383 kJ mol^{-1}, typical [L07] of C–H bonds in species with an α-C(O) group, and a BDE(O–H) of 218.0–182.9 + 375.4 = 411 kJ mol^{-1}, similar to that for benzeneperoxy carboxylic acid, $C_6H_5C(O)OO$–H, of 404 kJ mol^{-1}.

3.21.5.3 Results. Analysis identifies two hindered rotors, mode no. 16 with the O–O dihedral reduced barrier height (*V*/*RT*) = 13.5 and no. 18 with the C–C dihedral for which (*V*/*RT*) = 4.3.

T (K)	$S^o(T)$	$C_p^o(T)$	$H^o(T) - H^o(0)$
298.15	333.75	99.98	19.83
300.	334.37	100.30	20.02
400.	365.37	114.92	30.83
500.	392.13	124.68	42.84
600.	415.51	131.69	55.67
700.	436.24	137.23	69.12
800.	454.87	141.87	83.08
900.	471.82	145.85	97.47
1000.	487.37	149.32	112.23
1100.	501.75	152.34	127.32
1200.	515.12	155.00	142.69
1300.	527.62	157.33	158.30
1400.	539.36	159.39	174.14
1500.	550.42	161.22	190.17
1600.	560.88	162.85	206.38
1800.	580.22	165.63	239.23
2000.	597.80	167.93	272.59

References for peroxyglyoxylic; 2-oxo-ethaneperoxoic acids.

RF13 H. A. Rypkema and J. S. Francisco, "Atmospheric oxidation of peroxyacetic acid," J. Phys. Chem. A **117**(51), 14151 (2013).

MBT07 A. Maranzana, J. R. Barker, and G. Tonachini, "Master equation simulations of competing unimolecular and bimolecular reactions: Application to OH production in the reaction of acetyl radical with O_2," Phys. Chem. Chem. Phys. **9**(31), 4129–4141 (2007).

SU04 L. V. Serebrennikov and N. A. Uvarov, "Calculations of intermediates and transition states in the reaction of glyoxal with hydrogen peroxide and possible reaction channels," Z. Fiz. Khim. **78**(11), 2033–2039 (2004).

L07 Y.-R. Luo, *Comprehensive Handbook of Chemical Bond Energies* (CRC Press, Boca Raton, USA, 2007).

3.21.6. 1,2,3,4-Tetroxin

^1A g = 1 C_2 σ = 2 M_0 = 90.0355

There are very few references to this compound in the literature. Carbó and Fraga [CF72] used an all-valence electron SCF with the configuration interaction method to determine ionization potentials, electron affinities, dipole moments, and electron distributions for this species.

3.21.6.1 Species data.

6	0.004 785	0.664 010	1.133 968
6	−0.004 785	−0.664 010	1.133 968
8	−0.004 785	1.421 400	−0.011 418
1	−0.038 760	−1.268 938	2.025 465
8	0.004 785	−1.421 400	−0.011 418
8	−0.431 335	0.548 195	−1.092 242
8	0.431 335	−0.548 195	−1.092 242
1	0.038 760	1.268 938	2.025 465
B (GHz)	6.134 9	5.374 7	3.046 5

No.	$\bar{\upsilon}$ (cm^{-1})	x_{ii}	
1	3244.68	−27.85	*a*
2	1723.83	−5.29	*a*
3	1228.91	−0.11	*a*
4	1005.78	−1.68	*a*
5	899.09	−2.03	*a*
6	850.45	−0.80	*a*
7	606.57	−0.88	*a*
8	547.12	−2.15	*a*
9	533.18	0.31	*a*
10	414.81	−0.48	*a*
11	3226.72	−27.99	*b*
12	1370.04	−3.34	*b*
13	1061.92	−1.92	*b*
14	969.55	−0.79	*b*
15	818.64	−4.66	*b*
16	686.65	−0.30	*b*
17	588.97	−0.20	*b*
18	170.02	−10.15	*b*

3.21.6.2 Formation enthalpy, $\Delta_f H(0\ K)$. A well-balanced isodesmic reaction is difficult to frame but the following

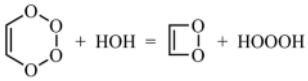

which relies on reference values for water (−238.931 ± 0.027 kJ mol^{-1}) and trioxidane (−81.43 ± 0.70 kJ mol^{-1}) and our previous value for 1,2-dioxete (140.68 ± 1.69 kJ mol^{-1}), provides a well-defined reaction enthalpy of 149.10 ± 0.90 kJ mol^{-1}, and hence $\Delta_f H°(0\ K)$ = 149.1 ± 2.1 kJ mol^{-1}, in accord with a multi-composite approach of 148.2 ± 6.7 kJ mol^{-1}. The corresponding value at 298.15 K is 136.0 kJ mol^{-1}.

3.21.6.3 Results. Hindered rotor corrections are unnecessary, and ring puckering modes are treated purely as anharmonics.

T (K)	$S°(T)$	$C_p°(T)$	$H°(T) - H°(0)$
298.15	296.56	81.65	15.71
300.	297.07	82.01	15.87
400.	323.13	99.36	24.97
500.	346.81	112.76	35.60
600.	368.32	122.94	47.41
700.	387.88	130.81	60.11
800.	405.78	137.05	73.52
900.	422.22	142.13	87.48
1000.	437.42	146.32	101.91
1100.	451.54	149.85	116.73
1200.	464.71	152.84	131.86
1300.	477.05	155.40	147.28
1400.	488.65	157.60	162.93
1500.	499.59	159.52	178.79
1600.	509.94	161.20	194.82
1800.	529.09	163.97	227.35
2000.	546.49	166.16	260.37

References for 1,2,3,4-tetroxin.

CF72 R. Carbó and S. Fraga, "AVE–CI–SCF studies in molecular structure .4. 6-membered heterocycles with nitrogen and oxygen," Ann. Fis. **68**, 21–28 (1972).

3.22. $C_2H_2O_5$

3.22.1. Dicarbonic acid

$^1A'$ g = 1 C_S σ = 1 M_0 = 106.0349

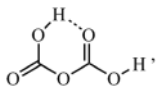

In an extensive recent set of DFT calculations of a series of polycarbonates C_nO_{2n+1} containing $(CO_2)_n$ units where n = 2–6, and so including dicarbonic acid, Bruna *et al.* [BGP11] discussed their structures and stabilities. For the species of interest *here*, they reported seven different rotational isomers with the lowest energy state possessing C_S symmetry and a single hydrogen atom bridge bonding to a carbonyl O-atom, as per the sketch above. Lewars [L96] in an earlier study reported different results. Our results show that the ground state is the O=C–O–H *anti* and H–O–C=O *syn* conformer above, but the *anti/anti* is only +1.5 kJ mol^{-1} higher; the rotational barrier amounts to 44 kJ mol^{-1}.

3.22.1.1 Species data.

6	−1.128 568	0.008 738	0.000 00
8	−1.219 635	−1.202 641	0.000 00
8	−2.161 854	0.840 281	0.000 00
1	−2.967 018	0.303 702	0.000 00
8	0.000 000	0.723 506	0.000 00
6	1.310 608	0.129 629	0.000 00
8	2.230 052	0.870 809	0.000 00
8	1.334 441	−1.181 387	0.000 00
1	0.410 741	−1.538 459	0.000 00
B (GHz)	6.323 7	2.009 8	1.525 1

No.	$\bar{\upsilon}$ (cm^{-1})	x_{ii}	
1	3771.16	−80.12	a'
2	3294.54	−191.28	a'
3	1948.68	−10.22	a'
4	1765.20	−9.12	a'
5	1486.28	−20.05	a'
6	1415.95	−5.37	a'
7	1220.47	−4.84	a'
8	1175.60	−2.68	a'
9	1034.10	−3.17	a'
10	851.26	−2.91	a'
11	703.26	−0.99	a'
12	637.17	0.18	a'
13	484.30	0.00	a'
14	443.17	−0.11	a'
15	279.48	−0.95	a'
16	843.62	−17.76	a''
17	786.43	−1.21	a''
18	761.53	1.11	a''
19	572.59	−14.34	a''
20	127.68	−2.64	a''
21	87.99	0.48	a''

3.22.1.2 Formation enthalpy, $\Delta_f H(0\ K)$. An isodesmic reaction $O(COOH)_2 + CH_4 \rightarrow O{=}C(OH)_2 + CH_3COOH$, which relates the dicarbonic acid to carbonic acid itself, has a reaction enthalpy of −19.37 ± 2.09 kJ mol^{-1}; this together with reference values for methane (−66.550 ± 0.057 kJ mol^{-1}), acetic (−418.38 ± 0.54 kJ mol^{-1}) and carbonic (−602.78 ± 0.79 kJ mol^{-1}) acids leads to $\Delta_f H^o$(0 K) = −935.2 ± 2.3 kJ mol^{-1} (−948.8 kJ mol^{-1} at 298.15 K), in agreement with $\Delta_f H^o$(0 K) = −935.7 kJ mol^{-1} from WMS and within the $\Delta_f H^o$(0 K) = −939.0 ± 6.6 kJ mol^{-1} from multiple composites.

3.22.1.3 Results. Hindered rotor analysis identifies mode nos. 19 and 20; a scan of the OCOC dihedral is problematic and since the "free" OH rotor, mode no. 19, contributes the most, just this is included.

T (K)	$S^o(T)$	$C_p^o(T)$	$H^o(T) - H^o(0)$
298.15	338.34	98.54	19.28
300.	338.95	98.96	19.46
400.	370.25	118.75	30.39
500.	398.42	133.53	43.04
600.	423.79	144.59	56.97
700.	446.75	153.15	71.87
800.	467.66	160.00	87.54
900.	486.84	165.61	103.83
1000.	504.54	170.29	120.63
1100.	520.96	174.24	137.86
1200.	536.27	177.60	155.45
1300.	550.61	180.49	173.36
1400.	564.07	183.00	191.53
1500.	576.78	185.20	209.94
1600.	588.79	187.13	228.56
1800.	611.03	190.39	266.32
2000.	631.23	192.99	304.66

References for dicarbonic acid.

BGP11 P. J. Bruna, F. Grein, and J. Passmore, "Density functional theory (DFT) calculations on the structures and stabilities of $[C_nO_{2n+1}]^{2-}$ and $[C_nO_{2n+1}]X_2$ polycarbonates containing chainlike $(CO_2)_n$ units (n = 2-6; X = H or Li)," Can. J. Chem. **89**(6), 671–687 (2011).

L96 E. Lewars, "Polymers and oligomers of carbon dioxide: *ab initio* and semi-empirical calculations," J. Mol. Struct.: THEOCHEM **363**(1), 1–15 (1996).

3.22.2. Diformyl trioxide

^1A g = 1 C_2 σ = 2 M_0 = 106.0349

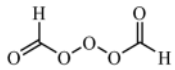

"Linear" *agga* and quasi-cyclic structures compete with the former slightly more stable by 0.4 kJ mol^{-1}.

3.22.2.1 Species data.

6	0.000 000	2.030 037	−0.053 888
1	0.978 530	1.991 669	0.438 922
8	−0.742 165	0.881 262	0.181 921
8	0.000 000	0.000 000	1.035 628
8	0.742 165	−0.881 262	0.181 921
6	0.000 000	−2.030 037	−0.053 888
1	−0.978 530	−1.991 669	0.438 922
8	0.460 348	−2.897 680	−0.714 184
8	−0.460 348	2.897 680	−0.714 184
B (GHz)	9.714 6	1.184 4	1.136 7

No.	$\bar{\upsilon}$ (cm^{-1})	x_{ii}		No.	$\bar{\upsilon}$ (cm^{-1})	x_{ii}		No.	$\bar{\upsilon}$ (cm^{-1})	x_{ii}	
1	3050.47	−30.69	*a*	8	430.21	−1.28	*a*	15	1047.45	−3.11	*b*
2	1875.87	−5.24	*a*	9	301.33	−0.17	*a*	16	1027.44	−1.16	*b*
3	1367.88	−4.50	*a*	10	178.	0.48	*a*	17	787.24	−4.55	*b*
4	1076.95	−3.87	*a*	11	58.59	−0.10	*a*	18	621.50	−1.59	*b*
5	1028.28	−1.16	*a*	12	3050.22	−30.65	*b*	19	448.28	−1.59	*b*
6	945.86	−3.34	*a*	13	1863.30	−5.07	*b*	20	189.39	0.48	*b*
7	658.23	−0.78	*a*	14	1368.05	−4.55	*b*	21	110.95	−1.09	*b*

3.22.2.2 Formation enthalpy, $\Delta_f H(0\ K)$. An isodesmic reaction utilizing reference values for dihydrogen and trioxidane (−81.43 ± 0.70 kJ mol^{-1}) in conjunction with *trans*-glyoxal (−206.91 ± 0.52 kJ mol^{-1})

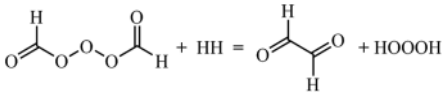

yields a reaction enthalpy of 52.28 ± 4.47 kJ mol^{-1}, which translates to $\Delta_f H^o(0\ K)$ = −340.6 ± 4.6 kJ mol^{-1} (−351.7 kJ mol^{-1} at 298.15 K) for the "linear" species; WMS gives $\Delta_f H^o(0\ K)$ = −341.1 kJ mol^{-1}.

A C–H bond dissociation energy of 218.0 + (−155.2) − (−351.7) = 414 kJ mol^{-1} emerges, which is comparable to that in methyl formate [L07] $CH_3OC(O)$–**H** of 399.2 ± 8.4 kJ mol^{-1}.

3.22.2.3 Results. Four hindered rotors are identifiable, mode nos. 11, 21, 10, and 20; none have a significant impact in isolation.

T (K)	$S^o(T)$	$C_p^o(T)$	$H^o(T) - H^o(0)$
298.15	348.29	104.42	21.16
300.	348.94	104.79	21.35
400.	381.68	123.18	32.77
500.	410.86	138.32	45.87
600.	437.18	150.32	60.33
700.	461.08	159.66	75.85
800.	482.90	166.90	92.19
900.	502.89	172.55	109.17
1000.	521.31	177.03	126.65
1100.	538.36	180.65	144.54
1200.	554.21	183.64	162.76
1300.	569.01	186.15	181.25
1400.	582.89	188.29	199.98
1500.	595.95	190.13	218.90
1600.	608.27	191.71	237.99
1800.	631.00	194.27	276.60
2000.	651.57	196.16	315.64

References for diformyl trioxide.

L07 Y.-R. Luo, *Comprehensive Handbook of Chemical Bond Energies* (CRC Press, Boca Raton, USA, 2007).

3.22.3. Formyl carboxyl peroxide

^1A g = 1 C_1 σ = 1 M_0 = 106.0349

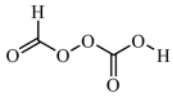

The ground state can be described (O=COO/COOC/OOC=O/O=COH) as *sgss*; the *sgsa* lies 4.5 kJ higher. The O–O bond length of 1.432 Å is longer than the corresponding bond length in the tetroxide compound, where it is 1.380 Å.

3.22.3.1 Species data.

8	0.963 402	−0.759 563	−0.660 357
8	−0.197 859	−0.911 693	0.164 229
6	−1.099 057	0.085 809	−0.120 932
6	1.882 099	0.079 191	−0.084 161
1	2.737 673	0.073 718	−0.773 620
8	1.772 325	0.674 347	0.934 188
8	−0.950 304	0.989 206	−0.881 466
8	−2.165 410	−0.188 955	0.635 002
1	−2.813 161	0.509 555	0.471 404
B (GHz)	5.762 3	1.878 6	1.843 1

No.	$\bar{\upsilon}$ (cm^{-1})	x_{ii}	No.	$\bar{\upsilon}$ (cm^{-1})	x_{ii}	No.	$\bar{\upsilon}$ (cm^{-1})	x_{ii}
1	72.55	−1.52	8	668.59	−0.22	15	1161.10	−5.40
2	95.32	0.00	9	771.29	−0.04	16	1361.18	−5.18
3	227.41	−0.36	10	836.18	−1.59	17	1386.67	−4.06
4	316.45	−0.49	11	893.11	−2.19	18	1849.89	−5.96
5	400.29	−0.95	12	971.57	−0.73	19	1885.03	−6.01
6	495.16	−2.70	13	1010.57	−2.00	20	3028.77	−61.26
7	501.57	−1.06	14	1047.11	−6.78	21	3785.18	−79.99

3.22.3.2 Formation enthalpy, $\Delta_f H(0\ K)$. The isodesmic reaction

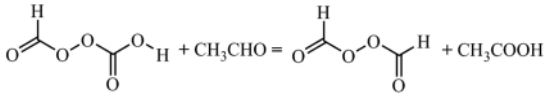

uses the computed reaction enthalpy of −39.62 ± 0.45 kJ mol^{-1} and reference values for the chaperones acetaldehyde (−154.97 ± 0.28 kJ mol^{-1}) and acetic acid (−418.51 ± 0.52 kJ mol^{-1}), together with our value for diformyl peroxide (−406.7 ± 1.5 kJ mol^{-1}), and yields $\Delta_f H^o(0\ K)$ = −630.6 ± 1.7 kJ mol^{-1} (−642.8 kJ mol^{-1} at 298.15 K). This is in excellent agreement with $\Delta_f H^o(0\ K)$ = −631.1 kJ mol^{-1} from WMS.

The 298.15 K value, plus data for the radicals formed on breaking the O–O bond, gives a BDE(O–O) of −131.7 + (−369.0) − (−642.8) = 142 kJ mol^{-1}; this value is midway between the corresponding value for the diformyl peroxide and dicarboxyl peroxide of 154 kJ mol^{-1} and 132 kJ mol^{-1}, respectively.

3.22.3.3 Results. Hindered rotor analysis ascribes four modes as impacted (nos. 1, 2, 5, and 6) with only a slight effect due to reduced barrier heights (*V*/*RT*)s greater than 10.8; here, we treat the lowest frequency mode as a hindered rotor, with a relaxed potential energy scan about the dihedral C–O–O–C, and use anharmonic frequencies.

T (K)	$S^o(T)$	$C_p^o(T)$	$H^o(T) - H^o(0)$
298.15	348.78	100.89	20.48
300.	349.41	101.24	20.66
400.	381.02	118.83	31.69
500.	409.13	133.09	44.32
600.	434.44	144.44	58.21
700.	457.41	153.52	73.13
800.	478.41	160.88	88.86
900.	497.72	166.94	105.26
1000.	515.58	172.01	122.21
1100.	532.18	176.30	139.63
1200.	547.68	179.96	157.44
1300.	562.21	183.11	175.60
1400.	575.88	185.85	194.05
1500.	588.79	188.24	212.75
1600.	601.01	190.35	231.68
1800.	623.64	193.87	270.12
2000.	644.22	100.89	309.18

3.22.4. 2-Hydroperoxy-2-oxoacetic acid

$^1A'$ g = 1 C_S σ = 1 M_0 = 106.0349

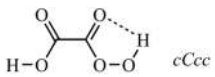

A considerable number of low lying conformers exist, which can be categorized as *cis* or *trans* in the order: HOC=O, O=CC=O, O=COO, and COOH. At the G4 level, the zero-point corrected electronic energies are given in the table relative to the lowest. Note that at CBS-QB3 (values in brackets), the order of the two lowest is reversed.

Conformer	*cCcc*	*cTcc*	*cTct*	*cCct*	*tTtc*
Relative energy (kJ mol^{-1})	0.00 (0.30)	0.10 (0.00)	10.5 (11.4)	11.9 (13.4)	18.0 (15.4)

3.22.4.1 Species data.

C	0.273 819 503	0.340 075 019	0.000 000
C	−1.218 368 395	−0.031 920 561	0.000 000
O	−2.069 580 444	0.805 632 002	0.000 000
O	0.676 522 603	1.471 399 551	0.000 000
O	−1.416 445 932	−1.355 363 514	0.000 000
H	−2.374 206 822	−1.507 888 930	0.000 000
O	1.066 437 085	−0.739 149 378	0.000 000
O	2.451 584 928	−0.357 885 503	0.000 000
H	2.376 093 289	0.621 944 791	0.000 000
B (GHz)	5.661 7	2.002 9	1.479 5

No.	$\bar{\upsilon}$ (cm^{-1})	x_{ii}		No.	$\bar{\upsilon}$ (cm^{-1})	x_{ii}		No.	$\bar{\upsilon}$ (cm^{-1})	x_{ii}	
1	3730.54	−81.88	a'	8	1164.65	−5.06	a'	15	210.47	0.80	a'
2	3502.37	−105.59	a'	9	945.32	−5.27	a'	16	821.77	−0.39	a''
3	1848.61	−9.21	a'	10	921.68	−1.62	a'	17	654.36	−3.14	a''
4	1808.89	−8.88	a'	11	695.26	0.25	a'	18	511.88	−4.01	a''
5	1493.25	−9.22	a'	12	492.58	−0.21	a'	19	429.10	−16.03	a''
6	1373.40	−5.19	a'	13	411.51	−0.55	a'	20	180.75	−0.52	a''
7	1204.71	−5.92	a'	14	369.96	−0.89	a'	21	12.32	−29.04	a''

3.22.4.2 Formation enthalpy, $\Delta_f H(0\ K)$. An isodesmic reaction

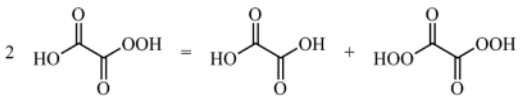

which ras is to be expected, and based on ourelates this compound to oxalic (−724.5 ± 1.5 kJ mol^{-1}) and peroxalic (−512.2 ± 2.5 kJ mol^{-1}) acids, seems sensible; the reaction enthalpy of −14.66 ± 1.30 kJ mol^{-1} leads to $\Delta_f H^o(0\ K)$ = −611.0 ± 3.2 kJ mol^{-1} (−623.3 kJ mol^{-1} at 298.15 K), in congruence with a multi-averaged atomization result of $\Delta_f H^o(0\ K)$ = −615.0 ± 6.6 kJ mol^{-1} and a WMS of $\Delta_f H^o(0\ K)$ = −613.6 kJ mol^{-1}.

An CO–H bond energy of 218.0 + (−375.9) − (−623.3) = 465 kJ mol^{-1} is in line with many of the listed values for carboxylic acids [L07] and the OO–H bond energy of 218.0 + (−440.1) − (−623.3) = 401 kJ mol^{-1} is similar to those for hydroperoxides [L07].

3.22.4.3 Results. A relaxed potential energy scan about the carboxylic moiety faces a barrier in excess of 48 kJ mol^{-1}, whereas that about COOH is much lower at 16 and about the C–C bond is lower again at 3 kJ mol^{-1}; the highest barrier is found for rotation about O=COO. Hindered rotor analysis identifies mode nos. 21, 19, and 17 with the first having the biggest contribution to change in entropy of −2.2, which is somewhat offset by +0.6 correction for the other two modes, thus resulting overall in a change of −1.6 J K^{-1} mol^{-1}. An anharmonic treatment replacing the highly anharmonic mode no. 21 by a hindered rotor is used.

T (K)	$S^o(T)$	$C_p^o(T)$	$H^o(T) - H^o(0)$
298.15	354.88	100.99	19.97
300.	355.51	101.37	20.16
400.	387.28	119.75	31.25
500.	415.65	134.54	43.99
600.	441.25	146.13	58.05
700.	464.47	155.06	73.12
800.	485.65	161.94	88.99
900.	505.04	167.29	105.46
1000.	522.90	171.54	122.40
1100.	539.41	174.98	139.73
1200.	554.77	177.83	157.38
1300.	569.10	180.25	175.28
1400.	582.53	182.34	193.41
1500.	595.18	184.17	211.74
1600.	607.12	185.80	230.24
1800.	629.17	188.62	267.68
2000.	649.17	191.01	305.65

References for 2-hydroperoxy-2-oxoacetic acid.

L07 Y.-R. Luo, *Comprehensive Handbook of Chemical Bond Energies* (CRC Press, Boca Raton, USA, 2007).

3.23. $C_2H_2O_6$

3.23.1. Diformyltetroxide

^1A g = 1 C_2 σ = 2 M_0 = 122.0343

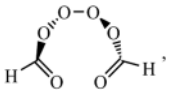

UV photo-oxidation in solid O_2 of glyoxal at 12–18 K has been shown to yield some diformyl tetraoxide among a number of initial and secondary products [TL84]. The most stable conformer has an O–O–O–O dihedral of −98.3°; the OO–OO bond at 1.345 Å is shorter than that in diformyl peroxide at 1.445 Å—this apparent counter-intuitive finding mirrors the situation for the hydrogen polyoxides [DO09].

3.23.1.1 Species data.

8	−0.157 879	0.653 783	1.364 728
8	0.157 879	−0.653 783	1.364 728
8	0.761 604	1.369 060	0.446 705
8	−0.761 604	−1.369 060	0.446 705
6	−0.157 879	−1.688 080	−0.734 534
1	−0.907 480	−2.276 245	−1.285 340
6	0.157 879	1.688 080	−0.734 534
1	0.907 480	2.276 245	−1.285 340
8	−0.934 004	1.399 595	−1.099 866
8	0.934 004	−1.399 595	−1.099 866
B (GHz)	2.965 9	1.908 9	1.503 6

No.	$\bar{\nu}$ (cm^{-1})	x_{ii}		No.	$\bar{\nu}$ (cm^{-1})	x_{ii}	
1	3007.86	−31.62	*a*	13	63.43	−2.65	*a*
2	1850.80	−5.31	*a*	14	3008.36	−31.59	*b*
3	1367.97	−4.46	*a*	15	1837.71	−5.28	*b*
4	1048.39	−2.91	*a*	16	1362.47	−4.33	*b*
5	1014.82	−1.13	*a*	17	1017.12	−1.20	*b*
6	952.25	−2.61	*a*	18	997.73	−2.26	*b*
7	822.50	−0.49	*a*	19	831.86	−0.81	*b*
8	589.92	−0.79	*a*	20	725.92	−3.69	*b*
9	446.46	−2.70	*a*	21	584.51	−1.50	*b*
10	337.73	−0.40	*a*	22	301.80	0.12	*b*
11	243.11	−0.47	*a*	23	220.60	−1.33	*b*
12	114.89	−0.21	*a*	24	80.76	0.78	*b*

3.23.1.2 Formation enthalpy, $\Delta_f H$(0 K). An isodesmic reaction

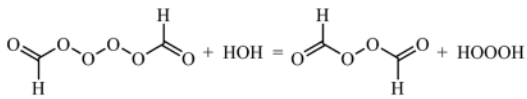

relies on a value for trioxidane [DO09] of −81.71 ± 0.72 kJ mol^{-1} and our previous number for diformyl peroxide of −406.7 ± 1.5 kJ mol^{-1} together with a reaction enthalpy of 39.80 ± 0.74 kJ mol^{-1} to yield $\Delta_f H^o$(0 K) = −289.0 ± 1.8 kJ mol^{-1}.

An additional reaction that uses our previous value for formic acid anhydride (−466.99 ± 0.68 kJ mol^{-1}) as well as a not particularly well-categorized number for tetraoxidane [TL84] (−33.6 ± 2.4 kJ mol^{-1}), H_2O_4, has an averaged enthalpy change of 28.86 ± 1.64 kJ mol^{-1}, which results in $\Delta_f H^o$(0 K) = −290.5 ± 3.0 kJ mol^{-1},

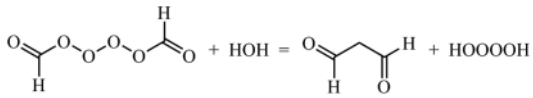

A weighted average of $\Delta_f H^o$(0 K) = −289.4 ± 1.6 kJ mol^{-1} thus emerges (−302.9 kJ mol^{-1} at 298.15 K).

In turn, this implies a BDE(OO–OO) of 2 × (−92.7) − (−302.9) = 118 kJ mol^{-1}, which is somewhat stronger than the equivalent bond in tetraoxidane HOOOOH [DO09] and a C–H BDE of 218.0 + (−111.7) − (−302.9) = 409 kJ mol^{-1}, typical of aldehydic C–H bonds.

3.23.1.3 Results. Hindered rotor analysis picks out four modes as significant, but these result in only slight changes to the entropy and hence an anharmonic oscillator treatment is used.

T (K)	$S^o(T)$	$C_p^o(T)$	$H^o(T) - H^o(0)$
298.15	367.73	113.10	23.17
300.	368.43	113.49	23.38
400.	403.86	133.18	35.74
500.	435.36	149.07	49.88
600.	463.69	161.61	65.44
700.	489.38	171.57	82.12
800.	512.83	179.62	99.69
900.	534.38	186.22	117.99
1000.	554.29	191.72	136.89
1100.	572.79	196.35	156.30
1200.	590.05	200.32	176.14
1300.	606.22	203.73	196.34
1400.	621.43	206.71	216.86
1500.	635.78	209.32	237.67
1600.	649.37	211.63	258.71
1800.	674.53	215.48	301.44
2000.	697.39	218.54	344.85

References for diformyltetroxide.

TL84 T. L. Tso and E. K. C. Lee, "Mechanism of photo-oxidation of glyoxal and formadehyde in solid O_2 at 12–18 K," J. Phys. Chem. **88**, 5465–5474 (1984).

DO09 P. A. Denis and F. R. Ornellas, "Theoretical characterization of hydrogen polyoxides: HOOH, HOOOH, HOOOOH and HOOO," J. Phys. Chem. **113**, 499–506 (2009).

3.23.2. Ethanediperoxoic acid; peroxalic acid

^{1}A g = 1 C_2 σ = 2 M_0 = 122.0343

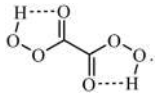

Peroxalic acid is an intermediate species encountered in the studies of the chemiluminescent behavior of 1,2-dioxetanedione—the so-called peroxylate chemiluminescence [TBDL08]. The lowest energy conformer, one of the many examined, corresponds to the sketch above with five-membered hydrogen-bonded rings [SS15].

3.23.2.1 Species data.

8	1.124 306	1.333 659	0.000 120
8	−1.124 306	1.358 731	0.000 249
6	−0.082 671	0.760 000	0.000 250
6	0.082 671	−0.760 000	0.000 250
8	−1.124 306	−1.333 659	0.000 120
8	−1.008 612	−2.760 958	−0.000 564
1	−0.033 047	−2.877 865	0.000 061
8	1.008 612	2.760 958	−0.000 564
1	0.033 047	2.877 865	0.000 061
8	1.124 306	−1.358 731	0.000 249
B (GHz)	5.705 3	1.216 7	1.002 8

No.	$\bar{\upsilon}$ (cm^{-1})	x_{ii}		No.	$\bar{\upsilon}$ (cm^{-1})	x_{ii}	
1	3508.11	−51.49	*a*	13	24.33	−11.54	*a*
2	1813.24	−5.13	*a*	14	3507.57	−51.54	*b*
3	1499.20	−4.95	*a*	15	1795.50	−5.31	*b*
4	1300.29	−6.03	*a*	16	1492.35	−4.50	*b*
5	991.00	−2.42	*a*	17	1185.03	−4.72	*b*
6	944.90	−0.78	*a*	18	922.32	−1.49	*b*
7	587.59	−1.29	*a*	19	853.82	−0.29	*b*
8	497.60	0.52	*a*	20	803.63	−0.09	*b*
9	411.88	−11.31	*a*	21	434.46	−15.85	*b*
10	381.92	−0.43	*a*	22	380.20	−0.42	*b*
11	333.64	−0.30	*a*	23	230.79	−0.47	*b*
12	140.27	−0.54	*a*	24	165.99	0.17	*b*

3.23.2.2 Formation enthalpy, $\Delta_f H$(0 K). An isodesmic reaction

$$\mathrm{HOOC(O)-C(O)OOH + HOH}$$

$$= \mathrm{HOC(O)-C(O)OH + HOOOH},$$

which attempts to match the "closed" nature of the peroxalic acid with the equally internally H-bonded conformer *tTt* oxalic acid, has a reaction enthalpy of −51.80 ± 1.75 kJ mol^{-1} from which $\Delta_f H^o$(0 K) = −515.6 ± 2.2 kJ mol^{-1} (−526.5 kJ mol^{-1} at 298.15 K) is derived based on our work for *tTt* oxalic acid of −724.9 kJ mol^{-1} q.v. together with the well-known chaperones, water (−238.931 ± 0.027 kJ mol^{-1}) and trioxidane (−81.43 ± 0.70 kJ mol^{-1}).

Adoption of the most recent ATcT value for oxalic acid of −721.8 kJ mol^{-1} drives the peroxalic acid value up to −512.5 kJ mol^{-1}, which is incompatible with our results. Multi-composite and WMS atomizations of $\Delta_f H^o$(0 K) = −518.0 ± 8.9 kJ mol^{-1} and $\Delta_f H^o$(0 K) = −517.5 kJ mol^{-1} round out the picture. Note that at the WMS level the reaction enthalpy of the above-mentioned isodesmic is −52.60 kJ mol^{-1}, which is well within the uncertainty of 1.75 kJ mol^{-1} listed above.

3.23.2.3 Results. The very low frequency mode no. 13 is replaced by a hindered rotor based on the OC–CO dihedral scan.

T (K)	$S^o(T)$	$C_p^o(T)$	$H^o(T) - H^o(0)$
298.15	373.79	118.36	23.04
300.	374.53	118.77	23.26
400.	411.55	138.96	36.17
500.	444.40	155.50	50.92
600.	473.97	168.76	67.16
700.	500.80	179.14	84.58
800.	525.27	187.11	102.91
900.	547.67	193.16	121.93
1000.	568.27	197.74	141.49
1100.	587.29	201.22	161.44
1200.	604.92	203.90	181.70
1300.	621.32	206.00	202.20
1400.	636.65	207.67	222.88
1500.	651.03	209.03	243.71
1600.	664.56	210.16	264.67
1800.	689.42	211.89	306.88
2000.	711.81	213.11	349.39

References for ethanediperoxoic acid; peroxalic acid.

TBDL08 S. A. Tonkin, R. Bos, G. A. Dyson, K. F. Lim, R. A. Russell, S. P. Watson, C. M. Hindson, and N. W. Barnett, "Studies on the mechanism of the peroxyoxalate chemiluminescence reaction," Anal. Chim. Acta **614**(2), 173–181 (2008).

SS15 J. M. Simmie and K. P. Somers, "Benchmarking compound methods (CBS-QB3, CBS-APNO, G3, G4, W1BD) against the active thermochemical tables: A litmus test for cost-effective molecular formation enthalpies," J. Phys. Chem. A **119**(28), 7235–7246 (2015).

3.23.3. Peroxydicarbonic acid

^{1}A g = 1 C_2 σ = 2 M_0 = 122.0343

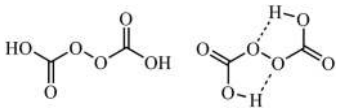

Peroxydicarbonic acid is apparently involved in photosynthetic oxygen evolution [CLS07] but is otherwise little known. A number of conformers exist with the lowest energy structure characterized by a C–O–O–C dihedral near 87.7°, O=C–O–O dihedrals of ~0°, and H–O–C=O of ~0°. The O–O bond length of 1.421 Å is *longer* than the corresponding bond in the tetroxide at 1.363 Å. The quasi-cyclic conformer shown lies some 16.5 kJ mol^{-1} higher in energy.

3.23.3.1 Species data.

8	−0.444 637	−0.554 461	0.869 411
8	0.444 637	0.554 461	0.869 411
6	0.034 060	1.477 393	−0.065 488
6	−0.034 060	−1.477 393	−0.065 488
8	−0.876 079	1.370 226	−0.824 013
8	0.876 079	−1.370 226	−0.824 013
8	0.876 079	2.503 817	0.076 596
1	0.627 265	3.164 981	−0.583 029
8	−0.876 079	−2.503 817	0.076 596
1	−0.627 265	−3.164 981	−0.583 029
B (GHz)	5.250 1	1.273 8	1.265 8

No.	$\bar{\nu}$ (cm^{-1})	x_{ii}		No.	$\bar{\nu}$ (cm^{-1})	x_{ii}	
1	3786.92	−40.65	*a*	13	77.61	−0.97	*a*
2	1893.85	−5.06	*a*	14	3786.02	−40.61	*b*
3	1395.80	−2.98	*a*	15	1864.57	−5.03	*b*
4	1171.83	−3.17	*a*	16	1368.17	−3.43	*b*
5	1068.78	−5.00	*a*	17	1153.34	−2.74	*b*
6	906.05	−1.89	*a*	18	923.81	−4.40	*b*
7	779.30	−0.01	*a*	19	765.11	−0.06	*b*
8	650.81	−0.08	*a*	20	742.62	−0.84	*b*
9	496.98	−7.19	*a*	21	564.13	0.12	*b*
10	413.02	−0.25	*a*	22	494.00	−6.84	*b*
11	338.51	−0.45	*a*	23	344.13	−0.27	*b*
12	95.56	−0.38	*a*	24	87.68	−0.22	*b*

3.23.3.2 Formation enthalpy, $\Delta_f H$(0 K). An isodesmic reaction that makes use of our previous value for diformyl peroxide (−405.5 ± 1.2 kJ mol^{-1}) together with references methanal (−109.32 ± 0.11 kJ mol^{-1}) and formic acid (−371.12 ± 0.22 kJ mol^{-1})

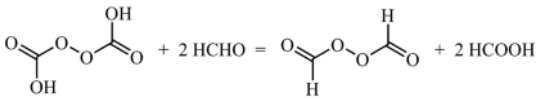

has a reaction enthalpy of −81.96 ± 1.03 kJ mol^{-1} and thereby $\Delta_f H^o$(0 K) = −855.2 ± 1.6 kJ mol^{-1} (−869.5 kJ mol^{-1} at 298.15 K), in comparison to a multi-averaged atomization value of −860 ± 9 kJ mol^{-1}. A WMS value of $\Delta_f H^o$(0 K) = −855.4 kJ mol^{-1} is in excellent agreement.

The bond dissociation energy, BDE(O–O), of 2 × (−369.0) − (−869.6) = 132 kJ mol^{-1} is noticeably *stronger* than the corresponding bond in the tetroxide.

3.23.3.3 Results. A hindered rotor analysis is quite complex with five vibrational modes implicated but two, mode nos. 24 and 12, are quite minor; the dihedral about the central O–O bond, mode no. 1, and the two OH rotors (mode nos. 9 and 22) each contributes approximately the same correction of ca. +0.4 J K^{-1} mol^{-1} to the entropy over the whole temperature range from 300 to 2000 K. The relaxed potential energy scans are not well behaved, except for those of the HOCO dihedral, which impinge on mode nos. 9 and 22.

T (K)	$S^o(T)$	$C_p^o(T)$	$H^o(T) - H^o(0)$
298.15	358.07	117.26	22.31
300.	358.80	117.74	22.53
400.	395.92	140.33	35.49
500.	429.11	156.79	50.39
600.	458.81	168.81	66.69
700.	485.54	177.95	84.05
800.	509.80	185.25	102.22
900.	531.98	191.34	121.06
1000.	552.42	196.57	140.45
1100.	571.37	201.15	160.34
1200.	589.05	205.19	180.66
1300.	605.62	208.77	201.36
1400.	621.21	211.91	222.40
1500.	635.92	214.64	243.73
1600.	649.85	216.98	265.31
1800.	675.63	220.57	309.08
2000.	699.00	222.87	353.44

References for peroxydicarbonic acid.

CLS07 P. A. Castelfranco, Y.-K. Lu, and A. J. Stemler, "Hypothesis: The peroxydicarbonic acid cycle in photosynthetic oxygen evolution," Photosynth. Res. **94**(2), 235–246 (2007).

3.24. $C_2H_2O_7$

3.24.1. Dicarboxyl trioxide

^{1}A g = 1 C_2 σ = 2 M_0 = 138.0337

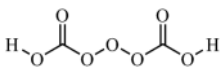

The lowest energy conformer (C_1, ^{1}A) has a hydrogen-bonded puckered eight-membered ring with an H••••O bond length of

1.760 Å; there is also a conformer with C_2 symmetry and *syn* HOC = O dihedrals, which is extremely close at +0.10 ± 0.39 kJ mol^{-1} and which is featured *here*.

3.24.1.1 Species data.

8	−0.743 979	−0.864 855	0.203 340
8	0.000 000	0.000 000	1.049 084
8	0.743 979	0.864 855	0.203 340
6	0.000 000	1.998 279	−0.074 629
6	0.000 000	−1.998 279	−0.074 629
8	−1.109 347	2.234 205	0.278 179
8	1.109 347	−2.234 205	0.278 179
8	−0.808 794	−2.756 866	−0.821 071
1	−0.321 268	−3.564 595	−1.032 141
8	0.808 794	2.756 866	−0.821 071
1	0.321 268	3.564 595	−1.032 141
B (GHz)	4.110 3	0.851 0	0.806 8

No.	$\bar{\nu}$ (cm^{-1})	x_{ii}		No.	$\bar{\nu}$ (cm^{-1})	x_{ii}		No.	$\bar{\nu}$ (cm^{-1})	x_{ii}	
1	3782.09	−40.30	*a*	10	513.42	−6.28	*a*	19	902.77	−3.52	*b*
2	1887.14	−5.29	*a*	11	389.38	−0.98	*a*	20	845.86	−2.83	*b*
3	1380.52	−2.97	*a*	12	222.89	0.04	*a*	21	778.37	−0.08	*b*
4	1166.22	−2.82	*a*	13	64.95	−0.34	*a*	22	685.38	−0.77	*b*
5	1010.99	−2.39	*a*	14	54.12	1.20	*a*	23	523.01	−0.15	*b*
6	905.92	−1.90	*a*	15	3781.45	−40.27	*b*	24	511.96	−6.22	*b*
7	783.90	−0.06	*a*	16	1883.65	−5.23	*b*	25	387.52	−0.27	*b*
8	689.77	−1.66	*a*	17	1362.89	−3.29	*b*	26	144.24	−0.06	*b*
9	592.95	−0.12	*a*	18	1146.79	−2.59	*b*	27	66.37	0.65	*b*

3.24.1.2 Formation enthalpy, $\Delta_f H$(0 K). The isodesmic reaction

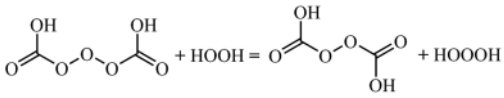

which uses the "linear" conformer of dicarboxyl trioxide in order to best mirror the structures on the right-hand side, is related to peroxydicarbonic acid (−855.2 ± 1.6 kJ mol^{-1}) q.v. via hydrogen peroxide (−129.472 ± 0.064 kJ mol^{-1}) and trioxidane (−81.43 ± 0.70 kJ mol^{-1}); the reaction enthalpy of −17.93 ± 0.51 kJ mol^{-1} gives rise to $\Delta_f H^o$(0 K) = −789.2 ± 1.8 kJ mol^{-1} (−805.4 kJ mol^{-1} at 298.15 K), in good agreement with the $\Delta_f H^o$(0 K) = −791.7 kJ mol^{-1} from WMS.

3.24.1.3 Results. Six modes are identified as potential hindered rotors, but individually their impact is slight.

T (K)	$S^o(T)$	$C_p^o(T)$	$H^o(T) - H^o(0)$
298.15	385.20	129.16	24.76
300.	386.00	129.68	25.00
400.	426.90	154.81	39.28
500.	463.61	174.02	55.76
600.	496.68	188.54	73.92
700.	526.61	199.50	93.35
800.	553.82	207.81	113.73
900.	578.68	214.20	134.84
1000.	601.52	219.20	156.52
1100.	622.60	223.22	178.65
1200.	642.17	226.52	201.14
1300.	660.42	229.31	223.93
1400.	677.50	231.71	246.98
1500.	693.56	233.83	270.26
1600.	708.71	235.70	293.74
1800.	736.67	238.89	341.20
2000.	761.97	241.44	389.24

3.24.2. Formyl carboxyl tetroxide

^{1}A g = 1 C_1 σ = 1 M_0 = 138.0337

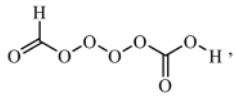

Conformational analysis reports a large number of conformers, which is unsurprising, given six rotatable bonds; here, we take the *agggss* (O=COO/COOO/OOOO/OOC=O/O=COH) as the ground state. The central O–O bond length of 1.380 Å is shorter than the corresponding bond in the formyl peroxide of 1.432 Å.

3.24.2.1 Species data.

6	−2.844 138	0.154 854	0.066 199
1	−2.704 028	1.131 984	0.544 388
8	−1.691 670	−0.300 652	−0.541 905
8	−0.638 500	0.691 191	−0.381 908
8	0.058 229	0.394 458	0.771 803
8	1.038 910	−0.612 038	0.463 539
8	−3.831 698	−0.498 961	0.019 522
6	2.189 385	−0.004 687	−0.002 553
8	2.358 347	1.156 350	−0.193 780
8	3.051 629	−1.007 174	−0.187 538
1	3.870 565	−0.618 385	−0.524 131
B (GHz)	6.099 5	0.681 8	0.647 4

No.	$\bar{\upsilon}$ (cm^{-1})	x_{ii}	No.	$\bar{\upsilon}$ (cm^{-1})	x_{ii}	No.	$\bar{\upsilon}$ (cm^{-1})	x_{ii}
1	3778.71	−80.21	10	974.76	−2.03	19	509.72	−7.30
2	3040.73	−62.09	11	902.40	−3.48	20	441.69	−0.56
3	1880.07	−10.1	12	860.49	−4.14	21	337.61	−0.16
4	1861.42	−10.1	13	780.01	−0.12	22	270.12	−0.16
5	1376.35	−8.31	14	723.98	−1.21	23	176.52	−0.05
6	1373.02	−5.31	15	666.70	−1.38	24	121.38	−0.11
7	1157.91	−5.36	16	637.38	−2.49	25	81.80	0.31
8	1077.71	−7.75	17	599.05	−1.11	26	55.71	−0.92
9	1029.05	−2.72	18	513.95	−0.55	27	52.44	−1.94

3.24.2.3 Formation enthalpy, $\Delta_f H(0\ K)$. The isodesmic reaction

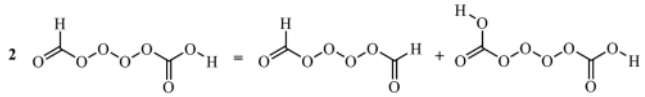

is near thermoneutral, −3.54 ± 1.05 kJ mol^{-1}, as is to be expected, and based on our previous values for the diformyl- (−288.4 ± 1.4 kJ mol^{-1}) and dicarboxyltetroxides (−747.2 ± 1.6 kJ mol^{-1}) yields $\Delta_f H^o$(0 K) = −516.0 ± 2.4 kJ mol^{-1} (−526.9 kJ mol^{-1} at 298.15 K), just in agreement with the $\Delta_f H^o$(0 K) = −518.8 kJ mol^{-1} from WMS.

The BDE(OO–OO) is calculated from the radicals *trans* peroxyformyl and carboxydioxy, specifically **R3**, as = (−107.8) + (−320.2) − (−526.9) = 99 kJ mol^{-1}, which fits the pattern that in tetroxides the central O–O bond is *shorter but weaker* than in peroxides.

3.24.2.3 Results. Six vibrational mode (nos. 1–5 and 9) are identified, all with reduced barrier heights (*V*/*RT*)s greater than 9.5; their complex nature means that we present a default anharmonic treatment.

T (K)	$S°(T)$	$C°_p(T)$	$H°(T) - H°(0)$
298.15	410.44	128.66	26.16
300.	411.23	129.08	26.40
400.	451.28	149.46	40.36
500.	486.41	165.38	56.14
600.	517.71	177.80	73.32
700.	545.88	187.61	91.61
800.	571.47	195.51	110.77
900.	594.88	202.00	130.66
1000.	616.45	207.42	151.13
1100.	636.44	212.02	172.11
1200.	655.07	215.97	193.51
1300.	672.49	219.39	215.28
1400.	688.86	222.38	237.37
1500.	704.30	225.01	259.74
1600.	718.89	227.33	282.36
1800.	745.90	231.18	328.22
2000.	770.42	234.18	374.76

3.25. $C_2H_2O_8$

3.25.1. Dicarboxyltetroxide

^1A g = 1 C_2 σ = 2 M_0 = 154.0331

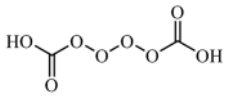

A conformationally diverse molecule whose dihedrals H–O–C=O, O=C–O–O, C–O–O–O, and O–O–O–O can be summarized as ssgG′gss for the lowest energy conformer. The central O–O bond length of 1.366 Å is *shorter* than the corresponding bond length in peroxydicarbonic acid of 1.445 Å, paralleling the situation for the hydrogen polyxides [DO09] and the diformyl polyoxides as seen in *this work*.

3.25.1.1. Species data.

8	0.326 272	−0.599 941	1.650 016
8	−0.326 272	0.599 941	1.650 016
8	−0.382 198	−1.522 914	0.778 109
8	0.382 198	1.522 914	0.778 109
6	−0.273 688	1.646 794	−0.422 395
6	0.273 688	−1.646 794	−0.422 395
8	1.223 080	−1.031 235	−0.795 497
8	−1.223 080	1.031 235	−0.795 497
8	−0.382 198	−2.610 833	−1.073 546
1	0.039 965	−2.703 383	−1.938 283
8	0.382 198	2.610 833	−1.073 546
1	−0.039 965	2.703 383	−1.938 283
B (GHz)	2.127 0	1.052 9	0.852 1

No.	$\bar{\upsilon}$ (cm^{-1})	x_{ii}		No.	$\bar{\upsilon}$ (cm^{-1})	x_{ii}	
1	3782.52	−40.02	*a*	16	66.67	0.17	*a*
2	1867.55	−5.28	*a*	17	3781.38	−39.99	*b*
3	1386.89	−2.98	*a*	18	1860.53	−5.20	*b*
4	1167.22	−2.87	*a*	19	1367.21	−3.29	*b*
5	1003.88	−1.82	*a*	20	1148.36	−2.72	*b*
6	931.66	−1.56	*a*	21	929.68	−2.45	*b*
7	780.61	−0.07	*a*	22	864.12	−3.59	*b*
8	710.64	−0.41	*a*	23	773.26	−0.02	*b*
9	621.91	−0.09	*a*	24	679.52	−0.87	*b*
10	551.76	−1.45	*a*	25	612.94	−0.30	*b*
11	502.76	−4.99	*a*	26	498.96	−5.10	*b*
12	411.60	−0.85	*a*	27	440.13	−0.42	*b*
13	291.33	−0.56	*a*	28	290.76	−0.48	*b*
14	135.72	−0.37	*a*	29	127.74	−0.13	*b*
15	79.95	−1.57	*a*	30	60.76	−1.59	*b*

T (K)	$S^o(T)$	$C_p^o(T)$	$H^o(T) - H^o(0)$
298.15	410.41	147.49	28.43
300.	411.32	147.99	28.70
400.	457.25	171.21	44.72
500.	497.39	188.37	62.74
600.	532.93	201.32	82.25
700.	564.75	211.32	102.90
800.	593.50	219.27	124.44
900.	619.72	225.75	146.70
1000.	643.79	231.15	169.55
1100.	666.04	235.75	192.90
1200.	686.73	239.73	216.68
1300.	706.06	243.22	240.83
1400.	724.20	246.33	265.30
1500.	741.29	249.13	290.08
1600.	757.45	251.66	315.12
1800.	787.36	256.12	365.90
2000.	814.54	259.90	417.51

3.25.1.2 Formation enthalpy, $\Delta_f H(0\ K)$. No really satisfactory isodesmic presents itself, but this species can be related back to dicarboxyl peroxide or peroxydicarbonic acid (-855.2 ± 1.6 kJ mol^{-1}) q.v. together with references water (-238.931 ± 0.027 kJ mol^{-1}) and trioxidane (-81.71 ± 0.72 kJ mol^{-1}) via

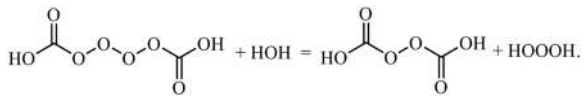

The reaction enthalpy of 48.15 ± 1.71 kJ mol^{-1} results in $\Delta_f H^o(0\ K) = -746.1 \pm 2.5$ kJ mol^{-1} (-763.3 kJ mol^{-1} at 298.15 K).

A BDE(OO–OO) of 113 kJ mol^{-1} can be derived from this result together with that for carboxydioxy radical (the **R4** conformer); this is *weaker* than the corresponding bond in peroxydicarbonic acid of 132 kJ mol^{-1}.

3.25.1.3 Results. Hindered rotor analysis identifies four mode (nos. 1, 5, 10, and 11), but the overall effect is small, the entropy increasing by just +1.4 J K^{-1} mol^{-1}, at room temperature. The relaxed scan about O–O is problematic, so a default anharmonic treatment is used.

References for dicarboxyl tetroxide.

DO09 P. A. Denis and F. R. Ornellas, "Theoretical characterization of hydrogen polyoxides: HOOH, HOOOH, HOOOOH and HOOO," J. Phys. Chem. **113**, 499–506 (2009).

4. Conclusions

In summary, we have performed a systematic series of calculations for the structural and thermodynamical properties for a range of tri-elemental $C_xH_yO_z$ species and compared the said results against whatever exists in the chemical literature. The objectives were to produce an organized collection, or a database, of well-founded results, which could be used for testing new and/or improved methodologies for carrying out such computations, for comparing against new experimental determinations, and finally simply for providing needed information about singular species (Table 1).

The use of higher-level theoretical quantum chemical methods, higher than those used here, is constrained by computational expense and, while limiting, should decline as

TABLE 1. Summary of results [$\Delta_f H^o$ (kJ mol^{-1}); S^o and C_p^o (J K^{-1} mol^{-1})]

Species	$\Delta_f H^o$(0 K)	$\Delta_f H^o$(298.15 K)	S^o(298.15 K)	C_p^o(298.15 K)
$C_1H_1O_1$				
Formyl	41.4	41.8	224.33	34.55
Isoformyl	216.4	216.8	225.03	34.90
$C_1H_1O_2$				
Dioxiranyl	215.9	212.4	250.57	41.49
Dioxymethylene *anti*	342.9	347.0	255.92	47.75
Dioxymethylene *syn*	358.1	355.8	257.91	44.60
Formyloxy $^2A_1$	−130.0	−131.6	256.71	48.55
Formyloxy $^2B_2$	−123.8	−127.3	245.31	40.76
Hydroxyformyl *anti*	−183.2	−185.8	253.43	48.08
Hydroxyformyl *syn*	−176.7	−179.8	254.02	48.15
$C_1H_1O_3$				
3-Dioxyranyloxyl	80.1	74.4	275.35	56.10
3-Hydroxydioxyranyl *syn*	12.4	7.4	284.17	60.48
3-Hydroxydioxyranyl *gauche*	10.9	5.6	284.04	60.43
Hydroxyoxomethoxy	−362.4	−368.6	273.47	55.57
Hydroperoxyoxomethyl	−74.6	−78.6	291.65	62.29
Methylenetrioxygen	688.4	683.7	282.14	65.14

TABLE 1. (*Continued.*)

Species	$\Delta_f H^o$(0 K)	$\Delta_f H^o$(298.15 K)	S^o(298.15 K)	C_p^o(298.15 K)
Peroxyformyl *trans*	−102.5	−107.6	279.61	58.89
Peroxyformyl *cis*	−89.8	−94.8	282.12	58.86
Trioxetanyl	270.6	264.4	271.79	53.50
$C_1H_1O_4$				
Bis-dioxymethylene *ss*	177.2	170.3	297.40	75.21
Bis-dioxymethylene *sa*	178.7	171.2	301.48	72.15
Bis-hydroperoxymethylene	159.2	154.2	317.89	84.90
Carbonoperoxyl	−243.5	−249.9	316.38	74.11
Carboxydioxy	−333.4	−342.8	295.18	69.03
Dioxiraneperoxyl	49.6	41.8	303.37	69.96
Hydrogentrioxide oxomethyl	−23.0	−29.0	319.83	81.14
$C_1H_1O_5$				
Carbonodiperoxoic acid radical	−215.7	−222.1	341.79	100.90
Formylhydrotetroxide radical	26.5	19.4	352.08	102.91
$C_1H_2O_1$				
Hydroxymethylene *anti*	112.2	108.4	225.10	36.66
Hydroxymethylene *syn*	130.2	126.4	225.27	36.62
Hydroxymethylene triplet	217.1	214.3	244.12	42.70
Methanal	−105.9	−109.1	218.58	35.20
$C_1H_2O_2$				
Dihydroxycarbene	−200.1	−206.2	253.83	48.87
Dioxirane	8.9	1.1	240.53	42.00
Dioxymethane $^3A_2$	82.9	75.6	254.02	47.12
Dioxymethane $^3B_1$	122.3	115.1	252.72	46.42
Dioxymethyl	110.8	103.7	249.25	47.35
Formic acid *syn*	−372.7	−380.1	248.56	45.28
Formic acid *anti*	−355.8	−362.2	247.92	44.83
Hydroperoxycarbene	68.8	64.5	268.84	60.77
$C_1H_2O_3$				
Carbonic acid	−603.6	−613.0	267.36	66.23
Dioxiranol *syn*	−199.3	−209.4	268.39	58.84
Dioxiranol *anti*	−216.0	−226.2	268.25	58.82
Dioxyhydroxymethyl	−97.2	−106.1	275.87	63.99
Hydroxyhydroperoxycarbene	−144.6	−151.5	290.78	74.42
Methylenetrioxygen	423.0	413.3	266.48	63.83
Oxoformic acid	−54.3	−63.1	290.06	60.76
Peroxyformic acid	−281.6	−291.0	277.22	66.88
Trioxetane	102.9	92.7	270.26	50.53
$C_1H_2O_4$				
Bis-dioxymethylene	93.2	82.6	299.71	77.50
Bis-hydroperoxymethylene	−38.2	−45.7	327.33	87.87
Carbonoperoxoic acid	−504.7	−516.1	296.50	78.23
Dioxiranediol	−422.2	−432.3	295.60	85.18
Dioxydihydroxymethyl	−302.1	−315.0	297.14	78.99
Dioxyhydroperoxymethyl	−45.7	−57.2	301.38	72.74
Formyl hydrotrioxide	−223.3	−226.3	303.80	86.05
Oxodioxiranol	86.5	75.1	299.07	76.88
Oxyoxonium methyldioxy	247.3	237.7	316.33	84.62
Tetroxolane	69.9	57.0	285.30	66.46
$C_1H_2O_5$				
Carbonodiperoxoic acid *saas*	−396.6	−408.8	323.98	91.96
Carbonodiperoxoic acid *sasg*	−388.4	−398.8	336.00	95.12

TABLE 1. (*Continued.*)

Species	$\Delta_f H^o$(0 K)	$\Delta_f H^o$(298.15 K)	S^o(298.15 K)	C_p^o(298.15 K)
Formylhydrotetroxide	−165.6	−176.3	344.79	100.76
Pentoxane	95.8	79.5	298.90	81.88
$C_2H_1O_1$				
Ethynyloxy	175.5	176.5	247.38	51.65
Hydroxyethynyl	408.1	410.3	258.16	50.21
Oxirenyl	398.1	398.7	253.40	45.26
Oxoethylidyne	510.1	510.1	256.46	42.64
$C_2H_1O_2$				
Carboxymethylidyne *syn*	176.9	175.9	281.74	63.48
Carboxymethylidyne *anti*	181.0	179.9	280.98	63.94
Dioxyethenylidene *anti*	549.2	549.2	290.48	66.64
Dioxyethenylidene *syn*	551.8	552.1	295.	67.87
1,2-Dioxet-3-yl	421.9	419.3	271.85	52.69
Ethynylhydroperoxide	476.2	477.1	295.82	69.28
Ethynylperoxy	364.0	362.4	278.46	62.32
Formyloxymethylidyne	118.9	118.6	292.44	56.98
Hydroxyoxirenyl	256.1	254.6	279.19	61.16
Hydroxyoxoethenyl	31.3	29.5	275.12	59.62
Methylenedioxiranyl	374.7	372.8	276.06	63.20
Oxirenyloxy	39.9	38.2	277.82	58.16
Oxoethynyloxy	−64.3	−65.5	283.34	59.45
2-Oxo-2-oxy-ethylidene $^4A''$	261.1	258.8	281.27	59.80
2-Oxo-2-oxy-ethylidene $^2A'$	n/a	n/a	272.22	50.88
$C_2H_1O_3$				
Carboxyoxomethyl	−306.8	−310.6	310.29	75.38
Dioxiranyloxomethyl	75.3	71.3	309.44	67.52
Dioxoethoxy	−117.3	−121.3	304.73	71.45
Formyloxy oxomethyl *sa*	−283.3	−286.0	314.70	74.73
Formyloxy oxomethyl *aa*	−282.9	−282.2	309.87	74.03
Hydroperoxyketenyl	78.8	77.2	320.84	82.52
Hydroxyoxarinonyl	−146.3	−149.5	305.73	76.85
4-Oxo-1,2-dioxetan-3-yl	−8.3	−14.0	287.06	66.37
4-Oxo-1,3-dioxetan-2-yl	−229.1	−235.9	281.99	60.51
Peroxyketenyl *syn*	77.2	75.2	315.15	79.31
Peroxyketenyl *anti*	83.3	81.1	310.70	79.83
2,3,5-Trioxabicyclo[2.1.0]pentyl	260.0	253.6	281.91	65.11
2,4,5-Trioxabicyclo[1.1.1]pentyl	147.3	142.2	285.81	57.96
$C_2H_1O_4$				
Carboxyformyl ether radical	−452.7	−458.0	338.63	82.86
Carboxyoxomethoxy	−461.6	−468.1	323.97	84.96
Carboxyoxy oxomethyl	−517.9	−523.2	329.80	92.32
Dioxirane carboxylic acid no. 1	−88.4	−96.2	330.20	76.29
Dioxirane carboxylic acid no. 2	−145.1	−151.2	330.62	88.16
1,2-Dioxoethyldioxy	−178.2	−182.9	335.69	88.68
Formylperoxy oxomethyl	−208.0	−214.4	336.45	81.39
2-Hydroperoxy-1,2-dioxoethyl	−207.4	−210.9	346.24	98.32
$C_2H_1O_5$				
2-Carboxyl peroxoic acid radical	−368.5	−374.9	362.66	110.17
Dicarbonic acid radical	−678.2	−686.3	350.81	95.60
Diformyl trioxide radical	−148.3	−155.2	364.83	104.34
2-Oxo-2-peroxyl-2-ethanoic acid radical	−432.6	−440.1	358.74	101.83
$C_2H_1O_6$				

TABLE 1. (*Continued.*)

Species	$\Delta_f H^o$(0 K)	$\Delta_f H^o$(298.15 K)	S^o(298.15 K)	C_p^o(298.15 K)
Diformyltetroxide radical	−104.0	−111.7	398.23	118.65
Ethanodiperoxoic acid radical	−333.3	−342.2	383.77	119.15
Peroxydicarbonic acid radical	−605.4	−616.0	374.64	110.70
$C_2H_1O_8$				
Dicarboxyltetroxide radical	−500.7	−513.5	426.36	141.52
$C_2H_2O_1$				
Ethynol	95.0	92.5	247.49	56.08
Ketene	−45.9	−49.1	241.40	51.21
Oxirene	271.8	270.0	254.68	52.81
1-Oxo-1,2-ethanediyl	180.7	177.6	259.91	51.07
Oxybismethylene	500.1	497.2	243.27	51.24
2-Oxoethenyl *anti*	259.5	256.0	262.33	54.17
2-Oxoethenyl *syn*	264.9	261.6	261.65	54.61
$C_2H_2O_2$				
Carboxymethylene	13.1	7.0	281.80	67.69
Dihydroxyethenylidene	138.9	135.0	281.35	71.31
1,2-Dioxetan-3-ylidene	258.3	251.7	267.75	58.94
1,3-Dioxetane-2,4-diyl	57.3	50.6	267.10	55.14
1,2-Dioxabicyclo[1.1.0]butane	107.9	101.7	264.01	59.76
1,2-Dioxete	140.7	132.9	254.90	53.42
1,2-Ethynediol	−19.4	−22.8	282.55	72.39
Ethynylhydroperoxide	195.9	191.6	291.61	70.97
Formyloxy methylene	3.4	−2.3	274.98	61.50
Glyoxal *trans*	−208.8	−212.6	271.61	59.78
Glyoxal *cis*	−191.3	−196.9	273.45	59.95
Hydroxyethenone	−145.6	−150.6	285.56	66.03
Methylenedioxirane	111.6	104.8	261.75	59.58
Methyleneoxy oxomethyl	42.1	39.0	303.69	72.27
2-Oxarinone	−164.9	−172.4	263.99	54.05
2-Oxo-2-oxoethyl	16.6	10.4	276.04	63.30
1-Oxo-2-oxoethyl	83.2	78.5	298.75	64.87
$C_2H_2O_3$				
Dihydroxyethenone	−300.5	−307.6	296.76	81.41
2,4-Dioxabicyclobutanol	n/a	n/a	n/a	n/a
1,2-Dioxetan-3-one	−167.1	−177.4	282.18	65.08
1,3-Dioxetan-2-one	−432.0	−442.9	271.66	60.21
Dioxiranecarboxaldehyde	−93.9	−102.5	294.81	71.02
2,2′-Dioxo-ethan-1-ol	−181.9	−190.0	305.56	77.93
1-Dioxy-2-oxoethyl	+3.9	−3.7	301.26	75.00
Formic acid anhydride	−467.0	−474.5	305.86	74.67
Hydroperoxyethenone	−75.3	−81.3	321.32	81.37
2-Hydroxyl acetic acid	−255.3	−263.3	305.79	75.74
Hydroxy-2-oxarinone	−349.9	−358.2	300.14	76.41
2-Oxo-acetic acid	−464.5	−471.1	298.52	78.01
1,2,3-Trioxolene	132.0	121.3	282.78	62.06
2,3,5-Trioxabicyclo[2.1.0]pentane	15.1	3.8	273.47	62.04
2,4,5-Trioxabicyclo[1.1.1]pentane	−99.6	−110.0	270.54	60.36
$C_2H_2O_4$				
Carboxyformyl ether *ssa*	−702.2	−712.3	321.72	88.73
Carboxyformyl ether *aas*	−697.5	−708.5	312.11	82.55
Diformyl peroxide	−406.7	−416.9	317.82	82.08
Dioxirane carboxylic acid	−342.1	−352.3	323.89	84.01

TABLE 1. (*Continued.*)

Species	$\Delta_f H^o$(0 K)	$\Delta_f H^o$(298.15 K)	S^o(298.15 K)	C_p^o(298.15 K)
Oxalic acid *tTt*	−724.9	−735.2	310.50	91.20
Peroxyglyoxylic acid	−366.2	−375.4	333.75	99.98
1,2,3,4-Tetroxin	149.1	136.0	296.56	81.65
$C_2H_2O_5$				
Dicarbonic acid	−935.2	−948.8	338.34	98.54
Diformyl trioxide	−340.6	−351.7	348.29	104.42
Formyl carboxyl peroxide	−630.6	−642.8	348.78	100.89
2-Hydroperoxy-2-oxoacetic acid	−611.0	−623.3	354.88	100.99
$C_2H_2O_6$				
Diformyltetroxide	−289.4	−302.9	367.73	113.10
Ethanediperoxoic acid	−515.6	−526.5	373.79	118.36
Peroxydicarbonic acid	−855.2	−869.5	358.07	117.26
$C_2H_2O_7$				
Dicarboxyl trioxide	−789.2	−805.4	385.20	129.16
Formyl carboxyl tetroxide	−516.0	−526.9	410.44	128.66
$C_2H_2O_8$				
Dicarboxyltetroxide	−746.1	−763.3	410.41	147.49

improvements in hardware and software continue. More concerning is the paucity of robust, quasi-universal procedures for dealing with problematic vibrational modes; this seems to be a real stumbling block to future progress.

5. Supplementary Material

See the supplementary material for (a) a complete set of MultiWell/THERMO annotated input files, including a brief description of the sources for the fundamental physical constants employed by that application, and (b) a text file containing species name, xyz's, rotational constants, and frequencies.

Acknowledgments

Computational resources were supplied by the Irish Centre for High-End Computing (ICHEC) under Project Nos. nuig02, ngche048c, ngche065c, ngche071b, and gmche003c. We thank the ICHEC staff for providing vital assistance during many phases of this project.

We thank Professor H.-J. Werner (Universität Stuttgart) and Professor P. J. Knowles (Cardiff University) for the provision of MOLPRO and Lokesh Joshi (Vice President of Research, NUIG) for support. Scripts and tools provided by our colleague Dr. Kieran Somers (Ph.D. thesis, National University of Ireland, Galway 2014) were most useful. We would like to thank Professor Yan Zhao (Wuhan University) for assistance with WMS.

Data Availability

The data that supports the findings of this study are available within the article and its supplementary material.

6. References

1. V. Trimble, "The origin and abundances of the chemical elements revisited," Astro. Astrophys. Rev. **3**(1), 1–46 (1991).
2. L. Vereecken, B. Aumont, I. Barnes, J. W. Bozzelli, M. J. Goldman, W. H. Green, S. Madronich, M. R. Mcgillen, A. Mellouki, J. J. Orlando, B. Picquet-Varrault, A. R. Rickard, W. R. Stockwell, T. J. Wallington, and W. P. L. Carter, "Perspective on mechanism development and structure-activity relationships for gas-phase atmospheric chemistry," Int. J. Chem. Kinet. **50**(6), 435–469 (2018).
3. Z. Wang, D. M. Popolan-Vaida, B. Chen, K. Moshammer, S. Y. Mohamed, H. Wang, S. Sioud, M. A. Raji, K. Kohse-Höinghaus, N. Hansen, P. Dagaut, S. R. Leone, and S. M. Sarathy, "Unraveling the structure and chemical mechanisms of highly oxygenated intermediates in oxidation of organic compounds," Proc. Natl. Acad. Sci. U. S. A. **114**(50), 13102–13107 (2017).
4. R. T. Garrod, S. L. W. Weaver, and E. Herbst, "Complex chemistry in star-forming regions: An expanded gas-grain warm-up chemical model," Astrophys. J. **682**(1), 283–302 (2008).
5. A. Karton and D. Talbi, "Pinning the most stable $H_xC_yO_z$ isomers in space by means of high-level theoretical procedures," Chem. Phys. **436-437**, 22–28 (2014).
6. S. Iyer, M. P. Rissanen, and T. Kurtén, "Reaction between peroxy and alkoxy radicals can form stable Adducts," J. Phys. Chem. Lett. **10**(9), 2051–2057 (2019).
7. S. Amabilino, L. A. Bratholm, S. J. Bennie, A. C. Vaucher, M. Reiher, and D. R. Glowacki, "Training neural nets to learn reactive potential energy surfaces using interactive quantum chemistry in virtual reality," J. Phys. Chem. A **123**(20), 4486–4499 (2019).
8. Y.-P. Li, K. Han, C. A. Grambow, and W. H. Green, "Self-evolving machine: A continuously improving model for molecular thermochemistry," J. Phys. Chem. A **123**, 2142–2152 (2019).
9. C. A. Grambow, Y.-P. Li, and W. H. Green, "Accurate thermochemistry with small datasets: A bond additivity correction and transfer learning approach," J. Phys. Chem. A **123**(27), 5826–5835 (2019).
10. B. Narayanan, P. C. Redfern, R. S. Assary, and L. A. Curtiss, "Accurate quantum chemical energies for 133 000 organic molecules," Chem. Sci. **10**, 7449–7455 (2019).
11. P. Morgante and R. Peverati, "Statistically representative databases for density functional theory *via* data science," Phys. Chem. Chem. Phys. **21**, 19092–19103 (2019).
12. A. Menon, N. B. Krdzavac, and M. Kraft, "From database to knowledge graph—Using data in chemistry," Curr. Opin. Chem. Eng. **26**, 33 (2019).
13. Spartan'18, version 1.4.0, Wavefunction, Inc., Irvine, CA, USA.

14. M. J. Frisch, G. W. Trucks, H. B. Schlegel, G. E. Scuseria, M. A. Robb, J. R. Cheeseman, G. Scalmani, V. Barone, G. A. Petersson, H. Nakatsuji, X. Li, M. Caricato, A. V. Marenich, J. Bloino, B. G. Janesko, R. Gomperts,B. Mennucci, H. P. Hratchian, J. V. Ortiz, A. F. Izmaylov, J. L. Sonnenberg, D. Williams-Young, F. Ding, F. Lipparini, F. Egidi, J. Goings, B. Peng, A. Petrone, T. Henderson, D. Ranasinghe, V. G. Zakrzewski, J. Gao, N. Rega, G. Zheng, W. Liang, M. Hada, M. Ehara, K. Toyota, R. Fukuda, J. Hasegawa, M. Ishida, T. Nakajima, Y. Honda, O. Kitao, H. Nakai, T. Vreven, K. Throssell, J. A. Montgomery, Jr., J. E. Peralta, F. Ogliaro, M. J. Bearpark, ; J. J. Heyd, E. N. Brothers, K. N. Kudin, V. N. Staroverov, T. A. Keith, R. Kobayashi, J. Normand, K. Raghavachari, A. P. Rendell, J. C. Burant, S. S. Iyengar, J. Tomasi, M. Cossi, J. M. Millam, M. Klene, C. Adamo, R. Cammi, J. W. Ochterski, R. L. Martin, K. Morokuma, O. Farkas, J. B. Foresman, and D. J. Fox, Gaussian 16, Revision A.03, Gaussian, Inc., Wallingford, CT, 2016.
15. D. N. Tahchieva, D. Bakowies, R. Ramakrishnan, and O. A. von Lilienfeld, "Torsional potentials of glyoxal, oxalyl halides, and their thiocarbonyl derivatives: Challenges for popular density functional approximations," J. Chem. Theory Comput. **14**(9), 4806–4817 (2018).
16. B. Chan and L. Radom, "W2X and W3X-L: Cost-effective approximations to W2 and W4 with kJ mol^{-1} accuracy," J. Chem. Theory Comput. **11**(5), 2109–2119 (2015).
17. R. L. Jacobsen, R. D. Johnson, K. K. Irikura, and R. N. Kacker, "Anharmonic vibrational frequency calculations are not worthwhile for small basis sets," J. Chem. Theor. Comput. **9**, 951–954 (2013).
18. M. Piccardo, J. Bloino, and V. Barone, "Generalized vibrational perturbation theory for rotovibrational energies of linear, symmetric and asymmetric tops: Theory, approximations, and automated approaches to deal with medium-to-large molecular systems," Int. J. Quantum Chem. **115**(15), 948–982 (2015).
19. K. K. Irikura, "Anharmonic partition functions for polyatomic thermochemistry," J. Chem. Thermodyn. **73**, 183–189 (2014).
20. S. J. Klippenstein, L. B. Harding, and B. Ruscic, "*Ab initio* computations and active thermochemical tables hand in hand: Heats of formation of core combustion species," J. Phys. Chem. A **121**(35), 6580–6602 (2017).
21. J. Zádor and J. A. Miller, "Comment on influence of multiple conformations and paths on rate constants and product branching ratios. Thermal decomposition of 1-propanol radicals," J. Phys. Chem. A **123**(5), 1129–1130 (2019).
22. D. Ferro-Costas, M. N. D. S. Cordeiro, D. G. Truhlar, and A. Fernández-Ramos, "Q2DTor: A program to treat torsional anharmonicity through coupled pair torsions in flexible molecules," Comput. Phys. Commun. **232**, 190–205 (2018).
23. J. R. Barker, T. L. Nguyen, J. F. Stanton, C. Aieta, M. Ceotto, F. Gabas, T. J. D. Kumar, C. G. L. Li, L. L. Lohr, A. Maranzana, N. F. Ortiz, J. M. Preses, J. M. Simmie, J. A. Sonk, and P. J. Stimac, MultiWell-2017 Software Suite, J. R. Barker, University of Michigan, Ann Arbor, MI, USA, 2018, http://clasp-research.engin.umich.edu/multiwell/.
24. L. Vereecken, D. R. Glowacki, and M. J. Pilling, "Theoretical chemical kinetics in tropospheric chemistry: Methodologies and applications," Chem. Rev. **115**(10), 4063–4114 (2015).
25. C. F. Goldsmith, G. R. Magoon, and W. H. Green, "Database of small molecule thermochemistry for combustion," J. Phys. Chem. A **116**(36), 9033–9057 (2012).
26. written by H.-J. Werner, P. J. Knowles, G. Knizia, F. R. Manby, M. Schütz, P. Celani, W. Györffy, D. Kats, T. Korona, R. Lindh, A. Mitrushenkov, G. Rauhut, K. R. Shamasundar, T. B. Adler, R. D. Amos, S. J. Bennie, A. Bernhardsson, A. Berning, D. L. Cooper, M. J. O. Deegan, A. J. Dobbyn, F. Eckert, E. Goll, C. Hampel, A. Hesselmann, G. Hetzer, T. Hrenar, G. Jansen, C. Köppl, S. J. R. Lee, Y. Liu, A. W. Lloyd, Q. Ma, R. A. Mata, A. J. May, S. J. McNicholas, W. Meyer, T. F. Miller III, M. E. Mura, A. Nicklaß, D. P. O'Neill, P. Palmieri, D. Peng, K. Pflüger, R. Pitzer, M. Reiher, T. Shiozaki, H. Stoll, A. J. Stone, R. Tarroni, T. Thorsteinsson, M. Wang, and M. Welborn, MOLPRO, version 2018.1, a package of *ab initio* programs, http://www.molpro.net.
27. MRCC, a quantum chemical program suite written byM. Kállay, Z. Rolik, J. Csontos, P. Nagy, G. Samu, D. Mester, J. Csóka, I. Ladjánszki, L. Szegedy, B. Ladóczki, K. Petrov, M. Farkas, and B. Hégely, see also Z. Rolik, L. Szegedy, I. Ladjánszki, B. Ladóczki, and M. Kállay, *J. Chem. Phys.* **139**, 094105 (2013), see htpp://www.mrcc.hu.
28. Y. Zhao, L. Xia, X. Liao, Q. He, M. X. Zhao, and D. G. Truhlar, "Extrapolation of high-order correlation energies: The WMS model," Phys. Chem. Chem. Phys. **20**(43), 27375–27384 (2018).
29. J. A. Montgomery, M. J. Frisch, J. W. Ochterski, and G. A. Petersson, "A complete basis set model chemistry. VII. Use of the minimum population localization method," J. Chem. Phys. **112**(15), 6532–6542 (2000).
30. J. W. Ochterski, G. A. Petersson, and J. A. Montgomery, "A complete basis set model chemistry. V. Extensions to six or more heavy atoms," J. Chem. Phys. **104**(7), 2598–2619 (1996).
31. L. A. Curtiss, K. Raghavachari, P. C. Redfern, V. Rassolov, and J. A. Pople, "Gaussian-3 (G3) theory for molecules containing first and second-row atoms," J. Chem. Phys. **109**(18), 7764–7776 (1998).
32. L. A. Curtiss, P. C. Redfern, and K. Raghavachari, "Gaussian-4 theory using reduced order perturbation theory," J. Chem. Phys. **127**(12), 124105 (2007).
33. E. C. Barnes, G. A. Petersson, J. A. Montgomery, M. J. Frisch, and J. M. L. Martin, "Unrestricted coupled cluster and Brueckner doubles variations of W1 theory," J. Chem. Theory Comput. **5**(10), 2687–2693 (2009).
34. J. M. Simmie, G. Black, H. J. Curran, and J. P. Hinde, "Enthalpies of formation and bond dissociation energies of lower alkyl Hydroperoxides and related hydroperoxy and alkoxy radicals," J. Phys. Chem. A **112**(22), 5010–5016 (2008).
35. J. M. Simmie and J. N. Sheahan, "Validation of a database of formation enthalpies and of mid-level model chemistries," J. Phys. Chem. A **120**(37), 7370–7384 (2016).
36. K. P. Somers and J. M. Simmie, "Benchmarking compound methods (CBS-QB3, CBS-APNO, G3, G4, W1BD) against the active thermochemical tables: Formation enthalpies of radicals," J. Phys. Chem. A **119**(33), 8922–8933 (2015).
37. J. M. Simmie and K. P. Somers, "Benchmarking compound methods (CBS-QB3, CBS-APNO, G3, G4, W1BD) against the active thermochemical tables: A litmus test for cost-effective molecular formation enthalpies," J. Phys. Chem. A **119**(28), 7235–7246 (2015).
38. B. Ruscic and D. H. Bross, Active Thermochemical Tables (ATcT) values based on version 1.122 of the Thermochemical Network, 2016, available at https://ATcT.anl.gov.
39. *NIST-JANAF Thermochemical Tables*, 4th ed., Journal of Physical and Chemical Reference Data, Monograph Vol. 9, edited by M. W. Chase, Jr. (U.S. Department of Commerce, Gaithersburg, MD, 1963).
40. E. Goos, A. Burcat, and B. Ruscic, "Extended third Millennium ideal gas and condensed phase thermochemical database for combustion with updates from active thermochemical tables," Mirrored at http://garfield.chem.elte.hu/Burcat/burcat.html; 12 January 2018.
41. NIST Chemistry WebBook, Standard Reference Database No. 69, https://doi.org/10.18434/T4D303.
42. Y.-R. Luo, *Comprehensive Handbook of Chemical Bond Energies* (CRC Press, Boca Raton, USA, 2007).
43. B. Narayanan, P. C. Redfern, R. S. Assary, and L. A. Curtiss, "Accurate quantum chemical energies for 133 000 organic molecules," Chem. Sci. **10**, 7449 (2019).
44. J.-Y. Park, M. C. Heaven, and D. Gutman, "Kinetics and mechanism of the reaction of vinyl radicals with molecular-oxygen," Chem. Phys. Lett. **104**, 469–474 (1984).
45. I. R. Slagle, J. Y. Park, M. C. Heaven, and D. Gutman, "Kinetics of polyatomic free-radicals produced by laser photolysis. III. Reaction of vinyl radicals with molecular-oxygen," J. Am. Chem. Soc. **106**, 4356–4361 (1984).
46. H. Wang, B. Wang, Y. He, and F. Kong, "The gaseous reaction of vinyl radical with oxygen," J. Chem. Phys. **115**, 1742–1746 (2001).
47. A. Bacmann and A. Faure, "The origin of gas-phase HCO and CH_3O radicals in prestellar cores," Astro. Astrophys. **587**, A130 (2016).
48. A. C. Terentis and S. H. Kable, "Near threshold dynamics and dissociation energy of the reaction $H_2CO \rightarrow HC_2O + H$," Chem. Phys. Lett. **258**, 626–632 (1996).
49. M. C. Chuang, M. F. Foltz, and C. B. Moore, "T_1 barrier height, S_1-T_1 intersystem crossing rate, and S_0 radical dissociation threshold for H_2CO, D_2CO and HDCO," J. Chem. Phys. **87**, 3855–3864 (1987).
50. R. Becerra, I. W. Carpenter, and R. Walsh, "Time-resolved studies of the kinetics of the reactions of CHO with HI and HBr: Thermochemistry of the

CHO radical and the C–H bond strengths in CH_2O and CHO," J. Phys. Chem. A **101**(23), 4185–4190 (1997).
51. D. Feller, K. A. Peterson, and D. A. Dixon, "A survey of factors contributing to accurate theoretical predictions of atomization energies and molecular structures," J. Chem. Phys. **129**, 204105 (2008).
52. A. Karton, N. Sylvetsky, and J. M. L. Martin, "W4-17: A diverse and high-confidence dataset of atomization energies for benchmarking high-level electronic structure methods," J. Comput. Chem. **38**, 2063–2075 (2017).
53. A. V. Marenich and J. E. Boggs, "Coupled cluster CCSD(T) calculation of equilibrium geometries, anharmonic force fields and thermodynamic properties of the formyl (HCO) and isoformyl (COH) radical species," J. Phys. Chem. A **107**, 2343–2350 (2003).
54. L. V. Gurvich, I. V. Veyts, and C. B. Alcock, *Thermodynamic Properties of Individual Substances: Elements and Compounds* (Hemisphere, New York, 1989), Vol. 2.
55. T. H. Dunning, "Theoretical characterization of the potential energy surface of the ground state of the HCO system," J. Chem. Phys. **73**, 2304–2309 (1980).
56. M. Agundez, N. Marcelino, J. Cernicharo, and M. Tafalla, "Detection of interstellar HCS and its metastable isomer HSC: New pieces in the puzzle of sulfur chemistry," Astron. Astrophys. **611**, L1 (2018).
57. M.-B. Huang, B.-Z. Chen, and Z.-X. Wang, "Theoretical study of CH + O_2 reactions," J. Phys. Chem. A **106**(22), 5490–5497 (2002).
58. A. Mansergas and J. M. Anglada, "Reaction mechanism between carbonyl oxide and hydroxyl radical: A theoretical study," J. Phys. Chem. A **110**(11), 4001–4011 (2006).
59. E. H. Kim, S. E. Bradforth, D. W. Arnold, and R. B. Metz, "Study of HCO_2 and DCO_2 by negative ion photoelectron spectroscopy," J. Chem. Phys. **103**, 7801–7814 (1995).
60. M. Döntgen and K. Leonhard, "Reactions of chemically activated formic acid formed via HĊO + ȮH," J. Phys. Chem. A **120**(11), 1819–1824 (2016).
61. V. B. Oyeyemi, D. B. Krisiloff, J. A. Keith, F. Libisch, M. Pavone, and E. A. Carter, "Size-extensivity-corrected multireference configuration interaction schemes to accurately predict bond dissociation energies of oxygenated hydrocarbons," J. Chem. Phys. **140**(4), 044317 (2014).
62. E. Garand, K. Klein, J. F. Stanton, J. Zhou, T. I. Yacovitch, and D. M. Neumark, "Vibronic structure of the formyloxyl radical (HCO_2) via slow photoelectron velocity-map imaging spectroscopy and model Hamiltonian calculations," J. Phys. Chem. A **114**(3), 1374–1383 (2010).
63. D. Feller, D. A. Dixon, and J. S. Francisco, "Coupled cluster theory determination of the heats of formation of combustion-related Compounds: CO, HCO, CO_2, HCO_2, HOCO, HC(O)OH, and HC(O)OOH," J. Phys. Chem. A **107**(10), 1604–1617 (2003).
64. D. A. Dixon, D. Feller, and J. S. Francisco, "Molecular structure, vibrational frequencies, and energetics of the HCO, HOCO, and HCO_2 anions," J. Phys. Chem. A **107**, 186–190 (2003).
65. W. M. F. Fabian and R. Janoschek, "Thermochemical properties of the hydroxy-formyl radical, HOCO, and the formyloxy radical, HC(O)O, and their role in the reaction OH + CO → H + CO_2. Computational G3MP2B3 and CCSD(T)-CBS studies," J. Mol. Struct.: THEOCHEM **713**, 227–234 (2005).
66. D. Yu, A. Rauk, and D. A. Armstrong, "Radicals and ions of formic and acetic acids: An *ab initio* study of the structures and gas and solution thermochemistry," J. Chem. Soc. Perkin Trans. **2**, 2207–2215 (1994).
67. J. Warnatz, *Combustion Chemistry*, edited by W. C. Gardiner (Springer, New York, 1984), Chap. 5.
68. E. J. K. Nilsson and A. A. Konnov, "Role of HOCO chemistry in syngas combustion," Energy Fuels **30**, 2443–2457 (2016).
69. R. C. Fortenberry, X. Huang, J. S. Francisco, T. D. Crawford, and T. J. Lee, "The *trans*-HOCO radical: Quartic force fields, vibrational frequencies, and spectroscopic constants," J. Chem. Phys. **135**, 134301 (2011).
70. J. S. Francisco, J. T. Muckerman, and H.-G. Yu, "HOCO radical chemistry," Acc. Chem. Res. **43**(12), 1519–1526 (2010).
71. B. Ruscic and M. Litorja, "Photo-ionization of HOCO revisited: A new upper limit to the adiabatic ionization energy and lower limit to the enthalpy of formation," Chem. Phys. Lett. **316**, 45–50 (2000).
72. B. Nagy, J. Csontos, M. Kállay, and G. Tasi, "High-accuracy theoretical study on the thermochemistry of several formaldehyde derivatives," J. Phys. Chem. A **114**(50), 13213–13221 (2010).
73. T. L. Nguyen, B. C. Xue, R. E. Weston, Jr., J. R. Barker, and J. F. Stanton, "Reaction of HO with CO: Tunneling is indeed important," J. Phys. Chem. Lett. **3**, 1549 (2012).
74. R. C. Fortenberry, X. Huang, J. S. Francisco, T. D. Crawford, and T. J. Lee, "Vibrational frequencies, and spectroscopic constants from quartic force fields for *cis*-HOCO: The radical and the anion," J. Chem. Phys. **135**, 214303 (2011).
75. S. Ghoshal and M. K. Hazra, "Impact of OH radical-initiated H_2CO_3 degradation in the earth's atmosphere via proton-coupled electron transfer mechanism," J. Phys. Chem. A **120**, 562–575 (2016).
76. C. Puzzarini, M. Biczysko, K. A. Peterson, J. S. Francisco, and R. Linguerri, "Accurate spectroscopic characterization of the HOC(O)O radical: A route toward its experimental identification," J. Chem. Phys. **147**(2), 024302 (2017).
77. D. A. Armstrong, W. L. Waltz, and A. Rauk, "Carbonate radical anion—Thermochemistry," Can. J. Chem. **84**, 1614–1619 (2006).
78. G. da Silva, "Hydroxyl radical regeneration in the photochemical oxidation of glyoxal:kinetics and mechanism of the HC(O)CO + O2 reaction," Phys. Chem. Chem. Phys. **12**, 6698–6705 (2010).
79. S. N. Elliott, J. M. Turney, and H. F. Schaefer, "The *cis*- and *trans*-formylperoxy radical: Fundamental vibrational frequencies and relative energies of the (X) $^2A''$ and (A) $^2A'$ states," RSC Adv. **5**(130), 107254–107265 (2015).
80. In Ref. 79 above their Fig. 3 contradicts both the text and their Table 3 about which is the more stable conformer.
81. A. A. Nickel, J. G. Lanorio, and K. M. Ervin, "Energy-Resolved collision-induced dissociation of peroxyformate anion: Enthalpies of formation of peroxyformic acid and peroxyformyl radical," J. Phys. Chem. A **117**(6), 1021–1029 (2013).
82. S. M. Villano, N. Eyet, S. W. Wren, G. B. Ellison, V. M. Bierbaum, and W. C. Lineberger, "Photoelectron spectroscopy and thermochemistry of the peroxyformate anion," J. Phys. Chem. A **114**(1), 191–200 (2010).
83. P. Saenz Méndez, L. A. Eriksson, and O. N. Ventura, "Theoretical study of the structure of neutral, radical and anionic monoperoxo carbonic acid," J. Mol. Struct.: THEOCHEM **913**(1), 131–138 (2009).
84. C. Kolano, G. Bucher, H. H. Wenk, M. Jäger, O. Schade, and W. Sander, "Photochemistry of 9-fluorenone oxime phenylglyoxylate: A combined TRIR, TREPR and *ab initio* study," J. Phys. Org. Chem. **17**(3), 207–214 (2004).
85. J. Berkowitz, G. B. Ellison, and D. Gutman, "Three methods to measure RH bond energies," J. Phys. Chem. **98**, 2744 (1994).
86. C. M. Leavitt, C. P. Moradi, J. F. Stanton, and G. E. Douberly, "Helium nanodroplet isolation and rovibrational spectroscopy of hydroxymethylene," J. Chem. Phys. **140**, 171102 (2014).
87. D. Feller, K. A. Peterson, and D. A. Dixon, "Further benchmarks of a composite, convergent, statistically calibrated coupled-cluster-based approach for thermochemical and spectroscopic studies," Mol. Phys. **110**, 2381–2399 (2012).
88. T. L. Nguyen and J. F. Stanton, "A steady-state approximation to the two-dimensional master equation for chemical kinetics calculations," J. Phys. Chem. A **119**(28), 7627–7636 (2015).
89. K. D. Vogiatzis, R. Haunschild, and W. Klopper, "Accurate atomization energies from combining coupled-cluster computations with interference-corrected explicitly correlated second-order perturbation theory," Theor. Chem. Acc. **133**, 1446 (2014).
90. P. Zoogman, X. Liu, R. M. Suleiman, W. F. Pennington, D. E. Flittner, J. A. Al-Saadi, B. B. Hilton, D. K. Nicks, M. J. Newchurch, J. L. Carr, S. J. Janz, M. R. Andraschko, A. Arola, B. D. Baker, B. P. Canova, C. Chan Miller, R. C. Cohen, J. E. Davis, M. E. Dussault, D. P. Edwards, J. Fishman, A. Ghulam, G. González Abad, M. Grutter, J. R. Herman, J. Houck, D. J. Jacob, J. Joiner, B. J. Kerridge, J. Kim, N. A. Krotkov, L. Lamsal, C. Li, A. Lindfors, R. V. Martin, C. T. McElroy, C. McLinden, V. Natraj, D. O. Neil, C. R. Nowlan, E. J. O'Sullivan, P. I. Palmer, R. B. Pierce, M. R. Pippin, A. Saiz-Lopez, R. J. D. Spurr, J. J. Szykman, O. Torres, J. P. Veefkind, B. Veihelmann, H. Wang, J. Wang, and K. Chance, "Tropospheric emissions: Monitoring of pollution (TEMPO)," J. Quant. Spectrosc. Radiat. Transfer **186**, 17–39 (2017).

91. M. L. Delitsky, D. A. Paige, M. A. Siegler, E. R. Harju, D. Schriver, R. E. Johnson, and P. Travnicek, "Ices on Mercury: Chemistry of volatiles in permanently cold areas of Mercury's north polar region," Icarus **281**, 19–31 (2017).
92. R. Ono, "Optical diagnostics of reactive species in atmospheric-pressure nonthermal plasma," J. Phys. D: Appl. Phys. **49**(8), 083001-1–083001-34 (2016).
93. J. M. Simmie, "Detailed chemical kinetic models for the combustion of hydrocarbon fuels," Prog. Energy Combust. Sci. **29**(6), 599–634 (2003).
94. R. A. Fletcher and G. Pilcher, "Measurements of heats of combustion by flame calorimetry. Part 6. Formaldehyde, glyoxal," Trans. Faraday Soc. **66**, 794–799 (1970).
95. A. Karton, E. Rabinovich, J. M. L. Martin, and B. Ruscic, "W4 theory for computational thermochemistry: In pursuit of confident sub-kJ/mol predictions," J. Chem. Phys. **125**, 144108 (2006).
96. G. da Silva, J. W. Bozzelli, N. Sebbar, and H. Bockhorn, "Thermodynamic and *ab initio* analysis of the controversial enthalpy of formation of formaldehyde," Chem. Phys. Chem. **7**, 1119–1126 (2006).
97. G. Czakó, E. Mátyus, A. C. Simmonett, A. G. Császár, H. F. Schaefer, and W. D. Allen, "Anchoring the absolute proton affinity scale," J. Chem. Theor. Comput. **4**(8), 1220–1229 (2008).
98. B. M. Broderick, L. McCaslin, C. P. Moradi, J. F. Stanton, and G. E. Douberly, "Reactive intermediates in ^{4}He nanodroplets: Infrared laser Stark spectroscopy of dihydroxycarbene," J. Chem. Phys. **142**(14), 144309 (2015).
99. L.-P. Wang, A. Titov, R. McGibbon, F. Liu, V. S. Pande, and T. J. Martínez, "Discovering chemistry with an *ab initio* nanoreactor," Nat. Chem. **6**(12), 1044–1048 (2014).
100. I. Alkorta and J. Elguero, "A LFER analysis of the singlet-triplet gap in a series of sixty-six carbenes," Chem. Phys. Lett. **691**, 33–36 (2018).
101. M. Vasiliu, K. A. Peterson, A. J. Arduengo, and D. A. Dixon, "Characterization of carbenes via hydrogenation energies, stability, and reactivity: What's in a name?," Chem. - Eur. J. **23**(69), 17556–17565 (2017).
102. T. L. Nguyen, H. Lee, D. A. Matthews, M. C. McCarthy, and J. F. Stanton, "Stabilization of the simplest criegee intermediate from the reaction between ozone and ethylene: A high-level quantum chemical and kinetic analysis of ozonolysis," J. Phys. Chem. A **119**(22), 5524–5533 (2015).
103. P. R. Schreiner and H. P. Reisenauer, "Spectroscopic identification of dihydroxycarbene," Angew. Chem., Int. Ed. **47**, 7071–7074 (2008).
104. J. M. Anglada, R. Crehuet, and J. M. Bofill, "The ozonolysis of ethylene: A theoretical study of the gas-phase reaction mechanism," Chem. Eur. J. **5**(6), 1809–1822 (1999).
105. M. T. Nguyen, T. L. Nguyen, V. T. Ngan, and H. M. T. Nguyen, "Heats of formation of the Criegee formaldehyde oxide and dioxirane," Chem. Phys. Lett. **448**, 183–188 (2007).
106. A. Karton, S. Daon, and J. M. L. Martin, "W4-11: A high-confidence benchmark dataset for computational thermochemistry derived from first-principles W4 data," Chem. Phys. Lett. **510**, 165–178 (2011).
107. O. V. Dorofeeva, "Ideal gas thermodynamic properties of oxygen heterocyclic compounds. Part 1. Three-membered, four-membered and five-membered rings," Thermochim. Acta **194**, 9–46 (1992).
108. D. Cremer, R. Crehuet, and J. Anglada, "The ozonolysis of acetylene-A quantum chemical investigation," J. Am. Chem. Soc. **123**, 6127–6141 (2001).
109. S. J. Klippenstein (personal communication, 21 December 2018).
110. R. Criegee, "Mechanism of ozonolysis," Angew. Chem., Int. Ed. **14**, 745–752 (1975).
111. C. A. Taatjes, G. Meloni, T. M. Selby, A. J. Trevitt, D. L. Osborn, C. J. Percival, and D. E. Shallcross, "Direct observation of the gas-phase criegee intermediate (CH_2OO)," J. Am. Chem. Soc. **130**(36), 11883–11885 (2008).
112. Y.-T. Su, Y.-H. Huang, H. A. Witek, and Y.-P. Lee, "Infrared absorption spectrum of the simplest criegee intermediate CH_2OO," Science **340**, 174–176 (2013).
113. H.-G. Hu, S. Ndengue, J. Li, R. Dawes, and H. Guo, "Vibrational energy levels of the simplest Criegee intermediate (CH_2OO) from full-dimensional Lanczos, MCTDH, and MULTIMODE calculations," J. Chem. Phys. **143**, 084311 (2015).
114. K. Moshammer, A. W. Jasper, D. M. Popolan-Vaida, A. Lucassen, P. Diévart, H. Selim, A. J. Eskola, C. A. Taatjes, S. R. Leone, S. M. Sarathy, Y. Ju, P. Dagaut, K. Kohse-Höinghaus, and N. Hansen, "Detection and identification of the keto-hydroperoxide ($HOOCH_2OCHO$) and other intermediates during low-temperature oxidation of dimethyl ether," J. Phys. Chem. A **119**(28), 7361–7374 (2015).
115. T. B. Nguyen, J. D. Crounse, A. P. Teng, J. M. St. Clair, F. Paulot, G. M. Wolfe, and P. O. Wennberg, Rapid deposition of oxidized biogenic compounds to a temperate forest, Proc. Natl. Acad. Sci. U. S. A. **112**, E392–E401 (2015).
116. C. Vastel, C. Ceccarelli, B. Lefloch, and R. Bachiller, "The origin of complex organic molecules in prestellar cores," Astrophys. J. Lett. **795**, L2 (2014).
117. G. C. Sinke, "The heat of formation of formic acid," J. Phys. Chem. **63**, 2063 (1959).
118. N. D. Lebedeva, "Heats of combustion of monocarboxylic acids," Russ. J. Phys. Chem. **38**, 1435–1437 (1964).
119. J. P. Guthrie, "Hydration of carboxamides. Evaluation of the free energy change for addition of water to acetamide and formamide derivatives," J. Am. Chem. Soc. **96**, 3608–3615 (1974).
120. D. R. Burgess, Jr., ""Thermochemical data" and Glushko thermocenter, Russian Academy of Sciences, Moscow entropy and heat capacity of organic compounds," in *NIST Chemistry WebBook, NIST Standard Reference Database Number 69*, edited by P. J. Linstrom and W. G. Mallard (National Institute of Standards and Technology, Gaithersburg, MD, 2019) (retrieved October 4, 2019).
121. R. C. Millikan and K. S. Pitzer, "Infrared spectra and vibrational assignment of monomeric formic acid," J. Chem. Phys. **27**, 1305–1308 (1957).
122. J. Chao, K. R. Hall, K. N. Marsh, and R. C. Wilhoit, "Thermodynamic properties of key organic oxygen compounds in the carbon range C1 to C4. Part 2. Ideal gas properties," J. Phys. Chem. Ref. Data **15**, 1369–1436 (1986).
123. K. Fukushima, J. Chao, and B. J. Zwolinski, "Normal coordinate treatment and thermodynamic properties of the *cis-trans* isomers of formic acid and its deutero-analog," J. Chem. Thermodyn. **3**, 553–562 (1971).
124. K. Ohno and S. Maeda, "Global reaction route mapping on potential energy surfaces of formaldehyde, formic acid, and their metal-substituted analogues," J. Phys. Chem. A **110**(28), 8933–8941 (2006).
125. N. A. Richardson, J. C. Rienstra-Kiracofe, and H. F. Schaefer, "Examining trends in the tetravalent character of group 14 elements (C, Si, Ge, Sn, Pb) with acids and hydroperoxides," J. Am. Chem. Soc. **121**(46), 10813–10819 (1999).
126. R. Gutbrod, R. N. Schindler, E. Kraka, and D. Cremer, "Formation of OH radicals in the gas phase ozonolysis of alkenes: The unexpected role of carbonyl oxides," Chem. Phys. Lett. **252**(3), 221–229 (1996).
127. B.-Z. Chen, J. M. Anglada, M.-B. Huang, and F. Kong, "The reaction of CH_2 ($X\ ^3B_1$) with O_2 ($X\ ^3$): A theoretical CASSCF/CASPT2 investigation," J. Phys. Chem. A **106**(9), 1877–1884 (2002).
128. S. Lakshmanan, S. Pratihar, F. B. C. Machado, and W. L. Hase, "Direct dynamics simulation of the thermal $^3CH_2 + {}^3O_2$ reaction. Rate constant and product branching ratios," J. Phys. Chem. A **122**(21), 4808–4818 (2018).
129. C. C. Womack, M.-A. Martin-Drumel, G. G. Brown, R. W. Field, and M. C. McCarthy, "Observation of the simplest Criegee intermediate CH_2OO in the gas-phase ozonolysis of ethylene," Sci. Adv. **1**(2), e1400105 (2015).
130. J. M. Buth, "Ocean acidification: Investigation and presentation of the effects of elevated carbon dioxide levels on seawater chemistry and calcareous organisms," J. Chem. Educ. **93**(4), 718–721 (2016).
131. H. P. Reisenauer, J. P. Wagner, and P. R. Schreiner, "Gas-phase preparation of carbonic acid and its monomethyl ester," Angew. Chem., Int. Ed. **53**(44), 11766–11771 (2014).
132. J. Bernard, M. Seidl, I. Kohl, K. R. Liedl, E. Mayer, O. Gálvez, H. Grothe, and T. Loerting, "Spectroscopic observation of matrix-isolated carbonic acid trapped from the gas phase," Angew. Chem., Int. Ed. **49**, 1939 (2010).
133. N. A. Porter, H. Yin, and D. A. Pratt, "The peroxy acid dioxirane equilibrium: Base-promoted exchange of peroxy acid oxygens," J. Am. Chem. Soc. **122**, 11272–11273 (2000).
134. Y. Yoshioka, D. Yamaki, S. Kubo, M. Nishino, K. Yamaguchi, K. Mizuno, and I. Saito, "Theoretical study on electronic structures of oxygenated dipoles and

mechanisms of ozonolysis reaction," Electron. J. Theor. Chem. **2**, 236–252 (1997).
135. L.-C. Li, X.-W. Liao, X. Wang, and A.-M. ATian, "*Ab initio* investigation on reaction of ozone with singlet carbene," Huaxue Xuebao **59**(4), 516–519 (2001).
136. C. A. Grambow, A. Jamal, Y.-P. Li, W. H. Green, J. Zádor, and Y. V. Suleimanov, "Unimolecular reaction pathways of a γ-ketohydroperoxide from combined application of automated reaction discovery methods," J. Am. Chem. Soc. **140**(3), 1035–1048 (2018).
137. S. Maeda and Y. Harabuchi, "On benchmarking of automated methods for performing exhaustive reaction path search," J. Chem. Theor. Comput. **15**(4), 2111–2115 (2019).
138. Y. N. Indulkar, M. K. Louie, and A. Sinha, "UV photochemistry of peroxyformic acid (HC(O)OOH): An experimental and computational study investigating 355 nm photolysis," J. Phys. Chem. A **118**(31), 5939–5949 (2014).
139. M. Kieninger, P. Saenz Méndez, and O. N. Ventura, "On the experimental structure of monoperoxocarbonic acid and the enthalpy of formation of carbonic acid, peroxyformic acid and monoperoxocarbonic acid in gas phase," Chem. Phys. Lett. **480**(1), 52–56 (2009).
140. W. Klopper, B. Ruscic, D. P. Tew, F. A. Bischoff, and S. Wolfsegger, "Atomization energies from coupled-cluster calculations augmented with explicitly-correlated perturbation theory," Chem. Phys. **356**(1), 14–24 (2009).
141. A. S. Pell and G. Pilcher, "Measurements of heats of combustion by flame calorimetry. Part 3. Ethylene oxide, trimethylene oxide, tetrahydrofuran and tetrahydropyran," Trans. Faraday Soc. **61**, 71–77 (1965).
142. F. Wang, H. Sun, J. Sun, X. Jia, Y. Zhang, Y. Tang, X. Pan, Z. Su, L. Hao, and R. Wang, "Mechanistic and kinetic study of $CH_2O + O_3$ reaction," J. Phys. Chem. A **114**(10), 3516–3522 (2010).
143. P. Gisdakis and N. Rösch, "Olefin epoxidation by dioxiranes and percarboxylic acids: An analysis of activation energies calculated by a density functional method," J. Phys. Org. Chem. **14**(6), 328–332 (2001).
144. A. C. Voukides, K. M. Konrad, and R. P. Johnson, "Competing mechanistic channels in the oxidation of aldehydes by ozone," J. Org. Chem. **74**(5), 2108–2113 (2009).
145. L. Vereecken, A. R. Rickard, M. J. Newland, and W. J. Bloss, "Theoretical study of the reactions of Criegee intermediates with ozone, alkylhydroperoxides, and carbon monoxide," Phys. Chem. Chem. Phys. **17**(37), 23847–23858 (2015).
146. L. R. Brock, B. Mischler, and E. A. Rohlfing, "Laser-induced fluorescence spectroscopy of the $B\,^2\Pi$–$X\,^2A''$ band system of HCCO and DCCO," J. Chem. Phys. **110**, 6773–6781 (1999).
147. S. J. Klippenstein, J. A. Miller, and L. B. Harding, "Resolving the mystery of prompt CO_2: The HCCO + O_2 reaction," Proc. Combust. Inst. **29**, 1209 (2002).
148. M. Agúndez, J. Cernicharo, and M. Guélin, "Discovery of interstellar ketenyl (HCCO), a surprisingly abundant radical," Astron. Astrophys. **577**, L5 (2015).
149. V. Wakelam, J.-C. Loison, K. M. Hickson, and M. Ruaud, "A proposed chemical scheme for HCCO formation in cold dense clouds," Mon. Not. R. Astron. Soc. Lett. **453**, L48–L52 (2015).
150. P. G. Szalay, A. Tajti, and J. F. Stanton, "*Ab initio* determination of the heat of formation of ketenyl (HCCO) and ethynyl (CCH) radicals," Mol. Phys. **103**(15-16), 2159–2168 (2005).
151. V. S. Nguyen, R. M. I. Elsamra, J. Peeters, S. A. Carl, and M. T. Nguyen, "Experimental and theoretical study of the reaction of the ethynyl radical with nitrous oxide, $C_2H + N_2O$," Phys. Chem. Chem. Phys. **14**(20), 7456–7470 (2012).
152. T. Zeng, D. Danovich, S. Shaik, N. Ananth, and R. Hoffmann, "Tuning the ground state symmetry of acetylenyl radicals," ACS Cent. Sci. **1**(5), 270–278 (2015).
153. K. W. Sattelmeyer, Y. Yamaguchi, and H. F. Schaefer III, "Energetics of the low-lying isomers of HCCO," Chem. Phys. Lett. **383**, 266–269 (2004).
154. X.-l. Zhao, J.-x. Zhang, J.-y. Liu, X.-t. Li, and Z.-s. Li, "Theoretical study on the mechanism of the C_2H + O reaction," Chem. Phys. Lett. **436**, 41–46 (2007).
155. H. M. T. Nguyen, H. T. Nguyen, T.-N. Nguyen, H. Van Hoang, and L. Vereecken, "Theoretical study on the reaction of the methylidyne radical, $CH(X^2\Pi)$, with formaldehyde CH_2O," J. Phys. Chem. A **118**(38), 8861–8871 (2014).
156. R. Alcala, J. W. Shabaker, G. W. Huber, M. A. Sanchez-Castillo, and J. A. Dumesic, "Experimental and DFT studies of the conversion of ethanol and acetic acid on PtSn-based catalysts," J. Phys. Chem. B **109**, 2074 (2005).
157. R. Sumathi, J. Peeters, and M. T. Nguyen, "Theoretical studies on the $C_2H + O_2$ reaction: Mechanism for HCO + CO, HC≡CO + O and CH + CO_2 formation," Chem. Phys. Lett. **287**(1-2), 109–118 (1998).
158. M. C. Bowman, A. D. Burke, J. M. Turney, and H. F. Schaefer, "Mechanisms of the ethynyl radical reaction with molecular oxygen," J. Phys. Chem. A **122**, 9498–9511 (2018).
159. N. Sebbar, H. Bockhorn, and J. W. Bozzelli, "Structures, thermochemical properties (enthalpy, entropy and heat capaci-ty), rotation barriers, and peroxide bond energies of vinyl, allyl, ethynyl and phenyl hydroperoxides," Phys. Chem. Chem. Phys. **4**, 3691–3703 (2002).
160. K. S. Kim, S. P. So, and H. F. Schaefer, "Structure and energetics of realistic carbynes: (Carbohydroxy)carbyne (HOCOCĊ:)," J. Am. Chem. Soc. **104**, 1457–1461 (1982).
161. J. J. Orlando and G. S. Tyndall, "The atmospheric chemistry of the HC(O)CO radical," Int. J. Chem. Kinet. **33**(3), 149–156 (2001).
162. A. L. Cooksy, "Relocalization in floppy free radicals: The OCNO and OCCHO isoelectronic series," J. Am. Chem. Soc. **123**(17), 4003–4013 (2001).
163. M. C. Bowman (Private communication, University of Georgia, Athens, GA, USA, 23 November 2018).
164. Y.-Q. Ding, C. Wang, D.-C. Fang, and R.-Z. Liu, "Theoretical study on the doublet-state potential energy surface of the reactions between HCCO ($^2A''$) and O_2 ($^3\Sigma_g^-$)," Huaxue Xuebao **62**(15), 1373–1378 (2004).
165. J. K. Merle and C. M. Hadad, "Computational study of the oxygen initiated decomposition of 2-oxepinoxy radical: A key intermediate in the oxidation of benzene," J. Phys. Chem. A **108**(40), 8419–8433 (2004).
166. Z.-G. Wei, X.-R. Huang, Y.-B. Sun, and C.-C. Sun, "Theoretical study on the potential energy surface of the reaction of ketenyl radical ($HCCO^•$) with oxygen (O_2)," Gaodeng Xuexiao Huaxue Xuebao **25**(8), 1504–1506 (2004).
169. D. Ponomarev and V. Takhistov, "Thermochemistry of organic and heteroorganic species. Part XVI. Application of IR spectra of unsaturated aliphatic molecules to the thermochemistry of vinylic and allylic free radicals," Int. J. Mol. Des. **4**, 367–380 (2005).
170. A. Krivokapic, A. Sanderud, S. G. Aalbergsjoe, E. O. Hole, and E. Sagstuen, "Lithium formate for EPR dosimetry (2): Secondary radicals in X-irradiated crystals," Radiat. Res. **183**(6), 675–683 (2015).
171. R. W. Molt, A. M. Lecher, T. Clark, R. J. Bartlett, and N. G. J. Richards, "Facile C_{sp^2}–C_{sp^2} bond cleavage in oxalic acid-derived radicals," J. Am. Chem. Soc. **137**(9), 3248–3252 (2015).
172. K. T. Kuwata, T. S. Dibble, E. Sliz, and E. B. Petersen, "Computational studies of intramolecular hydrogen atom transfers in the β-hydroxyethylperoxy and β-hydroxyethoxy radicals," J. Phys. Chem. A **111**(23), 5032–5042 (2007).
173. J. Zádor, R. X. Fernandes, Y. Georgievskii, G. Meloni, C. A. Taatjes, and J. A. Miller, "The reaction of hydroxyethyl radicals with O_2: A theoretical analysis and experimental product study," Proc. Combust. Inst. **32**(1), 271–277 (2009).
174. T. G. Denisova and E. T. Denisov, "Estimation of the O–H bond dissociation energy from kinetic data for hydroperoxides with functional groups," Pet. Chem. **44**, 278–283 (2004).
175. Y. Furutani, Y. Dohara, S. Kudo, J.-I. Hayashi, and K. Norinaga, "Theoretical study on elementary reaction steps in thermal decomposition processes of syringol-type monolignol compounds," J. Phys. Chem. A **122**(3), 822–831 (2018).
176. S.-H. Jung, S.-C. Jang, J.-W. Kim, J.-W. Kim, and J.-H. Choi, "Theoretical investigation of the radical–radical reaction of $O(^3P)$ + C_2H_3 and comparison with gas-phase crossed-beam experiments," J. Phys. Chem. A **119**(49), 11761–11771 (2015).
177. V. M. Orlov, A. A. Krivoruchko, A. D. Misharev, and V. V. Takhistov, "Enthalpy of formation of ketene, ethynol, and their analogs in the gas phase," Bull. Acad. Sci. USSR, Div. Chem. Sci. **35**, 2404–2405 (1986).

178. S. Rayne and K. Forest, "Thermochemistry of mono- and disubstituted acetylenes and polyynes at the Gaussian-4 level of theory," Comput. Theor. Chem. **970**, 15–22 (2011).
179. F. Jiao, J. Li, X. Pan, J. Xiao, H. Li, H. Ma, M. Wei, Y. Pan, Z. Zhou, M. Li, S. Miao, J. Li, Y. Zhu, D. Xiao, T. He, J. Yang, F. Qi, Q. Fu, and X. Bao, "Selective conversion of syngas to light olefins," Science **351**(6277), 1065–1068 (2016).
180. E. E. Etim, P. Gorai, A. Das, and E. Arunan, "Theoretical investigation of interstellar C–C–O and C–O–C bonding backbone molecules," Astrophys. Space Sci. **363**(1), 6 (2018).
181. F. O. Rice and J. Greenberg, "Ketene. III. Heat of formation and heat of reaction with alcohols," J. Am. Chem. Soc. **56**, 2268–2270 (1934).
182. R. L. Nuttall, A. H. Laufer, and M. V. Kilday, "The enthalpy of formation of ketene," J. Chem. Thermodyn. **3**, 167–174 (1971).
183. B. Ruscic, M. Litorja, and R. L. Asher, "Ionization energy of methylene revisited: Improved values for the enthalpy of formation of CH_2 and the bond dissociation energy of CH_3 via simultaneous solution of the local thermochemical network," J. Phys. Chem. A **103**, 8625–8633 (1999); **104**, 8600 (2000).
184. J. M. Simmie, W. K. Metcalfe, and H. J. Curran, "Ketene thermochemistry," ChemPhysChem. **9**, 700–702 (2008).
185. A. L. L. East and L. Radom, "*Ab initio* statistical thermodynamical models for the computation of third-law entropies," J. Chem. Phys. **106**(16), 6655–6674 (1997).
186. Y. Girard and P. Chaquin, "Addition reactions of ^1D and ^3P atomic oxygen with acetylene. Potential energy surfaces and stability of the primary products. Is oxirene only a triplet molecule? A theoretical study," J. Phys. Chem. A **107**(48), 10462–10470 (2003).
187. C. Delamere, C. Jakins, and E. Lewars, "Reactions of oxiranylidene and dimethyloxiranylidene, and their generation by retro diels-alder-type reactions: A computational study," J. Mol. Struct.: THEOCHEM **593**, 79–91 (2002).
188. E. G. Lewars, *Computational Chemistry*, 2nd ed. (Springer, New York, NY, 2011) ISBN: 978-90-481-3861-6.
189. P. Farmanara, V. Stert, and W. Radloff, "Ultrafast photodissociation dynamics of acetone excited by femtosecond 155 nm laser pulses," Chem. Phys. Lett. **320**(5), 697–702 (2000).
190. W. J. Bouma, R. H. Nobes, L. Radom, and C. Woodward, "On the existence of stable structural isomers of ketene. A theoretical study of the C_2H_2O potential energy surface," J. Org. Chem. **47**, 1869–1875 (1982).
191. D. J. Goebbert, D. Khuseynov, and A. Sanov, "O^-+ acetaldehyde reaction products: Search for singlet formylmethylene, a wolff rearrangement intermediate," J. Phys. Chem. A **115**(15), 3208–3217 (2011).
192. J. Gimenez-Lopez, C. T. Rasmussen, H. Hashemi, M. U. Alzueta, Y. Gao, P. Marshall, C. F. Goldsmith, and P. Glarborg, "Experimental and kinetic modeling study of C_2H_2 oxidation at high pressure," Int. J. Chem. Kinet. **48**(11), 724–738 (2016).
193. J. Guan, K. R. Randall, H. F. Schaefer, and H. Li, "Formylmethylene: The triplet ground state and the lowest singlet state," J. Phys. Chem. A **117**(10), 2152–2159 (2013).
194. P. Pokhilko, R. Shannon, D. Glowacki, H. Wang, and A. I. Krylov, "Spin-Forbidden channels in reactions of unsaturated hydrocarbons with O(3P)," J. Phys. Chem. A **123**(2), 482–491 (2019).
195. D. Vijay and G. N. Sastry, "Relative energies of $C_2O_2H_2$ isomers and their ionized counterparts: Possibility of bond stretch isomerism," J. Mol. Struct.: THEOCHEM **714**, 199–207 (2005).
196. A. P. Scott, M. S. Platz, and L. Radom, "Singlet-triplet splittings and barriers to Wolff rearrangement for carbonyl carbenes," J. Am. Chem. Soc. **123**(25), 6069–6076 (2001).
197. Y. Xie and H. F. Schaefer, "Singlet-triplet splitting of carbohydroxycarbene," Mol. Phys. **87**(2), 389–397 (1996).
198. Y. Apeloig and R. Schreiber, "Theoretical *ab initio* investigation of substituted alkylidene carbenes," Tetrahedron Lett. **19**, 4555–4558 (1978).
199. A. Fahr and A. H. Laufer, "The reactions of electronically excited vinylidene radicals with molecular oxygen," J. Am. Chem. Soc. **109**(13), 3843–3846 (1987).
200. R. Kakkar, P. Chadha, and P. Rajni, "Density functional (DFT) study of acyloxy carbene-carbene rearrangements," J. Mol. Struct.: THEOCHEM **626**, 187–194 (2003).
201. K. B. Wiberg and R. A. Fenoglio, "Heats of formation of C_4H_6 hydrocarbons," J. Am. Chem. Soc. **90**, 3395–3397 (1968).
202. D. Bakowies, "Estimating systematic error and uncertainty in *ab initio* thermochemistry: II. ATOMIC(hc) enthalpies of formation for a large set of hydrocarbons," J. Chem. Theory Comput. **16**, 399–426 (2020).
203. C. Trindle and E. A. Halevi, "Spin-forbidden reaction pathways in the interaction of singlet and triplet molecular oxygen with acetylene," Int. J. Quantum Chem. **14**, 281–290 (1978).
204. T. H. Lay, T. Yamada, P.-L. Tsai, and J. W. Bozzelli, "Thermodynamic parameters and group additivity ring corrections for three- to six-membered oxygen heterocyclic hydrocarbons," J. Phys. Chem. A **101**(13), 2471–2477 (1997).
205. E. Lewars and I. Bonnycastle, "The effect of substituents on the thermodynamic and kinetic stabilities of alkynols: A semiempirical and *ab initio* survey of the effect of H, Li, BeH, BH_2, CH_3, NH_2, OH and F," J. Mol. Struct.: THEOCHEM **418**(1), 17–33 (1997).
206. N. Sebbar, J. W. Bozzelli, and H. Bockhorn, "Thermochemical properties, rotation barriers, bond energies, and group additivity for vinyl, phenyl, ethynyl, and allyl peroxides," J. Phys. Chem. A **108**, 8353–8366 (2004).
207. T.-M. Fu, D. J. Jacob, F. Wittrock, J. P. Burrows, M. Vrekoussis, and D. K. Henze, "Global budgets of atmospheric glyoxal and methylglyoxal, and implications for formation of secondary organic aerosols," J. Geophys. Res.: Atmos. **113**, D15303 (2008).
208. Thermodynamics Research Center, *Selected Values of Properties of Chemical Compounds* (Thermodynamics Research Center, Texas A&M University, College Station, Texas, 1997).
209. S.-Z. Xiong, Q. Yao, Z.-R. Li, and X.-Y. Li, "Reaction of ketenyl radical with hydroxyl radical over $C_2H_2O_2$ potential energy surface: A theoretical study," Combust. Flame **161**(4), 885–897 (2014).
210. R. Sumathi and W. H. Green, "Thermodynamic properties of ketenes: Group additivity values from quantum chemical calculations," J. Phys. Chem. A **106**, 7937–7949 (2002).
211. R. D. Bach and O. Dmitrenko, "The effect of carbonyl substitution on the strain energy of small ring compounds and their six-member ring reference compounds," J. Am. Chem. Soc. **128**, 4598 (2006).
212. D. Kovacs and J. E. Jackson, "$CH_2 + CO_2 \rightarrow CH_2O + CO$, one-step oxygen atom abstraction or addition/fragmentation via α-lactone?," J. Phys. Chem. A **105**(32), 7579–7587 (2001).
213. J. Lee and J. W. Bozzelli, "Thermochemical properties, reaction pathways and kinetics of the formylmethyl radical + O_2 reaction system," J. Phys. Chem. A **107**, 3778–3791 (2003).
214. N. U. M. Howes, J. P. A. Lockhart, M. A. Blitz, S. A. Carr, M. T. Baeza-Romero, D. E. Heard, R. J. Shannon, P. W. Seakins, and T. Varga, "Observation of a new channel, the production of CH_3, in the abstraction reaction of OH radicals with acetaldehyde," Phys. Chem. Chem. Phys. **18**(38), 26423–26433 (2016).
215. B. Chen, D. A. Hrovat, and W. T. Borden, "Calculations of the energies of the low-lying electronic states of dioxatrimethylenemethane (H_2CCO_2) and prediction of the negative ion photoelectron (NIPE) spectrum of its radical anion," J. Phys. Org. Chem. **30**(4), e3594 (2017).
216. W. Lin and G. C. Schatz, "Mechanisms of formaldehyde and C_2 formation from methylene reacting with CO_2 adsorbed on Ni (110)," J. Phys. Chem. C **122**, 13827–13833 (2018).
217. W. T. Borden (personal communication, University of North Texas, Denton, 1 August 2019), see Ref. 346.
218. H. Sun, Y.-Z. Tang, Z.-L. Wang, X.-M. Pan, Z.-S. Li, and R.-S. Wang, "DFT investigation of the mechanism of $CH_2CO + O(^3P)$ reaction," Int. J. Quantum Chem. **105**(5), 527–532 (2005).
219. C. Goedecke, M. Leibold, U. Siemeling, and G. Frenking, "When does carbonylation of carbenes yield ketenes? A theoretical study with implications for synthesis," J. Am. Chem. Soc. **133**, 3557 (2011).
220. R. Gershoni-Poranne and A. Stanger, "An MO-based identification of charge-shift bonds," ChemPhysChem **13**(9), 2377–2381 (2012).

221. R. Gershoni (private communication, Poranne (ETH Zurich), 18 June 2019).
222. A. Francés-Monerris, I. Fdez Galván, R. Lindh, and D. Roca-Sanjuán, "Triplet versus singlet chemiexcitation mechanism in dioxetanone: A CASSCF/CASPT2 study," Theor. Chem. Acc. **136**, 70 (2017).
223. A. W. Harrison, M. F. Shaw, and W. J. De Bruyn, "Theoretical investigation of the atmospheric photochemistry of glyoxylic acid in the gas phase," J. Phys. Chem. A **123**, 8109 (2019).
224. Y. Liu, W. Wang, W. Wang, and X. Lei, "Theoretical investigation on the ozonolysis mechanism of (E)-2-formylcinnamaldehyde in the atmosphere," Chem. Phys. Lett. **730**, 165 (2019).
225. L.-l. Xing, X.-y. Zhang, Z.-d. Wang, S. Li, and L.-d. Zhang, "New insight into the competition between decomposition pathways of hydroperoxymethyl formate in low temperature DME oxidation," Chin. J. Chem. Phys. **28**, 563–572 (2015).
226. L. Vereecken, "The reaction of Criegee intermediates with acids and enols," Phys. Chem. Chem. Phys. **19**, 28630–28640 (2017).
227. C.-A. Chung, J. W. Su, and Y.-P. Lee, "Detailed mechanism and kinetics of the reaction of Criegee intermediate CH_2OO with HCOOH investigated via infrared identification of conformers of hydroperoxymethyl formate and formic acid anhydride," Phys. Chem. Chem. Phys. **21**, 21445 (2019).
228. C. Cabezas and Y. Endo, "The Criegee intermediate-formic acid reaction explored by rotational spectroscopy," Phys. Chem. Chem. Phys. **21**, 18059 (2019).
229. H. M. Perks and J. F. Liebman, "Aspects of the energetics of carboxylic acids and their anhydrides," Struct. Chem. **11**(4), 265–269 (2000).
230. G. Wu, S. Shlykov, F. S. Van Alseny, H. J. Geise, E. Sluyts, and B. J. Van der Veken, "Formic anhydride in the gas phase, studied by electron diffraction and microwave and infrared spectroscopy, supplemented with ab-initio calculations of geometries and force fields," J. Phys. Chem. **99**, 8589–8598 (1995).
231. H. Kühne, T.-K. Ha, R. Meyer, and H. H. Günthard, "Formic acid anhydride. Matrix infrared spectra of five isotopic species, vibrational analysis, empirical and *ab initio* harmonic force field and thermodynamic functions," J. Mol. Spectrosc. **77**, 251–269 (1979).
232. S. Firth-Clar, C. F. Rodiquez, and I. H. Williams, "Hydroxyoxiranone: An *ab initio* MO investigation of the structure and stability of a model for a possible α-lactone intermediate in hydrolysis of sialyl glycosides," J. Chem. Soc., Perkin Trans. **2**(10), 1943–1948 (1997).
233. A. K. Eckhardt, A. Bergantini, S. K. Singh, P. R. Schreiner, and R. I. Kaiser, "Formation of glyoxylic acid in interstellar ices: A key entry point for prebiotic chemistry," Angew. Chem., Int. Ed. **58**, 5663 (2019).
234. S. Liu, S. L. Thompson, H. Stark, P. J. Ziemann, and J. L. Jimenez, "Gas-phase carboxylic acids in a university classroom: Abundance, variability, and sources," Environ. Sci. Technol. **51**, 5454 (2017).
235. G. Buemi, "DFT study of the hydrogen bond strength and IR spectra of formic, oxalic, glyoxylic and pyruvic acids in vacuum, acetone and water solution," J. Phys. Org. Chem. **22**, 933–947 (2009).
236. Y.-R. Luo, *Comprehensive Handbook of Chemical Bond Energies* (CRC Press, Boca Raton, USA, 2007), p. 313.
237. S. E. Wheeler, D. H. Ess, and K. N. Houk, "Thinking out of the black box: Accurate barrier heights of 1,3-dipolar cycloadditions of ozone with acetylene and ethylene," J. Phys. Chem. A **112**(8), 1798–1807 (2008).
238. A. Ebrahimi, F. Deyhimi, and H. Roohi, "Investigation of structural properties of heteropropellane compounds by *ab initio* methods," J. Chem. Res. **2000**(2), 93–95.
239. D. R. Reed, S. R. Kass, K. R. Mondanaro, and W. P. Dailey, "formation of a 1-bicyclo[1.1.1]pentyl anion and an experimental determination of the acidity and C–H bond dissociation energy of 3-tert-Butylbicyclo[1.1.1]pentane," J. Am. Chem. Soc. **124**(11), 2790–2795 (2002).
240. A. Fattahi, L. Lis, Z. A. Tehrani, S. S. Marimanikkuppam, and S. R. Kass, "Experimental and computational bridgehead C–H bond dissociation enthalpies," J. Org. Chem. **77**(4), 1909–1914 (2012).
241. H. K. K. Hall, Jr. and J. H. Baldt, "Thermochemistry of strained-ring bridgehead nitriles and esters," J. Am. Chem. Soc. **93**, 140–145 (1971).
242. A. A. Samarov, A. G. Nazmutdinov, and S. P. Verevkin, "Vapour pressures and enthalpies of vaporization of aliphatic esters," Fluid Phase Equilib. **334**, 70–75 (2012).
243 Thermochemical Data by D. R. Burgess, Jr., in *NIST Chemistry WebBook, NIST Standard Reference Database Number 69*, edited by P. J. Linstrom and W. G. Mallard (National Institute of Standards and Technology, Gaithersburg, MD, 2019) (retrieved October 18, 2019).
244. K. W. Frese, Jr., F. Wang, C. Chen, and K. Krist, "Partial oxidation of methane in aqueous electrochemical systems," Am. Chem. Soc., Div. Pet. Chem. **37**(1), 15–25 (1992).
245. K. Sugino, E. Inoue, K. Shirai, T. Koseki, and T. Gomi, "Slow oxidation of ethylene by silent electric discharge," Nippon Kagaku Zasshi **86**(11), 1200–1201 (1965).
246. T. Uchimaru, R. Hara, K. Tanabe, and K. Fujimori, "Acyloxyl radical pair intermediate for the initial stage of the thermal decomposition of diacyl peroxide: A density functional study," Chem. Phys. Lett. **267**, 244–250 (1997).
247. K. Sung, "Substituent effects on stability of oxiranes, oxirenes, and dioxiranes," Can. J. Chem. **78**(5), 562–567 (2000).
248. Z. Zhang and G. W. Huber, "Catalytic oxidation of carbohydrates into organic acids and furan chemicals," Chem. Soc. Rev. **47**, 1351 (2018).
249. K. Kawamura and S. Bikkina, "A review of dicarboxylic acids and related compounds in atmospheric aerosols: Molecular distributions, sources and transformation," Atmos. Res. **170**, 140 (2016).
250. C. Chen and S.-F. Shyu, "Conformers and intramolecular hydrogen bonding of the oxalic acid monomer and its anions," Int. J. Quantum Chem. **76**, 541–551 (2000).
251. O. V. Dorofeeva, V. P. Novikov, and D. B. Neumann, "NIST-JANAF thermochemical tables. I. Ten organic molecules related to atmospheric chemistry," J. Phys. Chem. Ref. Data **30**, 475–513 (2001).
252. R. C. Wilhoit and D. Shiao, "Thermochemistry of biologically important compounds. Heats of combustion of solid organic acids," J. Chem. Eng. Data **9**, 595–599 (1964).
253. R. S. Bradley and S. Cotson, "The vapour pressure and lattice energy of hydrogen-bonded crystals .Part II. α- and β-Anhydrous oxalic acid and tetragonal pentaerythritol," J. Chem. Soc. **1953**, 1684–1688.
254. M. Bilde, K. Barsanti, M. Booth, C. D. Cappa, N. M. Donahue, E. U. Emanuelsson, G. McFiggans, U. K. Krieger, C. Marcolli, D. Topping, P. Ziemann, M. Barley, S. Clegg, B. Dennis-Smither, M. Hallquist, Å. M. Hallquist, A. Khlystov, M. Kulmala, D. Mogensen, C. J. Percival, F. Pope, J. P. Reid, M. A. V. Ribeiro da Silva, T. Rosenoern, K. Salo, V. P. Soonsin, T. Yli-Juuti, N. L. Prisle, J. Pagels, J. Rarey, A. A. Zardini, and I. Riipinen, "Saturation vapor pressures and transition enthalpies of low-volatility organic molecules of atmospheric relevance: From dicarboxylic acids to complex mixtures," Chem. Rev. **115**(10), 4115–4156 (2015).
255. D. Feller, D. H. Bross, and B. Ruscic, "Enthalpy of formation of $C_2H_2O_4$ (oxalic acid) from high-level calculations and the active thermochemical tables approach," J. Phys. Chem. A **123**, 3481–3496 (2019).
256. H. A. Rypkema and J. S. Francisco, "Atmospheric oxidation of peroxyacetic acid," J. Phys. Chem. A **117**(51), 14151 (2013).
257. A. Maranzana, J. R. Barker, and G. Tonachini, "Master equation simulations of competing unimolecular and bimolecular reactions: Application to OH production in the reaction of acetyl radical with O_2," Phys. Chem. Chem. Phys. **9**(31), 4129–4141 (2007).
258. L. V. Serebrennikov and N. A. Uvarov, "Calculations of intermediates and transition states in the reaction of glyoxal with hydrogen peroxide and possible reaction channels," Z. Fiz. Khim. **78**(11), 2033–2039 (2004).
259. R. Carbó and S. Fraga, "AVE–CI–SCF studies in molecular structure .4. 6-membered heterocycles with nitrogen and oxygen," Ann. Fis. **68**, 21–28 (1972).
260. P. J. Bruna, F. Grein, and J. Passmore, "Density functional theory (DFT) calculations on the structures and stabilities of $[C_nO_{2n+1}]^{2-}$ and $[C_nO_{2n+1}]X_2$ polycarbonates containing chainlike $(CO_2)_n$ units (n = 2-6; X = H or Li)," Can. J. Chem. **89**(6), 671–687 (2011).
261. E. Lewars, "Polymers and oligomers of carbon dioxide: *ab initio* and semi-empirical calculations," J. Mol. Struct.: THEOCHEM **363**(1), 1–15 (1996).

262. T. L. Tso and E. K. C. Lee, "Mechanism of photo-oxidation of glyoxal and formadehyde in solid O_2 at 12–18 K," J. Phys. Chem. **88**, 5465–5474 (1984).
263. P. A. Denis and F. R. Ornellas, "Theoretical characterization of hydrogen polyoxides: HOOH, HOOOH, HOOOOH and HOOO," J. Phys. Chem. **113**, 499–506 (2009).
264. S. A. Tonkin, R. Bos, G. A. Dyson, K. F. Lim, R. A. Russell, S. P. Watson, C. M. Hindson, and N. W. Barnett, "Studies on the mechanism of the peroxyoxalate chemiluminescence reaction," Anal. Chim. Acta **614**(2), 173–181 (2008).
265. P. A. Castelfranco, Y.-K. Lu, and A. J. Stemler, "Hypothesis: The peroxydicarbonic acid cycle in photosynthetic oxygen evolution," Photosynth. Res. **94**(2), 235–246 (2007).